

Note: This thesis has been revised. The most recent version is available at <https://shareok.org/handle/11244/337569.2>

UNIVERSITY OF OKLAHOMA
GRADUATE COLLEGE

EXPERIMENTAL INVESTIGATION OF ELASTOMER PERFORMANCE FOR
UNDERGROUND HYDROGEN STORAGE WELLS

A THESIS
SUBMITTED TO THE GRADUATE FACULTY
in partial fulfillment of the requirements for the
Degree of
MASTER OF SCIENCE

By
DANIEL ADDOKWEI TETTEH
Norman, Oklahoma
2023

EXPERIMENTAL INVESTIGATION OF ELASTOMER PERFORMANCE FOR
UNDERGROUND HYDROGEN STORAGE WELLS

A THESIS APPROVED FOR THE
MEWBOURNE SCHOOL OF PETROLEUM AND GEOLOGICAL ENGINEERING

BY THE COMMITTEE CONSISTING OF

Dr. Saeed Salehi, Chair

Dr. Ramadan Ahmed

Dr. Hamidreza Karami

© Copyright by DANIEL ADDOKWEI TETTEH 2023

All Rights Reserved.

Acknowledgments

First and foremost, I would like to thank the Almighty God for his continuous grace, knowledge, wisdom, understanding, and strength as a graduate student. I could not have done anything without Him. May His name be forever praised. Amen.

I would also like to express my profound gratitude to Dr. Saeed Salehi, my advisor, mentor, friend, father figure, confidante, and cheerleader. Thank you for accepting me as your student, believing in me, pushing me extremely hard to unearth my potential, funding me, and being patient with me to learn and grow while appreciating the process. You taught me to be strong, grow, and develop both as a human being and as a professional. I am very grateful and will forever be indebted to you. Thank you!

I am also grateful to my thesis committee members, Dr. Ahmed Ramadan, and Dr. Karami Hamidreza. To Dr. Ahmed, thank you for your continuous guidance and coaching during this thesis work and for advising me when I had difficult decisions. I am very grateful to you for offering your research space and fume hood so I can carry out my experiment safely. For your unwavering desire to always assist me, I am very grateful. Also, a big “thank you” to Dr. Karami Hamidreza for your support during my entire work for this thesis. You also made time for me and advised me concerning issues related to other work outside my thesis. I am truly grateful.

I also express my sincere gratitude to Jeff McCaskill at the University of Oklahoma Well Construction Technology Center. I appreciate the coaching, guidance, and chastisement. They all worked to make me a better person. You also sacrificed your time to assist me throughout the experimental set-up. You pushed me to think and be innovative and, more importantly, you were a friend. I am grateful, Jeff.

I also thank all my friends and colleagues at the Well Construction Technology Center (WCTC). Your support as a team played a significant role in completing this thesis. I am also grateful to Garry Stowe for offering me some very vital experimental support, Sonya Grant, Kathleen Shapiro, and all the Staff and Faculty at the Mewbourne School of Petroleum and Geological Engineering at the University of Oklahoma who played one role or the other in making completion of this thesis a reality.

Lastly, I wish to thank my family, my prayerful mother, Maa Belinda, and my supportive father, Mr. Ankamah, my siblings, my loved ones, members of the Immanuel Presby Church, OKC Oklahoma, and my good friends Nabe Konate and Julius Tetteh of the University of Wyoming for your continuous support throughout my entire time as a graduate student.

Table of contents

Acknowledgments	iv
Table of contents	vi
List of Tables	vii
List of Figures	viii
Abstract.....	x
1. Introduction	1
1.1. Research Motivation.....	1
1.2. Research Statement.....	7
1.3. Objectives	14
2. Literature Review.....	15
2.1. The Hydrogen Economy.....	15
2.1.1. Hydrogen Production.....	18
2.1.2. Hydrogen Transportation and Distribution	27
2.1.3. Hydrogen Storage	29
2.2. Large-Scale Underground Hydrogen Storage	30
2.2.2. Hydrogen Blending with Natural Gas	44
2.2.3. Hydrogen Storage in Depleted Reservoirs: Challenges and Barriers	46
3. Elastomers	66
3.1. Elastomers Used in the Oil and Gas Industry	76
3.2. Elastomer Failure Modes.....	82
3.3. A Review of Elastomer Behavior in Gaseous Hydrogen Environments.....	87
4. Experimental Design and Methodology	100
4.1. Materials.....	101
4.1.1. Elastomers	101
5. Results and Analysis.....	115
6. Discussions.....	137
7. Summary and Conclusions.....	145
8. Recommendations For Future Work	148
9. References	151

List of Tables

Table 1: The Advantages and Limitations of Principal Reformation Methods for Hydrogen Production (Tetteh and Salehi, 2022; Kalamaras et al.,2013; Holladay et al.,2009)	22
Table 2: Global Locations of Underground Hydrogen Storage Sites in Salt Caverns (Zivar et al.,2021; Tarkowski and Uliasz-Misiak, 2022; Tarkowski, 2019; Panfilov et al.,2006).....	38
Table 3: Worldwide Potential Hydrogen Storage sites.....	42
Table 4: Advantages and Limitations of Principal Gas Storage Techniques (All Consulting LLC, 2016; Bunger et al., 2016; FERC, 2004; Kobos et al., 2011; Crotingo, 2010; Evans 2007).....	43
Table 5: A comparison of the properties of H ₂ , CH ₄ and CO ₂ (Ugarte and Salehi, 2022; Tarkowski, 2019; Alcock, 2001; Das, 2016)	47
Table 6: Summary of Implications of Subsurface Microbial Activities (Aftab et al.,2022)	57
Table 7: Summary of Applications of Elastomers in the Oil and Gas Field (Adapted and modified from Mody, 2013)	80
Table 8: Criteria for ranking elastomer damage based on NORSOK testing standard (Schrittesser et al., 2016).....	90
Table 9: Measured Data from Elastomer Hardness Tests.....	104
Table 10: Measured Data from Elastomer Hardness Tests.....	106
Table 11: Matrix of Selected Tests for Aging Experiment.....	110
Table 12: Summary of Sampled Data on the Number of Cavities for Statistical Analysis.....	132
Table 13: T-Test Results After aging in 100% Hydrogen.....	134
Table 14: T-Test Results After aging in (50% H ₂ + 50% CH ₄).....	135
Table 15: Diffusion Coefficient of Gases at Selected Temperatures for Ambient Pressures (The Engineering Toolbox, 2022).....	139

List of Figures

Figure 1: Energy Consumption by Fuel- as projected in the Annual Energy Outlook of the US Energy Information Administration (EIA, 2022).....	3
Figure 2: The Hydrogen economy (Adapted and modified from Tetteh and Salehi. 2022).....	5
Figure 3: Diagrammatic representation of the “Power-to-Gas” Concept.....	8
Figure 4: Potential gas leakage pathways in the wellbore (Gasda et al., 2004).....	12
Figure 5: Global target-specific policies in support of the Deployment of Hydrogen Systems. Based on data available up to May 2019.....	18
Figure 6: Share of industrial hydrogen production by source (Ewan, 2005).....	19
Figure 7: Hydrogen production via Electrolysis using Renewable Energy (Chi et al.,2018).....	25
Figure 8: The Colors of Hydrogen (Tetteh and Salehi, 2023).....	27
Figure 9: The Timeline of Underground Gas Storage in the United States (All Consulting LLC, 2016)...	32
Figure 10: Underground Hydrogen storage techniques; (a) Depleted hydrocarbon reservoirs; (b) Salt caverns (c) Aquifers (All Consulting, 2016)	33
Figure 11: Underground gas storage by type (Adapted and modified from FERC, 2004).....	34
Figure 12: Global Outlook of Underground Gas Storage at the end of 2017 (Carnot-Gandolphe, 2018) ..	35
Figure 13: Map of United States Geological Structures with Potentials for Underground Hydrogen Storage (Kobos et al., 2011)	40
Figure 14: Map of Salt Caverns and Formations in Europe (Bunger et al., 2016).....	41
Figure 15: Diagrammatic representation of biotic reactions in an Underground Hydrogen Storage Environment (Ebrahimiyejta, 2017)	50
Figure 16: Clay swelling and fracture formation in clay silts due to hydrogen diffusion (Liu et al., 2022) ..	51
Figure 17: SRB corrosion reaction on steel surface based on cathodic depolarization theory (adapted and modified from (Mori et al., 2012).....	56
Figure 18: Pictorial representation of (a) Hydrogen blistering (b) Hydrogen-induced cracking (Szummer, 1999).....	59
Figure 19: SEM micrograph of carbonated cement surface with CaCO ₃ nucleation (Galan et al., 2015) ..	61
Figure 20: Sulfate attack in cement resulting in ettringite and gypsum formation (Ugarte and Salehi, 2022)	62
Figure 21: Blister fracture in EPDM O-ring after exposure to H ₂ @ 35Mpa and 100°C for 15 hours (Nishimura, 2014).....	65
Figure 22: Geological uncertainties associated with large-scale underground hydrogen storage in depleted hydrocarbon reservoirs (Heinemann et al., 2021).....	66
Figure 23: Schematic diagram of a network of cross-linked carbon chains of an elastomer (Mahak, 2019)	67
Figure 24: Diagrammatic representation of (a) raw rubber and (b) vulcanized rubber. Cross-linkages are represented by black dots, and lines represent the elastomer chains.	71
Figure 25: Molecular structures of common general and special purpose elastomers	76
Figure 26: (a) Elastomer seal elements in packer; (b) Elastomer seal element in Blowout Preventer (BOP) (Patel et al.,2019).....	78
Figure 27: NBR elastomer (black) in Model D packer by Baker Hughes (Mody, 2013).....	79
Figure 28: Evolution of elastomer applications in the petroleum industry (Mody, 2013)	81
Figure 29: (a)FKM elastomer chemically degraded by inorganic acids (b) Chemically degraded EPDM elastomer. (Richter and Blobner, 2017).....	85

Figure 30: Diagrammatic representation of crack distribution in elastomers after decompression for (a) Elastomers in an uncompressed state (b) Elastomers in a compressed state (c) Elastomers after explosive decompression (Yamabe and Nishimura, 2012).....	89
Figure 31: Appearance of bubbles in rubber material after supersaturation with gaseous Argon at 2.4MPa after 1, 3, and 6 minutes (Gent, 1990)	94
Figure 32: (a)Dissolution of hydrogen in elastomer at the end of saturation (b) Gas bubble formulation by agglomeration of hydrogen molecules (c) Cavity formation due to stresses generated by gas bubbles (Yamabe and Nishimura, 2009).....	95
Figure 33: Elastomer samples prepared for Hardness (left) and Compression (right) tests	101
Figure 34: Shore A Durometer	102
Figure 35: Compression Test Machine.....	107
Figure 36: Experimental Set-up for Aging Tests.....	109
Figure 37: ThermoFisher Quattro S Scanning Electron Microscopy (SEM) Device.	113
Figure 38: Control Sample for Cavity Identification in SEM Imaging	114
Figure 39: (Left)Marked Spots on Elastomers for Samples Prepared for SEM Imaging (Right) Elastomer samples Placed in SEM Device for Imaging.	114
Figure 40: Effects of Gases on Elastomer Samples Aged at 25°C and 3MPa.	117
Figure 41: Effects of Aging Period on Hardness of Elastomers: (a) 100% H ₂ @ 25°C (b) 100% H ₂ @ 70°C (c) (50% H ₂ + 50% CH ₄) @ 25°C (d) (50% H ₂ + 50% CH ₄) @ 70°C.....	119
Figure 42: Effects of Temperature on Hardness of Elastomers: (a, b and c) Aging in 100% H ₂ ; (d, e, f) Aging in Equal Mixture of Hydrogen and Methane.....	122
Figure 43: Effects of Days and Temperature on Compressional Measurement of Elastomers after aging in 100% H ₂ : (a, b) @ 25°C and (c, d) @ 70°C.....	126
Figure 44: Effects of Days and Temperature on Compressional Measurement of Elastomers after aging in (50% H ₂ + 50% CH ₄): (a, b) @ 25°C and (c, d) @ 70°C.....	127
Figure 45: Effects of Aging Period and Temperature on Compressional Measurements of Elastomers after aging in both 100% H ₂ environment and (50% H ₂ + 50% CH ₄) environment based on maximum stress values.	129
Figure 46: (a) CBS image obtained from SEM at 500microns (b) Binary image of CBS image isolating cavities after processing (c) Count of Isolated Cavities for Statistical Analysis	131
Figure 47: SEM images for morphological analysis for aging tests conducted in 100% H ₂ , 3MPa, and 70°C; (a) EPDM before Exposure, (b) EPDM after exposure, (c) NBR before exposure, (d) NBR after exposure (e) FKM before exposure (f) FKM after exposure.....	136
Figure 48: Schematic depiction of plasticization effect (Bhattacharya et al.,2013).....	139

Abstract

The "Power-to-Gas" concept is vital in the envisaged Hydrogen Economy as it ensures sustainability and energy security. The process involves converting surplus energy from various sources like conventional fossils, wind and solar into hydrogen for storage in underground structures and reproducing them during periods of high energy demand. Depleted hydrocarbon reservoirs are the most common underground structures for hydrogen storage. Being a relatively new concept, Underground Hydrogen Storage (UHS) in depleted hydrocarbon reservoirs is associated with challenges related to several aspects of well integrity, including elastomers as seen in well bore seal assemblies.

This study investigates the behavior of general-purpose oil and gas industry elastomers in UHS environments. Three general-purpose elastomers, Ethylene Propylene Diene Monomer (EPDM), Fluoroelastomers (FKM), and Nitrile Butadiene Rubber (NBR), are exposed to varied gas mixtures at different aging conditions via autoclave aging experiments and their physio-mechanical properties examined. In addition, observed cavities on the elastomers are statistically analyzed to ascertain the onset of elastomer failure due to cavity formation. Furthermore, changes in the surface morphology of elastomers due to aging were also investigated via Scanning Electron Microscopy (SEM). The result showed that exposure of elastomers to gaseous hydrogen environments at the specified environmental conditions causes changes in their physio-mechanical properties which may subsequently result in material failure.

Furthermore, two main phenomena were identified to be the primary cause the changes in the mechanical properties of elastomers samples for the given test conditions: Plasticization effect by gases and elastomer chain rupture or cross-linkage formations due to chemical ageing. Carbon dioxide was identified to have the most deteriorative effect on the mechanical properties of

elastomers due to its low diffusivity coefficient and high plasticization effect on polymer chains. The effects of pure hydrogen and hydrogen-methane mixtures on the mechanical properties of elastomers were identified to be similar. EPDM showed increased hardness and compressional resistance when aged in 100% hydrogen and hydrogen-methane mix environments at high temperatures and poor compressional resistance at low temperatures. EPDM also maintained its thermal resistance properties in gaseous hydrogen environments. The most significant elastomer degradation in gaseous hydrogen environments was seen in NBR. FKM remained thermally stable in gaseous hydrogen environments, although its compressional resistance reduced at elevated temperatures. Furthermore, SEM showed rougher surfaces of EPDM and NBR elastomers after aging in a pure hydrogen environment at 70°C for 7 days, which was proposed to be due to the formation of cross-links. Also identified on the surface of these elastomers after aging are haphazardly distributed micro-cavities and precipitates proposed to be additives used in material production. Finally, statistical analysis indicated that for all samples aged in 100% H₂ and (50% H₂ + 50% CH₄) for 3 days at 70°C, there is statistical evidence of cavity formation due to aging except for NBR samples aged in 100% H₂ at 70°C for 3 days.

1. Introduction

1.1. Research Motivation

For several decades, energy has proven to be a vital prerequisite for global civilization, economic sustainability, and human survival (Asif and Muneer, 2007; Midilli et al.,2006). Due to the rapidly increasing global population and advancement in industrialization and urbanization, energy demand is rising (Abdalla et al., 2018; Huang, 2014). In 2008, a report by Crabtree et al. (Crabtree et al., 2008) estimated global energy usage to double by 2050. Currently, the primary resources for generating heat and energy are fossil fuels (Gradisher et al., 2015). Petroleum (crude oil and natural gas) and coal are used mainly in the industrial technology and transportation sector (Agrawal et al.,2007). Also, they contribute to about 85% of the overall world energy consumption (Abdalla et al., 2018). In the United States alone, about 225 million registered light vehicles were recorded for the last decade, which cover about seven (7) billion miles a day and use as much as 8 million oil barrels daily (Holladay et al., 2009). This number rose to about 276 million vehicles in 2019 and is increasing steadily with time. Similarly, China, one of the largest global economies, reported a vehicle population of 240 million in 2018 (Wang et al., 2018). Thus, there is a considerable strain on fossil fuels which are finite resources that take a long time to recharge. Fossil resources are depleting alarmingly, and fuel prices are increasing daily.

Furthermore, excessive consumption of these resources contributes immensely to some of the major global environmental issues. They release carbon dioxide, other greenhouse gases, and pollutants into the atmosphere, facilitating the dreaded global warming (Wuebbles et al.,2001). Vehicular emissions contain chemicals like carbon monoxide and nitrogen oxides (NO_x) in large enough quantities that to some extent threaten the quality of life. In the same vein, the extraction of these fossil resources also adversely impacts land and marine environments (Shamoon et

al.,2022). In addition, exploration techniques may also discomfort marine life, whereas drilling and production operations may also cause pollution of fresh and saline water resources (Siddique et al.,2017; King and King, 2013). Coal mines have a notable reputation for releasing methane gas, nitrogen oxides, particulate matter, and volatile organic compounds that, in many ways, adversely impact the environment and may be lethal to plant and animal life (Warmuzinski, 2008). Evidently, despite the numerous benefits of fossil fuels, they are partly responsible for some of the world's crucial economic and environmental challenges. The stability of the earth's climate is threatened due to their excessive use.

In line with finding solutions to the challenges posed by fossils, the global citizenry has shifted its attention towards renewable, environmentally clean, and sustainable energy alternatives. Most developed countries and governmental agencies are pushing projects that envision a clean energy future. At the United Nations Framework Convention on Climate Change (COP21),2015, in Paris, participating countries made pledges to put structures in place to significantly minimize Green House Gas (GEG) emissions (Obergassel et al., 2016). The US Senate Committee on Energy and Natural Resources reported that 80% of electricity usage in the United States must come from environmentally friendly technologies by 2035, as specified by the Clean Energy Standards. Also, a total of USD 16 billion was invested in clean energies by the American Recovery and Reinvestment Act in 2009 (O'Hara, 2009; Aldy, 2012).

Over the last few decades, primary renewable sources have included solar, wind, geothermal, nuclear, and hydrogen. In fact, the share of these renewable energy alternatives in the energy consumption market is increasing as the global energy demand rises. From less than three (3) quadrillion British Thermal Units (BTUs) in 2000 to close to nine (9) quadrillion BTUs in 2020, the United States Energy Information Administration (EIA) in their annual energy outlook,

projects renewable energy consumption to grow to about 20 quadrillion BTUs in the United States (EIA, 2022). In addition, most of the renewable energy consumption is expected to be in the industrial and transportation sectors, as shown in **Figure 1**.

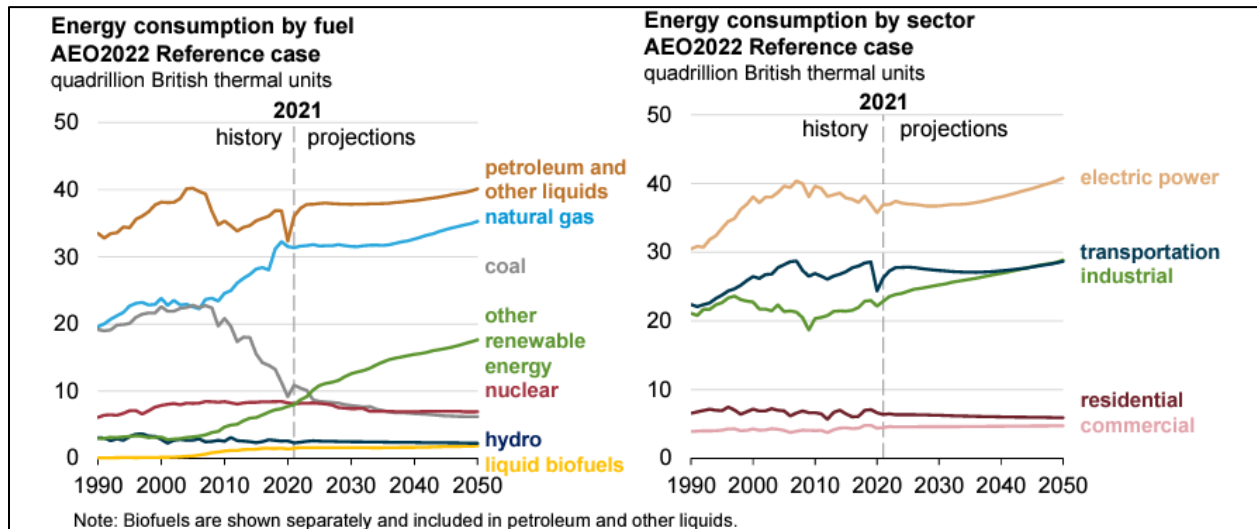


Figure 1: Energy Consumption by Fuel- as projected in the Annual Energy Outlook of the US Energy Information Administration (EIA, 2022)

Despite its numerous advantages, the renewable energy industry is still inchoate and plagued with environmental, technological, and economic limitations. For instance, solar and wind energy is highly weather dependent, affecting their ability to continuously meet energy demands without interruptions. On the other hand, nuclear energy has a very high initial cost of establishment and generates significant radioactive waste, while geothermal still produces some greenhouse gases (Deutch et al., 2003). Despite its current cost limitations and complications with storage, hydrogen has been proposed by many industry stakeholders as an essential energy carrier for a clean and sustainable future energy system (Xu et al., 2019).

Hydrogen occurs in nature as a hydrogen molecule with the molecular formula (H₂). It does not exist in nature as a fuel. It is a secondary energy carrier and thus needs to be produced from other resources like fossil fuels, water, and biomass (Tetteh & Salehi, 2022). Furthermore, it is abundant

and widely distributed worldwide without respect to national boundaries (Crabtree et al., 2004). Also, electrical energy generated from intermittent energy resources like solar, wind, and tidal power can be stored in hydrogen, making it a suitable energy storage medium (Edwards et al.,2007). As a fuel, hydrogen is highly versatile and efficient. Compared to gasoline, its energy density by mass is greater than that of gasoline. i.e., 120MJ/kg of hydrogen compared to 45 MJ/kg of gasoline (Tashie-Lewis et al.,2021; Clarkin, 2003). However, the volumetric energy density of hydrogen is 8MJ/L compared to 32MJ/L of gasoline (Zheng et al., 2021; Nehrir and Caisheng, 2009).

Similarly, hydrogen has a higher heating value of 141.8kJ/g at a temperature of 298K, and its range of specific energy is very broad; thus, it possesses a high potential of being transformed (Noor et al.,2013). Also, it has a high diffusivity, and its range of flammability is vast; hence, it burns readily in engines, requiring only little energy to ignite (Cashdollar et al.,2000). The fuel has also been shown over the years to possess a vast potential of being produced on an industrial scale. Stemming from the numerous advantages of hydrogen over conventional energy sources, it has gained a global reputation as the primary energy source for the next generation's clean and sustainable energy system; thus, the concept of the "Hydrogen Economy" has been proposed. The hydrogen economy (**Figure 2**) is an envisioned sustainable energy system powered by "emission-free" hydrogen energy (Tetteh & Salehi, 2022).

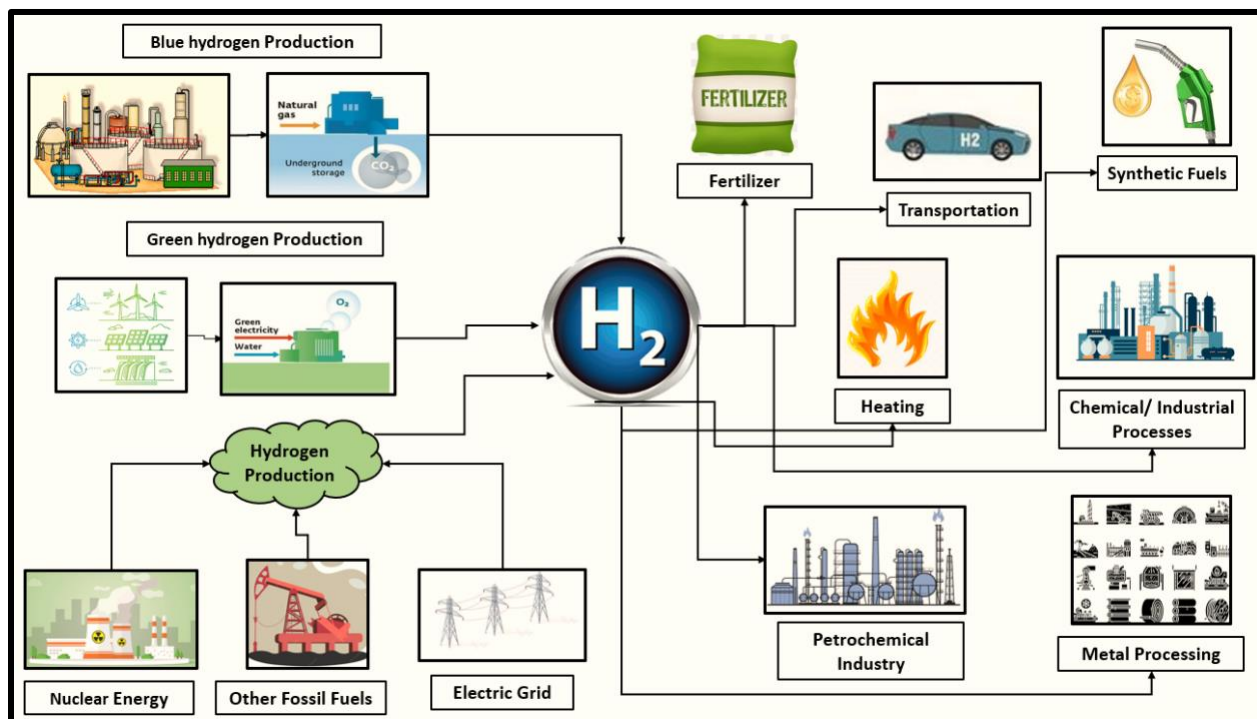


Figure 2: The Hydrogen economy (Adapted and modified from Tetteh and Salehi. 2022)

The hydrogen economy has some major components: production, storage, distribution, safety, and utilization (Dawood et al., 2020). As previously mentioned, hydrogen is a secondary form of energy and must be produced from either renewable or non-renewable resources using energy from different sources. Factors like cost, efficiency, technological availability, and system integration influence the choice of hydrogen production method (Sinigaglia et al., 2017). Also, when hydrogen is produced, it needs to be stored, distributed, and brought to final use (Bossel and Eliasson, 2003). Furthermore, safety concerns regarding each of these stages in the hydrogen chain need to be addressed. Hydrogen production is a very crucial stage in the hydrogen energy pathway. The process can be put under two main categories; production from primary non-renewable sources (i.e., fossil-based resources like coal, natural gas, and crude oil) (Cormos, 2011); Zhang et al. (2021)) and production from renewables (i.e., production from the water using electrolysis or from biomass through petrochemical processes) (Gardner, 2009; Hosseini et al., 2019). Steam

Reformation (SR), Partial Oxidation (PO) and Autothermal Reformation, Hydrocarbon pyrolysis, Coal gasification, Plasma reforming, and thermal cracking are some of the highly researched fossil-centric hydrogen production techniques. Hydrogen storage systems are dependent on the intended use of the commodity. i.e., either for transportation or stationary applications, and each is associated with specific requirements and limitations (Edwards et al., 2007). Hydrogen can also be stored on a large scale in underground facilities for future use. Common hydrogen storage techniques for stationary applications include liquefaction, compression, and storage in hydrides, either physically or chemically, carbon-based storage, and liquid carrier-based storage (Al-Hallaj and Kiszynski, 2011). Presently hydrogen is distributed via underground pipelines (as compressed gas) or tankers (as liquid hydrogen) to their consumers (Sherif et al., 2003). Hydrogen can be transformed into valuable forms of energy in hydrogen combustion engines, jet and rocket engines, catalytic combustion to produce heat, metal hydrides, and electrochemical processes to generate electricity as in fuel cells.

Despite its promising outlook for the future and the current massive global support it is enjoying, there are still significant challenges that need to be addressed in reaching a full hydrogen economy (Biol, 2019). Besides, principal scientific, technological, and socio-economic hurdles need to be addressed in each of the principal components of the hydrogen economy for it to become a reality (Edwards et al., 2007).

1.2. Research Statement

The Hydrogen Economy presents an envisioned energy system where renewable, carbon-free hydrogen energy is deployed and utilized on a large scale, mainly in the transportation and industrialization sector. For such a system, the potential challenge of not being able to supply enough energy to meet seasonal energy demand exists. The need to moderate this seasonal energy demand and ensure that there is continuity in energy supply regardless of the season necessitates large-scale underground hydrogen storage (Amid et al., 2016). A concept of interest associated with storing energy on a large-scale in periods of excess supply to meet future demands is the “Power-to-Gas” concept (Götz et al., 2016; Ozturk et al., 2019) as shown in **Figure 3**. The process involves converting surplus energy (typically wind and solar) into hydrogen for large-scale underground storage during periods of peak energy supply. The stored hydrogen is converted back to energy for usage during periods where there is a shortage in energy supply. The process requires the storage of hydrogen in a frequent charging and discharging process (Ozturk et al., 2019).

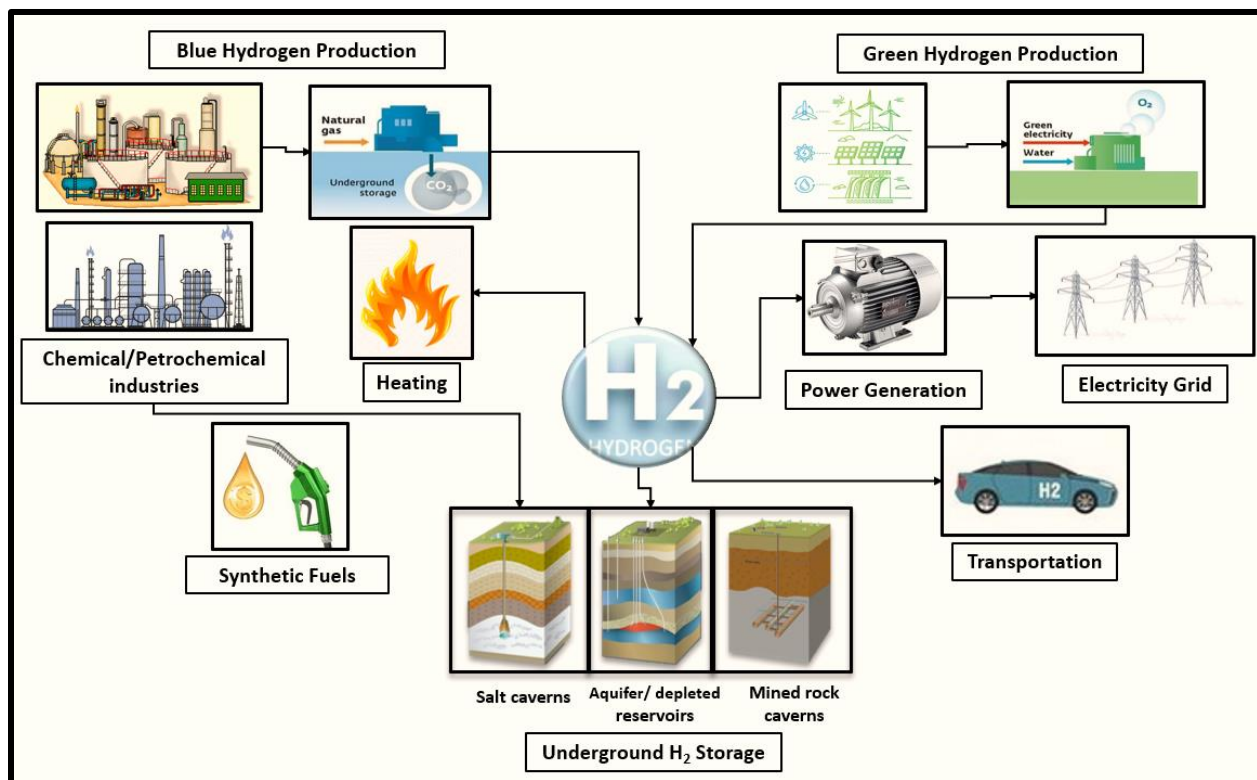


Figure 3: Diagrammatic representation of the “Power-to-Gas” Concept

The principal techniques for large-scale underground hydrogen storage (UHS) include depleted oil and gas reservoirs, salt caverns, aquifers, and hard rock caverns. The most common UHS facilities are depleted oil and gas reservoirs. These facilities usually have the requisite surface and sub-surface installations for safe and efficient storage and have proven integrity. Usually, hydrocarbons occur in geological traps. The trap consists of a reservoir rock (which contains the accumulated hydrocarbon), a seal, and an underlying aquifer. The seal is an impervious rock that keeps the hydrocarbons in place (Tarkowski, 2019). Depleted reservoirs used for underground gas storage purposes have good seals with proven capability of holding gases in place, adequate permeability to meet flow requirements during operations, and good porosity for storage requirements (Lord et al., 2014). Existing wells on the fields on which these reservoirs are located are primarily used for gas injection, although additional wells may be drilled where necessary (Bai et al. 2014). The

procedure is facilitated mainly by the fact that the geology of the formation is already known, the cushion gas requirement is minimal, and the cost of operation is reasonably low.

Salt caverns on the other hand are created by injecting fresh water in large salt domes or bedded salt deposits and leaching large cavities (Peng et al.,2023). The cavities are usually surrounded by impervious salt, making it feasible for gas storage. This method of storing hydrogen has a relatively low leak rate of about 1%, as the only possible leakage path of the gas is through wells. An aquifer is a large underground porous water-bearing rock usually employed for gas storage in areas where depleted reservoirs are unavailable. Its geological makeup and storage procedure are similar to depleted hydrocarbon reservoirs, with suitable candidates possessing ample porosity and permeability, adequate formation pressures, and storage capacities (Lord et al., 2014; Raad et al.,2022; Crotofino,2022). Due to the high level of uncertainty associated with the geology of aquifer rocks and the lack of infrastructure, these storage media are usually more expensive to employ (Crotofino, 2022; Lord et al., 2022). A relatively new avenue for the geological storage of gases is the employment of hard rock caverns. Here, large caverns are created in hard rocks and lined with steel or plastic materials (Lemieux et al., 2019). These linings serve as an impermeable layer to prevent unwanted gas escape. This is usually employed in areas where salt deposits and porous underground formations are unavailable.

Underground storage of hydrogen is a reasonably new area with minimal research and experience. Practical applications of a similar process are only present in the storage of town gas (consisting of a mixture of methane, hydrogen, and minute quantities of carbon dioxide and carbon monoxide, natural gas storage, and helium gas storage. Some studies have been conducted on the feasibility of underground geological storage of hydrogen at different geographical locations (Pudlo et al., 2013); (Lankof and Tarkowski. 2020); (Lemieux et al., 2020); (Liu et al., 2020); (Sainz-Garcia et

al. 2017) and results have shown promising potential for storage in most cases. However, some peculiar critical challenges exist in the UHS process. These challenges are related to the properties of hydrogen as a fluid, geochemical reactions between hydrogen, rock, and formation fluids, reservoir microbial activities (Heinemann et al., 2021), well integrity and completions, and material requirements (Bai et al., 2014).

According to the Norwegian standard for Well integrity in drilling and well operations, NORSOK D-010, WELL INTEGRITY is the application of technical, operational, and organizational solutions to reduce the risk of uncontrolled release of formation fluids throughout the life cycle of a well (Norge, 2013). It encapsulates all the measures put in place to prevent fluid escaping to the surface. The integrity of wells is paramount in gas storage as wells should be capable of withstanding harsh conditions during their entire service life without any leakage or corrosion problems (Freifeld et al., 2016; Zhao, 2019). Poor integrity of wells in hydrogen storage can be fatal as it could lead to explosions and, consequently, loss of lives and properties. As far as its integrity is concerned, some significant areas of a well are the cement type and configuration, casing (steel), packers, fittings, and valves. Downhole seals and packer elements in gas storage wells also have elastomers as crucial components, which play a vital role in the well's integrity. Typical well integrity challenges associated with cement in UHS include diffusion of hydrogen molecules through cement due to its smaller molecular size and higher diffusivity compared to other gases like carbon dioxide and natural gas (methane) (Bai et al., 2014; Reitenbach et al., 2015; Thiyagarajan et al., 2022). Common diffusion pathways of hydrogen in cement include micro-annuli within the cement, the bond between casing and cement (shear bonds), and the bond between cement and formation (hydraulic bonds). Furthermore, there exists a possibility of chemical reactions between hydrogen gas and cement minerals, thus creating micro-pore spaces within the cement that become

conduits for gas leakage (Zeng et al., 2022). Cement pores are mostly filled with water, and the extent of diffusion of hydrogen in cement materials is affected by water saturation, the concentration of hydrogen in cement material, as well as temperature and pressure variations (Sercombe et al., 2007). Generally, cement binders with low silica concentration are recommended to reduce hydrogen permeability in cement with variations in water saturation (Bai et al., 2014).

Another aspect of the well, susceptible to hydrogen attack and affecting the overall integrity of the well, is the casing strings (Watfa, 1991). These are typically made of steel and may undergo blistering. Hydrogen attack can also cause the formation of cavities or “blisters” on the surface of steel metals due to hydrogen gas accumulation in the pores within the metals. The hydrogen molecules accumulated within the pores react within the pores and build up pressures beneath the pores, thus forming blisters on the surface of the metal. This significantly reduces the tensile strength of the metal (Boersheim et al., 2019) and could also lead to hydrogen-induced cracking and hydrogen embrittlement (Revie, 2008; Ghasemi, 2011), which may create conduits within the material. These conduits may become potential pathways for hydrogen gas leakage (Ugarte and Salehi, 2022).

Elastomers are polymeric materials whose applications in the oil and gas industry are seen in drilling completions and wellhead equipment. They are usually found in seal elements in Blowout Preventers (BOP), subsurface safety valves, packers, O-rings, and liner hangers (Patel et al., 2019; Chen et al., 2021); This equipment is mainly used as a seal or well barrier elements. Potential failures in elastomers due to hydrogen gas activities include explosive decompression failures, which may cause material cracking and blistering, cavitation failures, and material deterioration, as seen in the changes in their structural and mechanical properties (Ugarte and Salehi, 2022; Balasooriya et al., 2018).

Elastomers usually exist in compressed states in downhole conditions, with their pores filled with gas molecules. When there is a release of surrounding gases, gas molecules rapidly escape these pores in a process known as explosive decompression, which may cause cracking and blistering in the material when gas energy is greater than the strength of the elastomer. This phenomenon is not usually experienced in underground gas storage. The potential gas leakage pathways from a wellbore are shown in **Figure 4**.

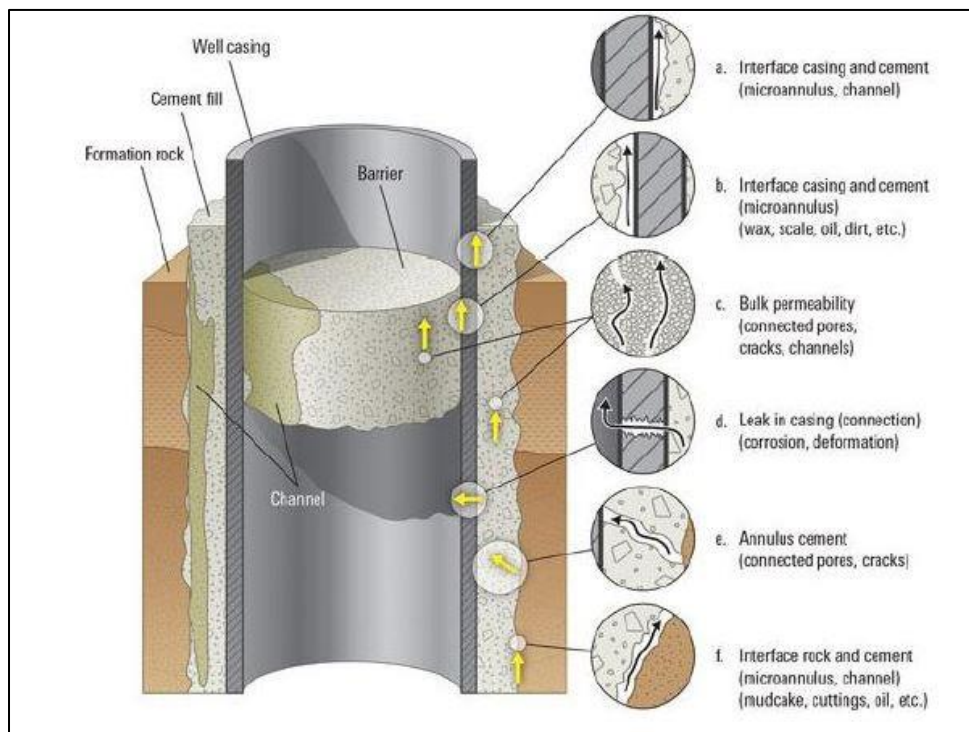


Figure 4: Potential gas leakage pathways in the wellbore (Gasda et al., 2004)

Generally, well integrity failures in underground gas storage are associated with high risks, have very catastrophic implications, and can lead to loss of life and properties. Notable examples of underground gas storage accidents caused by loss of well integrity include the Yaggy incident, which occurred in a storage site in Kansas, the Moss Bluff incident in Texas, Liberty County, The Magnolia facility incident in Bayou Louisiana, the infamous Southern California Gas' Aliso

Canyon incident, and the Clute Cavern storage facility incident in Brazoria County in Texas (Miyazaki, 2009). The first three incidents involved gas explosions caused by loss of casing integrity in salt cavern storage facilities. Furthermore, the primary cause of the Aliso Canyon incident, according to a report by the California Public Utilities Commission (CPUC), was the rupture of a 7-inch well casing due to microbial corrosion resulting from the casing's contact with groundwater (Tabibzadeh et al., 2017).

It is thus evident that although some substantial industrial experience exists for large-scale underground storage of natural gas (methane), storage of hydrogen in underground facilities is fairly novel. A few experimental works have been done on the behavior of well components such as cement, casing, and elastomer seal elements on exposure to carbon dioxide, methane, and hydrogen sulfide (H₂S) gas. Typically, these experiments investigate the changes in mechanical and structural properties of these wellbore elements on exposure to the gases.

Studies have also been conducted on the chemical effects of hydrogen on cement structure, whose results showed a minimal risk of chemical alteration (Reitenbach et al. 2014; Boersheim et al. 2019). However, it is unknown what the effects of exposure of cement to various concentrations of methane, hydrogen, and CO₂, as seen in hydrogen storage in depleted natural gas reservoirs, are on cement sheaths under specified pressure and temperature conditions. Some research has also been conducted on the effects of hydrogen on stainless steel and reasonable conclusions have been drawn. Stress changes such as pressure and temperature variation during well-completion operations may favor hydrogen embrittlement. The effects of a mixture of resident gases at different concentrations in these environmental conditions on the casing are also yet to be investigated.

Similarly, studies have shown that there exist some elastomer elements that are resistant to hydrogen gas damage. Also, some work has been conducted to investigate the performance and failure modes of general-purpose elastomers in high-pressure hydrogen environments. The impacts of hydrogen-methane gas blends on the physical dimensions of elastomer materials have also been investigated (Shi et al., 2020), as well as the deterioration of elastomers due to cavitation (Kane-Diallo et al., 2016; Briscoe et al., 1992; Jaravel et al., 2011). However, a gap in research exists in the effects of varied combinations of downhole gases, typically methane, hydrogen, and carbon dioxide, on elastomers' mechanical properties at different storage conditions (i.e., varied temperatures and pressures). Furthermore, the changes in structural and mechanical properties of general-purpose elastomers in gaseous hydrogen environments are not well understood.

1.3. Objectives

In this research, efforts were made to understand the behavior of general-purpose oil and gas elastomers in gaseous hydrogen environments, as seen in large-scale underground hydrogen storage (UHS) in depleted hydrocarbon reservoirs. The study is in line with the “Power-to-Gas Concept” and efforts to implement the envisioned Hydrogen Economy. Hydrogen typically exists in the presence of carbon dioxide and methane gas in depleted hydrocarbon reservoirs repurposed of UHS. More so, the recent interest in hydrogen blending with natural gas during storage or transportation as a near-term strategy for reaching a hydrogen economy further necessitates the need to investigate the effects of varied combinations of these gases on elastomer performance. The main objectives of this research are reported as follows.

1. Investigate the effects of hydrogen gas on the structural and mechanical properties of general-purpose oil and gas elastomers in UHS.

2. Investigate the effects of hydrogen-methane gas mixtures on the structural and mechanical properties of general-purpose oil and gas industry elastomers in comparison to pure hydrogen.
3. Investigate the effects of aging conditions (i.e., temperature, pressure, and time of exposure) on the mechanical and morphological characteristics of general-purpose oil and gas elastomers in UHS.
4. Investigate potential failures in general-purpose elastomers via cavitation due to exposure to gaseous hydrogen environments, as seen in UHS.

2. Literature Review

In this section, a comprehensive review of the concept of the hydrogen economy and its major components, relevant issues, and significant challenges are discussed. Also, the concept of large-scale underground hydrogen storage as a significant component of the hydrogen economy is discussed with elaborations on the various storage techniques and associated challenges. Furthermore, hydrogen storage in depleted gas reservoirs as the most common and economically feasible technology is reviewed while discussing significant well integrity challenges associated with the process.

2.1. The Hydrogen Economy

The hydrogen economy concept was introduced in the 20th Century by a famous scientist known as John Bockris as a conceptualized future energy system powered by hydrogen energy with no greenhouse gas emissions (Hardy, 2003). It is worth mentioning that the interest in and use of hydrogen as a source of energy has been in existence for some time. In the late 1800s, hydrogen was used as fuel for lamps and formed a significant component of “town gas,” which was used as a primary energy source until the advent of oil and gas (Ohi, 2005). Presently, it is mainly used in

fuel refineries and the manufacturing of fertilizers (Fan et al.,2021). It is also gaining popularity in Europe and some parts of Asia and America as a competitive fuel in the transportation sector (Ball and Marcel, 2015). Like other alternative energy sources, hydrogen has attracted global interest in the past and was pursued to make it a primary energy source for a sustainable energy system. These attempts, however, failed due to several reasons.

About four (4) decades ago, stemming from the rise in fossil fuel prices and the adverse effects they had on climate change, there became a global interest in pursuing hydrogen as a principal source of energy. This led to the creation of the International Journal of Hydrogen Energy and the formation of the International Energy Agency's Hydrogen and Fuel Cell Technology as strategic pillars for achieving this goal. Unfortunately, this vision was very ephemeral as significant quantities of petroleum resources were discovered during the same time. The abundance of these fossils led to a reduction in fuel prices and thus abating the desire for hydrogen. Similarly, in the early 1990s, several countries resorted to pursuing hydrogen energy due to critical concerns about climate change expressed by many countries. For instance, the Japanese government invested about five (5) billion Japanese yen into its World Energy Network project geared towards transforming renewable energy into a secondary form of energy (hydrogen) for usage in its major industrial sectors (Mitsugi et al.,1998; Ohira, 2004). Around the same time, The European Commission, together with Quebec, committed to extensive research into viable methods for storing hydrogen for applications in the transport sector, a project worth about thirty-three (33) million Canadian dollars (Drolet and Gretz, 2002). The period also recorded numerous cases of investments by automobile companies launching fuel cell vehicles for promoting the use of fuel cell technology. Just like the previous waves of enthusiasm for hydrogen energy, fossil fuel prices were optimal in this period, and thus the projects could not attract the much-needed support in

order to thrive. In the early 2000s, a massive resurgence in the interest in hydrogen occurred, and this was primarily fueled by the urgent need to end climate change caused by overdependence on fossil fuels. This resurgence was focused on encouraging hydrogen fuel usage in the transport sector, and thus novel policies were developed in that light. A notable one was the International Partnership for Hydrogen and Fuel Cells launched by the United States in 2003 to deploy FCV operating on hydrogen energy (Chalk and Lauren, 2004). The project did not, however, fully manifest due to the major challenges it faced with infrastructural development.

Recently, the interest in hydrogen has stirred up and has amassed a new wave of enthusiasm that has shown tremendous potential than in the past in terms of policy implementation, infrastructural development, and establishing ready markets for sustainability. In 2017, the Hydrogen Council was formed and had a number of important private sector contributors to the “New Hydrogen Economy.” Currently, it has over 50 influential stakeholders who are working towards implementing relevant policies to ensure the development of hydrogen infrastructure (Hydrogen Council, 2017). In addition, the number of countries formulating and implementing policies to ensure the promotion of the hydrogen economy for various sectors has equally risen. **Figure 5** shows hydrogen-energy deployment policies for various target sectors as of 2019.

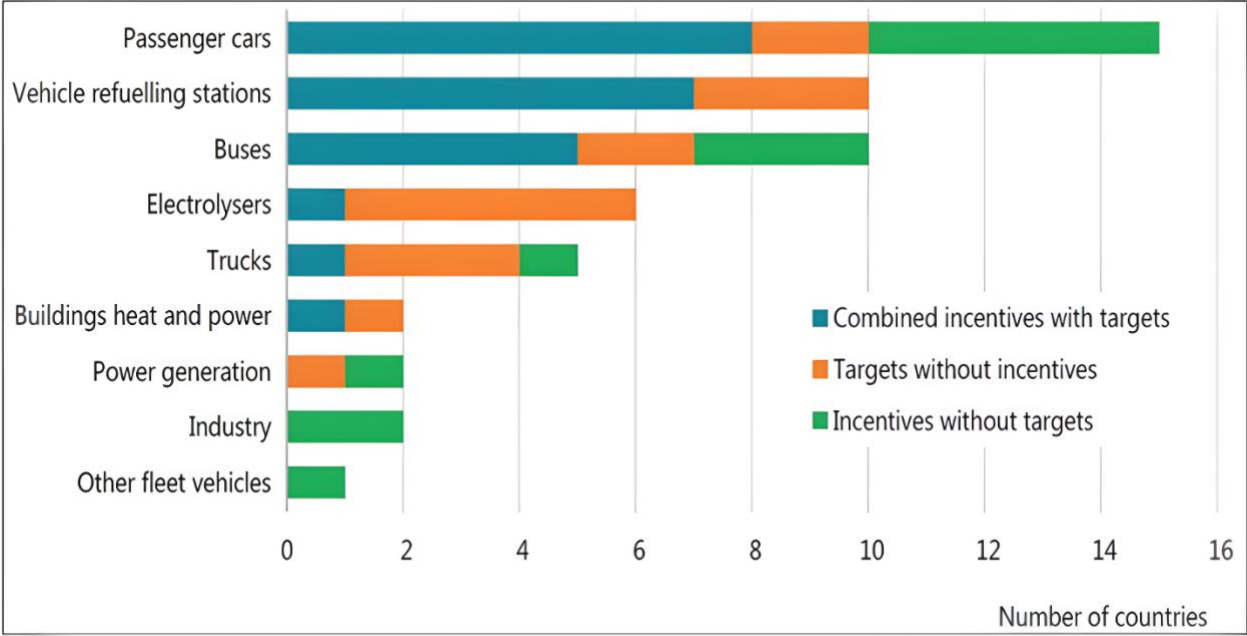


Figure 5: Global target-specific policies in support of the Deployment of Hydrogen Systems. Based on data available up to May 2019.

The hydrogen economy has some principal components, hydrogen production, distribution, storage, transportation, and utilization. These components are discussed herein, as well as some related challenges.

2.1.1. Hydrogen Production

Hydrogen production is a very important component of the hydrogen economy. Unlike fossils, hydrogen is a secondary energy carrier and is produced from other forms of energy. Thus, the production of hydrogen can be put under two broad categories: Production via electrolysis of water using renewable energy and production from fossils (Cormos, 2011). The fossil-centric hydrogen production methods include Steam Reformation, Partial Oxidation, Autothermal Reformation, hydrocarbon pyrolysis, coal gasification, plasma reformation, and thermal cracking, with the first three being the most common and industrially feasible (Kalamaras et al.,2013). Furthermore, it is worth noting that over 90% of the total industrial hydrogen production is from fossil resources,

making hydrogen production from fossil fuels the most common (Iqbal et al.,2022). The share of industrial hydrogen production based on the source material is shown in **Figure 6**. The principal hydrogen production techniques are discussed as follows.

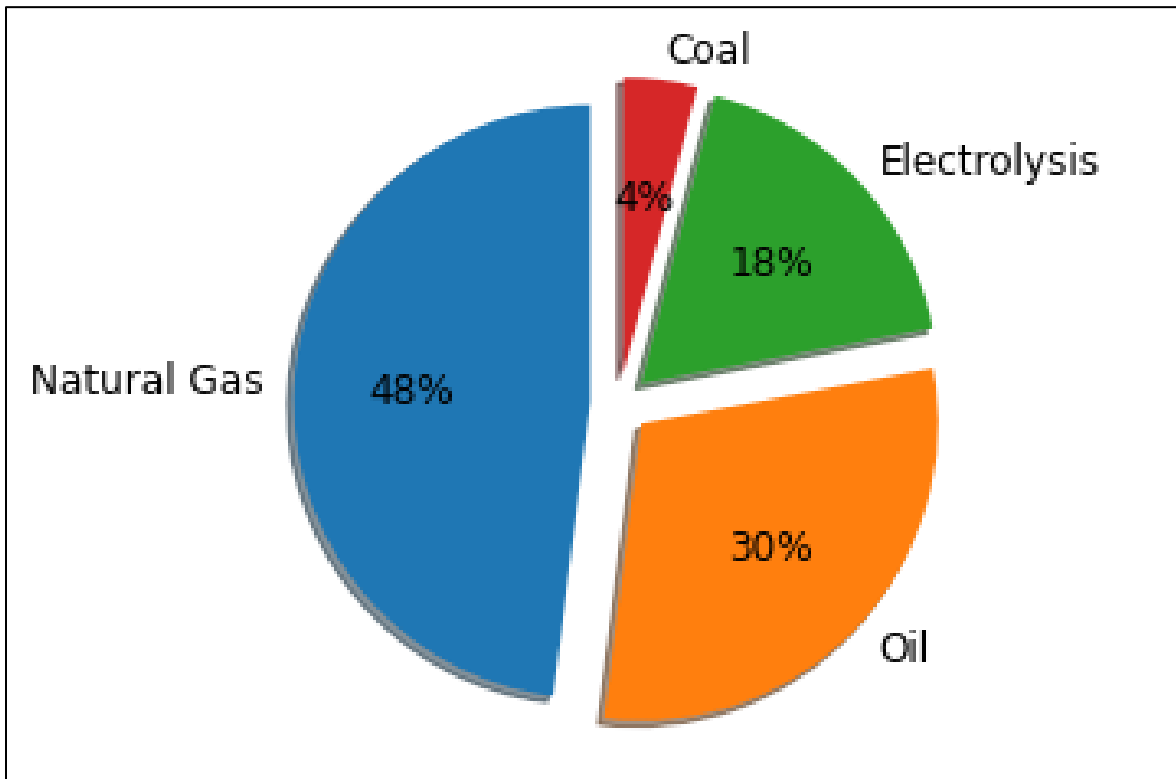


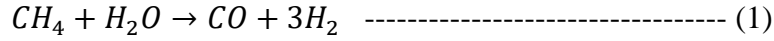
Figure 6: Share of industrial hydrogen production by source (Ewan, 2005)

2.1.1.1. Steam Reformation

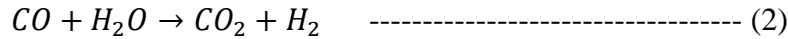
The process involves a catalytic reaction between hydrocarbons (usually methane) and steam to yield hydrogen and carbon oxides as the main products of the reaction. There are three main stages in the reformation process: syngas generation, water-gas shift (WGS) reaction, and gas purification (selective methanation) (Garbis & Jess, 2019). The first stage is an endothermic reaction process that results in syngas formation. The gas-shift reaction converts carbon monoxides into additional hydrogen and carbon dioxides as byproducts whereas the final stage involves purification of the

produced hydrogen based on the type of feedstock used. Equations (1) to (3) show the reactions involved in the steam reformation of methane.

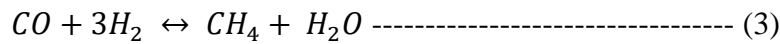
Reformation reaction



Water-gas shift reaction



Selective Methanation Reaction



2.1.1.2. *Partial Oxidation (PO)*

The process involves a catalytic exothermic reaction between methane, oxygen, and steam to produce hydrogen and carbon dioxide (Chao et al., 2008). The reactions occur at operating temperatures of about 950°C. Alternatively, a non-catalytic partial oxidation mechanism can be used, which usually occurs at temperatures between 1150°C to 1315°C (Li et al.,2018). The higher temperature in this alternative is essential to ensure complete combustion and conversion of the raw materials without the formation of sooth. In a like manner as steam reformation, PO also produces syngas which undergoes a gas-shift reaction to yield more hydrogen gas. The partial oxidation reactions are shown in equations (4) to (6).

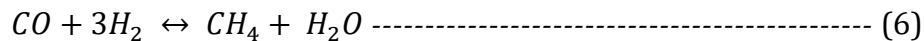
Reformation reaction



Water-gas shift reaction



Selective methanation reaction



2.1.1.3. Autothermal Reformation

In autothermal reformation, the Steam Reformation and Partial Oxidation processes are combined in a manner that the heat from PO is used in the hydrocarbon reformation process to increase the amount of hydrogen gas produced (Rabenstein and Viktor, 2008). In this method of hydrogen production, the reformation and oxidation process occur concurrently by filling the reformer with steam and oxygen. It is the most suitable reformation method for preventing the sintering and deactivation of catalysts (Balopi et al., 2022). This is because the reaction is usually neutral or slightly endothermic. It usually occurs at temperatures ranging from 950°C to 1100°C at pressures close to 10 MPa (1450.38) psi. The ATR reactor vessel is very compact and can easily be modified to produce the required quantity of hydrogen gas needed to meet hydrogen demand. Equation (7) below shows the equation for the Autothermal Reaction of methane gas. A summary of the pros and cons of the three principal hydrocarbon reformation methods for hydrogen production is shown in **Table 1**.

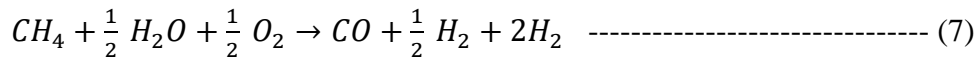


Table 1: The Advantages and Limitations of Principal Reformation Methods for Hydrogen Production (Tetteh and Salehi, 2022; Kalamaras et al.,2013; Holladay et al.,2009)

Hydrocarbon Reformation Method	Advantages	Limitations
Steam Reformation	<ul style="list-style-type: none"> • A practical approach and viable method for large-scale industrial use 	<ul style="list-style-type: none"> • High CO₂ emissions
	<ul style="list-style-type: none"> • Does not use oxygen (no oxygen supply cost) 	<ul style="list-style-type: none"> • Maintenance cost is high as energy-intensive conditions adversely impact reaction tubes and catalysts.
	<ul style="list-style-type: none"> • Higher H₂ yield due to high H₂:CO ratio compared to other reformation methods 	
	<ul style="list-style-type: none"> • Requires the lowest temperature compared to PO and ATR 	
Partial Oxidation	<ul style="list-style-type: none"> • Tolerant to sulfur (low desulfurization cost) 	<ul style="list-style-type: none"> • Low H₂ yield due to low H₂:CO ratio compared to SR.
	<ul style="list-style-type: none"> • Less energy-intensive compared to SR 	<ul style="list-style-type: none"> • Has the highest processing temperature compared to SR and ATR
	<ul style="list-style-type: none"> • Reactors are relatively smaller compared to SR 	<ul style="list-style-type: none"> • Associated with soot production, which contributes to a major challenge.
	<ul style="list-style-type: none"> • It may not require catalysts (for non-catalytic PO reaction) 	
Autothermal Reformation	<ul style="list-style-type: none"> • Does not require an external heat source. 	<ul style="list-style-type: none"> • High oxygen supply cost
	<ul style="list-style-type: none"> • The processing temperature is low compared to PO. 	<ul style="list-style-type: none"> • Limited commercial-scale experience.
	<ul style="list-style-type: none"> • Good sulfur-tolerating ability 	<ul style="list-style-type: none"> • High risk of reformer explosion
	<ul style="list-style-type: none"> • Overall efficiency is higher 	
	<ul style="list-style-type: none"> • Produces high-purity hydrogen 	

2.1.1.4. Coal Gasification

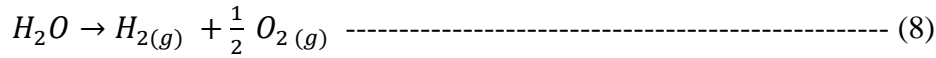
The gasification process involves the use of carbon-based feedstock such as coal, petroleum coke and biomass to produce essential commodities to meet market needs (Midilli et al.,2021). In hydrogen production, coal is the primary feedstock used in the gasification process. In the reaction process, a mixture of coal, oxygen and steam are reacted at temperatures greater than 1400°C (2552

°F) and pressures ranging from 20-70 MPa (~2900 – 10153 psi) through coal devolatilization (Stiegel et al., 2006; Higman et al., 2008). The reaction produces syngas, which chiefly consists of hydrogen and carbon monoxide and CO₂ as a by-product. In a like manner as SR, PO, and AR, the syngas produced are transferred to a water-gas shift reactor to produce more hydrogen gas. The gasification of coal to produce hydrogen is efficient, and its negative impacts on the environment are minimal. Another important aspect of this method is its easy adaptability for use in carbon capture and storage, as seen in blue hydrogen production plants (Lin et al., 2002; Stiegel et al., 2006; Ratafia-Brown et al., 2002).

2.1.1.5. Water Electrolysis

The electrolytic process of hydrogen production involves the passing of direct current through water, resulting in its breakdown into its elemental components. i.e., hydrogen and oxygen gas (Rashid et al., 2015; Ursua et al., 2011). The technology has been in existence for several years and has gained much industrial interest in recent years due to the global desire for hydrogen energy. Electrolysis occurs in a device known as the electrolyzer, which consists of electrodes (i.e., an anode and cathode) (Zoulias et al., 2004). The electric current in an electrolytic process flows between the separated electrodes, which are immersed in an electrolyte to increase electric conductivity. The electrodes used must exhibit good electrical conductivity, resist corrosion, demonstrate good structural integrity, and be suitable catalysts (Yu et al., 2019). Another critical component of the electrolyzer is a diaphragm that prevents the recombination of the separated hydrogen and oxygen molecules and short-circuiting the electrodes. Similar to electrodes, diaphragms also require high physical and chemical stability. The process of hydrogen production is as follows; first, at the electrode surfaces, electrons are either generated or taken in creating a multi-phase gas-solid liquid system. Two specific reactions occur: a reduction half-reaction and an oxidation half-reaction. The former occurs at the cathode, which is negatively polarized due to

the flow of electrons from the outside region of the circuit. The latter half-reaction occurs at the anode, where electrons leaving it causes it to become positively charged. This results in the production of hydrogen at the cathode and oxygen at the cathode. The electrolytic reaction is shown in equation (8).



The electrolysis process can be put under three main categories based on the type of electrolyte and the temperature at which the reaction occurs, namely, Alkaline water electrolysis (as seen in alkaline electrolyzers with sodium hydroxide (NaOH), potassium hydroxide (KOH), or hydrogen sulfate (H₂SO₄) as electrolytic material), polymer electrolyte membrane electrolysis and solid oxide electrolyte electrolysis (Gallandat et al., 2017). The latest usually occurs at high temperatures (Brisse et al., 2008). It is worth noting that electrolysis is a thermodynamic process that converts electrical and thermal energy to chemical energy, as seen in the hydrogen produced. The thermodynamic equation for the electrolytic process is shown in equation (9). The electricity for the electrolytic process can be harnessed from varied sources; Wind energy can be converted to electricity for use by electrolyzers to produce hydrogen. Photocatalytic splitting and photoelectrolysis are processes that use energy from the sun to split water into hydrogen and oxygen (Scott, 2019). Nuclear energy can also be used in thermochemical processes to drive a series of chemical reactions to generate hydrogen in a closed-loop system where the chemicals can be reused (El-Emam et al., 2020). **Figure 7** shows the water electrolytic process using energy from renewable sources.

$$\Delta G = \Delta H - Q = \Delta H - T \cdot \Delta S \quad \text{----- (9) (Ursua et al., 2011)}$$

$\Delta H =$ Enthalpy change of the process

$\Delta G =$ Gibbs free energy change

$Q =$ Thermal energy

$T =$ Process temperature

$\Delta S =$ Entropy change

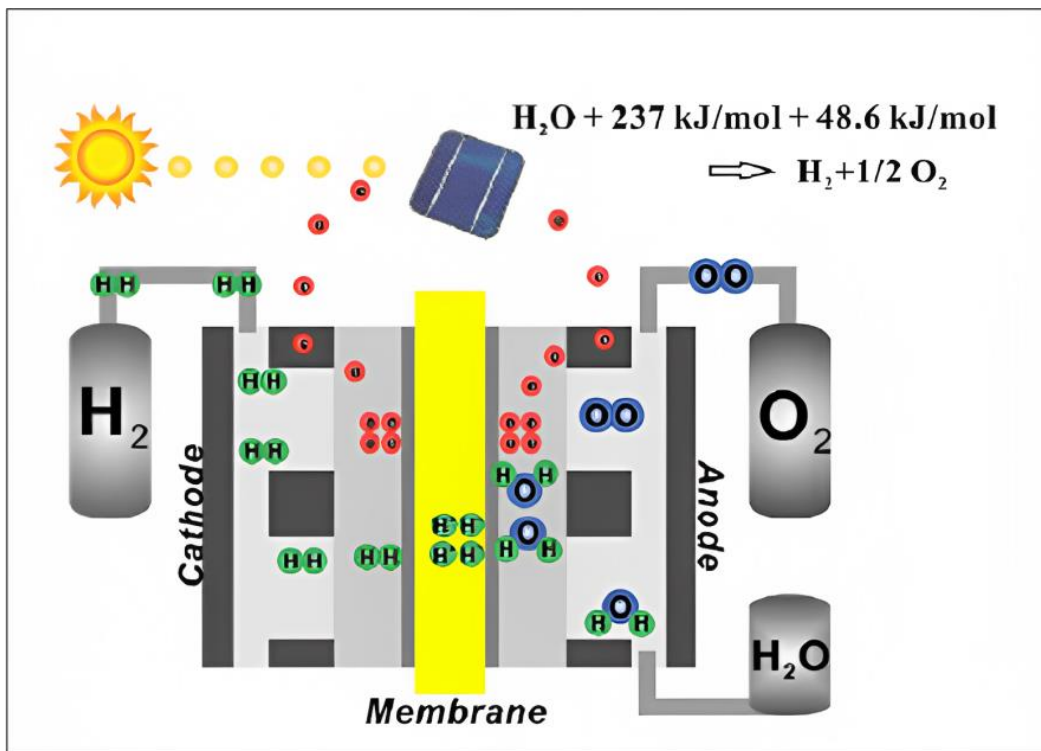


Figure 7: Hydrogen production via Electrolysis using Renewable Energy (Chi et al.,2018)

2.1.1.6. The Colors of Hydrogen

Hydrogen can be categorized as brown, black, grey, blue, turquoise, pink, yellow, or green. This classification is based on the type of technology, raw materials, source of energy, and environmental emissions associated with the production process (Hermesmann and Muller, 2022; Ajanovic, 2022). Brown and black hydrogen are produced via coal gasification, where CO₂ and

CO are produced as by-products (Panić et al.,2022). The term brown hydrogen is used when lignite coals are used in hydrogen production, whereas black is used for bituminous coals, which produce more carbon. On the one hand, when hydrogen is produced from natural gas without carbon capture, and storage (CCS), it is referred to as gray hydrogen (Ehlig-Economides et al.,2021).

On the other hand, blue hydrogen is used when natural gas is the raw material used in hydrogen production but is associated with carbon capture and storage. Blue hydrogen has become of great interest amongst stakeholders in the hydrogen energy industry due to the tremendous potential of becoming a competitive clean energy alternative for the near-to-mid-term energy transition (Howarth et al., 2021). Hitherto, there is no exact quantification of the carbon that needs to be captured and stored in the blue hydrogen production process. However, the recorded values in most implemented projects, as seen in the literature, range between 85% and 95% (IRENA, 2020). Similar to blue hydrogen is turquoise hydrogen (Hermesmann and Muller, 2022; Finckle, 2002). Here, hydrogen is mainly produced via methane pyrolysis with the associated production of solid carbon-based material; thus, gaseous CO₂ emissions are significantly reduced. Regarded as an ideal candidate for the hydrogen economy is Green Hydrogen (Dincer, 2012). It involves the production of hydrogen from renewable resources like water and biomass using energy from renewable sources, and thus, there are no emissions associated with the hydrogen production chain. Commonly, Green hydrogen is produced via electrolysis of water using renewable energies like solar and wind energy.

In some cases, it is produced via biomass gasification using routes associated with no greenhouse gas emissions. Pink hydrogen is hydrogen produced via electrolysis using nuclear energy (Seyed, 2022). In cases where the energy used in the electrolytic process is from a mixture of different sources (both renewable and non-renewable) as and when they become available, the hydrogen

produced is referred to as yellow hydrogen. **Figure 8** gives a summary of the color-code classification of hydrogen.

Colors	Energy Source	Process	Energy Description
Green	Solar energy Wind energy	Electrolysis of water	Renewable Energy Carbon Neutral
Blue	Methane	SMR, POx or ATR with CCS	Non-renewable Carbon Neutral
Yellow	Mixture (renewable/ non-renewable)	Electrolysis of water	Renewable Energy Carbon Neutral
Turquoise	Methane	Pyrolysis	Non-renewable Can be retrofitted with CCS plant for carbon neutrality
Black	Anthracite and Bituminous Coals	Coal Gasification	Non-renewable Carbon Neutral
Grey	Methane	SMR, POx or ATR	Non-renewable Produces CO ₂
Brown	Lignite Coal	Coal Gasification	Non-renewable Can be retrofitted with CCS plant for carbon neutrality
Purple	Nuclear Energy	Electrolysis of water	Alternative Energy Carbon Neutral
Pink	Nuclear Energy	Electrolysis of water	Alternative Energy Carbon Neutral

Figure 8: The Colors of Hydrogen (Tetteh and Salehi, 2023)

2.1.2. Hydrogen Transportation and Distribution

Produced hydrogen needs to be safely and efficiently transported to end users. Distribution of hydrogen from the site of manufacture to end-users is uniquely plagued with enormous challenges, chiefly on safety and cost. These challenges are mainly due to the properties of hydrogen. i.e., high diffusivity, extremely low density as a fluid, and high range of flammability compared to hydrocarbons (Rigas and Amyotte, 2013; Lanz et al.,2001). Enormous infrastructure is required to transport and dispense hydrogen as a fuel for automobiles or stationary usage, irrespective of its production methods (Morgan, 2006). At present, hydrogen is transported and distributed from

production sites to end-use locations via a local network of pipelines, pressurized gas in large cylinders usually made of steel at pressures of about 180-200 bar (2611- 2901psi), or as liquefied hydrogen under cryogenic conditions (i.e., extremely low temperatures) (Edwards et al.,2007). These methods are employed due to hydrogen's low volumetric energy density. Liquid hydrogen distribution is usually employed when large volumes of hydrogen need to be distributed in the absence of pipelines.

Tankers and compressed gas usually transport liquid hydrogen by tube trailers. Hydrogen can also be transported using rails or barges. For Fuel Cell Vehicles, hydrogen is delivered like gasoline to cars with internal combustion engines at a refueling station. Current transportation and distribution methods are costly, contributing to the overall unit cost of hydrogen, and posing another major hurdle in reaching a hydrogen economy. Hydrogen transportation as compressed gas through pipelines is only cost-efficient over short distances due to the high energy requirements involved in the process (Morgan, 2006). Key hurdles in hydrogen delivery and transportation include reducing the cost of delivery, improving energy efficiency in delivery, and maintaining hydrogen purity levels during transport while ensuring the maintenance of safety protocols in the entire delivery process (e.g., reducing hydrogen leakages). New methods and technologies that mitigate delivery costs while maintaining high safety levels need to be developed. This includes but is not limited to developing cheaper compressors, sensors, controls, and hydrogen refueling infrastructure (i.e., filling stations). In an ideal hydrogen economy, long-term hydrogen delivery should involve a complex network of pipelines linking localized production facilities with filling stations and end-users.

2.1.3. Hydrogen Storage

Hydrogen storage is one of the “hot topics” in transitioning into a hydrogen economy. The concept is vast, crucial, and plagued with significant challenges and hurdles. As a result, the concept is highly researched (Sharma and Ghoshal, 2015). The techniques and technologies used in hydrogen storage depend on factors ranging from the volume required in storage, the storage period, the cost, the needed phase of the gas, and the intended usage (Noussan et al., 2020). Storage options include storage at refueling stations, onboard vehicles, and storage at ports for some time after being supplied by ships and barges and large-scale geological storage.

On the one hand, hydrogen storage for the transportation or mobile industry has rigid storage requirements (Edwards et al., 2007). On the other hand, there are no stringent restrictions on the stationary storage of hydrogen besides the fact that it is usually affected at higher temperatures and pressures. Issues associated with these storage applications are mainly due to the type of materials used. Hydrogen storage techniques in this context include compressed hydrogen gas storage, cryogenic liquid hydrogen storage, liquid carrier-based storage, and storage in solid materials (i.e., metal hydrides, chemical hydrides, and carbon-based materials) (Al-Hallaj et al., 2011).

An average light-duty vehicle consumes about 24kg (6.34 gal) of petroleum, covering a mileage of about 400km. To cover the same distance, a hydrogen fuel cell vehicle requires four (4) kilograms of hydrogen. Fuel cell vehicles' onboard storage media, amongst other characteristics, must store this much hydrogen to compete with gasoline-based internal combustion engines. Also, to meet the envisaged hydrogen economy requirements, a fuel cell vehicle onboard storage material must be a highly secure, lightweight, inexpensive, and compact medium (Rivard et al., 2019). Besides, it should have fast kinetics in absorbing and releasing hydrogen, multicycle reversibility in this hydrogen uptake and release (over 500 cycles), low operating pressure

conditions, and high values for gravimetric (% weight of hydrogen per unit weight of storage material) and volumetric (weight of hydrogen per unit volume of storage material) densities. i.e., a gravimetric density of not less than 9% per weight of hydrogen and a volumetric hydrogen density greater than 70g/L (Edwards et al., 2007). At present, none of the hydrogen storage methods can meet all the above-mentioned criteria.

Large-scale underground hydrogen storage is a crucial aspect of hydrogen storage, given its role in ensuring sustainability in the envisioned hydrogen economy. Furthermore, it forms a crucial aspect of this study. The ensuing sessions present a thorough review of large-scale underground techniques, focusing on storage in depleted hydrocarbon reservoirs. Furthermore, the concept of well integrity in UHS in these storage facilities and associated challenges will be discussed. Finally, a thorough exegesis of commonly used elastomers in the oil and gas industry, their functions, as seen in wellbore seal elements, previous works conducted on their performance, and knowledge gaps existing on their fitness for use in UHS in depleted gas reservoirs will be presented.

2.2. Large-Scale Underground Hydrogen Storage

2.2.1. Underground Gas Storage

Gases are stored on a large scale in underground geological structures for several purposes. These may include storage for later use in energy or power generation or as a means of reducing greenhouse gas emissions. In the case of the former, gases are usually stored during periods of high supply for later strategic withdrawal and utilization based on a certain market and commercial factors. This ensures the provision of utility and industrial services without any form of interruption as well as favorable commodity pricing.

In the United States, a constant, uninterrupted supply of energy is vital for the sustainability of the nation's economy (All Consulting LLC, 2016). As of 2016, natural gas contributed a share of 29% of the total US energy requirements and is currently experiencing a significant rise in demand. Given the importance of natural gas in the US energy mix, geological storage of natural gas is crucial to ensure a cushion between a relatively constant natural gas supply and variations in its demand. Hence, this results in reasonable stable natural gas prices regardless of the season (i.e., whether there is peak supply or disruptions in supply). The maiden underground gas storage project was established in Ontario, Canada, in 1915 (Evans, 2009). The facility stored chiefly natural gas. In the ensuing year, the United States established its first underground gas storage project in Buffalo, New York. It is hitherto the longest-operating gas storage project in the US (Knepper, 1997; Schultz and Evans, 2020).

Furthermore, by 1930, nine gas storage projects existed in the United States, spanning six states, as shown in **Figure 9**. Besides natural gas (mainly consisting of CH_4), other gases that are recently stored on a large scale in underground geological formations include carbon dioxide (CO_2), Hydrogen (H_2), and Helium (He). Storage of gas on a large scale for energy facilitates its integration into the energy mix (Gabielli et al., 2020), increases energy security (Azuni and Breyer, 2018), and ensures more efficient management of the energy network (Blanco et al., 2018). Underground gas storage is usually characterized by several volumetric measures that distinguish between the properties of the storage facilities and the fluid (Folga et al., 2016). The total gas capacity is the maximum volume of gas that can be stored in a storage facility based on its design. Total gas in storage is the volume of gas in the storage facility at a given time. In contrast, the base or cushion gas refers to the gas in the storage reservoir required to maintain adequate pressure and deliverability. In addition, the native and working gas is the gas present in the reservoir formation

before the commencement of the gas injection process and the volume of gas available for the market, respectively (Katz et al., 1981; Kanaani et al.,2022).

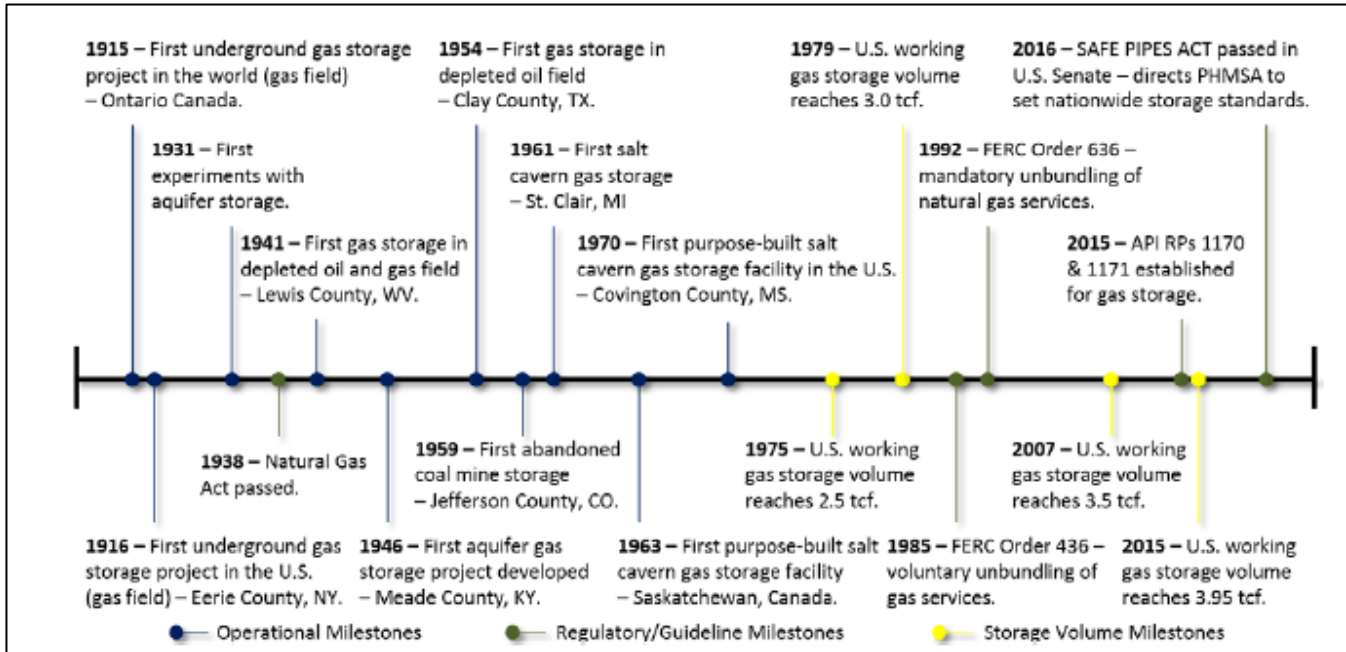


Figure 9: The Timeline of Underground Gas Storage in the United States (All Consulting LLC, 2016)

2.2.1.1. Underground Hydrogen Storage

As previously discussed, the primary techniques employed in underground gas storage are depleted oil and gas reservoirs, aquifers, and salt caverns (**Figure 10**). The concepts, advantages, and limitations of these techniques in relation to UHS are discussed.

Depleted oil and gas reservoirs are the most predominant underground gas storage facilities in the United States, with over 300 currently in operation (All Consulting LLC, 2016). According to a report by the Energy Information Administration (EIA) in 2001, these facilities contributed about 86% of the total underground gas storage in the United States. They were the most prominent, easiest to operate, and most economically feasible compared to the other gas storage techniques (**Figure 11**) (FERC, 2004). In a more recent report by CEDIGAZ INSIGHTS in 2017, 73% of the

total gas storage sites in the world are depleted oil and gas field facilities contributing about 80% of the total working gas capacity (**Figure 12**) (Carnot-Gandolphe, 2018). Gas storage in depleted hydrocarbon reservoirs involves injecting gases into reservoir formations (All Consulting LLC, 2016). Subsequently, the injected gas spreads out underneath the impervious seal after displacing the in-situ pore fluid, usually a sodium chloride (NaCl) solution (Heinemann et al., 2018). The gas is then reproduced during periods when it is needed.

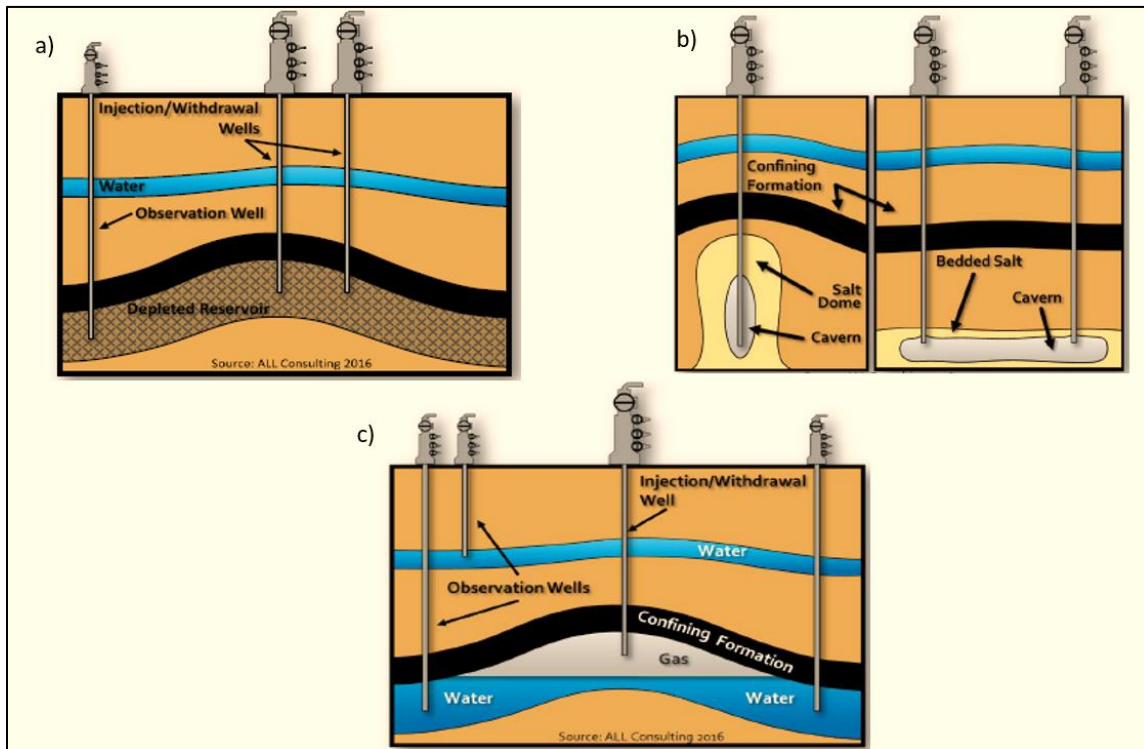


Figure 10: Underground Hydrogen storage techniques; (a) Depleted hydrocarbon reservoirs; (b) Salt caverns (c) Aquifers (All Consulting, 2016)

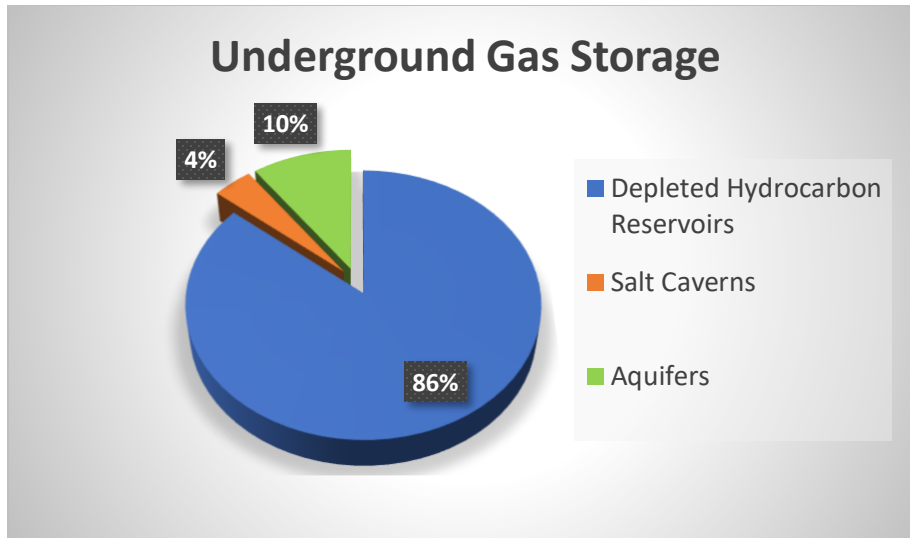


Figure 11: Underground gas storage by type (Adapted and modified from FERC, 2004)

Furthermore, it is the most cost-effective gas storage technique in the United States mainly due to readily available infrastructure (i.e., wells and pipelines) and subsurface installations necessary for its implementation. Also, the cushion gas injection requirement is minimal as depleted gas reservoirs tend to have a certain amount of gas already existing in the formation. In addition, the cost of reservoir characterization for geological storage of gases in depleted hydrocarbon reservoirs is usually low as there is usually existing data from the previous characterization of the formation from the production of hydrocarbons. These formations have proven integrity as some gas has been contained in them for several years.

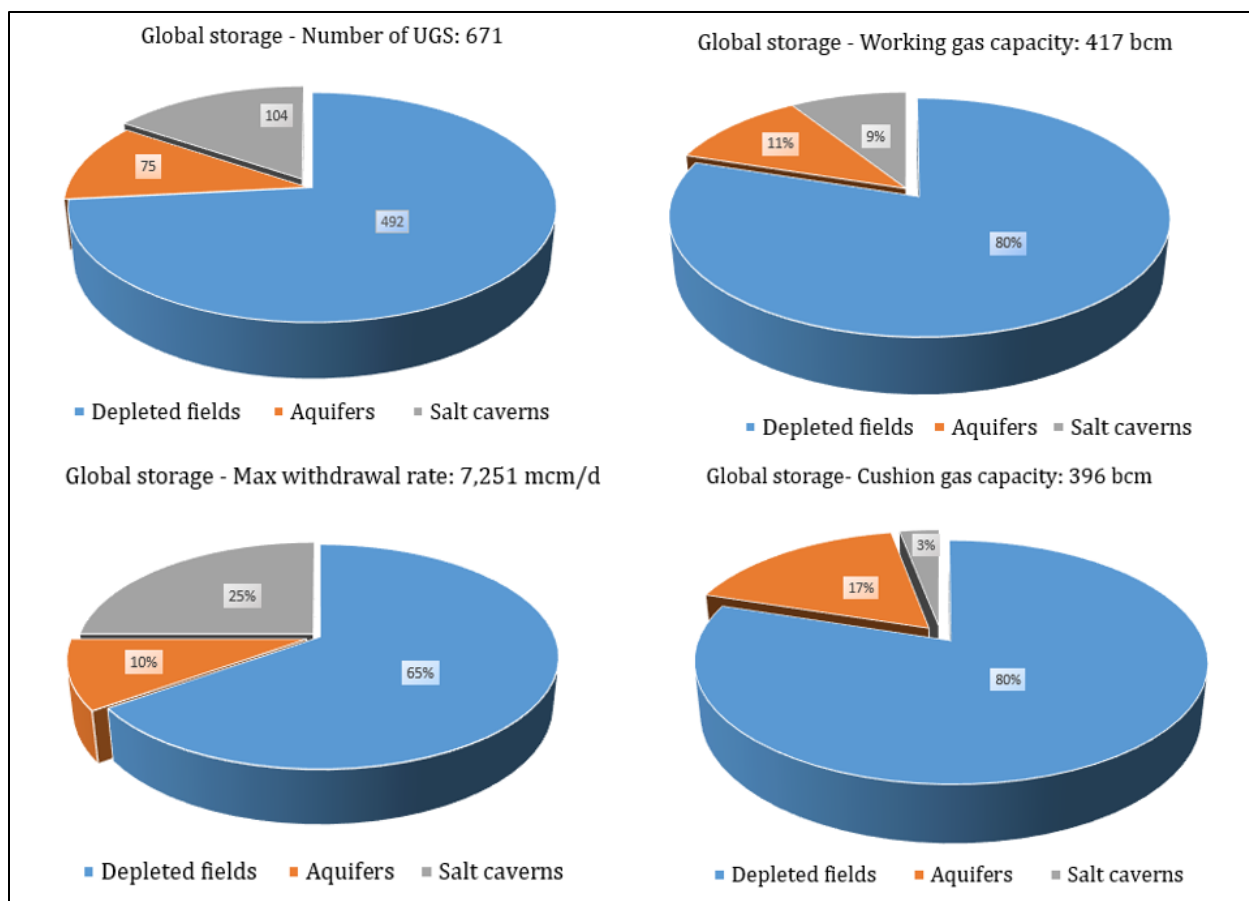


Figure 12: Global Outlook of Underground Gas Storage at the end of 2017 (Carnot-Gandolphe, 2018)

Depleted oil reservoirs are not ideal for hydrogen gas storage as hydrogen may diffuse and react with residual oil to produce other substances leading to a complete loss of hydrogen. As a result, depleted gas reservoirs are preferable. Besides the requirements of the primary reservoir and geological conditions that need to be met before underground hydrogen storage, additional requirements for practical storage of hydrogen gas in depleted gas reservoirs include sufficiently compressing and controlling the gas. This is done while ensuring that the gas pressure is kept within the limits of the hydraulic and overburden pressure gradients. For new reservoirs with no history of gas storage, the integrity of the caprock and the expected injection pressure must be thoroughly examined to ensure adequate pressure and reservoir tightness before beginning the storage program (Reitenbach et al.,2015). This is essential in preventing leakage problems in UHS.

When the reservoir has been formerly used for natural gas storage, leakage problems may be minimal. The operation of depleted gas reservoirs is typically associated with prolonged cycles, usually, an injection period ranging from 200-250 days and a withdrawal period ranging from 100-150 days (Ahmadpour, 2022).

Aquifers are similar to depleted gas reservoirs in terms of gas storage and operations, although they are more expensive to deploy due to infrastructural and cushion gas requirements (Zamehrian and Sedaee, 2022). Analogous to depleted gas reservoirs, they have long cycle periods; however, their deliverability could be much higher (Xiao et al., 2006). The process involves hydrogen storage in geological formations where gas confinement is achieved with a water-bearing rock called an aquifer. Unlike depleted gas reservoirs, a thorough geophysical exploration program is required to validate the suitability of the geological resource for hydrogen storage. This is essential in determining the storage capacity and the properties of the flow (Bunger et al., 2016). Compared to hydrogen storage in salt caverns, aquifer storage may result in chemical reactions between reservoir rock minerals, in-situ fluids, or micro-organisms with hydrogen gas, making it a more challenging option. The reactions may reduce the total hydrogen gas in storage or cause the closure of the pore spaces, adversely impacting deliverability. The process is usually associated with high capital expenditures, stemming from the need to drill new wells for injection, withdrawal, and observational purposes (Singh, 2010). Also, the cushion gas requirement for aquifer storage is about 80% of the total gas volume, as no initial native gas is present (Raad et al., 2020). Also, unlike depleted natural gas reservoirs, extraction of these cushion gas in aquifers is accompanied by significant adverse effects, the principal of which is damage to the formation.

Salt caverns are also renowned for being one of the primary techniques for UHS. Their fundamental principle of operation is significantly different from that of depleted gas reservoirs

and aquifers. In this technique, gas is stored in an empty void created by injecting fresh water at high pressures into large salt domes, forming large cavities for gas storage (Peng et al.,2023; Warren and Warren, 2016). This is known as the solution mining process and produces large quantities of brine that need to be disposed of in an eco-friendly way (Bunger et al., 2016). Although the technique is recently gaining much recognition in some parts of Europe and Asia, it is nonetheless an expensive alternative (Karakilcik et al., 2016). The high capital expenditure results from high mining and disposal, infrastructural development, and geological formation characterization costs. The technique is also ideal for gas storage when short-to-medium-term gas demand fluctuations occur. It allows several injection and production periods annually and has rapid production rates and a high rate of deliverability (Heinemann et al., 2021). This is mainly because the technique does not involve gas storage in pore spaces; hence there is no gas travel within pores during injection and withdrawal. Despite this high rate of deliverability, it is incumbent to stay within the allowable pressure-time gradient limits (1MPa/day) during operations, as exceeding this limit can damage the integrity of the cavern walls. The cushion gas requirement for this hydrogen storage alternative is also lower compared to aquifers and depleted gas reservoirs (Caglayan et al.,2020). It has, over the years, proven to be a good alternative for hydrogen storage due to the visco-elastic properties of rock salts, making it very tight to the gas (i.e., has very minimal to no permeability to hydrogen gas).

Furthermore, there is usually no reaction between rock salts and hydrogen gas. This characteristic of salt caverns makes it renowned for underground hydrogen storage. In the United States, natural gas storage in salt caverns contributes 10% of the total underground gas storage (FERC, 2004). Hydrogen has been stored at Teeside (UK) for over 30 years and on the United States Gulf Coast.

Large-scale underground storage of hydrogen is a new technology. Although lessons learned from the underground storage of natural gas are useful in its applications, it is still associated with some challenges and shortcomings peculiar to it. According to a report by the Sandia National Laboratories in 2011, three known hydrogen storage locations presently have been identified worldwide and are all salt cavern storage facilities (Kobos et al., 2011). Two of these hydrogen storage facilities are in Texas and are operated by ConocoPhillips and Praxair (Kobos et al., 2011, Leighty, 2008). The third is in the United Kingdom, operated and managed by Sabic Petrochemicals (Kobos et al., 2011; Crotagino., 2008; Panfilov., 2006). **Table 2** summarizes some known salt cavern hydrogen storage sites globally and their associated properties.

Table 2: Global Locations of Underground Hydrogen Storage Sites in Salt Caverns (Zivar et al.,2021; Tarkowski and Uliasz-Misiak, 2022; Tarkowski, 2019; Panfilov et al.,2006)

Characteristics	Teesside (UK)	Clemens (US)	Moss Bluff (US)	Spindletop (US)
Year Commissioned	1972	1983	2007	2014
Geology	Salt bed	Salt dome	Salt dome	Salt dome
% H ₂ stored	95% H ₂ , 3-4% CO ₂	95% H ₂	95% H ₂	95% H ₂
Volume (m ³)	3 X 70000	580000	566000	>580000
Depth (m)	350	930	820	-
Pressure (bar)	45	70-135	55-152	-
The energy of the stored H ₂ [GWh]	25	92	120	>120

Also, several regions worldwide have shown excellent potential for UHS using some or all discussed techniques. The choice of storage technique usually depends on several factors, including techno-economic constraints, geologic formation availability, and governmental policies. Despite some associated technological challenges in the United States, potential areas for applying all three primary gas storage techniques have been identified, as shown in **Figure 13**. In 2014, the European Union completed research on the potential for large-scale hydrogen storage in

salt caverns in Europe under the HyUnder project (Correas, 2013). In the same vein, similar projects like the H2STORE, InSpEE, and HyINTEGER have accessed and evaluated issues associated with hydrogen storage and utilization (Pudlo et al., 2013; Donadei et al., 2015; Rudolph, 2019). Due to the availability of large salt deposits, formations, and caverns, cavern hydrogen storage on a large scale has shown enormous potential in Europe. Germany and the Netherlands have substantial salt deposits in their northern regions, while France has most of its salt formations in the southeastern regions. Identified along the Mediterranean coasts of Spain are also large salt deposits with good potential for UHS. The identified salt formations in Europe with the potential for large-scale underground hydrogen storage are shown in **Figure 14**. Zivar et al. (Zivar et al., 2021) provided a comprehensive summary of some potential global sites for large-scale underground hydrogen storage, as shown in **Table 3**. Furthermore, the advantages and limitations of each gas storage technique are summarized in **Table 4** below.

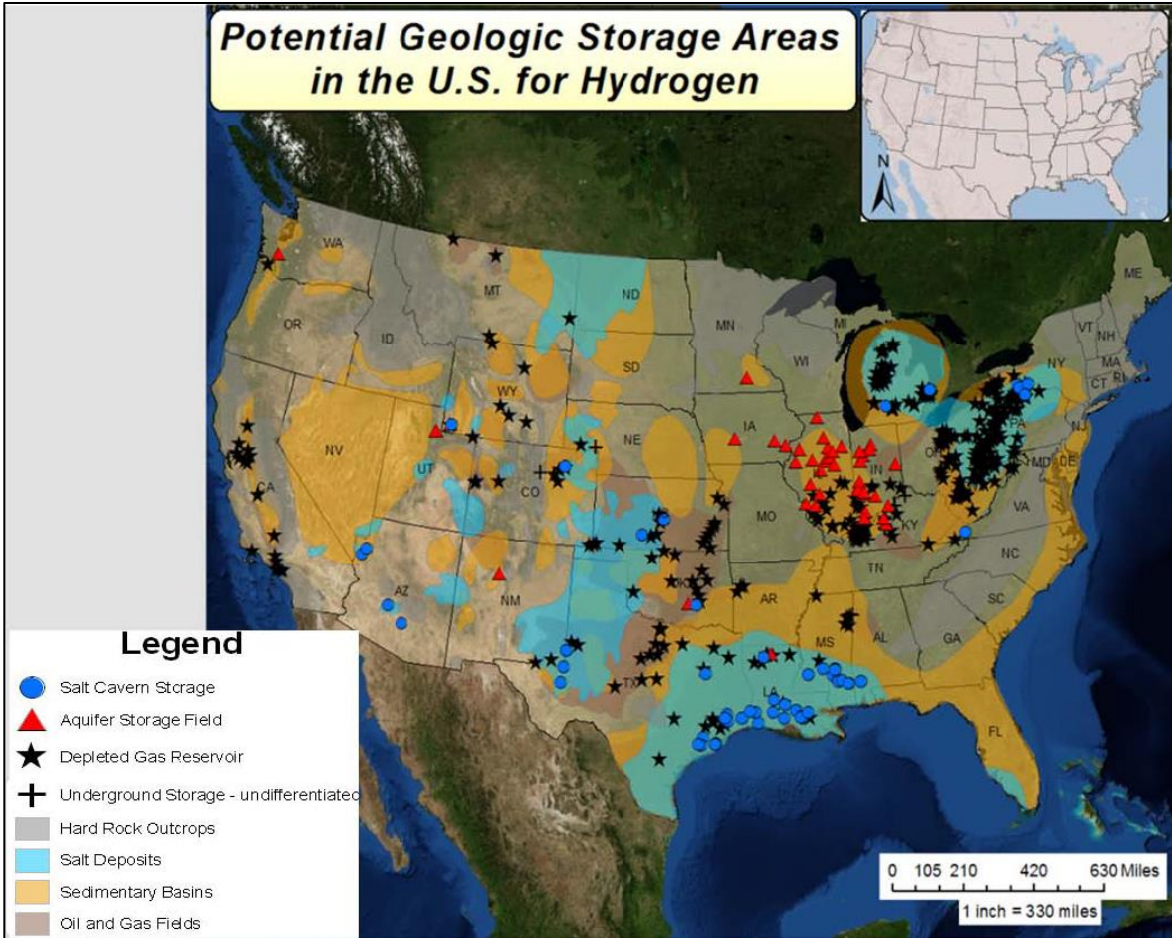


Figure 13: Map of United States Geological Structures with Potentials for Underground Hydrogen Storage (Kobos et al., 2011)

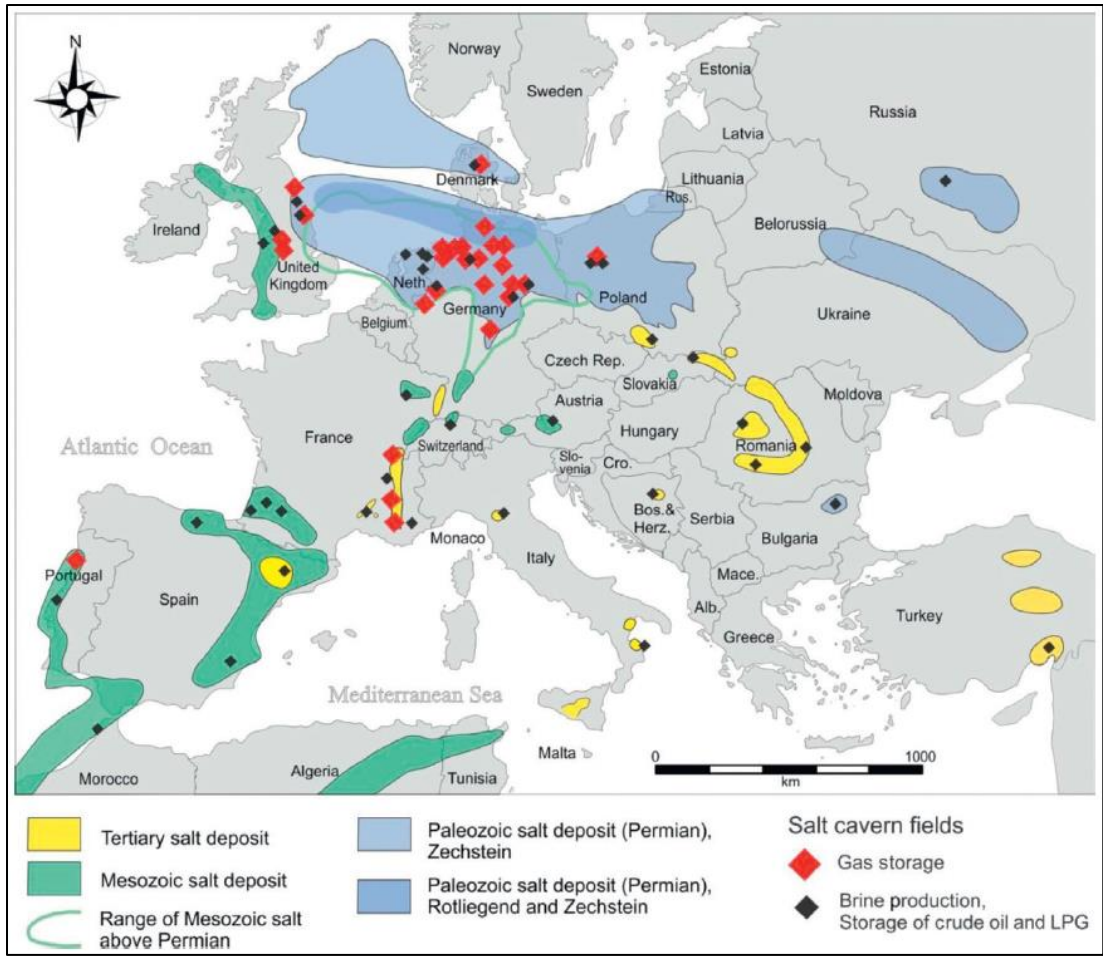


Figure 14: Map of Salt Caverns and Formations in Europe (Bunger et al., 2016)

Table 3: Worldwide Potential Hydrogen Storage sites

Location	Storage type	Properties	References
<ul style="list-style-type: none"> San Pedro belt, Spain 	Saline aquifer	Porosity (ϕ) = 0.2 Permeability (k) = 100mD	Sainz-Garcia et al.,2017
<ul style="list-style-type: none"> Rough gas storage facility, UK 	Depleted natural gas reservoir	Capacity= 48 million m ³ ϕ = 0.2 k= 75mD Depth = 2743m Pressure = 50 - 100 bar Period= 120 days	Amid et al.,2016
<ul style="list-style-type: none"> Ocna Mures Targu Ocna Ocnele Mari Cacica 	Salt Cavern	Not reported	
<ul style="list-style-type: none"> Romania Northern Nordrhein Westfalen Northwest Germany Central Germany 	Salt Cavern	Capacities= <ul style="list-style-type: none"> 2.4 billion m³ 4.6 billion m³ 1.8 billion m³ 	Lordache et al.,2014 Michalski et al., 2017
Salina B and A2, Ontario Canada	Saline aquifer	B- Depth= 400m Thickness = 90m Capacity = 6.4 million m ³ A2- Depth= 525m Thickness= up to 45m Capacity = 9.5 million m ³	Lemieux et al.,2019
Mount Simon aquifer, Ontario, Canada	Saline aquifer	Depth = 800m ϕ = 5-15% Pressure = 76 bar (~1102psi) Salinity= 100k- 300k mg/l Capacity= 725 million tons of CO ₂	Lemieux et al.,2019
Midland Valley, UK	Oil reservoir	k= 60-80mD Thickness 100-1000m	Heinemann et al.,2018
<ul style="list-style-type: none"> Rogozno Damaslawek Lanieta Lubien Goleniow Izbica Kujawska 	Salt Cavern	Not reported	

<ul style="list-style-type: none"> • Debina 			
<ul style="list-style-type: none"> • Gora Region, Poland 	Salt structure	Not reported	Tarkowski and Czapowski, 2018 Lewandowska-Smierchalska et al.,2018
<ul style="list-style-type: none"> • Chabowo T, Poland 	Aquifer	Not reported	Lewandowska-Smierchalska et al.,2018
<ul style="list-style-type: none"> • Przemysl, Poland 	Natural gas field	Not reported	Lewandowska-Smierchalska et al.,2018

Table 4: Advantages and Limitations of Principal Gas Storage Techniques (All Consulting LLC, 2016; Bungler et al., 2016; FERC, 2004; Kobos et al., 2011; Crotingo, 2010; Evans 2007)

Hydrogen Storage Technique	Advantages	Limitations
Depleted Hydrocarbon Reservoirs	<ul style="list-style-type: none"> • Most predominant gas storage technique • Cost-effective and economically attractive • Minimal cushion gas requirement • Proven integrity of storage formations 	<ul style="list-style-type: none"> • Operations are associated with prolonged cycles. (200-250 days of injection; 100-150 days of withdrawal). Thus, favorable for balancing seasonal fluctuations in demand. • Possess a gas leakage risk factor and can result in costly hydrogen contamination challenges. • Possible reaction between stored hydrogen, rock minerals, micro-organisms, and in-situ fluids.
Salt Caverns	<ul style="list-style-type: none"> • Suitable for regions where there is a short-to-medium term gas demand fluctuation. • Good sealing abilities due to self-healing property. • Low cushion gas requirements. • Gas-tight with theoretical leakage rates of 0.01% per annum. • Very little to no mineralogical and microbial reactions with hydrogen 	<ul style="list-style-type: none"> • Expensive technique compared to depleted gas reservoirs. • Limited by permissible pressure gradients during injection and withdrawal cycles (maximum allowable: 1MPa/day). • Limitations on shape and height of salt domes for storage due to stability requirements. • The challenge of cavern convergence with time due to salt creep

<p>Aquifer</p>	<ul style="list-style-type: none"> • May have higher deliverability despite prolonged cycles. • Allows for several injection and production periods annually. 	<ul style="list-style-type: none"> • More expensive to deploy due to cushion gas and infrastructural requirements. (i.e., cost of drilling new wells. etc.) • High cost associated with thorough geophysical exploration and reservoir characterization. • Challenges associated with in-situ reactions within storage formations (i.e., reaction with rock minerals, fluids, and micro-organisms). • Reduction in volume of hydrogen due to in-situ reactions. • High cushion gas requirements. • Higher injection pressure requirements compared to depleted reservoirs
----------------	---	---

2.2.2. Hydrogen Blending with Natural Gas

A concept of interest with the recent wave of enthusiasm for hydrogen energy is the blending of H₂ gas with methane, given its numerous identified benefits in heat and power generation (Kong et al., 2021; Melaina et al., 2013). Also, recent studies have indicated that hydrogen mixtures with compressed natural gas (CNG) in internal combustion engines have benefits, including an increase in thermal efficiencies, an increase in combustion performance, a decrease in time of combustion, and a reduction in carbon dioxide and other pollutant emissions (Chugh et al.,2016; Deng et al.,2011; Singh et al.,2016). Moreso, The European Network of Transmission System Operators for Gas, as part of its 2050 road maps for gas grids for a carbon neutral system, identified hydrogen blending into gas grids as the most viable amongst a number of identified alternatives in meeting the set goals for the short-to-mid-term (ENTSOG, 2019; Pellegrini et al.,2020). Typical hydrogen blending ratios range from 5-15% of hydrogen in natural gas and usually occur in large natural gas pipeline transportation networks (Melaina et al.,2013). It is essential also to note that the hydrogen percentage in hydrogen-natural gas blends may vary depending on the specific application and

other factors such as storage, regulations, distributions, metering, and the specific applications (Miroslav et al.,2022). Furthermore, the impact of hydrogen-methane blends on both underground and surface facilities is an issue of concern under investigation (Altfeld and Pinchbeck, 2013; Shi et al., 2020). Although green and blue hydrogen have considerable environmental benefits, on the one hand, there is currently no infrastructure to handle such gases.

On the other hand, building new infrastructure for such gases is economically risky as there is a high level of uncertainty associated with their demand chain. Hydrogen blending also comes in handy in such cases as a viable solution to the infrastructural challenges associated with blue and green hydrogen (Meliana et al., 2013). Hydrogen blended with natural gas is usually recovered at Fuel Cell Vehicle refueling stations after separation and purification. In some cases, it may be impossible to recover all the hydrogen, and such natural gas mixtures may be used in combustion with the added benefits, as discussed (Di Lullo et al., 2021).

Despite its numerous benefits, blending hydrogen with natural gas is associated with some uncertainties and challenges. To begin with, the impact of the percentage of hydrogen on end-use appliances and end-use facilities is not thoroughly understood as it has most often been addressed on a case-by-case basis. However, the hydrogen percentage in blends will inevitably impact the associated costs and the precautions that must be taken to operate such facilities (Meliana, 2013). Safety is another issue of concern with hydrogen blending as H₂ can ignite under a broader range of conditions compared to natural gas; thus, there is a higher chance of ignition for H₂-methane blends than pure natural gas. The ignition energy of hydrogen is significantly lower than methane's, making its blending with methane risky (Miroslav et al.,2022). Furthermore, although H₂-CH₄ blends are likely to reduce greenhouse emissions due to the higher probability of hydrogen leakage (given its higher mobility) in pipeline transportation systems, there is also an associated risk given

hydrogen's high flammability (Mahajan et al.,2022). Mixing hydrogen with methane also increases the overall temperature of combustion in household appliances and may result in equipment overheating (Leicher et al., 2022). The potential for hydrogen embrittlement in steel pipelines due to the transportation of the gas mixture is another area of concern. Embrittlement reduces the mechanical properties of the metal and could subsequently lead to hydrogen-induced cracking, a fatal incident that could result in gas leakage (Gangloff and Somerday, 2012).

2.2.3. Hydrogen Storage in Depleted Reservoirs: Challenges and Barriers

Depleted hydrocarbon reservoirs, as mentioned above, are the most common and cost-effective UHS facilities globally. Furthermore, although similar in many ways compared to natural gas storage and CO₂ sequestration, hydrogen storage in this depleted hydrocarbon formation differs in some technical respects due to difference in the properties of the gases. The properties of hydrogen (**Table 5**) are thus discussed relative to its storage and, in comparison, with methane and carbon dioxide. Furthermore, the challenges and barriers in hydrogen storage in depleted reservoirs are evaluated with a focus on well integrity issues.

At the freezing point of water (0°C) and a pressure of 1 bar, hydrogen exists in a gaseous phase at a density of 0.089kg/m³. When the temperatures drop to about -262°C (-439.6°F), the gas is converted to a solid (Tarkowski, 2019). These properties of hydrogen are essential in understanding the dynamics of its storage in depleted reservoirs, as the storage process involves compressing the gas to increase the quantity of stored gas. Hydrogen properties also affect the injection and withdrawal process during storage and its reversibility. The density of hydrogen is about 8 times lower than that of methane and 22 times lower than carbon dioxide. Also, compared to methane and carbon dioxide, hydrogen has higher permeability and thus higher chances of leakage through potential pathways in the wellbore, caprocks, or geological traps. Although the

presence of water in pore spaces in depleted reservoirs reduces the chances of hydrogen leakage due to low hydrogen permeability in water, the reaction of hydrogen with the formation rocks may be another challenge that requires a thorough understanding of hydrogen properties. Furthermore, the viscosity of hydrogen is lower than that of methane and carbon dioxide, thus, making retention of hydrogen gas in depleted reservoir formations a major challenge (Muhammed et al., 2023).

Table 5: A comparison of the properties of H₂, CH₄ and CO₂ (Ugarte and Salehi, 2022; Tarkowski, 2019; Alcock, 2001; Das, 2016)

Properties	Hydrogen	Methane	Carbon dioxide
Molar mass	2.016	16.043	44.01
Density at standard conditions (kg/m ³)	0.08375	0.6682	1.87
Autoignition temperature (°C)	585	540	NA
The diffusion coefficient in the air at standard conditions (cm ² /s)	0.61	0.16	0.139
Solubility in pure water at standard conditions (g/L)	16X10 ⁻⁴	22.7X10 ⁻³	1.45
Critical Temperature (°C)	-239.95	-81.9	30.98
Critical Pressure(atm)	12.83	45.349	72.83

As earlier established, only a few projects in UHS have been implemented while majority are still at the research and development (R&D) phase. Although some experience can be borrowed from underground storage of natural gas, helium, and carbon dioxide in implementing and operating hydrogen storage, some unique uncertainties and potential technical barriers and challenges still exist. These challenges are related to the properties of hydrogen as a fluid, geochemical reactions between hydrogen and rock and formation fluids, reservoir microbial activities, well integrity and

completions, and material requirements, which are discussed herein (Heinemann et al., 2021; Bai et al., 2014).

2.2.3.1. Effects of In-situ Geochemical Reactions

As discussed earlier, the depleted hydrocarbon formations for hydrogen storage consist of geological traps. The traps comprise a reservoir rock (a porous rock containing the gas), a seal (an impervious caprock for keeping the hydrocarbons in place), and an underlying drive mechanism. The integrity of the caprock and the quantity and quality of the stored gas is vital in large-scale underground hydrogen storage. In the storage process, there exists a possibility of geochemical reactions between the formation water, reservoir rocks, and dissolved gases, which could impact the integrity of caprocks, cause a reduction in the total gas volume stored as well as a result in the dissolution of minerals and the production of other harmful gases such as H₂S (Heinemann et al., 2021). Dissolving minerals may result in gas injectivity issues and, along with other factors, affect caprocks' integrity, creating pathways for gas leakage.

The failure of caprocks, which are essential components of the trapping mechanisms in underground hydrogen storage, is usually due to changes in porosity, permeability, interfacial tension, wettability, contact angles, and capillary pressures (Muhammed, 2023; Thiyagarajan, 2022). Caprocks have very low permeabilities and are usually saturated with formation water making them gas-tight until their threshold capillary pressure is exceeded (Reitenbach, 2015). They form the primary mechanism for gas trapping. In most underground hydrogen storage environments, commonly used caprocks are clays and salts, as they provide the needed tightness for sealing (Ugarte & Salehi, 2021). Besides, other geological rocks can be used as caprocks, provided the buoyancy pressure within the rocks is less than the minimum entry capillary pressure (Evans, 2007).

Given that the capillary pressure threshold is not exceeded, stored gas can remain trapped for several years during the gas storage period. When this pressure is exceeded, the caprock becomes permeable to gas as the water within the pore spaces is drained. Caprock wettability is also another factor that affects its integrity. Although some studies have been conducted to determine the combined impacts of contact angle, interfacial tension, and wettability, more R&D work is required to thoroughly understand these concepts (Yekta, 2018; Hashemi, 2021; Bo et al., 2021; Iglauer, 2021).

Besides, the integrity of caprock is also affected by dissolution and precipitation reactions (Labus et al., 2022; Rezaee et al., 2019; Gultinan et al., 2017). Usually, the integrity of the caprock is maintained when the precipitation rate exceeds the dissolution rate. Inferentially, there is an increase in the porosity and permeability of the caprock at a low precipitation rate, resulting in leakage of the stored gas. In some situations, stored hydrogen may induce geochemical reactions indirectly, affecting the caprock's integrity (Crotofino et al. 2010). Such processes usually involve hydrogen reactions with in-situ sulfates to change the pH of the formation fluid leading to dissolution reactions (Hematpur, Heineman; Hassanpouryouzband, 2021; Xu et al., 2021). These reactions are hydrogen-driven redox reactions that alter rock matrices' mechanical strengths, creating a gas leakage pathway. Still, on caprocks, there is an associated risk of hydrogen diffusion through the caprock. This occurs by hydrogen dissolution in the formation of water of the caprock and subsequently through the caprock itself (Amid et al., 2016). It is also worth noting that the extent to which these in-situ gas reactions occur is unknown (Kampman et al., 2016, Heineman et al., 2021; Reitenbach, 2015). Besides a theoretically reported value of 1.5-2% loss of stored hydrogen due to compromise in caprock integrity (Krooss, 2008), the in-situ geochemical reactions can also lead to the formation of H₂S, which affects the overall quality of the stored hydrogen and

can adversely impact hydrogen infrastructure as well (Gaucher et al., 2009). **Figure 15** is a diagrammatic representation of the hydrogen-related in-situ geochemical reactions in underground hydrogen storage in depleted reservoirs.

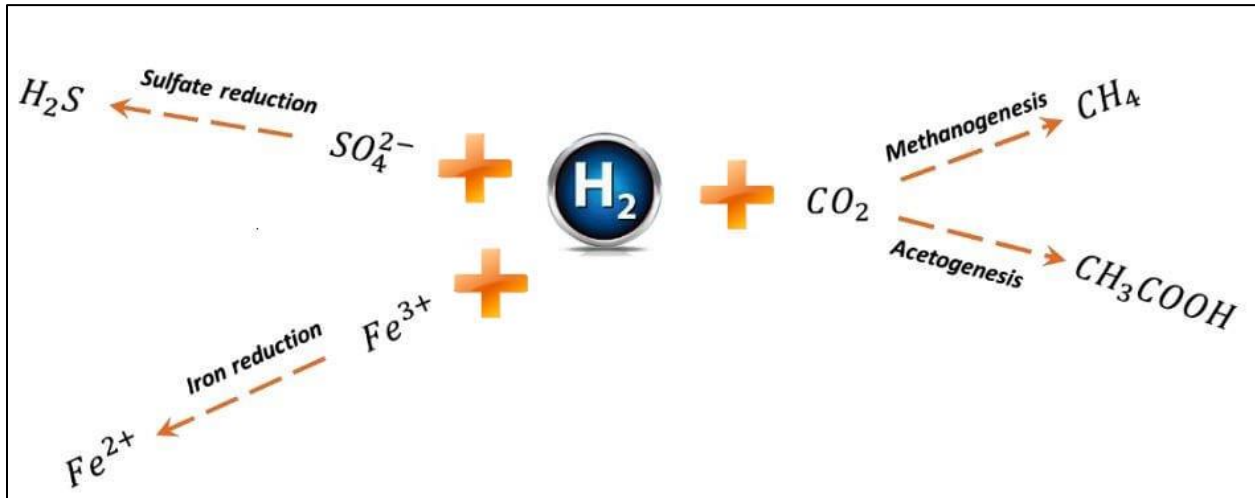


Figure 15: Diagrammatic representation of biotic reactions in an Underground Hydrogen Storage Environment (Ebrahimiyehta, 2017)

2.2.3.2. Geomechanical Barriers

The continuous cyclic injection of cold pressurized hydrogen into the storage formation and subsequent withdrawals could lead to variations in the mechanical and transport behavior of in-situ rock formations. In addition, changes in the pore pressures are also experienced due to continuous injection of the gas. These pressure changes can also reduce the porosity of the reservoir rock due to compaction, formation subsidence, and reactivation of faults (Ostermeier, 1995; Dautriat, 2009; Doornhof, 2006). Another potential challenge of these pressure changes is the flexure of the caprock, which can affect its sealing integrity by creating gas leakage pathways within it. Furthermore, due to chemical reactions, there is a potential for the dissolution of weight-bearing minerals in in-situ rock matrices. This may weaken the reservoir's ability to bear in-situ

loads due to a combination of elastic and inelastic deformations further enhanced by the injection and production cycles.

Furthermore, the knowledge base from the production of hydrocarbons over a long period has shown that minute compactions during the process at the reservoir level could result in subsidence at the surface and induce seismicity. It is, therefore, incumbent to investigate the effects of injected hydrogen gas and the injection rates on grain deformations. This can help to determine the extent to which grain-scale deformation occurs in long-term injection and production cycles during hydrogen storage. Another potential geomechanical barrier in underground hydrogen storage is the swelling of clay due to the absorption of the injected hydrogen and subsequent desorption, as shown in **Figure 16**. The process may result in the creation of fracture pathways in downhole rock matrices (Cornelio, 2019; Liu et al., 2022).

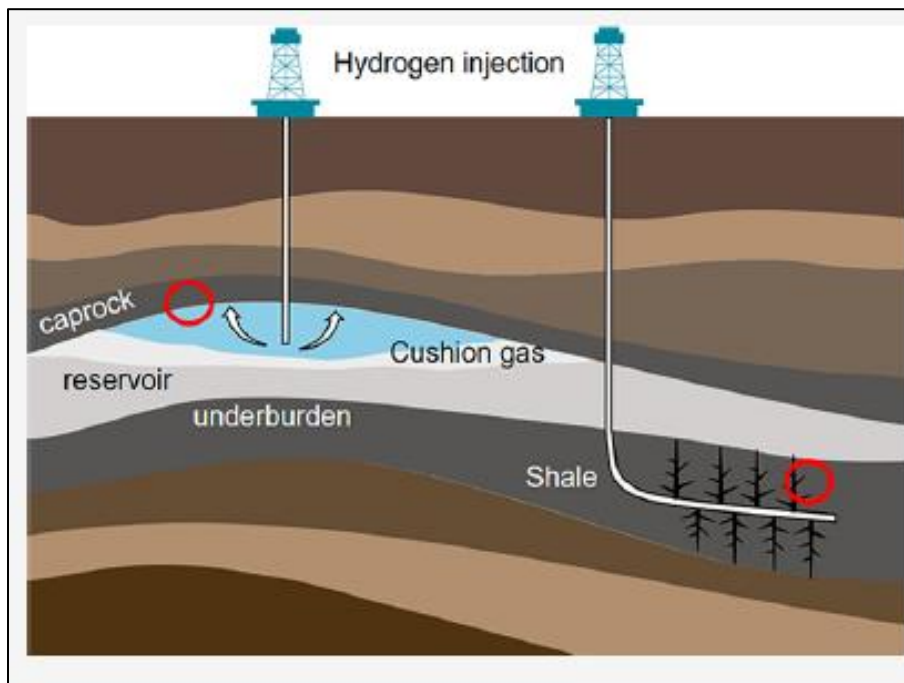


Figure 16: Clay swelling and fracture formation in clay silts due to hydrogen diffusion (Liu et al., 2022)

2.2.3.3. Microbial Activities in the Reservoir

A significant challenge in UHS is the impacts of microbial activities downhole (Hemme and Van Berk, 2018; Thaysen et al., 2021). The presence of microbes in underground hydrogen storage environments may result from some factors, including pumping, drilling, mining, and completion operations (Thiyagarajan et al., 2022). Hydrogen is a universal donor of electrons for prokaryotes (i.e., bacteria and archaea). Thus, bacteria activity can be reduced to very low volume concentrations (less than 1% vol) when the appropriate terminal electron receptors are present (Reitenbach, 2015; Cord-Ruwisch, 1998). A limited number of studies have indicated the presence of microorganisms in underground hydrogen storage environments at the subsurface whose activities result in the consumption of downhole gases at some given conditions (Muhammed et al., 2021; Dopffell et al., 2021). These microorganisms are mostly methanogens, homoacetogenic bacteria, sulfate-reducers, and iron (III) reducers (Eddaoui et al., 2021). Factors like concentration of salt, pH value, temperature, and pressure affect the activities of these microorganisms. The primary concern regarding microbial activities in UHS is the reduction of hydrogen volume downhole due to consumption by these micro-organisms. This usually involves hydrogen conversion into products like H₂S and CH₄, changing the stored gas mixture (Zeng Lingping, 2022). Furthermore, the loss of hydrogen by these microbial activities can also cause an increase in the porosity of the reservoir leading to further loss of the stored gas. This is usually predominant in fractured reservoirs. (Hemme and Van Berk, 2018; Dopel et al., 2021; Jiang et al., 2016). Previous reports on gas storage projects have shown different ranges of gas consumption due to microbial activities. For instance, In Beyenes, France, town gas (which has hydrogen as a constituent) storage showed 0% hydrogen consumption, whereas a 17% reduction in the overall volume of hydrogen produced was recorded in Lobodice (Czech Republic) (Stolten.,2016; Amigan,1990). In the case of the latter, the reduction in hydrogen volume was associated with a

simultaneous reduction in carbon dioxide (CO₂) and an increase in methane (CH₄) after seven months of operation. Other reports of microbial conversion of hydrogen to methane were also reported in the Sun-Storage project in Austria, where about 3% of the total hydrogen stored was converted to methane by methanogens (Pichler, 2019).

Furthermore, sulfate-reducing bacteria can also cause corrosion problems in steel components of the wellbore (i.e., casing strings) at the subsurface (Kleinitz and Boehling, 2005). An indirect consequence of casing corrosion is a reduction in the sealing capacities of wellbore cement (Deveci, 2018). Sulfate-reducing bacteria are very adaptive and can exist in both oxygenated and non-oxygenated environments. The activities of these sulfate-reducing bacteria become more severe when hydrogen is blended with natural gas as this causes procreation of these sulfate-reducing bacteria.

Another problematic aspect of microbial activity in underground gas storage environments is the formation of biofilms that could potentially clog the pore spaces in rock matrix for gas storage. This process is generally referred to as biomass plugging. It is caused by the rapid growth of the microbial cells resulting in the formation of these biofilm structures within the pores of the reservoir rocks (Davey et al., 1998). This reduces the gas injectivity rate into the porous reservoir rocks. This phenomenon is new, with little to no research (Chou, 2003; Heineman et al., 2021). Thus, research and development studies are required to investigate and quantify the impacts of biofilms in large-scale underground gas storage. A similar concept known as Microbial Induced Carbonate Precipitation has been discussed recently in underground hydrogen storage environments (Thiyagarajan et al., 2022), requiring more R&D work.

2.2.3.4. Well Integrity Barriers

Well integrity is one of the critical issues of concern in large-scale underground hydrogen storage, as wells must withstand the potential harsh storage conditions to prevent any form of gas leakage (Bo et al., 2021; Rezaee et al., 2019). The International Standards Organization (ISO) defines Well Integrity as the ability of a drilled well to remain in shape and intact throughout its lifecycle. It also refers to the application of technical, operational, and organizational solutions to reduce the risk of uncontrolled release of formation fluids throughout the lifecycle of the well (Norge, 2013). As discussed in section 1.2, loss of integrity of wells can be fatal and lead to failure of the storage project, loss of lives and properties, and financial losses. In this section, well integrity challenges related to various aspects of the wellbore, including cement, casing strings, elastomeric materials including packers, fittings, and valves, amongst others, are discussed.

2.2.3.4.1. Microbial Induced Corrosion (MIC)

Microbial-induced corrosion is a principal challenge in large-scale underground hydrogen storage, typically affecting steel infrastructure at both surface and sub-surface locations. The phenomenon is usually caused by microbes whose activities result in methanogenesis and sulfate and iron reductions (Muhammed, 2023; Reitenbach, 2015). Generally, at favorable pH, salinity, temperature, and pressure conditions, the activities of microbes result in the formation of biofilms on the surface of steel casings. These biofilms are made up of cells surrounded by complex networks of nucleic acids, proteins, and sugars that protect the microbes from harsh external environments. Underneath the biofilms, microbial activity causes steel corrosion and severe impairment of metallic downhole components, negatively impacting the overall storage integrity of the wellbore (Dopffel, 2021). The principal microbes involved in this process include sulfate-reducing bacteria (SRB) (which are formed by the mineral dissolution of calcium sulfate, iron-

reducing bacteria (IRB), and Methanogens Archaea (Ebigbo, 2013; Thaysen, 2023; Boopathy; 1991; Edyvean, 1997). SRB causes corrosion on the metallic surface either chemically via the production of H₂S or electrically by the withdrawal process. For the former, one of the earliest proposed theories was the cathodic depolarization theory by Von Wolzogen Keuhr and Van der Vlugt in 1934 (Kuhr et al., 1934). The process involves the consumption of hydrogen by SRB to reduce sulfate ions (SO₄²⁻) to H₂S at the cathodic site. At the anode, about a quarter of the Fe²⁺ reacts with H₂S to form FeS while the remaining forms FeCO₃ precipitate, facilitating the overall corrosion reaction.

SRB usually thrives optimally in temperatures around 38°C where pH conditions are neutral (i.e., about 6 to 7.5) although other factors like porosity, salinity, and pressure may affect it (Thaysen,2023). Besides SRB, IRB's also cause casing corrosion via a metabolic reaction involving the consumption of H₂ by ferric oxides (i.e., iron (III) oxide) although their impact is less severe compared to SRBs. Although both bacterium types can thrive in the same environment and facilitate the corrosion process, IRBs activities supersedes that of SRBs in an environment that is rich in iron oxides and organic carbon (Ugarte and Salehi, 2022; Labus et al., 2022). This is because IRBs have very high affinity to H₂. Methanogens are also another group of microbes that cause casing corrosion in UHS. The activities of these microbes cause consumption of H₂ as a donor while CO₂ is used as a receptor in producing methane (CH₄). Although the methane formed is not highly corrosive, its availability in the presence of CO₂ and H₂S can facilitate the corrosion process in casing. The activities of these microbes are summarized in **Table 6**. **Figure 17** also shows the reactions on the surface steel casing in SRB induced microbial corrosion based cathodic depolarization theory by Mori et al. (Mori et al., 2010).

MIC is often difficult to detect first due to its similarity with chemical corrosion and secondly because it shows a wide range of corrosion rates and occurrences (Thiyagarajan, 2022).

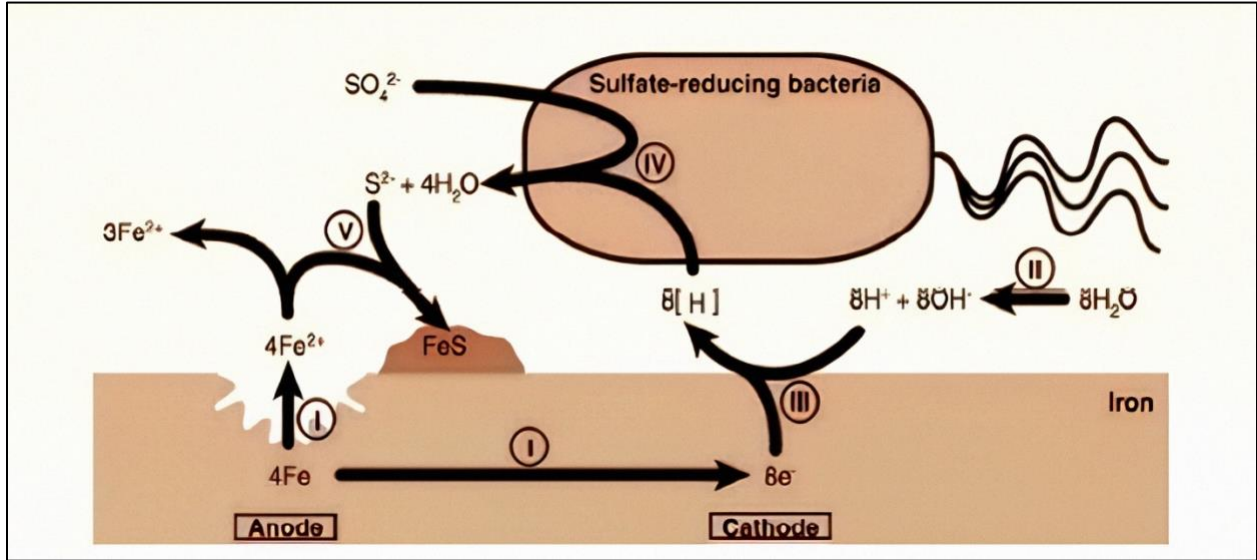

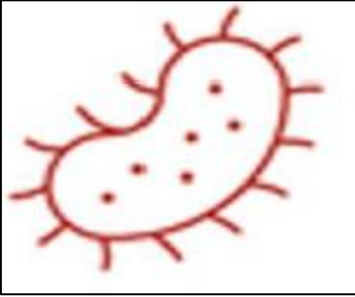



Figure 17: SRB corrosion reaction on steel surface based on cathodic depolarization theory (adapted and modified from (Mori et al., 2012))

Table 6: Summary of Implications of Subsurface Microbial Activities (Aftab et al.,2022)

Hydrogenotrophic microbes	Reaction and potential mineralization	Potential Impact on LSUHS
<p>Sulfate Reducing Bacteria (SRB)</p> 	<ul style="list-style-type: none"> • $SO_4^{2-} + 5H_2 \leftrightarrow H_2S + 4H_2O$ • H_2 reacts with anhydrite and other inorganic sulfate sources and reduces sulfate to sulfide. 	<ul style="list-style-type: none"> • H_2 sulfide release. • Gas mixing effect • Iron corrosion • pH reduction • Hydrogen embrittlement • Mineral precipitation
<p>Iron Reducing Bacteria (IRB)</p> 	<ul style="list-style-type: none"> • $H_2 + 3Fe_2O_3 \leftrightarrow 2Fe_3O_4 + H_2O$ • Microbes can reduce film. E.g., ferric components on metal surfaces. • Water can release and occupy sandstone's interstitial pore space by-product, causing excess water saturation and mineral dissolution. 	<ul style="list-style-type: none"> • Low sulfide reduction • Metal corrosion • Carbon steel corrosion • Mineral dissolution
<p>Methanogens Archaea</p> 	<ul style="list-style-type: none"> • $4H_2 + 3Fe_2O_3 \leftrightarrow CH_4 + 2H_2O$ • Microbes attach to the edges of clay surfaces. e.g., kaolinite to prevent CH_4 flow. • The presence of Aluminium ions in the kaolinite can be toxic to the growth of methanogens 	<ul style="list-style-type: none"> • Gas mixing effect • Reduces injection and withdrawal capacity due to plugging of pores • Permeability and porosity alteration.

2.2.3.4.2. Hydrogen Embrittlement

Typically, the effects of hydrogen on casing strings in underground hydrogen storage is seen in hydrogen embrittlement (sometimes referred to as hydrogen blistering or hydrogen-induced cracking) (Thiyagarajan et al., 2022; Ghasemi, 2011; Revie, 2008). Hydrogen embrittlement is the significant reduction in the strength of a material due to its introduction to hydrogen atoms in a gaseous hydrogen environment. The process also reduces the ductility, mechanical strength, and tensile strength of materials and is more severe at elevated temperatures (Dwivedi et al., 2008; Kim et al., 2017). Blistering occurs when atomic hydrogen is formed on a metal surface due to a dissociative chemical sorption process (Muhammed et al., 2023). Atomic hydrogen permeates into the steel metal matrix and into its lattice by diffusion and forms a cluster underneath the surface of the metal. In some instances, this atomic hydrogen may be trapped along the boundaries of the metal grain or around dislocations and vacancies (Reitenbach, 2015). The phenomenon can further lead to hydrogen-induced cracking as follows. Catalytic reactions on the surface of the metal cause hydrogen molecule formation, which further promotes nucleation reactions at the boundaries of the metal grains. This causes a pressure build-up at those boundaries, causing an extension of the distance between the grain interfaces. This causes the formation of micro-voids at the boundaries and subsequently results in blistering. Hydrogen blistering in itself is not an issue of grave concern. However, micro-void growth may occur when steel is subjected to high tensile stress, and crack formation may result from these micro-voids, a process referred to as hydrogen-induced cracking, HIC. This is a very problematic situation as it can result in sudden failure of the steel metal (casing) without any initial signs of metal weakening. The term hydrogen embrittlement stems from the fact that hydrogen blistering and HIC could lead to the breaking of metals without first bending or showing any signs of the onset of failure. The severity of hydrogen embrittlement is also contingent on factors like temperature, pressure, material properties, number of impurities, and grain

structures, amongst others. Also, SRBs, as discussed earlier, cause the release of H₂S and coupled with the diffusive behavior of H₂, facilitate the hydrogen embrittlement process, resulting in hydrogen leakage (Aftab, 2022).

Furthermore, hydrogen has a reputation for promoting the corrosion fatigue properties of steel, and this is critical in UHS as casing and other steel elements are subjected to periodic stress challenges due to production and injection cycles. Embrittlement is common in steel with high strength (i.e., steels with tensile strength greater than 900MPa). As a result, low-strength or medium-strength steel is preferable in UHS (Muhammed et al.,2023). Hydrogen blistering and hydrogen-induced cracking are shown in **Figure 18** below.

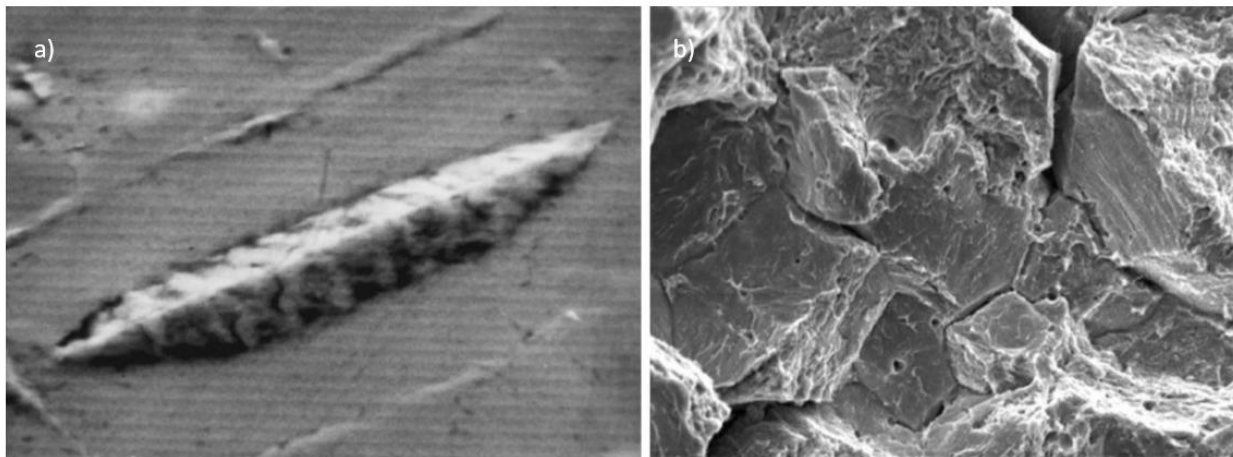


Figure 18: Pictorial representation of (a) Hydrogen blistering (b) Hydrogen-induced cracking (Szummer, 1999)

2.2.3.4.3. Cement Degradation

Cement is an essential component of well integrity in underground hydrogen storage. They are major barrier elements by the shear and hydraulic bonds they form between themselves and the casing and formation. Although cement usually has proven integrity in depleted hydrocarbon reservoirs, they are susceptible to failure over long periods under subsection to varying storage

conditions. Cement degradation may be due to chemical or mechanical processes at underground hydrogen storage conditions. The mechanical degradation process occurs when cement is subjected to varying stresses during loading and unloading processes in UHS. This is due to heat expansions, changes in pressure, and cement material volume expansion resulting from the hydration process.

Chemical degradation of cement, on the other hand, may be because of a reaction with CO₂ in the presence of water and the subsequent occurrence of two major processes; “carbonation” and “leaching” (Strazisar et al., 2009). Besides, an H₂S attack can also cause chemical degradation in the cement sheath. The two major binding elements formed during the hydration of cement are CH, sometimes referred to as portlandite (Ca (OH)₂), and the CSH phase. In the carbonation process, CO₂ first dissolves in the formation of water to form brine which reacts with the cementitious materials CH and CSH to form calcium carbonates (CaCO₃). CaCO₃ further precipitates to reduce the porosity and permeability of cement, increasing its mechanical strength in the process (de Sena Costa et al., 2018; Omozebi et al., 2016; Reitenbach, 2015). **Figure 19** is an SEM micrograph of a carbonated cement surface. At conditions where CO₂ is in excess at underground gas storage conditions, CaCO₃ and additional portlandite are further dissolved in a process known as leaching. This increases cement permeability and porosity and reduces its mechanical strength. At higher temperatures and pressures, the carbonation and dissolution process is typically higher in class G cement (Le Saout et al., 2006). Besides carbonation, cement may also undergo chemical attack by sulfates. Here, excessive H₂S formed by microbial activities is transformed into H₂SO₄, which attacks cement, leaches portlandite, and results in ettringite and gypsum formation, as shown in **Figure 20** (Ugarte and Salehi, 2022; Breysse, 2010). Carbonation of the cement sheath can be problematic, as seen in carbon capture and storage (CCS).

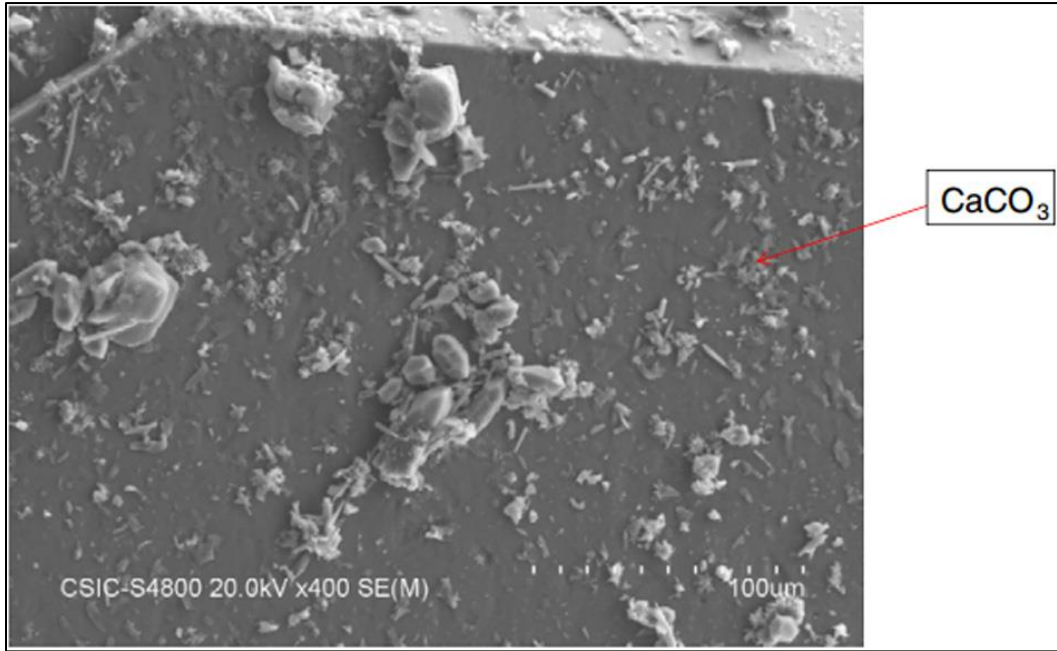


Figure 19: SEM micrograph of carbonated cement surface with CaCO₃ nucleation (Galan et al., 2015)

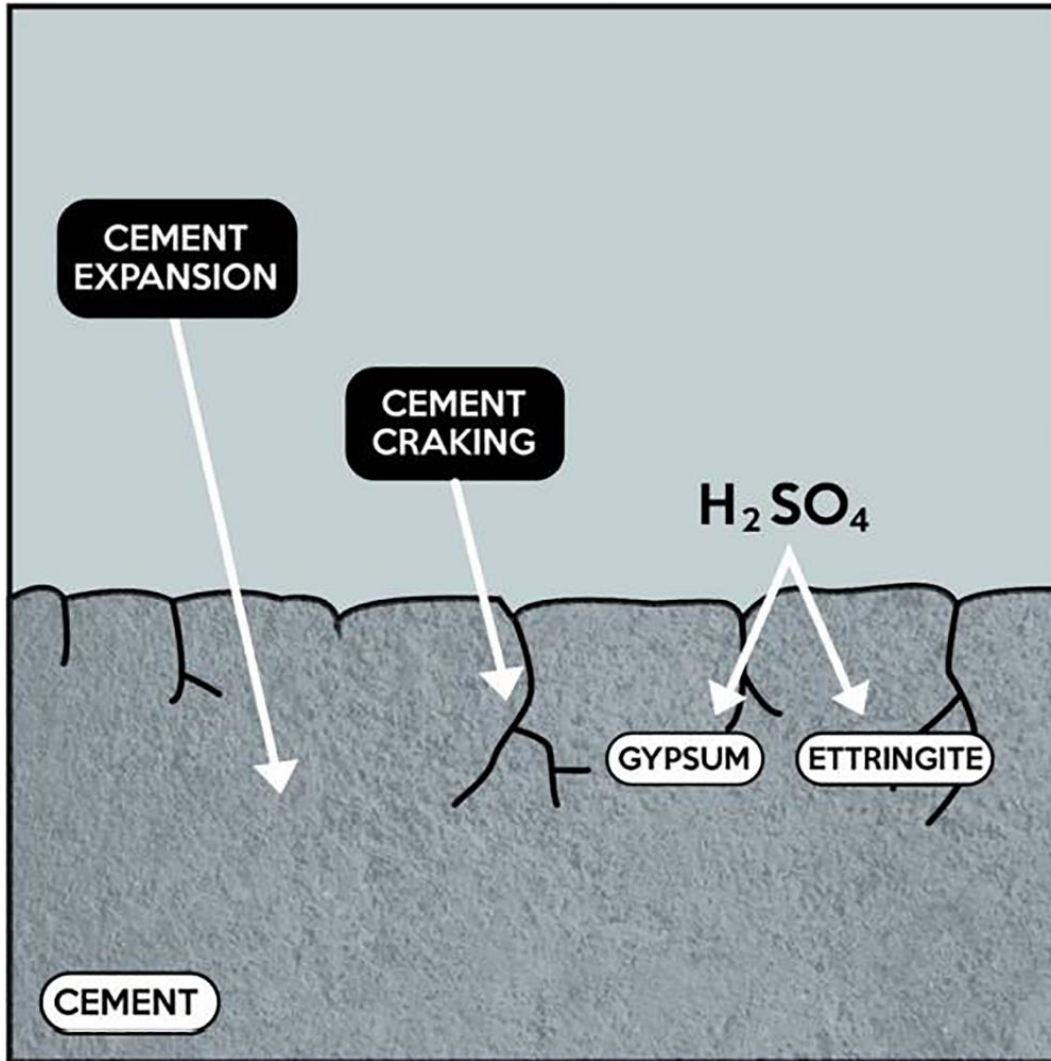


Figure 20: Sulfate attack in cement resulting in ettringite and gypsum formation (Ugarte and Salehi, 2022)

It can result in dissolution which reduces the compressive strength of the cement and increases cement porosity and permeability, creating a favorable condition for hydrogen leakage through cement. Since carbonation of cement is highly dependent on CO_2 concentration in underground hydrogen environments, it is important to appropriately select cushion gas to reduce CO_2 effects in cement degradation. As a result, depleted hydrocarbon reservoirs with minimal quantities of CO_2 are recommended for UHS. Also, in order to reduce the chances of gas leakage in underground hydrogen storage environments, it is recommended to use fine completion cements with low SiO_3

concentrations (Thiyagarajan et al, 2022). Besides cement degradation by carbonation, sulfate-reducing bacteria archaea can also cause deterioration of cement resulting from H₂S attack on the cement due to its reaction with the hydrogen molecule (H₂). Flesch et al., 2018 also showed an increase in porosity of cement due to hydrogen exposure at temperatures between 40°C (104°F) and 100°C (212°F) and pressures between 10 to 20 MPa (Flesch et al., 2018). Although identified to have the potential of being problematic, there is hitherto not enough research evidence on the suitability of general-purpose class G and H cement in underground hydrogen storage environments (Ugarte and Salehi, 2021).

2.2.3.4.4. Elastomer Degradation

Besides cement, elastomer performance is vital in ensuring well integrity in underground gas storage. These are viscoelastic polymeric materials with comparatively weak intermolecular forces, low young's modulus, and are more susceptible to strain failure compared to other materials (Muhammed, 2023). For underground hydrogen storage in depleted hydrocarbon reservoirs, their applications are seen as being important components of seal and barrier elements such as Blowout Preventers (BOP), packers, and liner hangers (Ahmed et al.,2020; Ahmed et al., 2019). Packers are mainly used for zonal isolation, while the BOP is a large valve situated at the top of the well and used to shut in the well during well control events (Shafiee et al.,2022; Ahmed et al.,2020; Ahmed et al.,2019). Typical elastomers used in these applications include Ethylene-propylene Diene Monomer (EPDM), Nitrile Butadiene Rubber (NBR), silicon rubber (VMQ), and Viton (FKM) (Reitenbach, 2015). At underground gas storage conditions, elastomers are susceptible to both chemical and physical damage when exposed to downhole gases (i.e., CO₂, CH₄, H₂, and H₂S). The chemical degradation process involves the reaction of the downhole gases with the molecular structures of the elastomers and usually occurs when the bond dissociation energies

(BDEs) of these gases are exceeded, i.e., the standard enthalpy change for bond cleavage by homolysis is attained. Chemical degradation of elastomers is also facilitated by the presence of downhole fluids like drilling and completion fluid, brine, and production fluids (Patel et al., 2019). Furthermore, research has shown that downhole micro-organisms such as SRB and methanogens may cause hydrogen reactions with H_2S and CO_2 to form CH_4 and H_2S . While CH_4 has minimal chemical effects on the chemical degradation of elastomers, H_2S can cause elastomer failure due to heterolysis and hemolysis as it increases subsurface reaction activities (Ugarte and Salehi, 2022; Kwatia, 2018). Evidence of elastomer chemical degradation includes changes in physical and mechanical properties such as hardness, and tensile and compressive strengths, amongst others. Besides, elastomers may also undergo physical damages such as blistering (Stevenson et al., 1995; Yamabe and Nishimura, 2009), buckling (Melnychuk et al., 2020; Reuda et al., 2012), and cavitation (Denecour and Gent, 1968; Kane-Diallo et al., 2016) due to permeation of hydrogen molecules through the elastomeric material. A notable failure mechanism in elastomers is rapid decompression (explosive decompression). This involves the expansion and escape of pressurized gas molecules absorbed in an elastomer at a compressed state due to a sudden reduction in the pressure of the surrounding gases. The phenomenon usually results in blister formation (**Figure 21**) on the surface of the elastomers and subsequently causes its failure (Stevenson et al., 1995). Previous works have shown that observable physical damage in elastomers in gaseous hydrogen environments usually occurs at high pressures (above 10MPa) (Yamabe & Nishimura, 2011) and temperatures (Yamabe, 2013; Jaravel et al., 2011). However, very minimal research exists on the behavior of general-purpose elastomers in comparatively low-pressure underground gas storage environments.

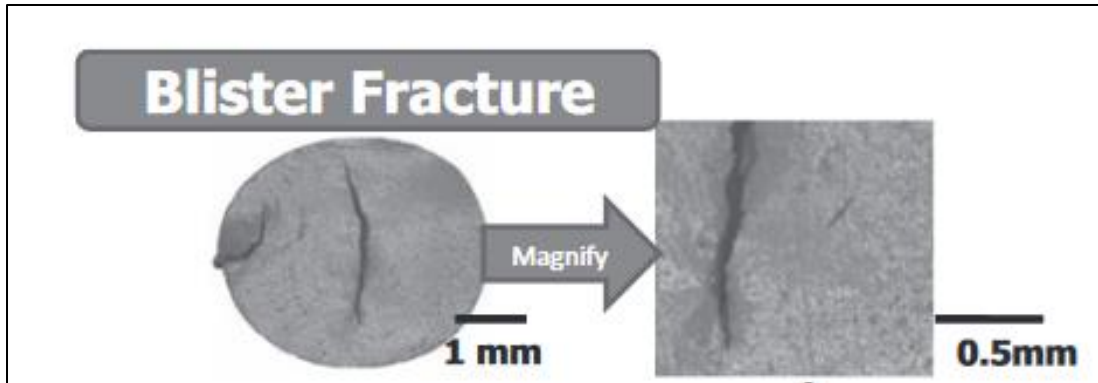


Figure 21: Blister fracture in EPDM O-ring after exposure to H₂ @ 35Mpa and 100°C for 15 hours (Nishimura, 2014)

In summary, large-scale underground hydrogen storage in depleted hydrocarbon reservoirs is plagued with several uncertainties, barriers, and challenges. These include but are not limited to caprock integrity failures and uncertainties, microbial activities and reactions downhole, cement degradation due to chemical attacks, and geomechanical uncertainties due to stress/strain changes in injection and withdrawal cycles, amongst others. There is evidently a need for extensive R & D work for safe and efficient storage of the gas. **Figure 22** depicts some geological uncertainties associated with large-scale underground hydrogen storage.

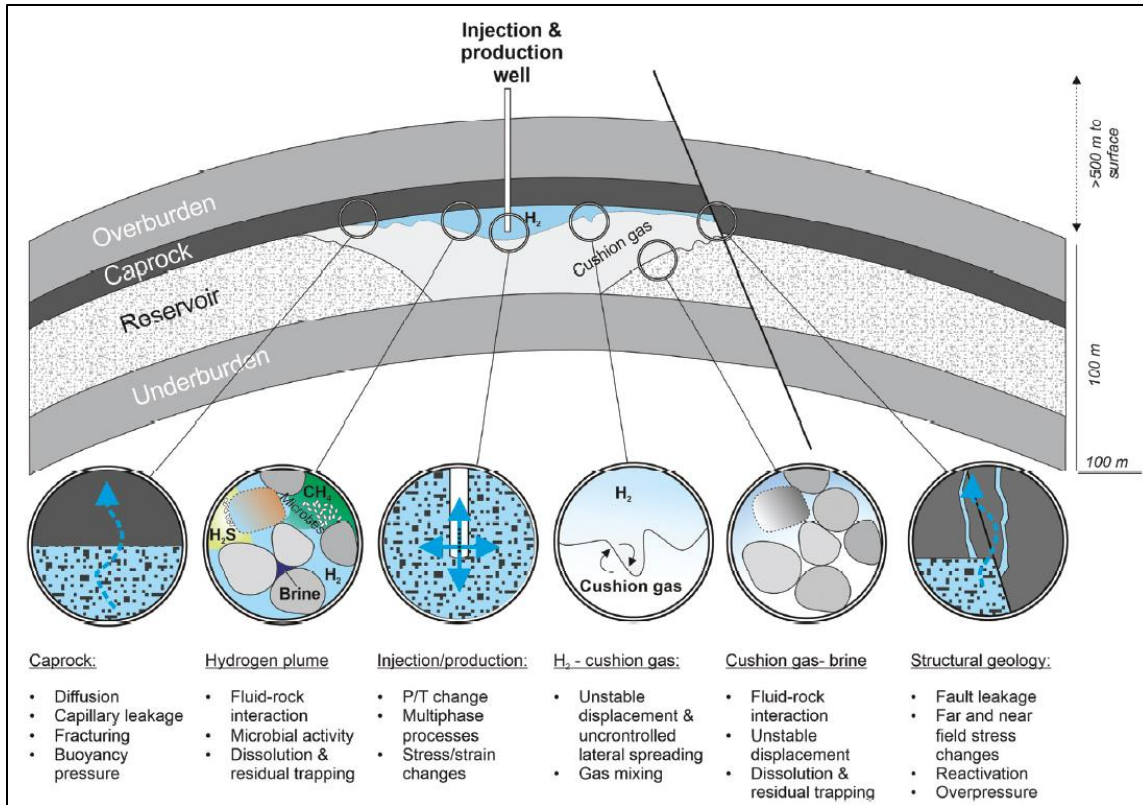


Figure 22: Geological uncertainties associated with large-scale underground hydrogen storage in depleted hydrocarbon reservoirs (Heinemann et al., 2021).

3. Elastomers

In this section, a thorough review of elastomers, their applications in the oil and gas industry as well as research works on their performance (as seen in seal assemblies) in hydrogenated environments is presented.

Elastomers are rubber materials formed by loose cross-linkage of amorphous polymers (Rinnbauer, 2007). They are a unique category of polymers whose molecular structure consists of sporadically distributed chains held together by cross-links, as shown in **Figure 23**. (Visakh, 2013). The cross-links are responsible for the rigidity of the elastomer molecular network, which otherwise maintains some freedom of movement between the molecular chains (Mahak, 2021).

Thus, elastomers show a quick and large reversible response to strain when subjected to stress (Shanks and Kong, 2013). Generally, elastomers are made of monomers that are in a cross-linkage bond with their neighbors and hence are pulled back into their original shape when stress acting on them is removed (Kwatia, 2018). According to the American Society of Testing and Materials (ASTM standard D1566), elastomers are high polymeric organic networks capable of absorbing large deformations in a reversible manner. Based on this property and the fact that elastomers can absorb stresses, they are used in the manufacture of products that reduces or dampens vibrations, permits motion between different parts of a system, and assist in seal formation, amongst others (Rinnbauer, 2007).

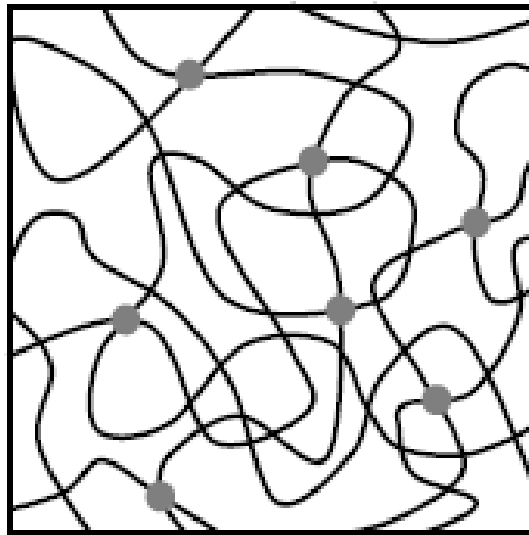


Figure 23: Schematic diagram of a network of cross-linked carbon chains of an elastomer (Mahak, 2019)

Elastomers are both entropy-elastic (Jaunich et al.,2011) and viscoelastic materials (Ginic-Markovic et al.,1998). For the former, a basic explanation is that entropy (the degree of disorder of elastomeric chains) is responsible for the elasticity of the polymeric material. Entropy is higher in a disordered, entangled elastomer state compared to an orderly and well-arranged elastomer

chain state. Viscoelastic behavior of elastomers implies that they exhibit both the reversible elastic behavior of solids as well as the irreversible behavior of viscous behavior of liquids (Christensen,2012). For a given loading and pressure and temperature conditions, one of the two properties is predominant over the other. Typically, elasticity is more prevalent at lower temperatures and higher deformation speeds whereas viscous behaviors is seen at higher temperatures and lower speed of deformation (Rinnbauer, 2007).

The production of elastomers is done in three major stages; selection of compounding ingredients, mixing, or compounding and finally, vulcanization to yield the final product (Rajesh et al.,2013; Rinnbauer, 2007; Visakh et al., 2013).

Material selection is an essential step in elastomer formulation as it determines the unique properties of the elastomer. It is also worth noting that one additive may improve a particular characteristic of an elastomer material while negatively affecting another (Drobny, 2014). Materials used in the rubber formulation include polymers which may be natural or synthetic, fillers (either reinforcing or non-reinforcing, processing aids (i.e. plasticizers, oils and tackifiers, age resisting additives such as antiozonants and antioxidants and other miscellaneous materials such as blowing agents, flame retardants and colorants. The system for vulcanization is also selected in the polymer formulation process.

The elastomer formulation process starts with mastication of the rubber material with chemicals called peptisers (Fancy et al.,2013). The process reduces the material nerviness and changes the distribution of the molecular chains between the polymer network junctions (Fries and Pandit, 1982). Subsequently, in the formulation process, fillers and other additives are added to the masticated rubber material and mixing is done in millers for high shearing mixing (Ponnamma et al.,2013; Rajesh et al.,2013; Visakh et al., 2013). Mastication also reduces the viscosity of the

material and increases the incorporation and proper distribution of chemicals and fillers within the material (Fancy, 2013). In the mixing process, additives are incorporated into the rubber as rubber flows around these additives resulting in the formation of a matrix of rubber. Typically, the raw rubber material flows around an agglomerated filler particle where it penetrates the spaces between these particles, resulting in a reduction in the compressibility and an increase in the density of the rubber. After this, rubber becomes immobilized and dispersive mixing occurs (Kodal and Ozkoc, 2021). Finally, curatives are added when mixing is done and when the mixture is homogenized, the elastomers are sheeted out in batches (Fancy, 2013; Nortey, 1999; Tokita, 1966).

Vulcanization is a chemical process that involves blending rubber with activators, accelerators, and sulfur at reasonably high temperatures (i.e., 140 -160C) to improve the mechanical properties of elastomers by introducing more cross-links (Heideman et al.,2004; Mahak, 2021). These chemical cross-links are formed along the backbone of the polymer and result in a reduction in the plasticity and tackiness of the elastomer (Rajesh et al.,2013). The process results in the formation of a complex three-dimensional elastomer network and reduces the deformation of the polymeric material due to mobility between its molecular chains (Mark, 2013). The elastomer is transformed from a viscoelastic material to an elasto-viscous material in the vulcanization process (Wood, 1957; Rajesh et al., 2013). **Figure 24** is a diagrammatic representation of elastomers before and after the vulcanization process. Several vulcanization techniques exist in elastomer formulation. These include Sulfur, accelerated sulfur, Peroxide, metal oxide, Resin Cure, mixed, radiation, and dynamic vulcanizations (Bhowmik and Mangaraj, 2018).

Sulfur vulcanization is one of the oldest vulcanization methods which involves heating the rubber material with sulfur (usually ground sulfur) (Nieuwenhuizen, 2001). In some situations, the sulfur vulcanization process can be sped up with the aid of accelerators (Aprem et al.,2005). These are

chemical substances that catalyze the vulcanization process at lower temperatures for a minimum time. Common accelerators include aniline, thiazoles, and sulfenamides (Rajesh,2013; Bhowmick, 2018; Datta, 2002). Besides sulfur, peroxides are also used in vulcanization (Speigelhalder and Preussmann, 1983; Simpson, 2002). By their interactions with the molecular structure of the polymers via free radicals, they change their polarity and increase the performance of the elastomers at high temperatures. They also speed up the vulcanization process and enable cross-linking in both saturated and unsaturated rubber materials (Dluzneski, 2001).

In elastomer production using chloroprene rubbers, vulcanization is usually done with zinc oxides complimented with magnesium oxides to ensure that final elastomer produced has adequate resistant to scorch (Morton, 1987). Besides, a mixed vulcanization process can also be employed to ensure that the final polymeric material possess the beneficial properties yielded by each of the individual vulcanization process (Coran, 1995). For instance, both sulfide and peroxide vulcanization processes can be combined during an elastomer formulation. The process can yield preferable elastomer properties from both sulphur vulcanization as well as peroxide vulcanization (vBevervoorde-Meilof, 1998).

Finally, in dynamic vulcanization, a thermoplastic is mixed with a rubber phase simultaneously with the cross-linking process, resulting in a homogeneous melt end-product known as thermoplastic vulcanizate (TPVs) (George et al.,2000; Akiba, 1997). Dynamic vulcanization requires high enough temperatures (usually higher than the melting point of the thermoplastic material) and significantly high shear stress to activate the process (Naskar, 2007).

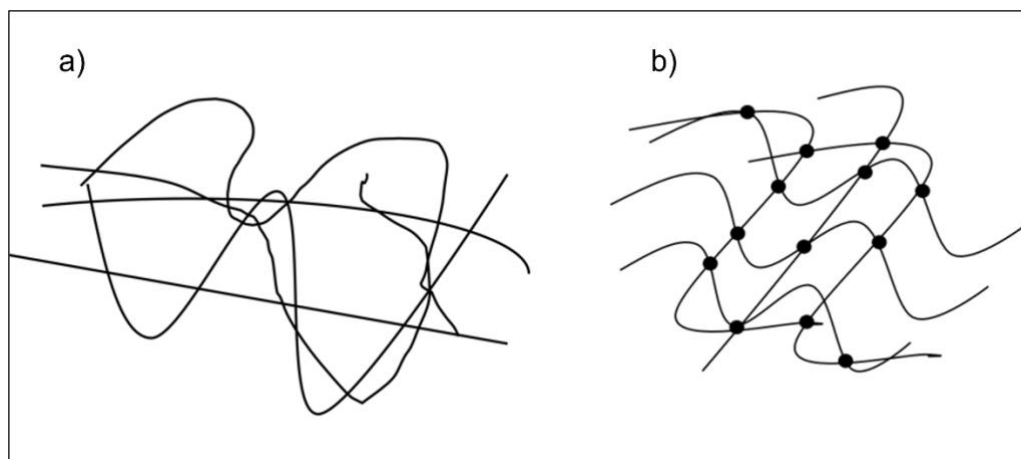


Figure 24: Diagrammatic representation of (a) raw rubber and (b) vulcanized rubber. Cross-linkages are represented by black dots, and lines represent the elastomer chains.

There are two broad categories of elastomers: thermosets and thermoplastics (Peters, 2002). Thermosets are three-dimensional polymer networks whose molecular structures are held strongly together by chemical bonds, mainly due to the vulcanization process (Princi, 2019; Mark, 2017; Amsden, 2008). They mostly swell due to solvent absorption but do not dissolve. Unlike thermosets, thermoplastic polymer networks are not primarily due to chemical bonds but rather due to the physical aggregation of their molecular parts into hard domains (Holden et al., 1969; Imato et al., 2016). Despite weaker cross-linkages, they have good elasticity and flexibility, as seen in most elastomers. However, thermosets are most common in end-use applications as they have better elasticity and are more durable. Common examples of thermoset elastomers include alkyl acrylate copolymer, bromobutyl (BIIR), chlorinated polyethylene (CPE), chlorosulphonated polyethylene (CSM), ethylene propylene diene monomer (EPDM), Fluoroelastomer (FKM), Natural Rubber (NR), Nitrile Butadiene Rubber (NBR), and Styrene Butadiene Rubber (SBR) amongst others (Simpson, 2002; Mark, 2017; Leung, 2018). The “F” in “FKM” represents “Flouro,” “K” is the German word “Kohlenstoff,” meaning “Carbon,” and “M” designates the saturated backbone of the rubber per American Society of Testing and Materials (ASTM)

definition. On the other hand, thermoplastic elastomers include Styrenic block copolymers, copolyether esters, and polyester amide elastomers (Holden, 1969; Bonart, 1979; Grady, 2005).

Elastomers can also be classified into general-purpose and special-purpose elastomers based on their specific application (Ponnamma et al., 2013; Deepalekshmi et al., 2013; Datta, 2004). As the name suggests, general-purpose elastomers are used in several applications (Shanks and Kong, 2013; Deepalekshmi et al., 2013). They are sometimes referred to as commodity elastomers due to their relatively cheaper costs and wide range of use (Princi, 2019; Colvin, 2004; Lee, 2003). Furthermore, they are mostly hydrocarbon polymers such as Styrene Butadiene Rubber (SBR), Natural Rubber (NR), polyisoprene rubber, polybutadiene, isobutylene, neoprene, silicone, polyurethane, and ethylene propylene diene monomer (EPDM) rubber amongst others. Typical usage of general-purpose elastomers is in producing vehicular tyres, as they possess excellent resistance to abrasion and good resilience properties (Colvin, 2004).

The most common general-purpose elastomer is Natural Rubber (NR), also called (cis-1,4 polyisoprene). It is resistant to abrasion and has high mechanical resilience and tensile strength (Subramaniam, 1987; Princi, 2019; Kohjiya, 2015). Also, despite having good electrical resistance and high resistance to acids, its resistance to oils and weathering is low (Deepalekshmi et al., 2013; Niyogi, 2007). The glass transition temperature of NR is about -70°C and thrives mostly in temperatures ranging from -50°C to 100°C (Princi, 2019; Loadman, 1985). The material is also highly processable with a low heat build-up property hence highly suitable for making trucks, aircraft, and giant off-the-road tires (Ponnamma et al., 2013; Elias, 2003; Jurkowska, 1998; Hirata and Ozawa, 2014). It is also used in the manufacture of non-linear, high-maintenance springs. EPDM has outstanding resistance to ozone and weathering, inorganic and polar chemicals, phosphates, alcohols, ketones, esters, and steam. However, its resistance to hydrocarbons is low

(Princi,2019; Stella, 1989; Karpeles and Grossi, 2000). This is because of its highly stable polymer backbone structure. Its usage is primarily seen in the manufacture of seals, steam hoses, electrical insulations, radiators, and roofing (Mishra, 2021). SBR, on the other hand, is a synthetic copolymer that consists mainly of styrene and butadiene. It has good chemical and abrasive-resistant properties (Shen et al., 2013). Its applications can be seen in the manufacture of conveyor belts, the soles of shoes, light vehicle cars, and rubber goods (Lodewijks, 2011; Bulbul et al.,2014). Polyurethane is another general-purpose elastomer which is a thermoplastic. They are versatile and exhibit variable hardness (Chen et al., 2007). They possess high mechanical strength, toughness, tensile and tear strength, and good resistance to abrasion and mineral oils, ozone, and oxygen. Besides, their heat resistance is low, and their electrical resistance properties leave much to be desired; hence, they are not commonly used in making insulators. However, their usage is mostly seen in manufacturing bellows fabrics, floorings, furnishing, composite wood, and cable jackets (Princi, 2019; Hilado, 1998). Like polyurethane, Styrenic block copolymers are another class of general-purpose thermoplastic elastomers. Their usage is mainly seen in enhancing the performance of bitumen or road paving. They also make adhesives and footwear (Visakh,2013; Princi; Temin, 1990).

Special purpose elastomers have specific applications in various jurisdictions as the name suggests. Typical examples include butyl rubbers, nitrile rubbers, Silicone rubbers, flouroelastomers, chlorosulfonated polythene and others (Deepalekshmi et al.,2013; Sweet, 1980; Yue, 2005). A few of them are described herein.

Butyl rubber is a special-purpose elastomer formed by the polymerization of about 95% or more isobutylene and about 1 -3 % of isoprene with the aid of $AlCl_3$ or BF_3 as catalysts (Gronowski, 2003). It is sometimes referred to as “isobutene-co-isoprene” (Deepalekshmi et al.,2013). Due to

its highly saturated hydrocarbon backbone, it is repellent to polar fluids and water. However, its philia for cyclic hydrocarbons and aliphatic hydrocarbons is high (Nohile et al.,2008). As a result, elastomer products made of butyl rubbers experience significant swelling when exposed to hydrocarbon solvents and oils and contrarily exhibit outstanding resistance to moist synthetic hydraulic fluids and plasticizers made of esters. Furthermore, it is notable for being highly impermeable to gases (i.e., hydrogen, CO₂, and nitrogen) stemming from its closely packed structure and exhibiting strong damping properties hence, its renowned usage and applicability in making sealants (Vohra et al.,2016). It is also used in making tubeless tyres, pneumatic springs, and accumulator bags amongst others. Butyl rubber can also be cross-linked with sulphur via organic accelerator or sulfur activation.

Nitrile Rubber (sometimes referred to as Nitrile-butadiene rubber), NBR is regarded as a “plodder” in industrial settings. It is highly resistant to industrial setting oils thus its usage in making hydraulic hoses, conveyor belts, oil and gas field packers, and plumbing and water-handling seals (Lachat, 2008). It has good resistance to compression, excellent elongation properties, and sufficient resilience for its applications (Visakh, 2013). NBR can be categorized as cold or hot, cross-linked hot, bound antioxidant or carboxylate nitrile NBRs (Lee, 1973; Ibarra and Alzorriz, 2007). It is formulated by a polymerization reaction of acrylonitrile and butadiene, aided by a catalyst. The catalysts are fed into the reactor vessel together with soaps and monomers resulting in the formation of latex coagulated with several materials. The final copolymer product usually has about 15 to 50% acrylonitrile present (Duffy et al, 1993; Blow, 1998).

Flouroelastomers are special-purpose elastomers with extremely high fluorine contents (typically 66 to 70% by weight) (Ameduri, 2001). As a result, they are highly resistant to mineral acids, chemicals, ozone, heat, harsh environments, oils, and lubricants. Compared to other elastomers,

their thermal stability is about 260C greater than most elastomers (Stevens, 2001; Ohm, 1990). They possess a totally amorphous nature with unique properties, thus, their special applications. The maiden flouroelastomers were polytetrafluoroethylene (PTFE) and polychlorotrifluoroethylene (PCTFE) with high and low molecular weights and were discovered in 1941 and 1937 respectively (Gardiner, 2014). The hydrolytic stabilities of these elastomers are very high. Hexaflouoropropylene (HFP) is another flouroelastomer developed in 1957 to meet the needs of the aerospace industry (Twum et al.,2013). More recent versions of flouroelastomers are produced by an emulsion polymerization process. In this process, the PTFE and HFPs are fed into reactors at high temperatures and pressures together with additives and some surfactants. The final product is then washed, dried, and packaged. Flouroelastomers are more thermally stable and have good mechanical properties (Lu et al.,2012). Furthermore, their resistance to chemicals and oil is not temperature dependent and is mainly due to the high bond dissociation energies of C-F and C-C bonds. They are used in the manufacture of shaft seals, O-rings, engine head gaskets, hydraulic hoses, fuel tanks, diaphragms, gaskets, valve seats, hoses, and tank lining with applications in chemical, petrochemical, and aerospace industries (Shanks and Kong, 2013).

Chlorosulphonated polyethylene elastomers are typically used in areas where solvent and chemical resistance is needed (Princi, 2019; John and John, 1992). They are usually formed when polyethylene is treated in a chlorine and sulfur dioxide solution. A common chlorosulphonated polyethylene elastomer is Hypalon which is highly resistant to extreme chemical and temperature levels and ultraviolet light. The elastomers discussed and their chemical structures are represented in **Figure 25**.

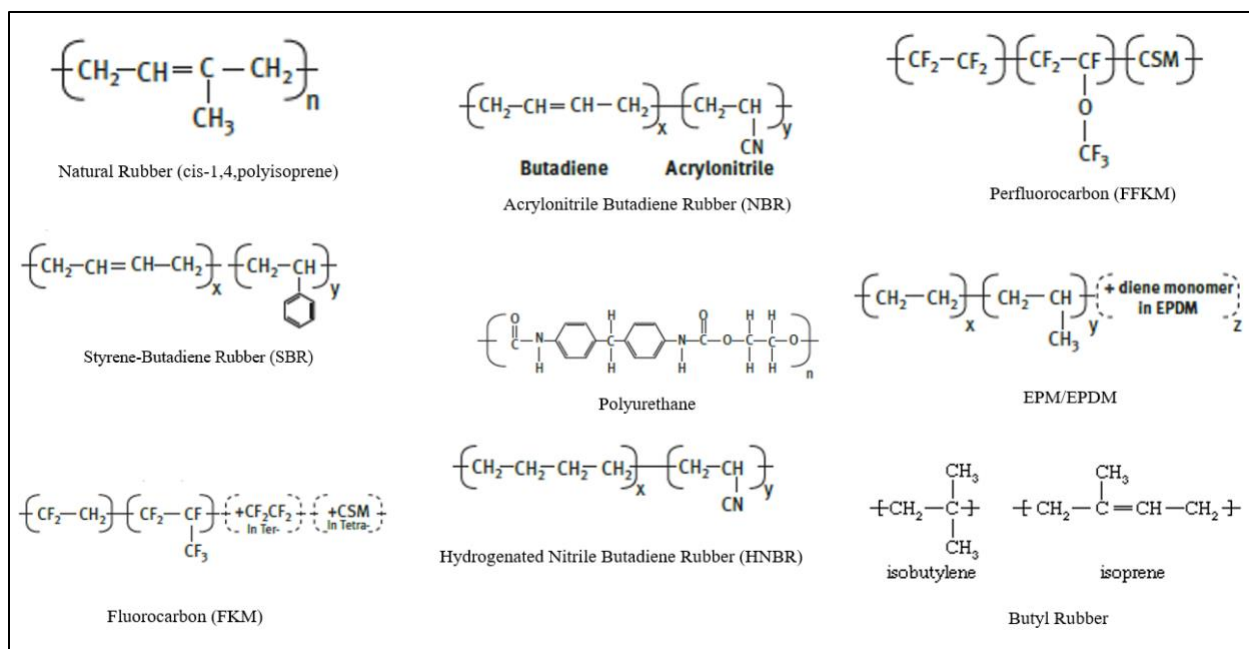


Figure 25: Molecular structures of common general and special purpose elastomers

As discussed in the review in this section, elastomers have a wide range of applications in the automotive, aerospace, chemical, petrochemical and oil and gas industries. They are used in manufacturing car tyres, static seals, shoe soles, flexible soles, conveyor belts, gaskets, boots, gloves, paints, stopers, cables, inner tubes and many more. The following section discusses specific use of elastomers in the oil and gas industry.

3.1. Elastomers Used in the Oil and Gas Industry

As discussed earlier, the petroleum industry is one of many industries that has a wide range of applications of elastomers. As compared to the automotive and aerospace industries, elastomers used in the oil and gas industry are subjected to relatively harsh conditions (i.e., high temperatures and pressures, acidic chemicals, oil-based drilling fluids, H₂S and soluble salts) (Mody et al., 2013). Their applications are mostly seen in drilling, completions and well control where they are used in making seal elements in packers, liner hangers, cement plugs, safety valves, O-rings, and Blowout Preventers (BOP) (Chen et al., 2021). These seal assemblies constitute the secondary well

barrier (fluid column forms the primary well barriers) against unwanted fluid influx from the reservoir (Patel et al.,2019; Skogdalen et al., 2011; Kiran et al.,2017). Other auxiliary applications are seen in their use in making drilling motors.

The Blowout preventer is a secondary well-barrier element used in well control in situations where there is a kick or a blowout (Patel et al., 2019; Fan, 2016). It is a large stack consisting mainly of a set of hydraulic valves used mainly in offshore drilling operations while drilling the intermediate and reservoir sections per a given well plan (Fan, 2016). It is typically a large valve with a donut-shaped elastomer. In a well control event, pressure is applied to this elastomer, causing it to expand and close around the drill pipe, sealing off the well in the process (Patel et al.,2019).

Packers, on the other hand, are mechanical devices that isolate the production tubing from the inner parts of the casing or liner (Zhong et al.,2022; Guo, 2011). Their mechanism of operation is such that they consist of a cone and slip assembly that energizes an elastomer element, causing it to compress and expand, offering the needed zonal isolation (Freyer and Huse, 2002; Kennedy et al.,2005). The elastomer elements, as described in BOP and packer elements, are shown in **Figure 26**. Production packers can be classified as permanent or retrievable. The former remains a downhole throughout the lifetime of the well and is usually milled through to get rid of them. The latter, on the hand, have a mechanism for retrieval using service tools. They are often used for brief periods during cementing, casing, or some other well-construction event, after which they are removed (Zhong, 2016).

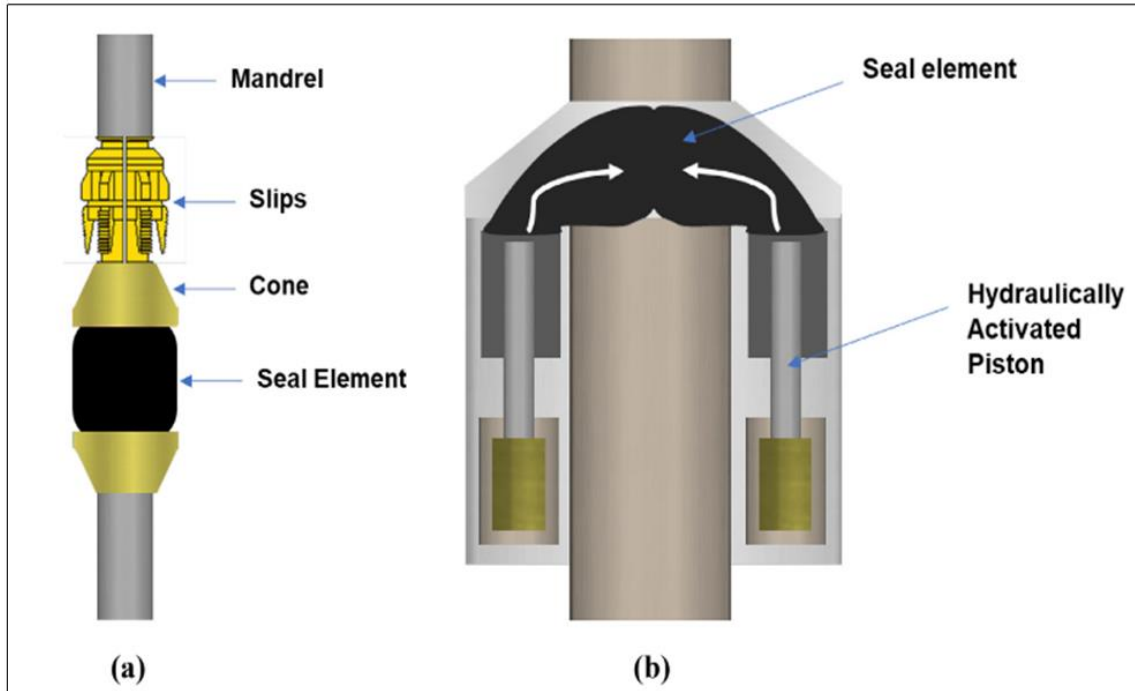


Figure 26: (a) Elastomer seal elements in packer; (b) Elastomer seal element in Blowout Preventer (BOP) (Patel et al.,2019)

Liner hanger systems are similar to casing strings; however, they are hung from the previous casing strings and do not extend all the way to the surface of the well. Like casing strings, they isolate the wellbore from the formation (Mohammed and Al-Zuraigi, 2013; Moore et al.,2002). A typical liner hanger arrangement is made up of a compression plate, an elastomer, and slips (Ahmed et al.,2019). Sealing is achieved by applying a hydraulic or mechanical force that pushes the slip towards the opposite surface. As the force is continuously applied, the elastomer is compressed and the compression plates at the bottom are anchored by slips (Patel et al.,2019, Speer, 2006).

According to (Mody, 2013), elastomers have been in existence in the oil and gas industry since the beginning of the 20th century, when Natural Rubber (NR) was the earliest and only available elastomer for use in the early 1900s. It was the main elastomer used in making seal elements in the industry despite its inability to withstand high temperatures and oils. A similar but more

advanced elastomer to NR, known as polychloroprene, was made in the 1930s (Johnson, 1976). It has a similar polymer chain compared to NR but for the addition of a chlorine atom in the chain. By 1934, NBR had been produced, and it became a household use elastomer in the oil and gas industry in the design of downhole seals. **Figure 27** shows NBR usage in a packer element by Baker Hughes.

Due to advancement in oil and gas drilling activities (i.e., drilling at higher depths and high temperature formations), a need arose for elastomers that have higher thermal and chemical resistivity compared to NBR. This necessitated the advent and usage of perfluoroelastomers between the 1950s and the 1970s as elastomers with high thermochemical stability for use in downhole equipment in oil and gas wells (Logethetis., 1989; Gaines, 2022).



Figure 27: NBR elastomer (black) in Model D packer by Baker Hughes (Mody, 2013)

Although highly thermally stable, its ability to maintain good mechanical stability at such high temperatures is restricted. Hydrogenated Nitrile Butadiene Rubbers (HNBR) came into play in the 1980s as elastomers with high stabilities even in chemically aggressive environments. **Figure 28** depicts a timeline of elastomer applications in the petroleum industry since its advent. **Table 7**, on the other hand, shows a list of several elastomer applications in petroleum engineering.

Table 7: Summary of Applications of Elastomers in the Oil and Gas Field (Adapted and modified from Mody, 2013)

Name of Seal Assembly	Function	Base Polymers	Conventional Sizes
Retrievable Packers	Pressure and Flow	NBR, HNBR, FEPM, FKM	Up to 50 cm OD, 1.25-5cm wall
Blow-out Preventers	Well Control	NR, EPDM, NBR	100 – 250kg
Inflatable Packers	Pressure and Flow Control, Zonal Isolation	EPDM, HNBR, NBR	4-20CM od, 0.3-0.6cm wall, 3m long
Production Tubing to Packer Seal: Rubber to Metal Bonded Seals	Pressure and Flow Control	NBR, HNBR, FKM, FEPM	10-20cm OD, 0.3-0.6cm wall, 10cm long
Swellable Packers	Zonal Isolation, Pressure, and Flow Control	NBR, EDPM	10-20CM OD, 1.25-5cm wall, 3m long
Production Tubing to Packer Seal: v-packing/ seal stacks	Pressure and Flow Control	NBR, HNBR, FEPM, FKM, FFKM	1.25-13cm OD, 0.3-0.6cm across section
Safety Valve Dynamic Seal O-ring/v-ring	Pressure and Flow Control	NBR, HNBR, FEPM, FKM, FFKM	1.25-13cm OD, 0.3-0.6cm across section

Drill Bit Dynamic Seals	Pressure and Flow Control	HNBR	1.25-20 cm OD
Mud Motor Stators/PCP Stators	Pressure and Flow Control	NBR, HNBR	5-15cm mean diameter, 0.3-1.25 cm radial cross section
Pressure Compensating Bladders	Fluid Separation, Pressure Compensation	NBR, HNBR, FKM	5-15 cm OD, 0.15-0.3cm wall

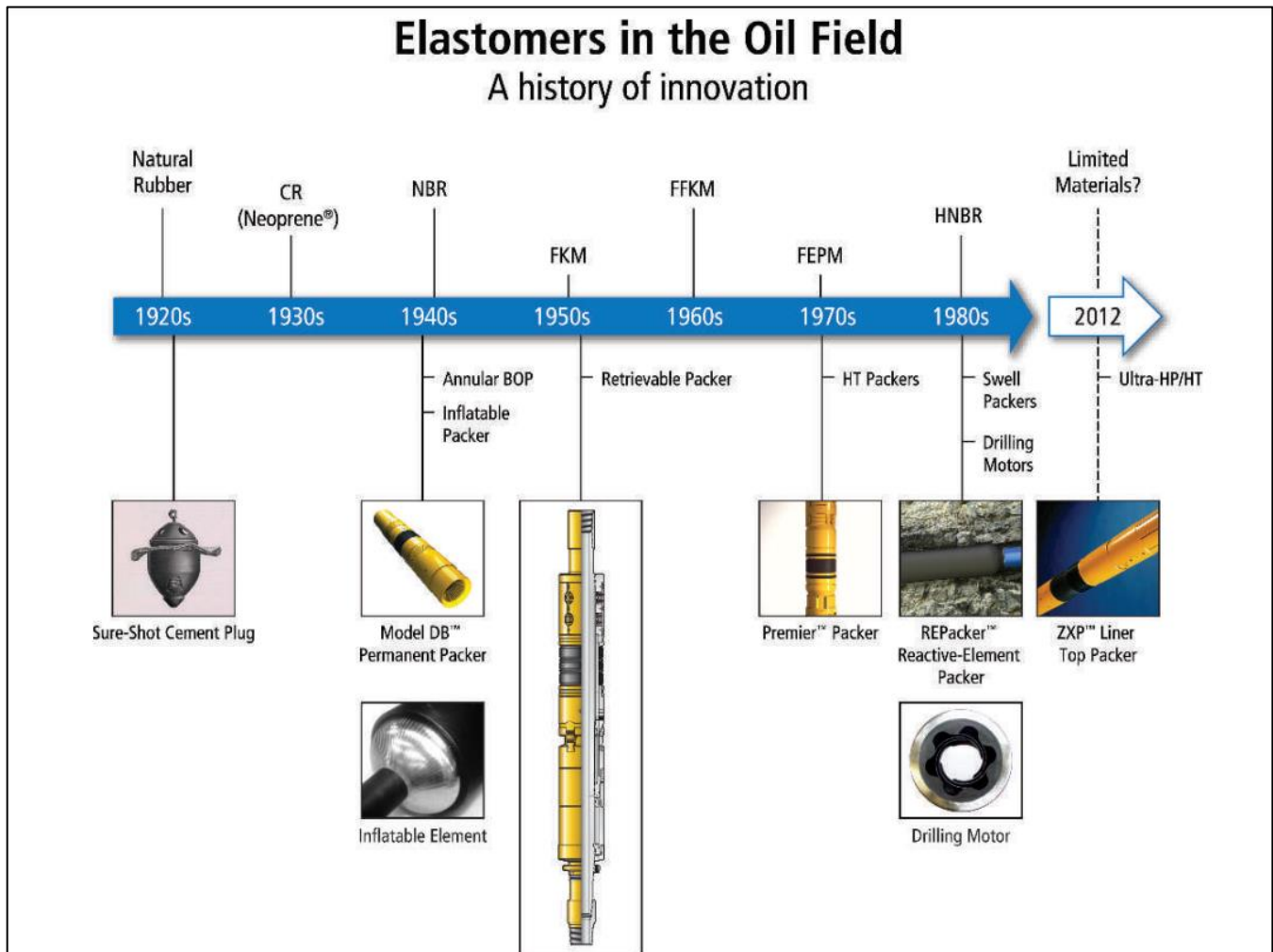


Figure 28: Evolution of elastomer applications in the petroleum industry (Mody, 2013)

Main challenges associated with elastomers include failures due to exposure to high temperatures and extreme chemicals as well as blistering, and cavitations due to explosive decompression. Thus, the selection of a particular type of elastomer for specific usage in the oil and gas industry depends on its ability to be non-susceptible to these challenges (Stahl, 2006; Patil et al., 2005).

Furthermore, on one hand, these elastomeric materials remain downhole for a significantly long period of time (about 20 to 30 years) under these harsh conditions. On the other hand, the properties of these elastomers need to be maintained over these long periods. Stemming from the fact that it is highly expensive to replace failed elastomers downhole, design and testing methods need to be put in place to ensure that the designed properties of elastomers are maintained over the long service periods. Testing and selection criteria for elastomers are based on the following standards: American Society of Testing and Materials (ASTM), American Petroleum Institute (API), International Organization for Standardization (ISO), and the National Association of Corrosion Engineers (NACE) and the American National Standards Institute (ANSI).

3.2. Elastomer Failure Modes

As discussed earlier, some commonly used elastomers in the oil and gas field include NBR, EPDM, FKM (Viton/Flouroelastomers), HNBR, and FEPM (Perflouroelastomers). Each of these elastomers is susceptible to failure due to degradation on exposure to harsh conditions downhole. i.e., high temperatures and pressures, corrosive fluids, and mechanical stresses.

Elastomers undergo degradation when exposed to chemicals, heat, UV light, gases, and ozone amongst others. The process results in a change in the mechanical properties (i.e., hardness, compressive and tensile strength), chemical changes in elastomeric chain structures, and formation

of cracks, blisters and microvoids (Hill 2019; Ahmed and Salehi, 2021; Mitra et al., 2004; Harwood, 1983). Depending on their chemical make-up, elastomers respond differently to degradation. In oil and gas applications, elastomers are energized (as seen in liner hanger seals and packers) to produce a firm contact pressure referred to as sealability (Ahmed and Salehi, 2021). Elastomer degradation may result in loss of elastomer sealability and ultimately resulting in failure of the seal assembly. Furthermore, on subjection to cyclic loading, especially during injection and withdrawal phases in gas storage and geothermal applications, degraded elastomers lose their physio-mechanical properties and structurally damage in the process resulting in ultimate failure (Bosma et al.,1999). In this section, some of the common failure modes of elastomers are discussed.

A common mode of failure of elastomers at downhole conditions is chemical degradation (Garfield et al., 2007; Tan et al.,2007). The process occurs when the elastomer comes in contact with a chemically corrosive material. First, the chemical causes erosion of the material surface, after which it spreads diffusively into the internals of the seal material. At this point, the chemical reacts with the polymeric structure and the cross-links of the rubber material. This could result in a break in the cross-links within the elastomer material (Slikkerveer et al.,1999; Hill, 2019). Another common term in elastomer chemical degradation is chemical ageing which usually occurs at high temperatures. The process can result in cross-link formation or elastomer chain scission and is facilitated by high temperatures (Zaghdoudi et al., 2019). A chemically degraded elastomer usually has reduced mechanical strength and becomes more relaxed (i.e., an indication of a loss of its sealing property) (Richter and Blobner, 2017). In oil and gas drilling and completions, elastomers in seal assemblies are exposed to drilling and completion fluids, hydrocarbons, organic and inorganic acids, and other corrosive chemicals (Kubena et al.,1991). These chemicals may cause

chemical degradation of these oil and gas field elastomers, as discussed (Campion et al.,2005). Chemical degradation of elastomers also depends on the temperature at which the rubber materials are exposed, the period of exposure and the polymeric structure of the rubber material (Richter and Blobner, 2017; Shakiba et al.,2021). More so, degradation is higher at higher temperatures (Patel et al.,2019).

Furthermore, physical traces and evidence of chemical degradation are not always seen (Campion et al., 2005; Richter and Blobner, 2017). Sometimes, a chemically degraded elastomer only shows high compression set signs (i.e., it does not return to its original state after compression). Besides, other evidence of a chemically degraded elastomer includes visible cracks on the medium (either with the eye or under a microscopic lens), softening with a sooty surface, and a loss in material elasticity. **Figure 29** shows examples of the chemical degradation of some elastomers used in the petroleum industry.

The potential for chemical degradation of elastomers in gaseous environments via reaction between the elastomers and gas molecules has been studied by several authors. Cong et al. (2013) exposed HNBR elastomers to H₂S gas at 1000psi and 212°F. From their results, they observed a deterioration in the hardness and tensile strength of the elastomers. Also, the authors reported acidic hydrolysis of the C≡N group in HNBR by H⁺ ions formed by heterolysis of the gaseous molecules. In addition, the C=O group in HNBR was also attacked by the HS⁻ ions from the heterolysis reaction. The reactions resulted in the formation of two new functional groups; C=S and C—C=S, indicating an alteration in the molecular structure of HNBR due to formation of new compounds. Besides H₂S, CO₂ attack on elastomers has also been studied. According to Salehi et al. (2019), stemming from the high bond dissociation energies of CO₂ (i.e., 749 kJ/mol), chemical reaction of CO₂ with elastomers is unlikely. However, the gas may dissolve in brine (where

present) to form carbonic acids which may chemically corrode elastomers. Daou et al., 2014 exposed FKM, EPDM, and PTFE elastomers to supercritical CO₂ and CO₂ saturated brine in a high-pressure-high-temperature (HPHT) autoclave reactor vessel at 122°F temperature and 3000psi pressure. The authors mentioned that CO₂ molecules migrate into the molecular structure of the elastomers and may cause swelling and alteration of the mechanical properties of the elastomers leading to tearing and extrusions on the material surface. Their results showed a 6%, 10% and about 40% swelling compared to the original volume for EPDM, PTFE and FKM elastomers respectively.

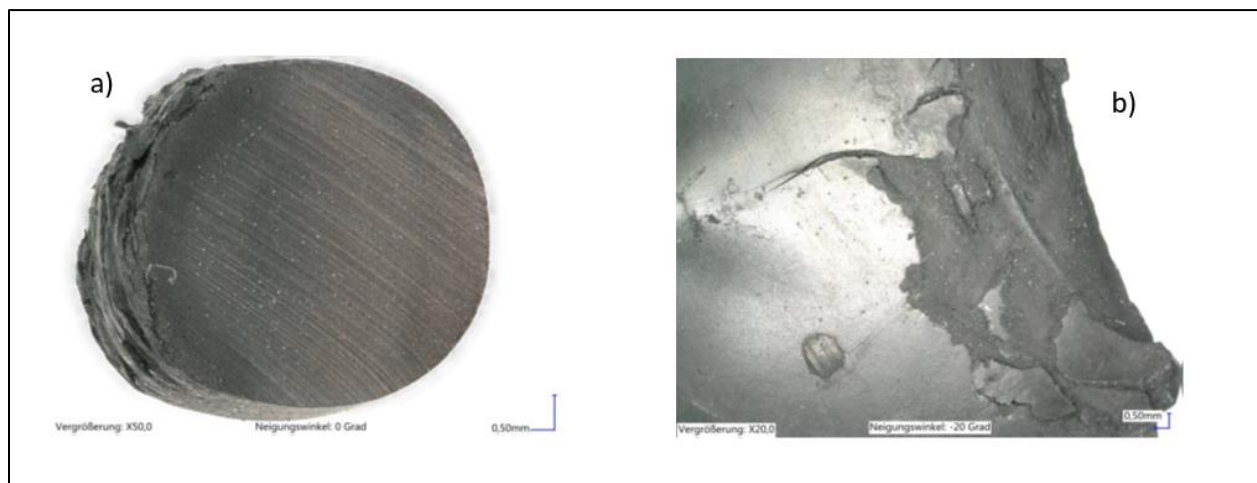


Figure 29: (a)FKM elastomer chemically degraded by inorganic acids (b) Chemically degraded EPDM elastomer. (Richter and Blobner, 2017)

Besides chemical degradation, elastomers may also swell on the absorption of downhole fluids resulting in another mode of failure known as extrusion (Elhard et al., 2017). Extrusion can be crucial, especially in downhole oil and gas equipment like the BOP (Chen et al.,2019). Usually, the contact surfaces in sealing assemblies have a small gap between them to permit motion. In some instances (when elastomers are subjected to high pressures and temperatures or are swollen due to fluid absorption), the elastomers undergo deformation and fill this gap. High-stress

concentrations occur at extrusion regions and may result in the deformation of the elastomer. With time, a fracture forms in this region to release the accumulated stress, creating a leakage pathway (Winslow and Busfield, 2019). In oil and gas seals, extrusion failures can also result in difficulty in retrieving the seal elements (Patel et al.,2019)

Another common type of failure in elastomers is abrasion failure, usually experienced during the installation (Patel et al.,2019). Lancaster defined abrasive wear as one caused by hard abrasive materials between two seal surfaces or on one of the surfaces in relative motion, resulting in a displacement of materials on the surface (Lancaster, 1969; Shen et al., 2016). The presence of debris and other solid matter at the sealing interface and improper lubrication of these surfaces are primary causes of abrasion failure (Patil and Coolbaugh, 2005; Feyzullahoglu, 2015). Other causes include corrosive materials in fluids between surfaces (Shen et al.,2016). It may also sometimes occur when there is no proper lubrication on the sealing surfaces (Feyzullahoglu, 2015).

Elastomers may also fail due to a well-known phenomenon referred to as explosive decompression (Briscoe et al.,1994; Edmond, 2003). Bottomhole conditions are usually associated with gases at high pressures which are usually absorbed into the voids in the molecular structure of elastomers (Balasooriya et al.,2022; Menon et al.,2016). On a sudden reduction in pressures of surrounding gases, the elastomers, in a compressed state, expand as absorbed gases forcibly escapes the elastomer. This leads to the formation of microvoids within the elastomers, which subsequently results in blister and crack formations (Kwatia et al., 2017; Schrittester et al., 2016; Patel et al., 2019; Ahmed et al., 2021). Blisters are bubbled defects on elastomer surfaces. It is usually caused by rapid expansion and release of gas molecules dissolved in elastomers due to decrease in surrounding gas pressure.

Furthermore, a phenomenon known as buckling may also occur during RGD. In this process, absorbed gas molecules can permeate through elastomers and coalesce at the interface between the liner material and the host composite (i.e., a tube or pipe). During RGD, stress is exerted on the outer layer of the liner by accumulated gas molecules, detaching the liner from its host. This structural defect is known as buckling collapse (Melnichuk et al., 2020; Reuda et al., 2012).

Cavitation in elastomers may also subsequently result in its failure. Cavitation is the existence and subsequent expansion of microscopic voids present intrinsically in a rubber matrix (Gent, 1990; Mahak, 2019). Micro voids may either be pre-existing in elastomer rubber matrix due to elastomer chain inhomogeneity during manufacture or caused by RGD. The latter leads to the loss of rubber materials and a subsequent reduction in material conformity hence the formation of microcavities (Mahak, 2019). These micro pores coalesce locally to form flaws which under the influence of external stresses result in crack formation and growth (Eirich, 1973).

3.3. A Review of Elastomer Behavior in Gaseous Hydrogen Environments

Based on the discussions so far, it is inevitable that elastomers in seal elements (i.e., secondary well barrier elements) in depleted oil and gas wells repurposed for large-scale gas storage operations stand a risk of failure due to many factors. Some of these factors include exposure to storage gases (i.e., H₂, CO₂, and methane) (Kulkarni et al., 2021; Simmons et al., 2021; Lorge et al., 1999; Ansaloni et al., 2020; Salehi et al., 2019), stresses from pressure cycling associated with stimulation, injection, and production operations (Ahmed and Salehi, 2021; Bosma et al., 1991; Dusseault et al., 2014), and pressure and temperature conditions (Balasooriya, 2018). In this

section, the deterioration of elastomers (by any of the discussed failure modes) due to the individual factors mentioned or a combination of them is presented.

As described earlier, one of the critical failure mechanisms of elastomeric seals in oil and gas wells is explosive decompression (i.e., rapid gas decompression). The phenomenon has been studied by different authors for different gases and at varied experimental conditions.

Yamabe and Nishimura (Yamabe and Nishimura, 2012) investigated rapid gas decompression failures in acrylonitrile butadiene rubber (NBR) on exposure to high-pressure hydrogen gas. In their study, the authors examined the relationship between the hydrogen content, the mechanical properties of the material, and the extent of blister damage in the explosive decompression failure process. Further investigations were also conducted to determine chemical deterioration within the rubber material. Experiments were carried out in a durability tester that allowed the exposure of the elastomeric materials (in the form of O-rings) to gaseous hydrogen at different experimental conditions. Some of the experimental samples were compressed at ratios ranging from 8 - 30% during experiments where they were exposed to hydrogen at atmospheric pressure to about 100MPa and temperatures ranging from -60°C to 100°C. According to the authors, exposure of O-rings to gaseous hydrogen in compressed state results in crack formation in a direction parallel to the compressional force applied after decompression. This is due to stress generated at the center of the specimen. Conversely, in an uncompressed state, cracks formed are ring-like and are distributed randomly. Furthermore, at high decompression rates, cracks appear on the surface of the elastomer. **Figure 30.** shows the crack distribution in elastomers at both compressed and uncompressed states after decompression. SEM images obtained for O-rings exposed repeatedly to hydrogen at 100MPa indicated that fatigue cracks started from within the elastomer and not on the surface. The authors also determined that decompression at high pressures for samples exposed

to hydrogen creates small-scale fractures within the elastomers due to bubble formation. However, these bubble defects rarely affect the tensile properties of the elastomers except only in cases where the bubbles result in the initiation of blisters.

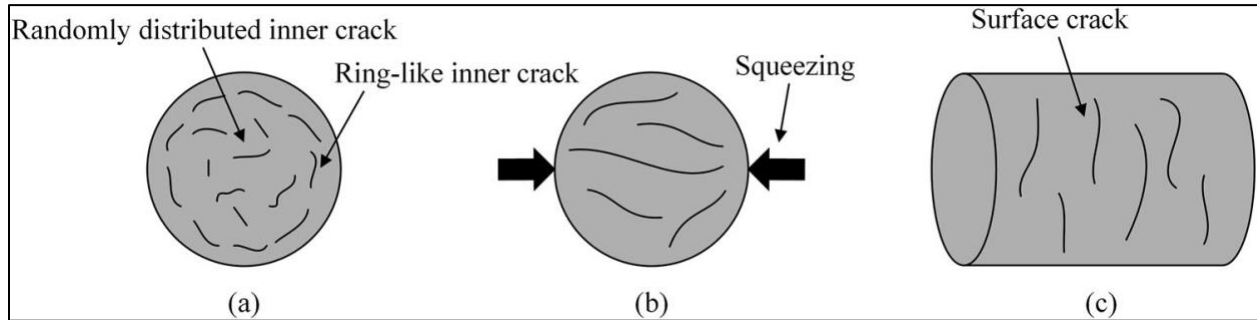


Figure 30: Diagrammatic representation of crack distribution in elastomers after decompression for (a) Elastomers in an uncompressed state (b) Elastomers in a compressed state (c) Elastomers after explosive decompression (Yamabe and Nishimura, 2012).

Schrittesser et al., 2016 also studied rapid gas decompression failures by exposing hydrogenated butadiene rubber with 36% acrylonitrile content to several gas mixtures at different temperatures and pressures and for different decompression rates. Experiments were conducted in an autoclave equipped with a customized camera system to observe and record the changes in the volume of elastomer due to exposure to experimental conditions. The authors used cylindrical specimens with heights and diameters of 8mm in their experimental investigations. Furthermore, the dimensions O-rings used in component testing had diameters of 15.44mm and thickness of 5.33mm. Experimental pressures were 50, 100, and 150 bar (~ 725.2, 1450.4, and 2175.6 psi) with temperatures ranging from 70°C (158°F) to 110°C (230°F), and exposure times were approximately 20 hours.

Furthermore, a constant depressurization rate of 10MPa/min was applied. The authors used a NORSOK ranking testing standard to characterize changes in material properties, as shown in **Table 8**. From their results, the authors concluded that increasing the test temperature results in a

decrease in the volumetric change of the material, thus, an increase in the Norsok ranking of the material. This is seen in the initial crack formation in the material and its subsequent breakdown at higher temperatures. Furthermore, the material performance is also dependent on the aging gas. The authors determined that an increase in the CO₂ content of the aging gas resulted in an increase in the volumetric change of the material during depressurization. Also, the observed Norsok ranking of the materials increases as the saturation pressure increases. On the effects of depressurization rates, the authors determined no solid connection between decompression rates and volumetric changes in a material, as changes in the Norsok rankings were insignificant.

Table 8: Criteria for ranking elastomer damage based on Norsok testing standard (Schrittesser et al., 2016)

Description	Rating
No internal cracks, holes, or blisters of any size.	0
Less than 4 internal cracks, each shorter than 50% of the cross section, with a total crack length less than the cross section.	1
Less than 6 internal cracks, each shorter than 50% of the cross section, with a total crack length of less than 2,5 times the cross section.	2
Less than 9 internal cracks of which max. 2 cracks can have a length between 50% and 80% of the cross section.	3
More than 8 internal cracks, or one or more cracks longer than 80% of the cross section.	4
Crack(s) going through entire cross section or complete separation of the seal into fragments.	5

Balasoorya et al., 2018 investigated the behavior of hydrogenated nitrile butadiene rubber (HNBR with 36% acrylonitrile content) for oil and gas applications. The elastomeric samples were exposed to different solvents and gases, as seen in oil and gas well settings at different aging conditions. Furthermore, the effects of aging conditions on the materials resistance to rapid gas decompression (RGD) was also investigated. This was done by testing the decompression resistance of the virgin samples and comparing it to the aged samples. Furthermore, changes in the mechanical properties of the material were also investigated via tensile testing of both virgins, swollen and de-swollen

samples. The authors further determined a correlation between the extent of material degradation and its level of swelling. Elastomer samples were machined into cylindrical shapes for RGD tests. The samples were aged in autoclaves exposed to 100% carbon dioxide (CO₂) at 90°C and 15MPa, and the depressurization rate was set at 10MPa/min. The autoclave is also equipped to conduct testing with CH₄ as aging gas. The effects of RDG were investigated with a light microscope at three different radial cut sections. The number and length of internal cracks within the elastomers were observed and ranked according to the NORSOK rating system as used by Schritteser et al., 2016. In their conclusion, the authors claim that given the test conditions, when the elastomer is de-swollen, it regains all its properties as it possesses in an unswollen state. Furthermore, on the one hand, the authors reported a relatively lower volumetric increase for swollen samples in the compression phase. On the other hand, the least volumetric increase was seen in the swollen sample, followed by the thermo-oxidative aged and pure unaged samples. Besides, when these samples were ranked based on the NORSOK rating system, the thermo-oxidative aged sample performed better compared to the others.

Ahmed et al.,2019 also studied RGD failures in two principal general-purpose oil and gas field elastomers, EPDM and NBR in line with developing testing protocols for verifying the behaviors of elastomer seal assemblies as used in liner hanger seal assemblies. The authors exposed the samples to a CO₂ saturated autoclave at approximately 4.14Mpa and room temperature for 72 hours. After aging and decompressing within less than a minute, the authors reported an observed visible cracks and blisters on the elastomer which was mainly because of the high rate of decompression. According to the authors, standard RGD test should be done at decompression rates between 290psi/min and 580psi/min. However, in this test, decompression rate was higher and thus deemed as an experimental limitation.

It is worth noting that rapid gas decompression failures are not typical in large-scale underground gas storage conditions due to relatively lower injection and withdrawal pressures. According to Brun and Rainer (Brun and Rainer, 2018), maximum withdrawal pressures at underground gas storage stations are usually less than 7MPa, with injection pressures typically within the range of 20-28MPa. Considering this, Yamabe et al. (Yamabe et al., 2008) exposed an Ethylene Propylene Diene Monomer (EPDM) and Nitrile Butadiene Rubber (NBR) to a gaseous hydrogen environment at pressures less than 10MPa and a temperature of 30°C. Their objective was to investigate the hydrogen permeation properties and damage due to blister formation. The authors observed that in a similar manner as other gases, hydrogen could cause blisters in elastomers; however, the damage is less severe when the concentration of hydrogen molecules decreases (Yamabe et al.,2008; Yamabe et al.,2009).

Besides RGD, elastomer degradation via cavitation in gaseous environments has been extensively studied. As discussed earlier, exposing elastomers to gases for an extended period results in absorption of gases into the molecular structure of the elastomer. Furthermore, stress generated by the absorbed gas results in microvoids (micro-cavity) formation. Subsequently, nucleation of these cavities occurs and propagates to form cracks, adversely affecting the performance of the elastomers in the process.

Gent conducted one of the earliest studies of cavitation in rubber materials (Gent and Tompkins, 1969; Gent, 1990). The author investigated internal fractures in elastomeric materials. In their methodology, they posited that while the critical stress required for internal rupture to occur is independent of other mechanical properties of the elastomer, it is proportional to the modulus of elasticity of the rubber. According to the author, elastomer failures result from very minute precursor cavities formed when the elastomeric material is subjected to stress from supersaturating

these elastomers with gases at high pressures. When the critical pressure of value $5E/6$ (where E represents the modulus of elasticity of the materials with rubberlike elasticity) of a given rubber material is exceeded, visible bubbles (precursor cavities) (**Figure 31**) appear in the interior of the rubber material and these cavities may grow infinitely when the applied pressure is increased. At pressures less than these critical values, bubbles do not appear. On reaching the maximum extensibility of the material due to increasing pressures, cavities will propagate into a crack on the material's surface. The author further observed that the critical value for internal precursor cavities to appear in the rubber material is greater than $5E/6$ for smaller volumes of the test samples. Also, the number of cracks on the surface was more when applied stress exceeded $5E/6$. Further reported was that at higher pressures, two types of cavities may appear: larger and relatively smaller ones surrounding the larger ones. According to the author, bubbles with smaller sizes are more hesitant to appear on the material's surface than larger voids due to their restriction by tensional forces at the material's surface. The author concluded that a possible cause of the anomaly is that rubber does not necessarily follow the kinetic theory of elasticity at significant deformation stresses. Furthermore, the microvoids in rubber materials have radii ranging from 0.1 microns to 1 mm as far as the rubber has a large enough volume to accommodate them. The author recommended further study on the effects of superimposed stress on the critical stress needed for cracks to be formed.

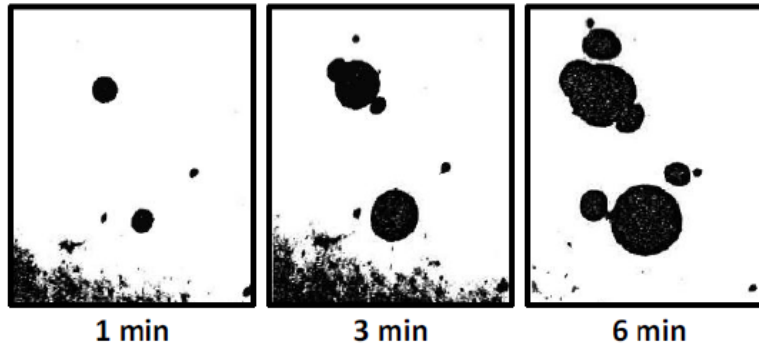


Figure 31: Appearance of bubbles in rubber material after supersaturation with gaseous Argon at 2.4MPa after 1, 3, and 6 minutes (Gent, 1990)

Stevenson and Morgan (Stevenson and Morgan, 1995) proposed a possible explanation for the principle of cavitation. According to the authors, due to inhomogeneity in elastomers during the manufacturing process, they tend to have regions of low cross-link density. Such regions have free volumes and, thus, pre-existing micro-voids. When saturated with gases, these pre-existing micro-voids swell to form cavities which subsequently initiate crack formation. Besides, Gent and Tompkins (Gent and Tompkins, 1969) already posited that cavities are more likely to form in regions in elastomers with defects and impurities due to their making. Another notable principle behind cavity formation was posited by Yamabe and Nishimura (Yamabe and Nishimura, 2009). The authors claim that during decompression (after saturation of elastomers with gases), gas molecules accumulate to form agglomerates in regions of the elastomers with low cross-link densities. As a result of the stresses generated by these agglomerates, they initiate cavity formation and, subsequently, crack generation and propagation within the elastomers, as shown in **Figure 32**.

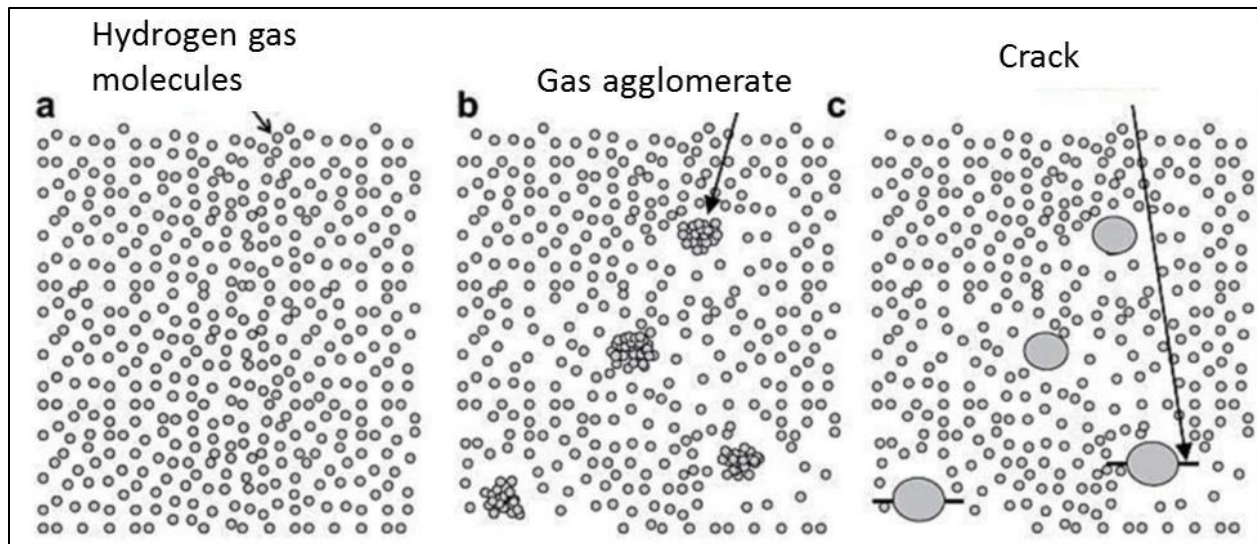


Figure 32: (a) Dissolution of hydrogen in elastomer at the end of saturation (b) Gas bubble formulation by agglomeration of hydrogen molecules (c) Cavity formation due to stresses generated by gas bubbles (Yamabe and Nishimura, 2009)

A more recent study on cavitations in rubber materials was conducted by Jaravel et al., 2011. The authors investigated parameters affecting the on-set of cavities in rubber materials after an explosive decompression in a pure saturated gaseous hydrogen environment. Silicon rubber (vinyltrimetoxysilane) was exposed to a pressurized hydrogen environment at pressures ranging from 0.1 to 27MPa in a temperature-regulated chamber. After gas saturation, depressurization was conducted at pressures from 1 to about 90 MPa. Two different depressurization tests were conducted to detect the effects of loading factors. The first involved depressurizing at different rates while maintaining the same saturation pressure, whereas the second was vice versa. i.e., the decompression rate was kept constant, but the saturation pressures were varied. As a safety measure, the chamber was purged with nitrogen to prevent its hazardous mixture with oxygen before carrying out experiments. The behavior of the elastomer was observed under a Sony XCD SX 90CCD camera that had an Avenir TV Zoom Lens, which took pictures at 1 picture per minute over the entire experiment. The authors first observed that damage in elastomers occurs primarily via an onset of cavities, and as proposed by Gent et al., 1990, two different cavity populations

occur a first population consisting of larger-sized cavities and a second consisting of smaller cavities surrounding the larger ones. The authors also concluded that explosive decompression in rubbers could be prevented when elastomeric samples are pressurized at low pressures and decompressed at slow depressurization rates.

Furthermore, the decompression rate also affects the cavitation process besides saturation pressures. On the one hand, when decompression rates are higher, the cavities appear faster in the elastomer material. On the other hand, higher saturation pressures result in a slower onset of gas bubbles (micro-cavities) in the elastomer. The authors also posited that during the pressurization state, it is possible to determine the time for which cavitation occurs; however, this is relatively very challenging during depressurization. Finally, the authors also concluded that increasing the mechanical loading on the elastomers via applied pressures from the saturation gas reduces the time of cavitation.

The effects of exposure pressures and decompression rates on the onset, growth, and nucleation of cavities to propagate crack formation in EPDM elastomers were studied by Kane-Diallo et al.,2016. The authors examined the statistics of the cavities, their rate of occurrence with time, and the effects of depressurization rates on their numbers and how they are distributed.

Experimental test temperatures were between atmospheric temperature and 150°C while pressures ranged from atmospheric pressures up to 40MPa. The decompression rates experimented with ranged from 0.75 to 30MPa/min. Stemming from the results obtained by in-situ camera-captured images, the authors observed that when saturation and decompression pressure increase, the number and size of the cavities also increase, but the relationship is non-linear. Furthermore, when decompression rates were lower, the observed cavities were separate and localized but later combined to form larger cavities at higher decompression rates. Similar studies on the growth and

evolution of cavities in elastomers on exposure to gases have also been studied by Briscoe et al.,1992.

Koga et al., 2013 investigated the effects of polymer type and gas on the initiation of blisters and subsequent blister damage for two major polymer types used in hydrogen equipment: EPDM (Ethylene Propylene Diene Monomer) and VMQ (Vinyl Methyl Polysiloxane) O-rings. Their approach involved the use of a high-pressure gas exposure container that facilitated the use of an optical microscope to visualize internal damages within the elastomer samples during pressurization and depressurization. The elastomer samples were exposed to three different gases: hydrogen, nitrogen, and helium, at temperatures and pressure of 25°C and 3MPa. After 0.3 seconds, the container was depressurized, and damage initialization was visualized. No blister damage was observed in VMQ. However, on the other hand, blister damage was seen in EPDM. They examined the initiation of the blisters and the extent of damage based on the size of the blisters. They observed that damage in a hydrogen environment was more severe than that of helium but less than in nitrogen. This was directly related to the diffusivity coefficient of the gases. The smaller the diffusivity coefficient, the less time it takes for the gas to diffuse out of the elastomer, and hence the greater the blister damage.

Also, Salehi et al., 2019 investigated the "fitness for service" of some commonly used oil and gas industry elastomers by exposing them to downhole corrosive conditions. Elastomers studied include NBR, EPDM, Fluoroelastomer (FKM), and Polytetrafluoroethylene (PTFE). All experiments were conducted at a constant pressure of 1000psi (6.89Mpa) at two different temperatures; 120F (48.8C) and 180F (82.2°C). The elastomers were aged for 1, 3, and 7 days with an aging vessel pressurized with three different gases: CO₂, H₂S with methane as a carrier, and CH₄. For some experimental batches, a mixture of these gases was used based on their partial

pressure ratios. All elastomers were aged in a brine phase or vapor from a brine phase. They studied the effects of temperature and gas variations on the mechanical properties of elastomers by measuring hardness, compressional strain, and volumetric swelling. Their results showed that generally, NBR and EPDM elastomers soften on exposure to higher temperatures, but hardness increases after some time of exposure. This was associated with elastomer chain growth. The behavior was, however, not seen in Viton elastomers exposed in a brine phase. They also observed that, on initial exposure, NBR, EPDM, and Viton elastomers had reduced hardness, but as aging time increased, elastomer hardness increased. The observation was consistent with all test temperatures. They concluded that an increase in the aging period at a constant temperature is analogous to an increase in temperature and, thus, the corresponding chain growth. In terms of gas variation, the authors concluded that the degradation of elastomers increased in the order of $\text{CO}_2 > \text{All gases} > \text{H}_2\text{S} > \text{CH}_4$. NBR experienced the highest deterioration of all the elastomers tested, while Viton had the least. The decompression resistance of Viton is, however, very low.

Shi et al. 2020 investigated the impacts of hydrogen-methane blends on elastomeric materials used in large-scale underground hydrogen storage in depleted natural gas reservoirs. Elastomers were aged in pressurized incubators with an $\text{H}_2\text{-CH}_4$ gas ratio of 13:87 at 26.2Mpa and 353.15K. They reported changes in the dimensions of 4 cylindrical and 2 rectangular elastomeric samples. Their results showed that the diameter of an elastomer aged in H_2 containing gas mixture increased by about 14.3% compared to a 3.05% increase for elastomers aged in a pure methane environment. On the other hand, the thickness of rectangular elastomeric sheets increased by 13.08% in hydrogen methane mixtures and 17.5% in purely natural gas mixtures. In their conclusion, they stated that only changes in structural dimensions were experimented on, thus the need to investigate the changes in mechanical and physical properties.

In the subsequent discussion, a thorough description of the current research done on attempts to investigate the changes in the structural and mechanical properties of general-purpose elastomers in the presence of varied combinations of hydrogen, methane, and carbon dioxide mixtures at different pressures and temperatures is provided.

4. Experimental Design and Methodology

As discussed in the review above, temperature, pressure, and downhole gases largely affect the performance of general-purpose elastomers used in oil and gas well settings. Furthermore, given the relatively low injection and withdrawal pressures associated with underground gas storage environments, RGD failures are not usually encountered. However, it is important to investigate the impacts of downhole gases at the said conditions on the structural and mechanical properties of the elastomers. As discussed in section 2.3.3, typical withdrawal pressures are below 7MPa, and injection pressures range between 20 and 28MPa at underground gas storage conditions. 3MPa was selected due to the limitations of the testing setup and equipment.

On the other hand, the temperature varied between 25°C (77°F) and 70°C (158°F) for different aging periods. Three different general-purpose elastomers were used for all the experiments; Acrylonitrile Butadiene Rubber (NBR), Ethylene Propylene Diene Monomer (EPDM), and Fluoroelastomer (FKM/ Viton). Three different gases (as seen in UHS environments), i.e., Hydrogen (H₂), Carbon Dioxide (CO₂), and Methane (CH₄), were used in the pressurization of an autoclave vessel for the aging experiments. In the experimental matrix, some of the tests involved aging elastomers in a pure singular gas environment (i.e., 100% H₂, 100% CO₂, and 100% CH₄), while other tests involved a mixture of these gases based on their partial pressure ratios. Focus was given to hydrogen-methane mixtures and their impacts on elastomer performance, given their relevance in a “Hydrogen Economy,” as discussed in Chapter 2.

As a means of quantitatively determining the deterioration of the elastomers, the mechanical properties of the elastomers (i.e., hardness and compressional strain) were measured before and after the aging experiments. Furthermore, characterization of the elastomers before and after aging experiments was conducted via Scanning Electron Microscopy (SEM). Specifically,

morphological changes in the elastomers due to exposure to aging conditions were investigated. In addition, an inferential statistical approach was used in analyzing the onset of elastomer failures due to cavity formations. The classical “hypothesis testing” technique was employed in this approach. The described techniques were utilized in determining hypothesized degradation of elastomers in large-scale underground storage of hydrogen in depleted hydrocarbon reservoirs.

4.1. Materials

4.1.1. Elastomers

Three different elastomers, as earlier mentioned, were used in all experiments: EPDM, NBR, and FKM. These elastomers were chosen stemming from their wide range of applications in the oil and gas industry, as discussed in previous sections. Cylindrical rods of each of the elastomer types were obtained, and two different test samples with specific dimensions were prepared for each elastomer. Samples used for the hardness test were approximately 1 inch (0.0245m) thick, with a three-quarter (0.75) inch (0.0191m) diameter. The compression test, on the other hand, was based on testing specifications provided by ASTM D575-91. The samples used had a thickness of approximately 0.33 inches (0.00838m), while a diameter of 0.75 inches was maintained for the samples for hardness tests. The experimental samples are shown in **Figure 33** below.

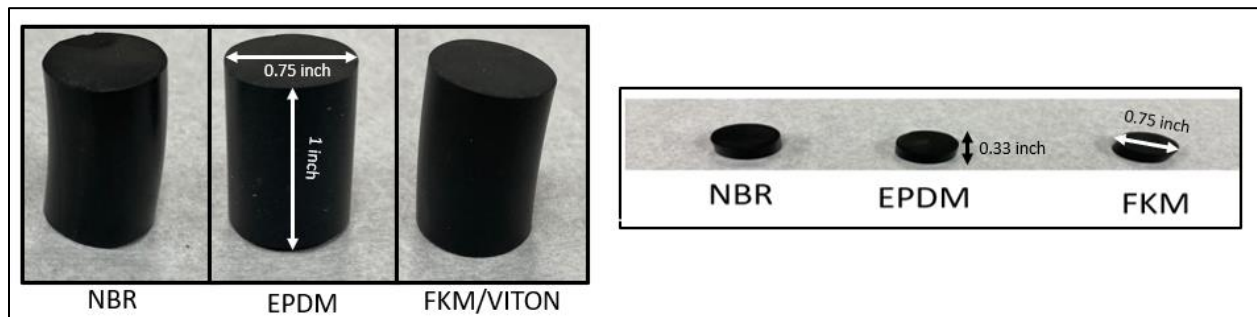


Figure 33: Elastomer samples prepared for Hardness (left) and Compression (right) tests.

4.1.2. Gases

The three distinct gases used for the aging experiments were hydrogen (H₂), methane (CH₄), and carbon dioxide (CO₂). From the literature review section, these are inevitably the principal gases in a large-scale UHS environment in depleted hydrocarbon reservoirs. Thus, it is relevant to investigate their ability to cause deterioration in the elastomeric components in the wellbore.

4.2. Experiments And Procedures

4.2.1. Hardness and Compression Tests

4.2.1.1. Hardness Test

The hardness test was an essential mechanical test to determine potential deterioration in the elastomer samples. Tests were carried out using a shore A durometer (**Figure 34**) according to the “*ASTM D2240 Standard Test Method for Rubber Property-Durometer Hardness*”. Before measuring the hardness of any of the elastomeric samples, the durometer was first zeroed. Hardness measurements were then taken at four different spots, two on each of the circular flat surfaces of each elastomer sample, and the average durometer reading and standard errors were determined. This was done to cater for errors that may result from uneven surfaces of the elastomers for some test samples and variable hardness on the measured surface. The measurements were taken with an error margin of +/-0.5 durometer units.



Figure 34: Shore A Durometer

4.2.1.2.Compression Test

The compression test was performed with a compression machine (**Figure 35**) following the ASTM D575-91 “Test Method B-Compressive stress at Specified Force” standard protocol for compression tests for rubber materials. The process involved applying a constant force to the compressive test sample for approximately 3 seconds, and the compressive strain in the material was recorded. The process was repeated for each elastomer in both “before” and “after” experiments, and similar to the hardness tests, average values and standard errors were determined. Due to the limitations of the compression machine set-up, compression forces used in this test were limited to 15lbf, 30lbf, 45lbf, 60lbf, 75lbf, and 90lbf. Different compressive strain measurements were taken for each sample, and the average strain for each force was measured.

The gathered data for hardness and compression tests for one of the test runs are shown in **Tables 3 and 4**. Hardness and compressive strain for all the samples were measured before and after aging.

Table 9: Measured Data from Elastomer Hardness Tests

Test Conditions	Sample	Before Exposure						
		Mass (g)	Average Thickness (in)	Duro 1	Duro 2	Duro 3	Duro 4	Average Duro
100% H2 3 DAYS 70°C	NBR	8.7	0.985	77.7	77.5	75.5	75.1	76.45
	EPDM	8.7	1.015	74.7	73.2	74	74.2	74.025
	FKM	13.3	0.98	76.9	77.8	75.5	76	76.55
H2:CH4 3 DAYS 70°C	NBR	8.7	0.945	76.4	75.7	76.8	76.2	76.275
	EPDM	8.7	1	74.4	73.9	74.8	75	74.525
	FKM	13.2	0.995	76	76.6	76.5	78	76.775
		After Exposure						
		Mass (g)	Average Thickness (in)	Duro 1	Duro 2	Duro 3	Duro 4	Average Duro

100% H ₂ 3 DAYS 70°C	NBR	8.7	0.985	74	73.5	75.5	76.2	74.8
	EPDM	8.7	1.015	74.6	75.1	75.2	74.2	74.775
	FKM	13.2	0.985	75.7	76.2	74	75.2	75.275
H ₂ :CH ₄ 3 DAYS 70°C	NBR	8.7	0.945	75.5	74	75	74.9	74.85
	EPDM	8.7	0.995	74.8	75.3	75.1	75.3	75.125
	FKM	13.2	1	77.6	76.9	75.3	76	76.45

Table 10: Measured Data from Elastomer Hardness Tests

Test Conditions	Sample	Before Exposure						After Exposure					
		Forces (lbf)	Area (in ²)	Length (in)	Avg Extension (in)	Stress (psi)	Strain	Forces (lbf)	Area (in ²)	Length (in)	Avg Extension (in)	Stress (psi)	Strain
H2:CH4 3 DAYS 25°C	NBR	15	1.662	0.33	0.0355	9.026	0.108	15	1.662	0.33	0.0355	9.026	0.118
		30	1.662	0.33	0.046	18.053	0.139	30	1.662	0.33	0.046	18.053	0.152
		45	1.662	0.33	0.0556	27.079	0.168	45	1.662	0.33	0.0556	27.079	0.188
		60	1.662	0.33	0.067	36.106	0.202	60	1.662	0.33	0.067	36.106	0.214
		75	1.662	0.33	0.079	45.132	0.238	75	1.662	0.33	0.079	45.132	0.245
		90	1.662	0.33	0.087	54.159	0.264	90	1.662	0.33	0.087	54.159	0.279



Figure 35: Compression Test Machine

4.2.2. Set-Up and Procedure for the Aging Experiment

The aging experiment aimed to create the necessary environment to test the effects of gases, temperature, and time on the properties of elastomers. The set-up (**Figure 36**) consisted of five (5) main components; an autoclave reactor (aging) vessel, a heating vessel, a temperature gauge, a gas cylinder rack with distinct cylinders each containing one of the individual aging gases (i.e., H₂, CO₂, and CH₄), and a gas inlet hose. The autoclave reactor vessel consists of an inner chamber with shelves on which the elastomer samples are stacked. The shelves are made of gauze with holes, permitting gases to flow uniformly around the samples. The top lid of the autoclave gas has two valves, inlet and outlet valves. Gases used for pressurizing the autoclave are routed through the inlet valve via the inlet line into the inner chamber of the autoclave.

On the other hand, the outlet valve is used for depressurizing the autoclave and is kept open during the purging of the autoclave. The top lid is also equipped with a pressure gauge for determining the pressure within the autoclave at any given time. The vessel is airtight, preventing gas leakage from any part of it into the surrounding environment. The autoclave is immersed in a heating vessel to generate the required temperatures for running experiments. The heating vessel consists of a heating element and a thermostat to regulate the temperature and keep it constant. A thermocouple measures the temperature in the vessel at any given time. The gas cylinders are kept in place with the racks.

4.2.2.1. Test Procedure

The samples are stacked on the shelves in the inner chamber of the autoclave and the vessel is sealed via the top lid such that it is airtight. The heating vessel is then heated to the appropriate temperature. Prior to pressurizing the vessel with the required gas/gas mixtures for any experiment, the vessel is purged with nitrogen gas to remove any trapped gas present in the inner chamber of the vessel. Both inlet and outlet valves were opened, and purging is done by allowing nitrogen gas to flow continuously in and out of the vessel. For experiments involving a pure singular gas, the outlet valve is closed, and vessel pressurized to the requisite pressure as determined by the gauge. For experiments involving a mixture of two or more gases, gas ratios are achieved using their partial pressure ratios. The aging period was varied between 1, 3 and 7 days with the airtight vessel (containing stacked elastomer samples) fully immersed in the heating vessel, heated to the appropriate test temperature. A constant pressure of 3MPa (~436 psi) was maintained for all experiments while temperatures were varied between 25 °C (+/- 3 °C) and 70 °C (+/- 3°C) to investigate the effects of temperature on elastomer degradation.

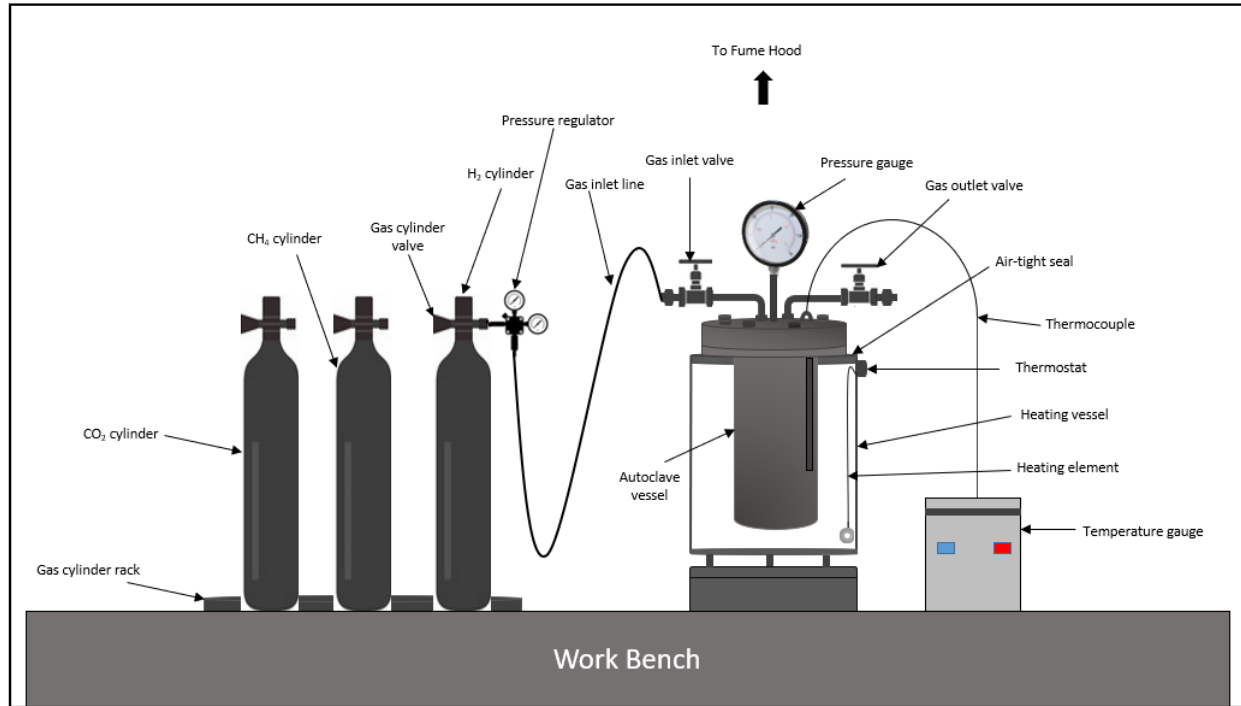


Figure 36: Experimental Set-up for Aging Tests

4.2.2.2. Test Matrix

Two different categories of tests were run. A preliminary test for all the stipulated gases/ gas mixtures which will be later described in this section. All preliminary tests were conducted at a pressure of 3MPa and temperature of 25°C for 24 hours (1 day). The main test category consisted mainly of aging in a pure hydrogen and an equal partial-pressure ratio mixture of hydrogen and methane for different temperatures while keeping pressure constant. Some auxiliary tests were also conducted for a pure methane aging environment in the main tests. The gas mixtures used in the experiment are presented as follows; 100% H₂, (50% H₂+ 50% CH₄), 100% CH₄, 100% CO₂, (50% H₂ + 50% CO₂), (33.1/3% H₂ + 33.1/3% CH₄ + 33.1/3% CO₂). A total of 29 different aging experiments with 174 different samples (all involving hardness and compressive strain measurements) were conducted. Table D is a representation of selected tests from the overall experimental matrix.

Table 11: Matrix of Selected Tests for Aging Experiment

No.	Gas Mix Ratios	Samples	Aging Conditions			Main Tests	Supplementary Tests
			Temperature (°C)	Pressure (MPa)	Time (Days)		
1.	100% H2	NBR, FKM, EPDM	25	3	1	<ul style="list-style-type: none"> • Hardness • Compression 	N/A
2.	100% H2	NBR, FKM, EPDM	25	3	7	<ul style="list-style-type: none"> • Hardness • Compression 	N/A
3.	H2:CH4 50:50	NBR, FKM, EPDM	25	3	3	<ul style="list-style-type: none"> • Hardness • Compression 	N/A
4.	H2:CH4 50:50	NBR, FKM, EPDM	25	3	7	<ul style="list-style-type: none"> • Hardness • Compression 	N/A
5.	100% H2	NBR, FKM, EPDM	70	3	3	<ul style="list-style-type: none"> • Hardness • Compression 	SEM for Cavitation Analysis
6.	H2:CH4 50:50	NBR, FKM, EPDM	70	3	3	<ul style="list-style-type: none"> • Hardness • Compression 	SEM for Cavitation Analysis
7.	H2:CH4: CO2 1: 1:1	NBR, FKM, EPDM	25	3	1	<ul style="list-style-type: none"> • Hardness • Compression 	N/A
8.	100% CH4	NBR, FKM, EPDM	25	3	3	<ul style="list-style-type: none"> • Hardness • Compression 	N/A
9.	100% H2	NBR, FKM, EPDM	70	3	7	<ul style="list-style-type: none"> • Hardness • Compression 	SEM for Morphological Analysis

10.	H ₂ :CH ₄ 50:50	NBR, FKM, EPDM	70	3	7	<ul style="list-style-type: none">• Hardness• Compression	N/A
-----	--	----------------	----	---	---	--	-----

4.2.3. Material Characterization and Statistical Analysis

4.2.3.1. Scanning Electron Microscopy

The Scanning Electron Microscope (SEM) is an instrument that produces magnified images of objects by use of electrons instead of light. The equipment has an electron gun that generates a beam of electrons and routes them through a vertical path of electromagnetic fields until it is focused on the samples. Afterward, electrons and X-rays are ejected from the sample, which falls on detectors. The detectors convert these x-rays and electrons into signals that are directed onto a screen to generate a final image. Scanning Electron Microscopy images were obtained for samples in selected tests from the experimental matrix. The SEM tests were put under two categories, each with a different objective. The first was an attempt to investigate the failure of elastomers (per given experimental conditions) due to cavitations. The second category aimed at investigating morphological changes within the elastomer on exposure to stipulated experimental conditions. The ThermoFisher Quattro S. Scanning Electron Microscopy (SEM) machine (**Figure 37**) was used in the imaging analysis. For both imaging experiments, circular backscattered (CBS) images were obtained for the test samples. The CBS detector is a Back-Scattered Electron detector with higher efficiency, has multiple segments, and consists of multiple rings, thus, produces images simultaneously (Wang et al., 2016).

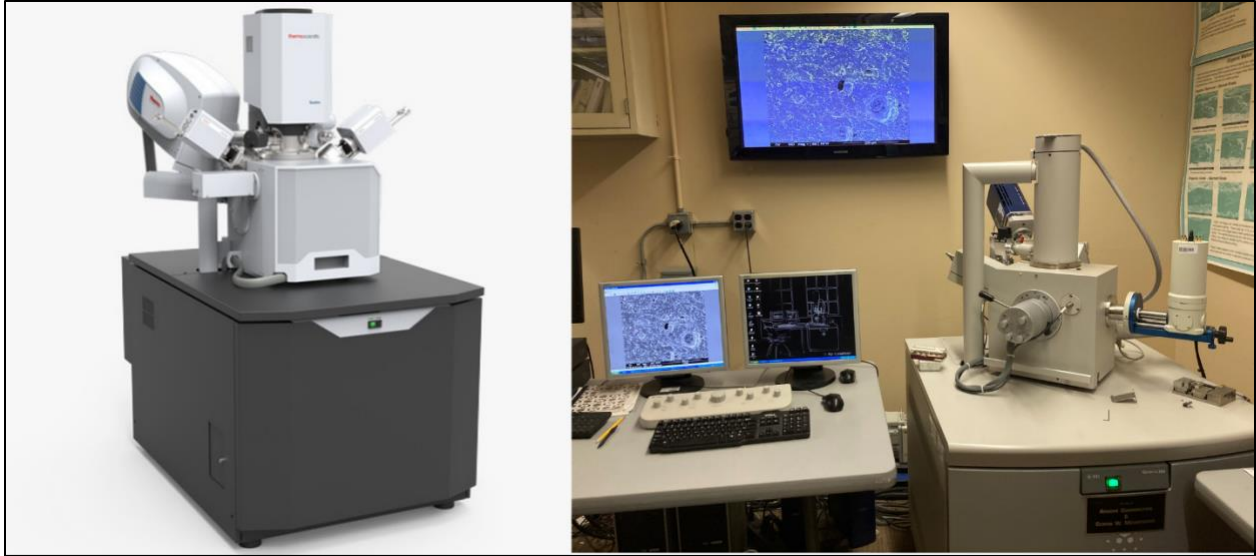


Figure 37: ThermoFisher Quattro S Scanning Electron Microscopy (SEM) Device.

4.2.3.2.SEM Imaging for Cavitation Analysis

As discussed earlier, cavitation is one of the key identified mechanisms by which elastomers deteriorate in seal assemblies. A statistical approach based on hypothesis testing was used to evaluate the onset and subsequent failure of elastomers due to cavitations. A control sample (**Figure 38**) was prepared by artificially creating a cavity in an elastomer sample. This was observed under the microscope, and a CBS image was generated to ascertain the existence of the cavity and how it appears in the SEM image. For the main test samples, five different spots were marked on the flat surfaces of each of the elastomers and three on the sides, resulting in a total of eight (8) marked spots on each type of elastomer. Images were obtained in the microneighborhoods (approximately close) for each marked spot before and after the aging tests. This was done to remove any form of bias in sampling the number of cavities present in the elastomer before and after aging experiments and to ensure that obtained images were representative. The number of cavities present in each obtained image was determined with the aid of image processing software,

as thoroughly described in the results section. These represented the sample space for statistical analysis. **Figure 39** shows samples prepared for SEM Imaging for cavitation failure analysis.

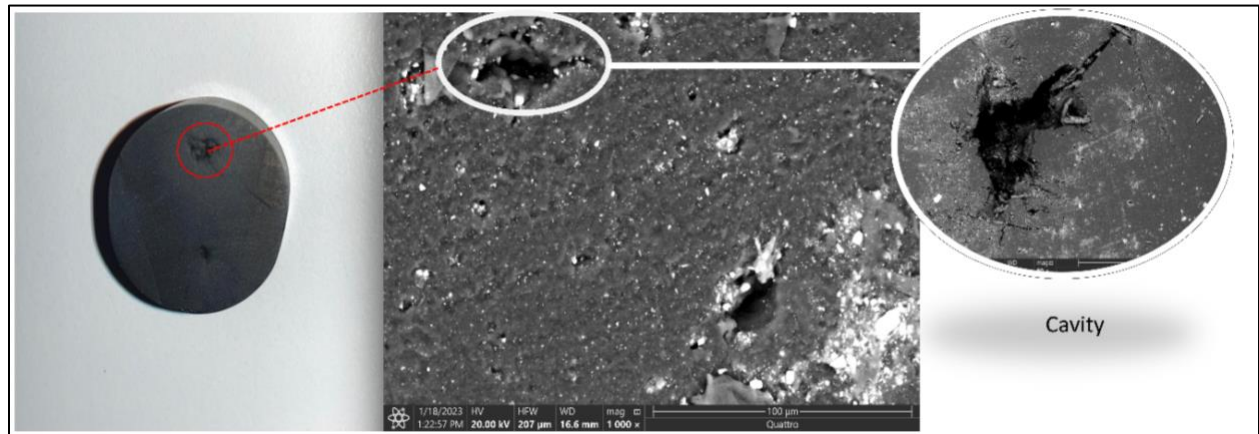


Figure 38: Control Sample for Cavity Identification in SEM Imaging

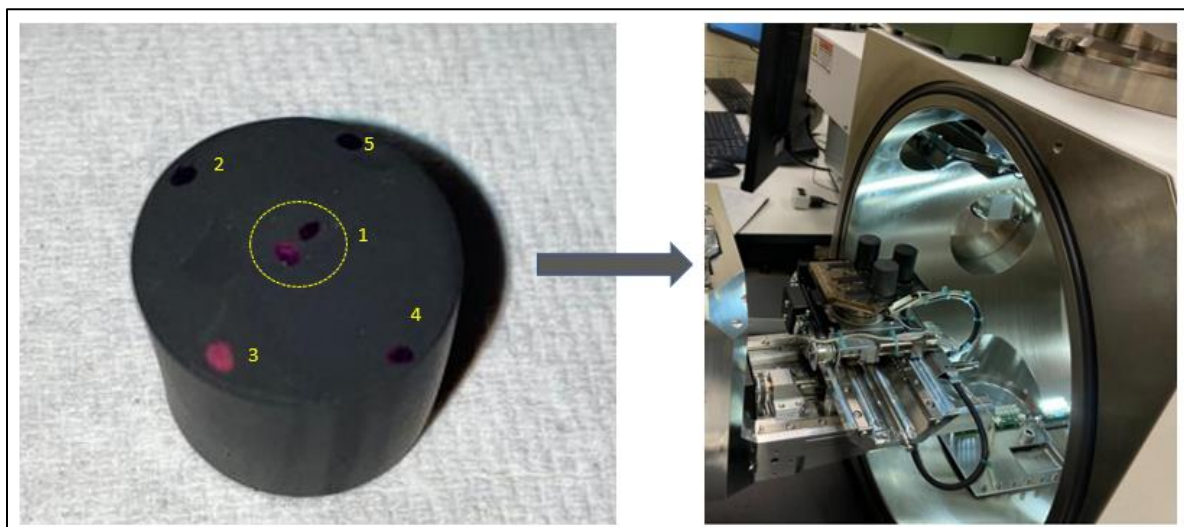


Figure 39: (Left) Marked Spots on Elastomers for Samples Prepared for SEM Imaging (Right) Elastomer samples Placed in SEM Device for Imaging.

4.2.3.3.SEM Imaging for Morphological Analysis

Besides imaging for statistical analysis, changes in the morphological structure of the elastomers were also investigated. This test was conducted purposely to determine high temperature effects on the morphological structure of elastomers aged in a pure hydrogen environment in relation to the observed changes in the mechanical properties of elastomers for such elevated temperatures. SEM images for a virgin and a corresponding aged sample per given experimental conditions were obtained, and both images were analyzed and compared.

5. Results and Analysis

In this section, the results from the preliminary and main tests are presented. Also, results from SEM imaging for both morphological and cavitation failure analysis are also discussed. The deterioration of elastomers due to aging conditions is evaluated based on changes in their mechanical properties. This is quantified by variations in hardness and compressive strain measurements before and after aging. Furthermore, as a supplementary test to ascertain the degradation in elastomer samples, an evidence-based inferential statistical method (i.e., hypothesis testing) is conducted with sample data, and the results are evaluated.

Furthermore, the results presented in this section will discuss the effects of aging temperature, gases, and time on the changes in the mechanical properties of elastomers as a means of ascertaining rubber deterioration. More focus is given to failures due to aging in pure hydrogen versus hydrogen-methane gas mixture environments.

5.1. Hardness Test

Potential damage in elastomers can be evaluated by analyzing changes in their hardness measurement after exposure to certain conditions (Kubena et al.,1991; Ertekin and Sridhar, 2009;

Embury, 2004). According to the American Society for Testing and Materials (ASTM D2240), the hardness of an elastomer is a measure of its resistance to indentation induced on it by a shore A or D durometer. The effects of gases, aging period, and temperature on hardness are presented.

5.1.1. Effects of Gases

The results from the hardness tests from the preliminary tests (**Figure 40**) are analyzed to determine the effects of gases on elastomer deterioration due to changes in hardness. The general trend from the results is a reduction in elastomer hardness aging for all preliminary experiments. For all samples aged in 100% H₂, 100% CH₄, and hydrogen-methane mixture environments, the observed reduction in hardness was less than 5%. However, the observed reduction in hardness for samples aged in hydrogen-methane mixtures was slightly higher than the former two (2), which had very close values. On the one hand, in samples aged in (50% H₂ + 50% CO₂) and (331/3% H₂ + 331/3% CH₄ + 331/3% CO₂) gas mixtures, the observed reduction in hardness was between 3-5%. On the other hand, samples aged in a 100% CO₂ environment caused the highest reduction in hardness of elastomeric samples (i.e., an observed 8% reduction in hardness). Furthermore, the highest reduction in hardness in the CO₂ environment was observed in NBR elastomers.

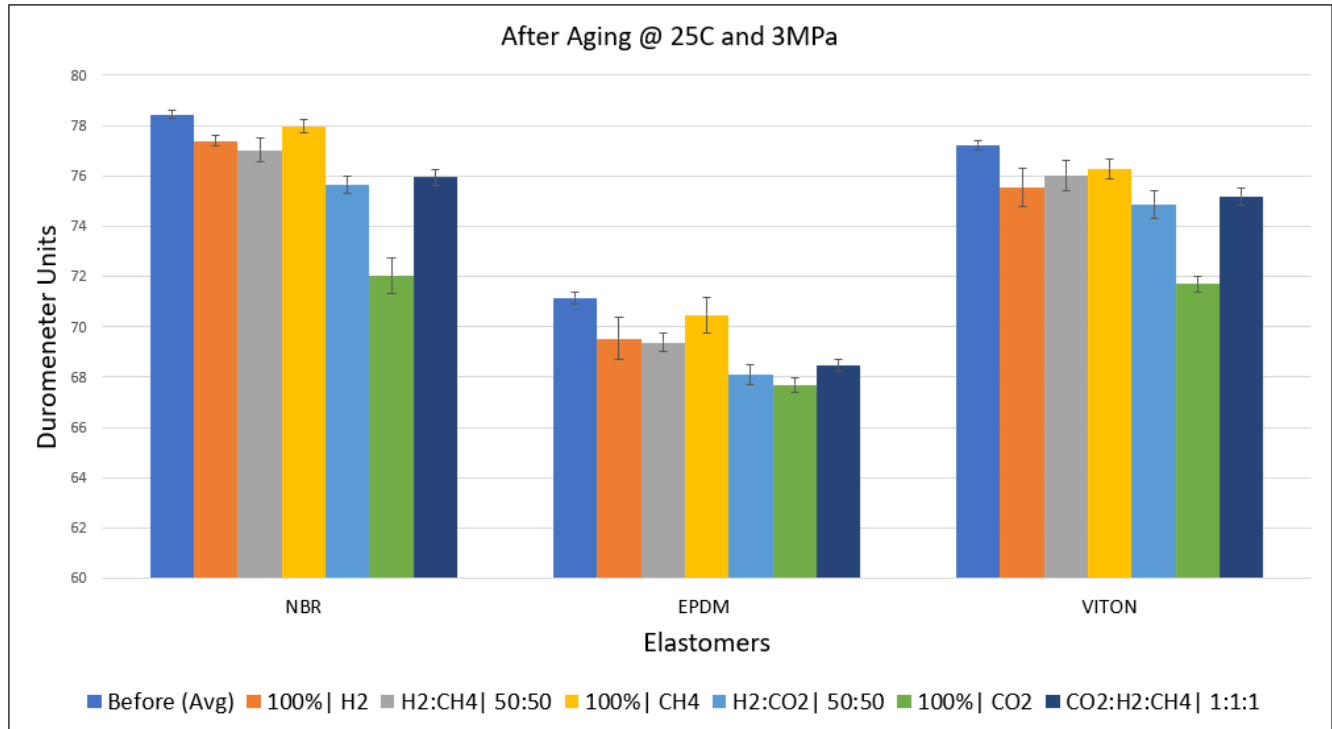


Figure 40: Effects of Gases on Elastomer Samples Aged at 25°C and 3MPa.

5.1.2. Effects of Aging Period

Besides gases, the period of exposure of elastomers to a given set of aging conditions also affects the level of material degradation, as seen in changes in hardness measurements. The effects of aging period on elastomer hardness were investigated for samples aged at pure hydrogen and a (50% H₂+ 50% CH₄) gas mixture conditions. The results for aging in both gaseous environments were analyzed at 25°C and 70°C, as shown in **Figure 41**. For both pure hydrogen and (50% H₂+ 50% CH₄) aging environments, the general trend observed was an initial reduction in the hardness of elastomers on exposure to gases, followed by a slow, steady increase in hardness as the aging time increases. This observation was consistent for aging at both 25°C and 70°C. However, this gradual increase was more profound at 25°C than at 70°C, indicating that the higher temperatures are influencing the behavior of the elastomers.

Furthermore, less than a 5% reduction in hardness is seen in all elastomer samples aged in pure hydrogen after 24 hours at 25°C. When all other conditions were maintained but the aging period increased to 7 days, the decrease in hardness observed did not exceed 3%. The highest reduction in hardness was observed in acrylonitrile butadiene rubber elastomers. Still on the samples aged in a pure hydrogen environment, an anomaly in the general trend was observed in EPDM elastomers aged at 70 °C. Instead of an initial reduction in hardness on exposure and a gradual increase as aging time increases, the samples showed a 1.4% increase in hardness after 1 day of aging and 1.7% increase after 7 days of aging.

The percentage changes in elastomer hardness for aging in a hydrogen-methane mixture were similar to that of a 100% hydrogen environment when temperature was kept at 25°C and aging period varied between 1 and 7 days. At 70°C, however, unlike the 100% hydrogen environment, an initial decrease in hardness was observed in EPDM after 1 day and only 0.19% increase in hardness (compared to unaged sample) was observed when aging period was increased to 7 days. The percentage change in hardness of FKM elastomers for both distinct aging gases at 70C was less than 1% for both 1 and 7 days of aging, indicating good thermal stability.

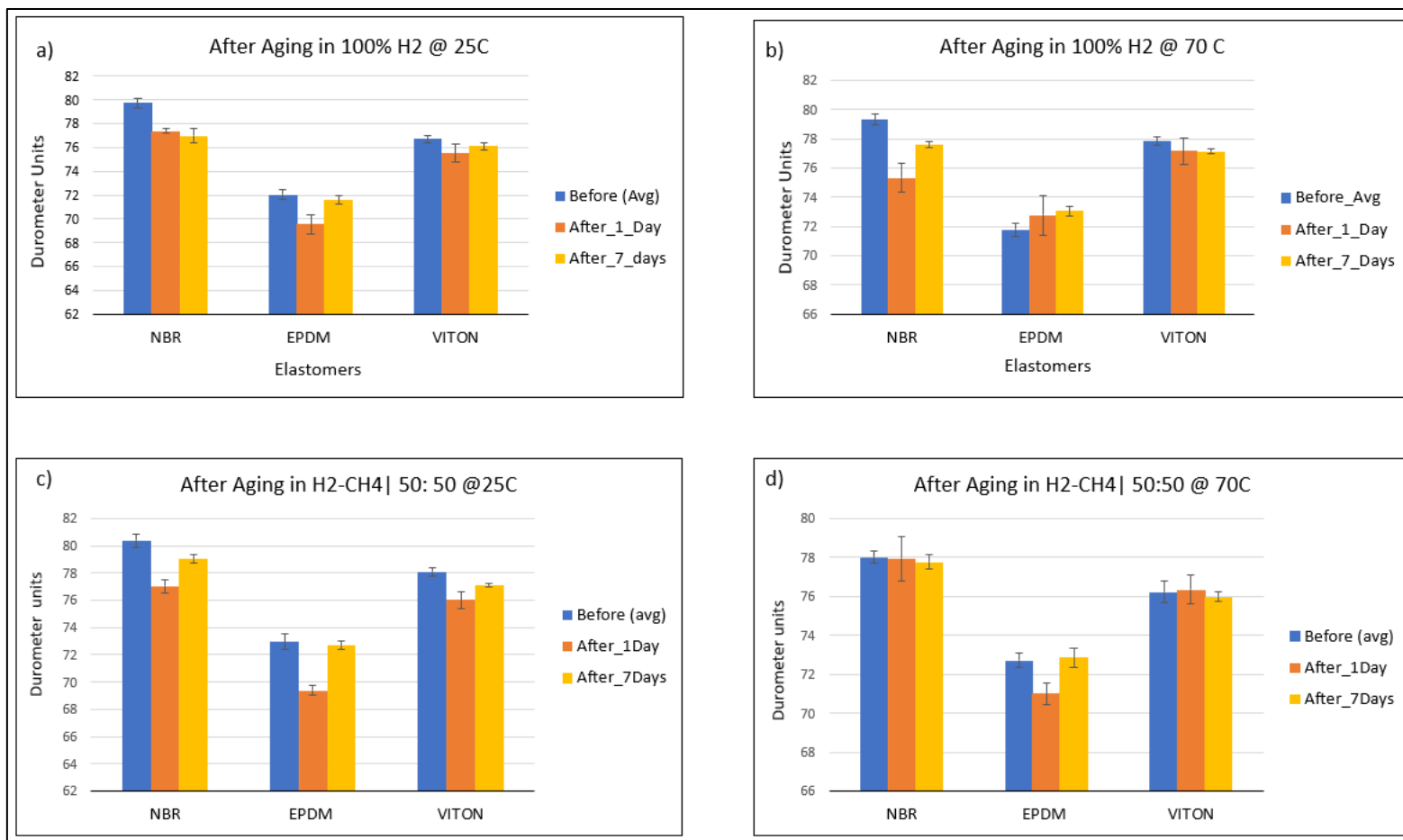


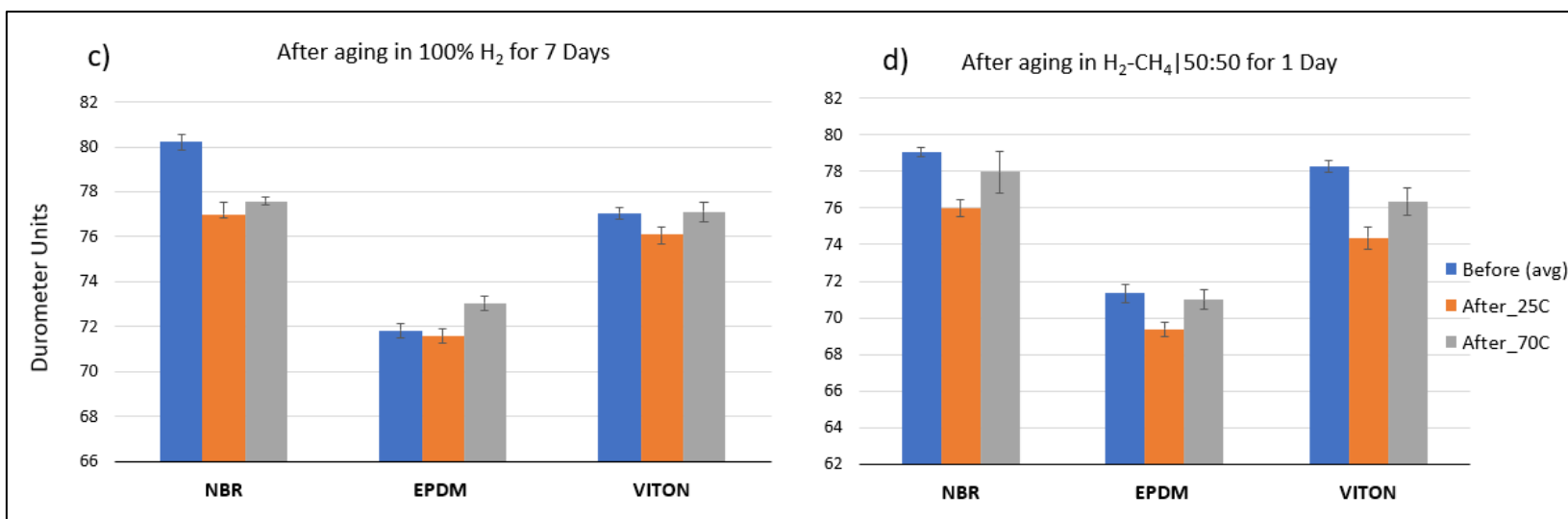
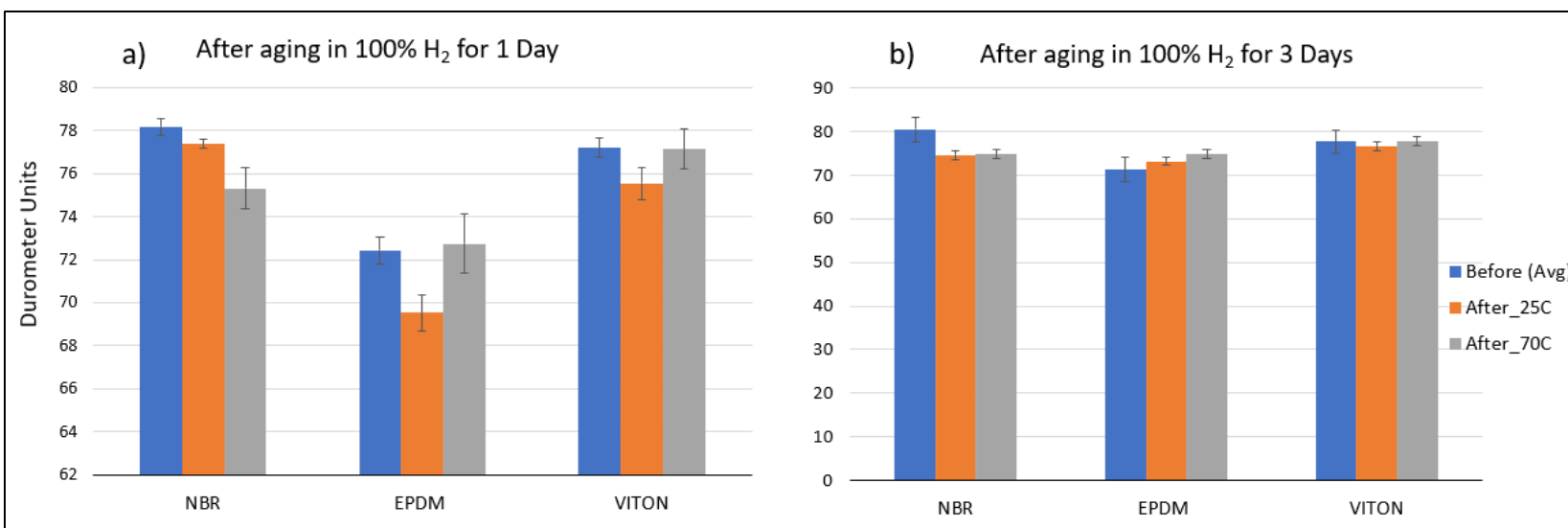
Figure 41: Effects of Aging Period on Hardness of Elastomers: (a) 100% H₂ @ 25°C (b) 100% H₂ @ 70°C (c) (50% H₂+ 50% CH₄) @ 25°C (d) (50% H₂+ 50% CH₄) @ 70°C

5.1.3. Effects of Temperature

The effects of the temperature on the hardness of tested elastomer samples were also evaluated, as shown in **Figure 42**. From the results, it was observed that for a 100% hydrogen aging environment, the general trend is an increase in elastomer sample hardness as the temperature increases from 25°C to 70°C regardless of how long the aging process took, although an anomaly in the pattern was observed in NBR elastomers after aging for 1 day. Furthermore, the observed pattern is seen to be more definite for a 7-day aging period compared to 1 and 3 days. Also, for a 7-day aging period, the increase in elastomer hardness from 25°C to 70°C is approximately less than 1.5% for NBR and Viton and about 2% for EPDM.

Furthermore, for samples aged in an equal partial pressure ratio mixture of hydrogen and methane, the trend of increase in elastomer hardness per increase in the temperature is also observed. This observed trend was most definite for samples aged for 1 day. Also, there were inconsistencies in the trends identified for acrylonitrile butadiene rubber after aging for 3 and 7 days as well as FKM after aging for 7 days. Generally, compared to measured durometer readings before aging, the percentage reduction in hardness for all elastomers after 1-day of aging at 25°C was less than 5% for all elastomers. Also, the observed reduction in hardness for NBR was approximately 3.2%, and instead of an increase as temperature increases to 70°C, a reduction of about 4.5% in hardness (compared to the virgin samples) was observed.

The results also show that generally, material degradation in a hydrogen-methane mixture environment is slightly more severe than in a 100% hydrogen environment.



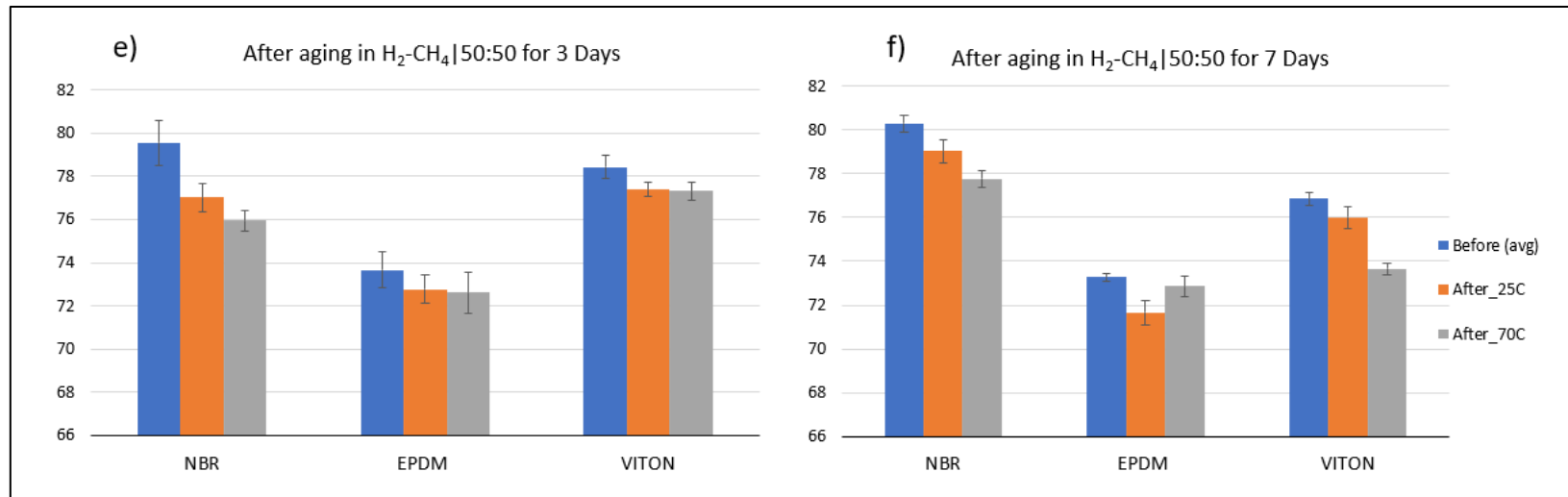


Figure 42: Effects of Temperature on Hardness of Elastomers: (a, b and c) Aging in 100% H₂; (d, e, f) Aging in Equal Mixture of Hydrogen and Methane.

5.2.Compression Test

The resistance of elastomers to compressive stress is another critical mechanical property besides hardness that helps to determine deterioration (both physical and chemical) within the rubber material.

Elastomers usually exist in compressed states in underground gas storage settings, as seen in downhole seal assemblies in liner hangers and BOPs. Furthermore, they are one of the well barrier elements prone to pressure cycling loads in gas storage wells, especially during injection and withdrawal cycles. These cycling loads may induce considerable compressive strain on the elastomer, which may change its physio-mechanical properties, ultimately resulting in material failure (Bosma et al., 1991; Ahmed and Salehi, 2021). Consequently, the sealing integrity of elastomers is compromised, resulting in gas leakage from the wellbore. Thus, it is vital to investigate the effects of aging on the compressive strain properties of elastomers employed in gas storage wells. The changes in the compressive strain of elastomers as a means of ascertaining physical and chemical damage in elastomers on exposure to different conditions have been studied by different authors (Woo et al., 2011; Chai et al., 2011; Akhlaghi et al., 2015).

In this work, the changes in the compressive strain of tested elastomer samples when a specific stress load was applied were observed before and after aging. The results for samples aged in both 100% hydrogen and the 50% H₂+ 50% CH₄ environments are analyzed. Furthermore, for both aging environments, the changes in the compressive strain of elastomers when maximum stress was applied were also analyzed. This was aimed at gaining a better understanding of the elastomer damage due to aging by compressional strain analysis. The results are represented in **Figures 43 and 44**.

5.2.1. Effects of Aging Period and Temperature

Figure 43 (a) and (b) show the changes in strain measurements before and after aging in 100% hydrogen for 1 and 7 days at 25°C. From the results, the general trend is an increase in the compressive strain for all elastomers after aging for both 1 and 7 days, with the most significant increase in the compressive strain values seen in EPDM after aging for 7 Days. When the aging temperature was increased to 70°C (**Figure 43** (c) and (d)), however, the increase in strain for EPDM elastomers was lower after aging for both 1 and 7 days compared to the results obtained when aging was done at 25°C. This shows that increasing the aging temperature increases the compressive resistance in EPDM elastomers. Also, this compressive resistance in EPDM is seen to be higher for the shorter aging period (i.e., 1 day) compared to the longer aging period (7 days). The temperature effects on the compressive strain of elastomers aged in a pure hydrogen environment can also be analyzed from **Figure 43**. The results show that NBR experienced a higher increase in compressive strain at a higher temperature of 70°C than at 25°C after aging for 1 day (**Figure 43** (a) and (c)). On the other hand, the compressive strain values for EPDM, before and after 1 day of exposure at 25°C, were very close. Besides, when the temperature was increased to 70°C, a significant reduction in the compressive strain values was observed. Furthermore, when the effects of temperature for an extended aging period (i.e., 7 days) are analyzed, the results indicated a larger increase in strain values for NBR and Viton from 25°C to 70°C (**Figure 43** (b) and (d)) and for EPDM, the observed trend is a reduction in the strain value measured as the temperature is increased from 25° C to 70°C.

The temperature and exposure time effect on the compressive resistance of elastomers is also analyzed for the equal-ratio-hydrogen-methane mixture aging environment, as shown in **Figure**

44. For samples aged at 25°C, the observed trend is generally an increase in the compressive strain for all elastomer samples after exposure. This observation was consistent for both 1-day and 7-day aging experiments. Also, at a higher temperature of 70°C, a similar trend was observed in all elastomer types except for EPDM, which showed a small reduction in compressive strain instead of an increase for the 7-day aging period.

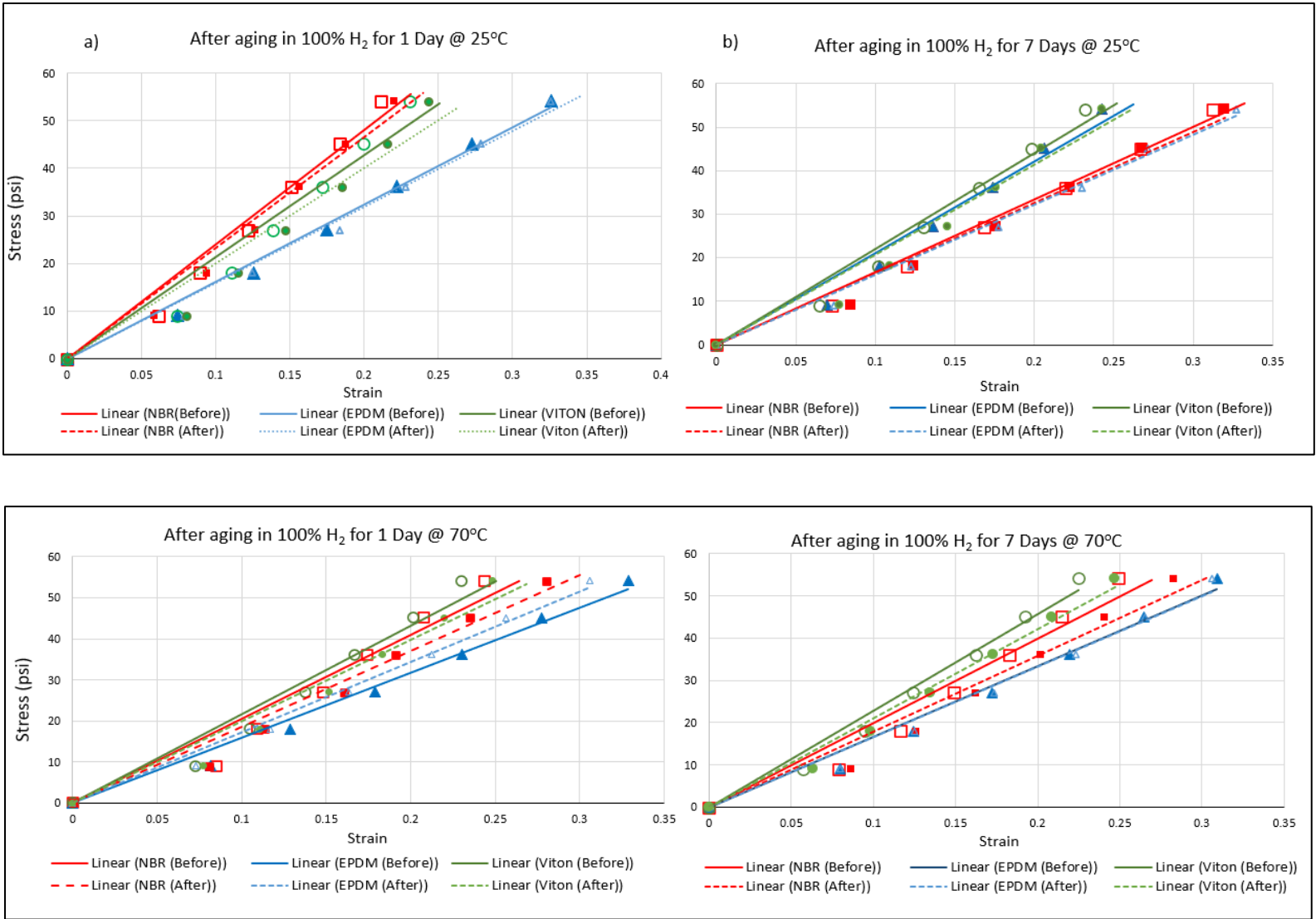


Figure 43: Effects of Days and Temperature on Compressional Measurement of Elastomers after aging in 100% H₂: (a, b) @ 25°C and (c, d) @ 70°C.

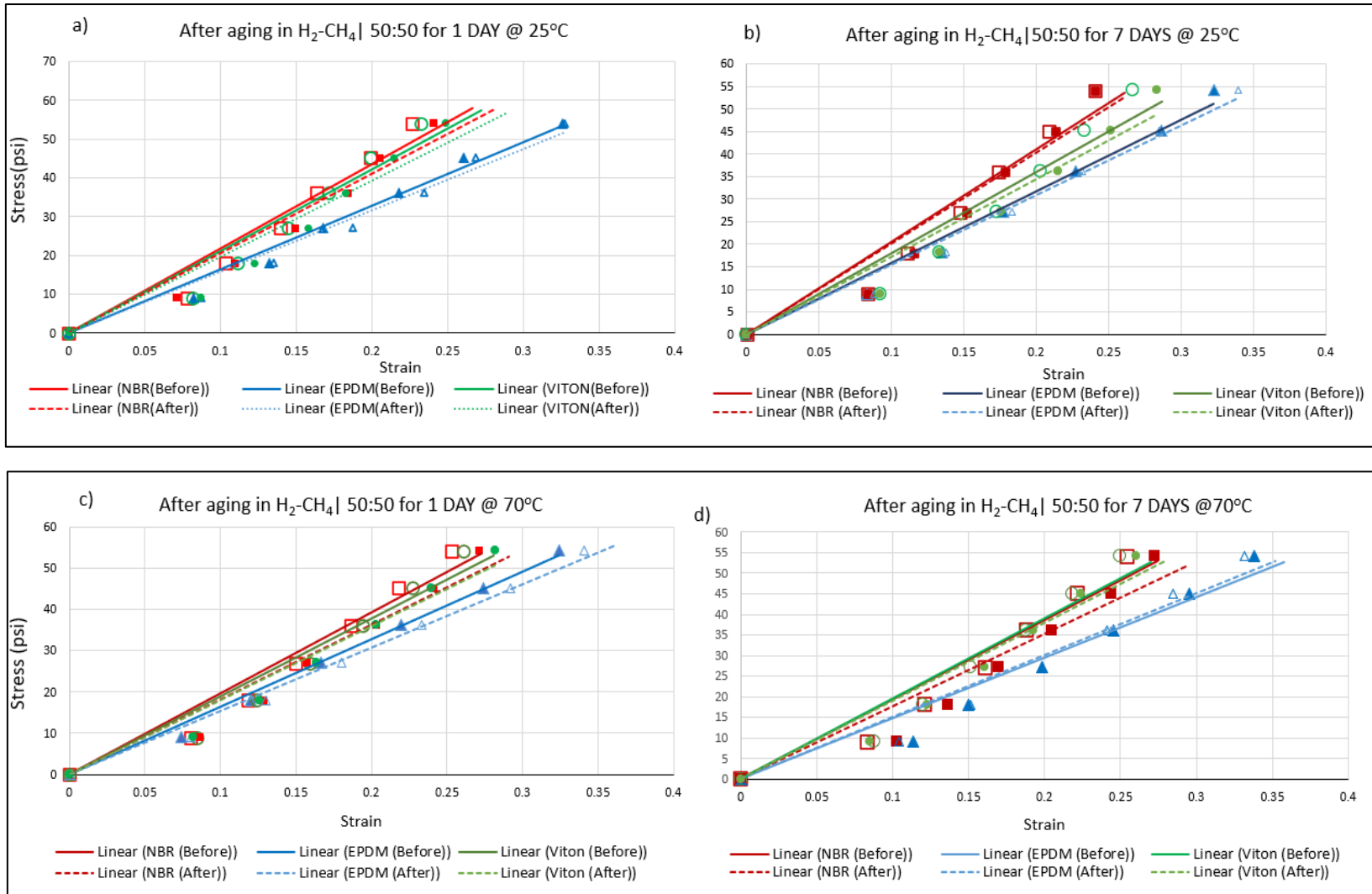


Figure 44: Effects of Days and Temperature on Compressional Measurement of Elastomers after aging in (50% H₂+ 50% CH₄): (a, b) @ 25°C and (c, d) @ 70°C.

To further investigate and thoroughly understand the degradation in elastomers by compressive strain measurements, the measured strain values for the maximum recorded stress values (i.e., 54.16psi) were evaluated against the aging period and temperature, as shown in **Figure 45**. A general trend observed is that for samples aged in a pure hydrogen environment, there is an increase in the strain values recorded after aging compared to the unaged samples. The trend was coherent for both aging temperatures in all elastomers except for EPDM, where a reduction instead of an increase in strain value was observed after aging for 1 day at 70°C. Comparing all the elastomer samples, the maximum increase in strain values was observed in acrylonitrile butadiene rubber after aging for 1 day at 25°C.

Similar trends were observed for compressive strains at maximum stress in test samples after aging in the equal ratio hydrogen-methane gas mixture (i.e., 50% H₂+ 50% CH₄) as compared to a pure hydrogen environment. However, the strain values measured for the EPDM elastomer at 70°C for 7 days was less than that of 1 day. This shows that at a high constant temperature, the compressive resistance of EPDM increases with an increase in aging period. The percentage reduction in compressive resistance from a 1-day aging period to a 7- day aging period for this case of EPDM is 2.6%. A similar behavior was observed for Viton under the same conditions (i.e., hydrogen-methane gas mixture aging environment and temperature of 70°C), however, the percentage reduction observed from 1 to 7 days was 7.52%.

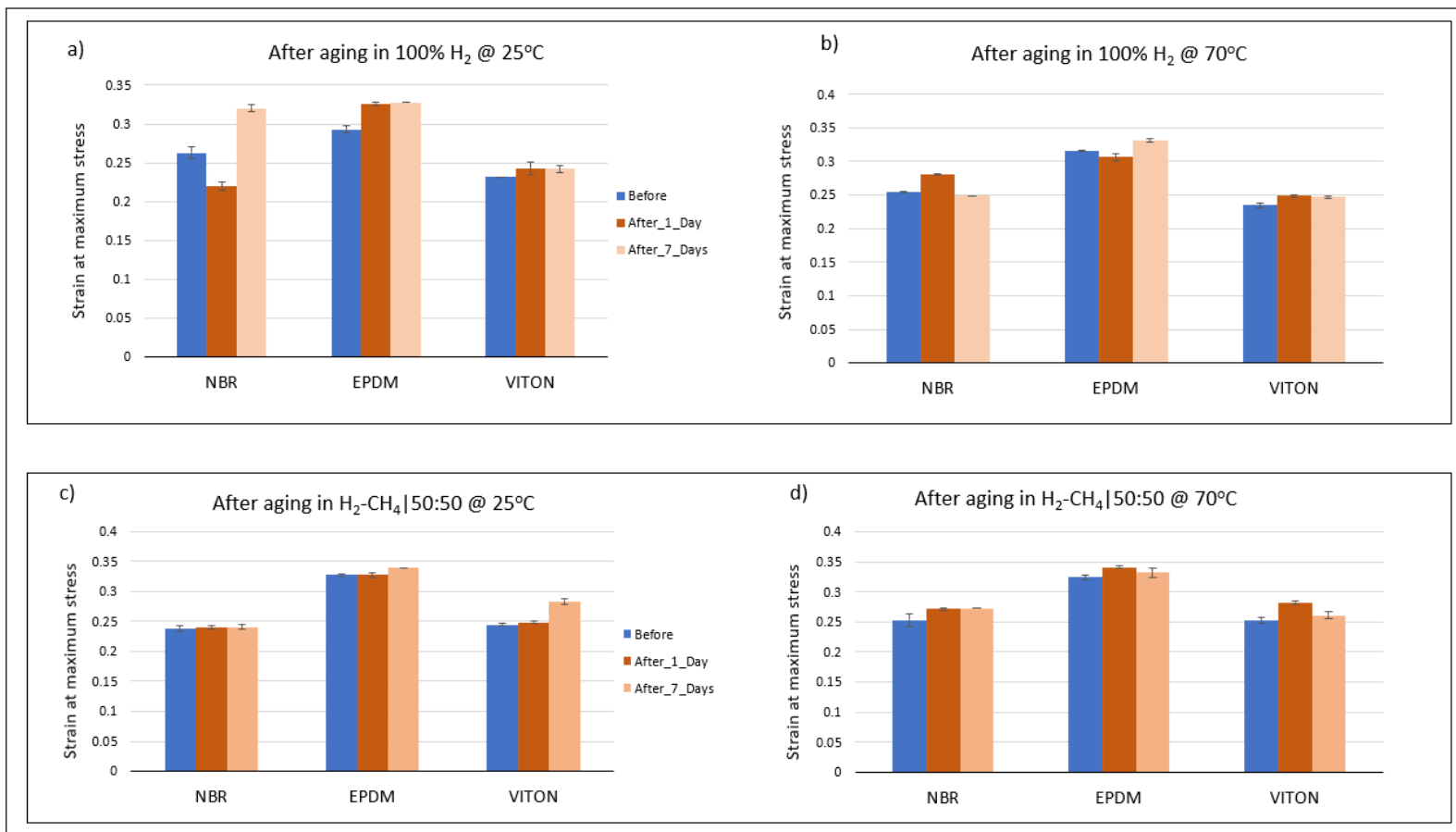


Figure 45: Effects of Aging Period and Temperature on Compressional Measurements of Elastomers after aging in both 100% H₂ environment and (50% H₂+ 50% CH₄) environment based on maximum stress values.

5.3. Statistical Analysis of Cavity Formation in Elastomers

In this section, the results of the statistical analysis of cavity formation in elastomers are presented.

The test was conducted for all elastomer samples before and after aging in both 100% H₂ and 50% H₂ + 50% CH₄ at 70°C for 3 days. This was done to comparatively analyze the results from both experiments. Furthermore, as described in the methodology, the number of observed cavities was obtained from thirteen (13) different sample points on each elastomer type (i.e., NBR, EPDM, and FKM) before and after aging in both stipulated aging environments at the given conditions. An image-processing software was used in identifying, isolating, and counting the number of cavities. To remove bias in cavity determination and counting, image processing was done by setting a fixed threshold value for analyzing the Circular Backscatter Detector (CBS) SEM images before and after aging, as shown in **Figure 46**. Furthermore, all images process were taken at 500 microns to ensure consistency in the results. A summary of the sampled data is given in Table 1.

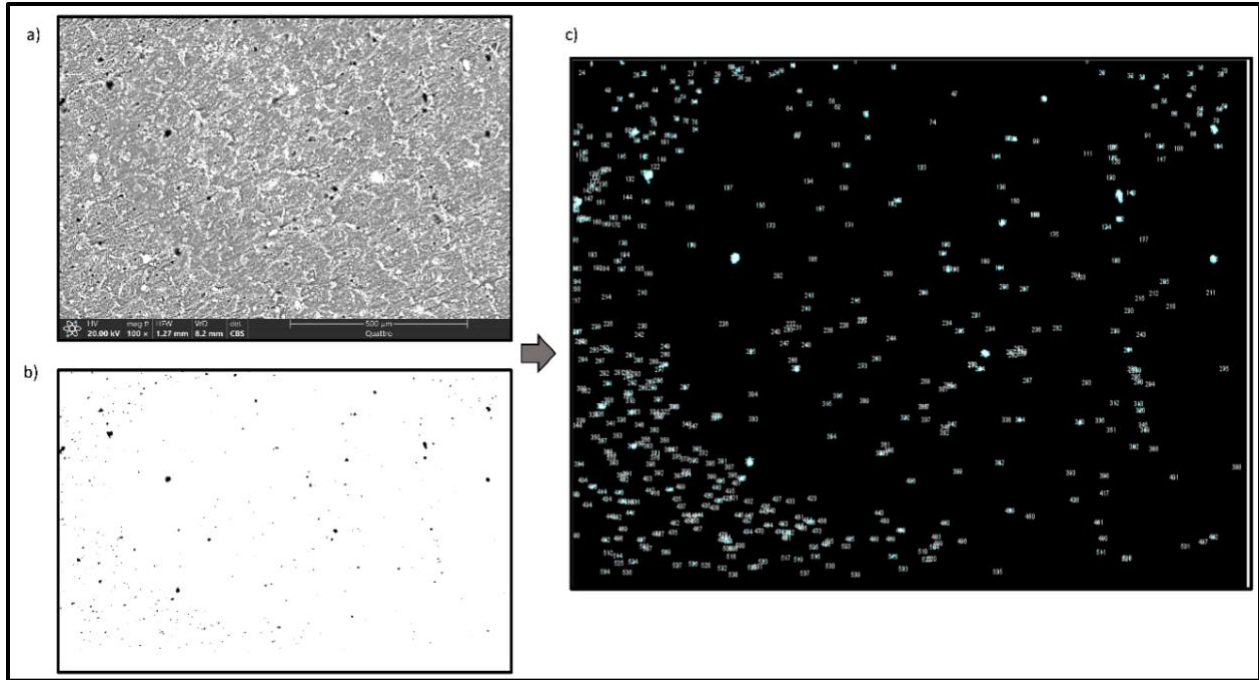


Figure 46: (a) CBS image obtained from SEM at 500microns (b) Binary image of CBS image isolating cavities after processing (c) Count of Isolated Cavities for Statistical Analysis

Table 12: Summary of Sampled Data on the Number of Cavities for Statistical Analysis

Aging Specifications			Number of Cavities												
Elastomers	Aging Gas	Condition	CA	CB	SP1A	SP1B	SP2A	SP2B	SP3A	SP3B	SP4A	SP4B	SP5	SP6	SP7
NBR	100% H ₂	BE	1082	709	1432	973	1478	2190	389	1365	813	1304	2043	341	540
NBR	100% H ₂	AE	852	1235	1933	1475	1081	1502	970	757	1146	1751	2836	1430	1841
EPDM	100% H ₂	BE	2124	56	260	557	539	1055	740	701	292	380	649	352	205
EPDM	100% H ₂	AE	2213	2041	1438	1393	1600	1419	1436	1574	692	539	735	1345	1241
VITON	100% H ₂	BE	5	5	135	183	409	483	181	152	1736	60	1490	1681	130
VITON	100% H ₂	AE	4742	734	563	258	2902	2054	177	2968	2230	2190	1471	1782	1229
NBR	H ₂ -CH ₄ 50:50	BE	773	1204	1745	1444	562	635	1382	1704	1684	1741	29	954	2045
NBR	H ₂ -CH ₄ 50:50	AE	2514	2148	2083	2056	3412	2774	3169	3349	3949	4535	217	675	439
EPDM	H ₂ -CH ₄ 50:50	BE	830	1874	1666	1434	1316	1233	988	1504	1357	1247	693	688	736
EPDM	H ₂ -CH ₄ 50:50	AE	4326	1274	4775	4999	4967	6885	3957	4529	3826	816	1423	806	499
VITON	H ₂ -CH ₄ 50:50	BE	81	669	2228	1377	1248	191	2541	1293	13858	2866	1914	1885	2929
VITON	H ₂ -CH ₄ 50:50	AE	12728	13317	5278	1566	5511	4539	2834	3621	14824	57022	2457	6172	3842

5.3.1. Hypothesis Testing

Hypothesis testing is a systematic statistical procedure of investigating whether there is enough statistical evidence to support a particular research claim. It involves putting to test some assumptions made about a particular population parameter and ensuring that experimental results have not occurred by chance. In this study, the classical hypothesis test was conducted for the difference in the mean number of cavities for a given sampled point for two different populations. The populations, in this case, are the number of cavities on the elastomers before aging and after aging. The “null hypothesis” proposed is that “*the mean number of cavities on a given elastomer sample “A” before gaseous exposure for the given experimental conditions is greater than or equal to the mean number of cavities after gaseous exposure.*” The alternate hypothesis is thus given as “*the mean number of cavities on a given elastomer sample A before gaseous exposure for the given experimental conditions is less than the mean number of cavities after gaseous exposure.*” The test was done for samples aged in both hydrogen and hydrogen-methane mixture environments. Furthermore, prior to testing the difference in mean between the two populations, an F-Test was conducted to determine if the variance of the individual populations is equal or not. This assisted in determining the correct formula for the test statistic in the T-test. Also, the conventional 95% confidence interval was used for the hypothesis testing. The T and F tests equations are shown in equations (1) and (2) in **Appendix A**. The hypothesis test indicated that on one hand, for all samples aged in 100% hydrogen, there was not enough statistical evidence to reject the null hypothesis for NBR samples. On the other hand, there was enough statistical evidence to reject the null hypothesis for EPDM and VITON samples. Furthermore, for all samples aged in (50% H₂ + 50% CH₄) gas mixture, there was enough statistical evidence to reject the null hypothesis for all elastomer samples. The results are thoroughly explained in the discussion

session. Also, **Tables 13 and 14** are a summary of the results from the T and F test for aging in both 100% hydrogen and hydrogen-methane gaseous environments respectively.

Table 13: T-Test Results After aging in 100% Hydrogen.

T-TEST RESULTS						
Aging in 100% Hydrogen						
	NBR		EPDM		VITON	
	Before Exposure	After Exposure	Before Exposure	After Exposure	Before Exposure	After Exposure
<i>F-Test Conclusions</i>	Population variances are unknown and equal		Population variances are unknown and equal		Population variances are unknown and unequal	
<i>Mean</i>	1127.6153	1446.8461	608.461538	1358.92307	511.538461	1792.30769
<i>Variance</i>	339940.7564	312035.141	278230.9359	236371.4103	432210.4359	1645646.897
<i>Observations</i>	13	13	13	13	13	13
<i>Pooled Variance</i>	325987.948		257301.173		NA	NA
<i>Hypothesized Mean Difference</i>	0		0		0	0
<i>df</i>	24		24		18	18
<i>t-Stat</i>	-1.4254784		-3.7719352		-3.2035735	
<i>P(T<=T) One-Tail</i>	0.0834480		0.0004678		0.0024618	
<i>One-tail critical value</i>	1.71088208		1.71088208		1.7340636	
<i>P(T<=T) Two-Tail</i>	0.166896007		0.000935659		0.004923656	
<i>Two-tail critical value</i>	2.063898562		2.063898562		2.10092204	
<i>T-Test Conclusions</i>	The null hypothesis is not rejected		The null hypothesis is rejected		The null hypothesis is rejected	

Table 14: T-Test Results After aging in (50% H₂ + 50% CH₄).

T-TEST RESULTS						
Aging in H ₂ -CH ₄ 50:50						
	NBR		EPDM		VITON	
	Before Exposure	After Exposure	Before Exposure	After Exposure	Before Exposure	After Exposure
<i>F-Test Conclusions</i>	Population variances are unknown and unequal		Population variances are unknown and unequal		Population variances are unknown and unequal	
<i>Mean</i>	1223.2307	2409.2307 6	1197.38461	3314	2544.61538	10285.4615
<i>Variance</i>	351501.525	1791205.0	148020.923	4318827.66	12409554.59	216386871.8
<i>Observations</i>	13	13	13	13	13	13
<i>Pooled Variance</i>	NA	NA	NA	NA	NA	NA
<i>Hypothesized Mean Difference</i>	0		0		0	
<i>df</i>	17		13		13	13
<i>t-Stat</i>	-2.92129231		3.61087960		1.845166214	
<i>P(T<=T) One-Tail</i>	0.00476136		0.00158265		0.043954648	
<i>One-tail critical value</i>	1.73960672		1.77093339		1.770933396	
<i>P(T<=T) Two-Tail</i>	0.00952272		0.00316531 6		0.087909296	
<i>Two-tail critical value</i>	2.109815578		2.16036865 6		2.160368656	
<i>T-Test Conclusions</i>	The null hypothesis is rejected		The null hypothesis is rejected		The null hypothesis is rejected	

5.4. Effects of Aging on the Morphology of Elastomers

The morphology of elastomers before and after aging in a pure hydrogen environment at 70°C and 7 days was probed as a means of characterizing the rubber material to further understand its behaviors for the given conditions. The test was conducted for all three elastomer types (i.e., NBR, EPDM, and FKM), and the results are presented. SEM images were obtained for each elastomer sample before and after aging at the same magnifications (500 microns) for comparative analysis.

In order to thoroughly scrutinize identified changes in morphology for samples after aging, secondary images were obtained for samples after aging at higher magnification (100 microns), as shown in **Figure 47**.

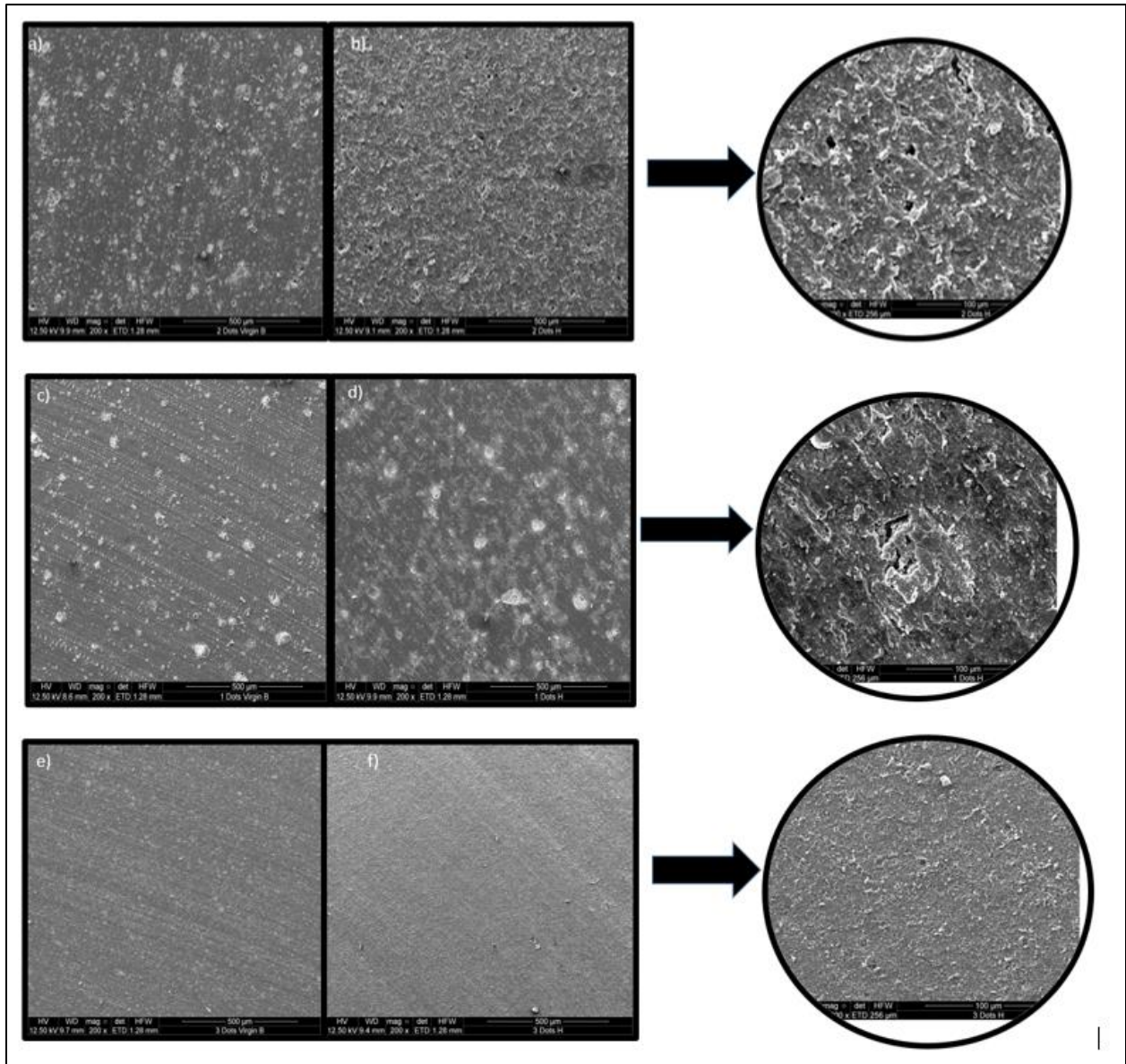


Figure 47: SEM images for morphological analysis for aging tests conducted in 100% H₂, 3MPa, and 70°C; (a) EPDM before Exposure, (b) EPDM after exposure, (c) NBR before exposure, (d) NBR after exposure (e) FKM before exposure (f) FKM after exposure.

6. Discussions

As discussed earlier, on the one hand, elastomers are polymeric materials consisting of randomly distributed chains connected to each other by cross-links (Visakh et al., 2012). These elastomer cross-links are responsible for its rigidity and thus its mechanical properties. On the other hand, deterioration of elastomers may be due to either physical or chemical processes or both.

Furthermore, Ono et al. (2018) and Fujiwara et al. (2015) studied elastomer degradation and concluded that mechanical deterioration of elastomers increases the free volume within the elastomers, permitting increased permeation and dissolution of surrounding gases into the elastomers. The process subsequently facilitates failure within the elastomers via swelling, buckling, and overflow fractures.

Chemical degradation in elastomers as described earlier may alter the molecular structures of elastomers when chemically corrosive substances react with the polymeric structure of the elastomers. The process can also affect the cross-linkage within the elastomer via chemical ageing process. In this work, elastomers were aged in a gaseous environment thus chemical degradation will occur when the bond dissociation energies (BDE) of aging gases is exceeded. i.e., the standard enthalpy for cleavage of bonds in gas molecules is attained by homolysis (Salehi et al., 2019). Bond dissociation energy can also be described as the strength of an existing chemical bond. Hitherto, the deterioration of elastomers by their chemical reaction with aging gases (i.e., H₂, CH₄, and CO₂) has been hypothesized. However, for the experiments carried out, the gases involved have relatively high bond dissociation energies and experiments were carried out at relatively low pressure and temperature conditions. Furthermore, besides NBR that has C≡N with relatively weak bond dissociation energies, EPDM has a carbon-carbon double bond with a high dissociation energy

of 611 kJ/mol while FKM has a carbon-fluorine single bond with a high dissociation energy of 450kJ/mol, making it highly stable (Salehi et al., 2019).

As a result, chemical alteration of the molecular structure of these elastomers is very minimal. The observed changes in the elastomers are proposed to be mainly due to chemical ageing (cross-linkage formation or scission) (Shaw et al., 2005; Baaser and Ziegler, 2006; Lion and Johlitz, 2012) and plasticization effect (Briscoe and Zakaria, 1991; Schrittester et al., 2016; Balasooriya et al., 2018; Mao et al., 2017). Cross-links are covalent bonds formed between the polymeric chains of the elastomers holding various portions of the elastomers together and giving the material its reversible elastomeric properties. During chemical ageing, new bonds are created (chain growth) or broken (chain scission) depending on the type of elastomer and the ageing conditions (Lago et al., 2017).

Plasticization effect is the change in mechanical properties (i.e., stiffness, hardness, tensile strength), glass transition temperature, and permeability of an elastomer due to the absorption of gas into the molecular structure of an elastomer (Bos et al., 1999; Ansaloni et al., 2020). Elastomers consist of cross-linked polymer (repeating monomer units) chains. On the molecular level, gases absorbed into the molecular structure of the elastomer act as a lubricant (i.e., a plasticizer) and minimize the interactions between molecules of the polymer chains, hence permitting easy movement of molecules past each other. The process also expands the matrix of the polymer and increases its free volume. The phenomenon facilitates macroscale deformation of the elastomers (Ansaloni et al., 2020). For gases, the extent of plasticization effect on elastomers is highly dependent on their diffusivity (or diffusion) coefficient. i.e., the amount of gas diffusing from one region to another through a unit cross-section of a material for a unit volume concentration gradient. When gases dissolve into the amorphous polymer structure of an elastomer, they generate

a continuous pressure loading that causes a gradual deterioration of the mechanical properties of elastomers. The effect of this phenomenon is greater for gases with a lower diffusivity coefficient as they stay longer within the elastomer polymeric structure (Balasooriya et al., 2021). **Figure 48** shows a schematic depiction of polymer plasticization by a gaseous phase, as studied by Bhattacharya et al. (Bhattacharya et al.,2013). The diffusion coefficient of the gases used in this experiment is shown in **Table 15**.

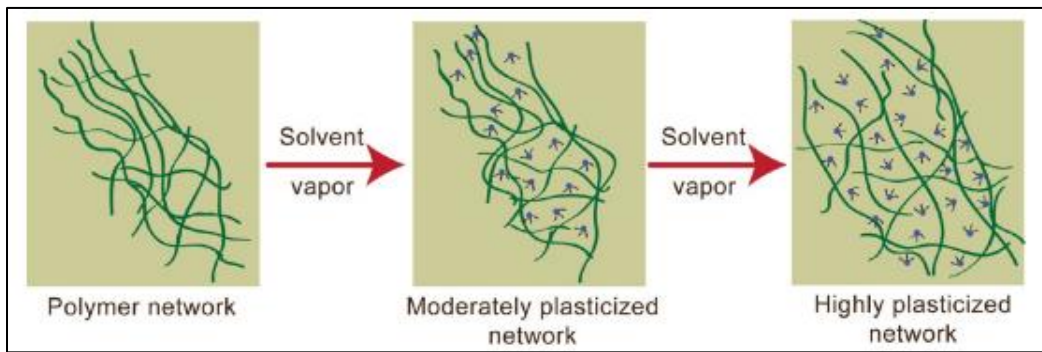


Figure 48: Schematic depiction of plasticization effect (Bhattacharya et al.,2013).

Table 15: Diffusion Coefficient of Gases at Selected Temperatures for Ambient Pressures (The Engineering Toolbox, 2022)

Gases in excess of air	The diffusion coefficient, D_{12} , (cm^2/s) at atmospheric pressure and given temperatures	
	20°C	100°C
Name		
Hydrogen	0.756	1.153
Methane	0.21	0.321
Carbon dioxide	0.16	0.252

As discussed earlier, elastomers consist of randomly distributed polymer chains held together by cross-links. The elastomeric chains can break, leading to a reduction in the cross-link density. Subsequently, the process results in elongation of the elastomer and thus a reduction in its

mechanical hardness and tensile strength. Besides, elastomer chain growth can also cause changes in the physical properties of the polymer material. The effect of this phenomenon is however the reverse of chain breakage/scission. i.e. an increase in the tensile strength of elastomers and reduction in its elongation (Schweitzer, 2000).

6.1. Hardness and Compression Tests

From the results on effect of gases on elastomer hardness, the observed reduction in hardness when samples were aged in 100% H₂, 100% CH₄ and (50% H₂ + 50% CH₄) gas mixture was less than 5%. Furthermore, the measured hardness values after aging were very close for a pure hydrogen and a pure methane aging condition. Referring to Table 4, the diffusion coefficient of hydrogen and methane is higher than that of carbon dioxide (CO₂). Thus, the plasticization effect of the former two gases is lower than that of carbon dioxide (CO₂). This also further explains why H₂ and CH₄ have a lower deterioration effect on tested elastomer samples compared to CO₂. This results also agrees with the conclusion of Shi et al. 2020 who suggested that methane's solubility in polymer materials should be as high as that of hydrogen and thus, both gases should have similar effects on the polymeric material. Furthermore, methane has a high bond dissociation energy (i.e., 438.892 +/- 0.065 kJ/mol) at 25°C (Ruscic,2015), thus, given the experimental conditions, the probability for the bonds to break for the gas to chemically react with and impact elastomer deterioration is very minimal. Also, the percentage reduction in hardness for samples aged in hydrogen-methane mixtures is slightly higher compared to the single gases as seen in the results. A possible explanation behind this observation is an overall higher plasticization effect by the mixture compared to aging in a pure hydrogen environment. In addition, CO₂ has a very high bond dissociation energy (i.e.,749 kJ/mol), making the compound highly stable (Cottrell, 1958) and thus has minimal chemical degradation effects on elastomers. As a result, its high deteriorative effect on the hardness of elastomer samples is due to its low diffusivity coefficient.

According to Jin et al., cross-linking in elastomers increases as temperature increases. This explains the general trend of an increase in elastomer hardness with increase in temperature in the results for effects of temperature for aging in both 100% H₂ and equal partial-pressure ratio mix of hydrogen and methane. A possible cause for the greater increase in hardness for EPDM, when aged in a pure hydrogen environment compared to the other elastomers, is that, for a pure hydrogen environment, the effect of cross-linkage formation is more prominent than the plasticization effect by hydrogen molecules, and this can be further supported by the relatively low pressures at which aging was carried out. Furthermore, the observed changes in the hardness of Viton (FKM) are minimal and this is due to the fact that the elastomer is thermally stable thus the least affected by temperature (Heller et al., 1999; Lu et al., 2012). The decompression rate for elastomers saturated with gases in aging experiments, to some extent, influences the deterioration of an elastomer (Kane-Diallo et al., 2016). An experimental limitation in this study was the failure to monitor and control the rate of decompression when unloading the autoclave. This was due to the low aging pressures and total volume of the vessel. Hence, this uncontrolled decompression rate may be a possible cause for the inconsistencies in the anomalies and deviation from the general trend of increase in elastomer hardness with increase in temperature for NBR after aging in pure hydrogen for 1 day and Viton after aging in hydrogen-methane mixture for 7 days at 70°C.

On the effects of aging time on elastomer hardness, Salehi et al. posited that when temperature is kept constant, an increase in aging period is analogous to a gradual and steady increase in temperature and thus an increase in elastomer cross-linkage formation (Salehi et al., 2019). This is hence, the reason for the general trend of an increase in hardness of elastomers with increased aging time. Furthermore, from the results obtained in investigating effects of aging time and effects of temperature on elastomers in this work, an initial drop in hardness was observed and this can

be explained to be due to chain scission or breakage (i.e., elastomer elongation) on initial exposure to aging conditions.

The results obtained for compressional tests of elastomers can be explained by similar principles as used in hardness tests. i.e., plasticization effect, chain growth and chain scission. An interesting observation from the compressive strain test results was the behavior of EPDM under thermal aging. Results showed that increasing aging temperature increases the compressive resistance for EPDM elastomers and more so, this resistance tends to be lower when aging period is increased. Evidently, both plasticization effect and chain growth (i.e., cross-linkage formation) occur during the aging process. At lower temperatures, and long aging periods, the plasticization effect and chain scission tend to be more dominant than chain growth (i.e., cross-linkage formation) and thus a gradual deterioration in physio-mechanical properties of the elastomer. However, when temperature is increased, chain growth dominates over plasticization effect and thus relatively lower observed compressive strain. This claim is further support by Kömmling et al., 2016, who concluded in their study that both chain scission and cross-linkage formation occurs in EPDM elastomers during aging, however, there exist a difficulty in determining the contribution of each in measurements conducted during experimental investigations. They also concluded that EPDM undergo cross-linkage formation when aged in air at higher temperatures. A similar study on the behavior on EPDM on aging was also conducted by Zaghdoudi et al. (Zaghdoudi et al., 2019) who concluded that EPDM is susceptible to both chain scission and cross-linkage formation during thermal aging. The authors concluded that both scission and cross-linkage formation continue to compete during long aging periods for EPDM elastomers.

6.2. Statistical Analysis of Elastomer Failure via Cavitations

The statistical analysis aimed to investigate the onset of failure of elastomer via cavity formation. From **Table 1**, the results show that based on the experimental conditions and the applied methodology, there was not enough statistical evidence to reject the null hypothesis for NBR samples aged in 100% H₂ for 3 days at 70°C. i.e., there is not enough statistical evidence to reject the claim that the number of cavitations present in NBR elastomer samples before aging in a 100% H₂ environment is greater than or equal to the number of cavitations present in the elastomer after aging, hence a higher probability of onset of elastomer failure in NBR via cavitation. However, there was enough statistical evidence to reject the null hypothesis for EPDM and Viton after aging in 100% hydrogen for the given conditions. This is further supported by the observed initial reduction in mechanical properties of elastomers after aging at higher temperatures compared to their virgin samples.

For the hydrogen-methane gas mixture environment there was enough statistical evidence to reject the null hypothesis for all tested elastomer samples. i.e., there is enough statistical evidence to reject the claim that the mean number of cavities before exposure is greater than the number after exposure for all three (3) tested elastomer samples. The result from the statistical analysis is reasonable and in sync with the results obtained in the mechanical property tests for these elastomers.

6.3. Material Characterization

6.3.1. Morphological Analysis Elastomers

From **Figure 47**, the SEM images showed that all elastomers had a relatively homogenous and smooth surface before aging, with very few observable microcavities haphazardly placed on the surface of NBR and EPDM elastomers. However, after thermal aging, NBR and EPDM surfaces became rougher. Furthermore, on the one hand, besides the observed roughness of the EPDM

elastomer, the microcavities observed on its surface became more visible but still haphazard. Thus, it is evident that thermal aging of EPDM elastomer in gaseous hydrogen environments has significant impact on its surface morphology. Furthermore, as established earlier, increase in aging temperature increases elastomer hardness (Jin et al.,2008), thus, a possible explanation for the roughness of the elastomer surface is the on-set of cross-linkage formation. This is supported by the increased hardness of EPDM elastomers as observed from experimental results. This observed morphological behaviour is similar to that of Liu et al. (Liu et al., 2015). The author observed similar roughness and microvoids on the surface of EPDM after thermal aging for 90 days and concluded that thermal aging proceeds predominantly with cross-linkage formation. The obtainable result from this study is also in tandem with the exceptional thermal aging resistance of EPDM as mentioned by several authors (Saleesung et al., 2015; Wang et al.,2022) and more so maintains this property in a gaseous hydrogen environment.

On the other hand, tiny white spots were observed on the surface NBR before and after aging. This may be due to surface impurities or precipitation of additives used in the elastomer manufacturing process. Furthermore, the observed roughness is also due to cross-linkage formation as in the case of EPDM. However, although NBR undergoes cross-linkage on exposure to a high temperature environment, its resistance to decompression is very low (Haroonabadi et al., 2018) and this explains its initial reduction in hardness and reduction in compressive resistance after decompression when aged at a higher temperature for a short period. The almost uniform surface morphology of Viton before and after aging can be best explained to be due to its high resistance to temperature and chemicals (Kalfayan et al.,1972; Stevens, 2001) and this supported by the results from the hardness and compression tests.

7. Summary and Conclusions

In this study, a number of experimental and experimental techniques are employed in investigating the behaviors of three major general-purpose elastomers, i.e., Acrylonitrile Butadiene Rubber (NBR), Ethylene Propylene Diene Monomer (EPDM) and Viton (FKM) as used in seal assemblies in large-scale underground hydrogen storage in depleted hydrocarbon wells. The mechanical properties of these elastomers are measured before and after aging in gaseous hydrogen environments. Mechanical properties tested include hardness and compressive resistance of the elastomers. An autoclave was used in simulating underground hydrogen storage conditions where elastomers were aged under varied conditions. The period of aging ranged from 1 to 7 days while temperatures varied between 25°C (77°F) and 70°C (158°F). Furthermore, the gas mixtures used for the aging experiments are as follows: 100% H₂, (50% H₂+ 50% CH₄), 100% CH₄, 100% CO₂, (50% H₂ + 50% CO₂), (33.1/3% H₂ + 33.1/3% CH₄ + 33.1/3% CO₂), although more focus was given to elastomer behaviors in pure hydrogen and hydrogen-methane mix environments. The effects of gases, aging period and temperature on potential degradation of elastomers due to changes in its mechanical properties were investigated.

In addition, an inferential statistical approach based on hypothesis testing was employed in investigating the onset of elastomer degradation due to cavity formation. This was used as a means of further ascertaining possible deterioration in the elastomer. Finally, changes in the surface morphology of elastomers aged in a pure hydrogen environment at elevated temperatures were investigated and characterized. The following were reached based on the experimental results from this work.

1. Exposure of general-purpose oil and gas elastomers to gaseous hydrogen aging environments at specified pressures, aging period and temperature conditions causes changes in their physical and mechanical properties.
2. The effects on the mechanical properties of general-purpose elastomers on exposure to a pure hydrogen environment and a hydrogen-methane blend environment are similar.
3. The trend of degradation in elastomers with respect to aging gases due to changes in the studied mechanical and physical properties is as follows: $100\% \text{ H}_2 < 100\% \text{ CH}_4 < (50\% \text{ H}_2 + 50\% \text{ CH}_4) < (33\frac{1}{3}\% \text{ H}_2 + 33\frac{1}{3}\% \text{ CH}_4 + 33\frac{1}{3}\% \text{ CO}_2) < (50\% \text{ H}_2 + 50\% \text{ CO}_2) < 100\% \text{ CO}_2$.
4. The changes in the mechanical properties of elastomers for the aging conditions in this work is mainly due to plasticization effect of gases, elastomer chain rupture (i.e., elastomer chain scission, elastomer elongation) and/ or elastomer chain growth (via cross-linkage formation) due to chemical ageing.
5. EPDM showed increased hardness and compressional resistance at higher temperatures in gaseous hydrogen environments. i.e., a 2% increase in hardness when the temperature was raised from 25°C to 70°C in a pure hydrogen aging environment after 7 days and a 1.7% increase in hardness for the same temperature change when aged in (50% H₂ + 50% CH₄) for 7 days. Also, after aging in pure hydrogen for 7 days, the measured compressive strain was reduced by 4% when the temperature was increased from 25°C to 70°C. This also ascertains the similarity in the effects of 100% H₂ and (50% H₂ + 50% CH₄) on the mechanical properties of elastomers. At lower temperatures, however, the compressional resistance of EPDM is poor. i.e., after aging at 25°C for 7 days, its compressive strain increased by 10% in a pure hydrogen environment and by about 4% in a hydrogen-methane

mixture environment for a given stress value. Overall, it maintains its good thermal resistance properties in a gaseous hydrogen environment.

6. NBR experienced the most significant deterioration in gaseous hydrogen environments and showed low decompression resistance. i.e., a 3% and 3.4% reduction in hardness when after aging in 100% H₂ for 1 and 7 days respectively at 25°C. Likewise for a (50% H₂ + 50% CH₄) environment, a 4% and 2% reduction in hardness was observed after 1- and 7-days aging period at 25°C. Furthermore, after aging in pure hydrogen at 25°C for 7 days, an 18% increase in compressive strain was observed for constant stress.
7. Viton remained thermally stable in gaseous hydrogen environments, although its compressional resistance is reduced at higher temperatures. i.e., at the same constant stress, a 5.48% and a 4.91% increase in compressive strain was observed after aging in 100% H₂ at 70°C for 1 and 7 days respectively. Similarly, for the hydrogen-methane mixture environment, a 10% and 3% increase in compressive strain was observed for a constant compressive stress after aging for 1 and 7 days respectively at 70°C.
8. The results from the statistical analysis showed that for all samples aged in 100% H₂ and (50% H₂ + 50% CH₄) for 3 days at 70°C, there is statistical evidence of cavity formation due to aging except for NBR samples aged in 100% H₂ at 70°C for 3 days.

8. Recommendations For Future Work

In this study, an autoclave was used to simulate wellbore conditions for Underground Hydrogen Storage in Depleted Hydrocarbon Reservoirs for a typical “Power-to-Gas” concept. The study focused on the behavior of general-purpose elastomers in such storage environments to understand the overall integrity of the wellbore. Despite the valuable results and relevant insights obtained, there were a few limitations based on which the following recommendations are proposed for further consideration in future works.

1. Due to the limitations of the vessel used, all experiments were run at a constant pressure of 3MPa and with temperatures at either 25°C or 70°C. In order to achieve a more thorough understanding of the effects of temperature and pressure on changes in the physio-mechanical properties and subsequent deterioration of elastomers, it is recommended to run experiments using a broader range of test pressures and temperatures.
2. All tests were run for either 1, 3, or 7 relatively short days. Typically, longer aging periods are required for gases to thoroughly saturate elastomers to study the effects of gas diffusivity on elastomeric properties effectively. Future work should be conducted at longer aging periods.
3. Furthermore, the aging vessel used was significantly small, thus imposing limitations on the number of samples that can be tested at a given time and the volume of test gases used. This was partly due to the uncertainty associated with the compatibility of stainless steel with hydrogen gas. Literature reports have shown a potential risk of hydrogen-induced cracking in steel. It is recommended that future experiments be carried out with larger

vessels with proven compatibility with hydrogen to allow for more test samples per experiment and larger gas volumes.

4. For future tests conducted with larger hydrogen-compatible vessels, larger gas volumes, longer aging periods, and a broader range of test pressures and temperatures, volumetric swelling of elastomers should be measured as one of the physical properties used in investigating potential damage in elastomers.
5. Reports from past studies on the behavior of elastomers have shown that the rate of decompression influences the deterioration rate in elastomers. However, in this study, the decompression rates after aging elastomers were not monitored nor controlled due to relatively low-test pressures and gas volumes. Future work should investigate the effects of decompression rate on material deterioration.
6. In this study, the employed statistical method for investigating the onset of elastomer degradation due to cavitation was conducted for only samples aged at 70°C for 3 days. Future work should further improve this by investigating the onset of cavity failures in elastomers at different aging conditions (i.e., temperature, pressure, aging time, etc.)
7. The hydrogen-methane gas mixtures used in this work were in the ratio 1:1 based on their partial pressures. However, this may not always be the case at downhole conditions or extensively in gas transportation through pipelines at the surface. Hence, it is recommended that future work investigate the effects of different hydrogen-methane mixture ratios on the changes in the physio-mechanical properties of elastomers to ascertain deterioration in the material.
8. In the statistical analysis of cavitation failure, image processing software was used to identify, isolate and count the number of cavities based on a set threshold value. However,

the software did not identify and quantify other materials on the surface of the elastomer (i.e., impurities or precipitates of additives used in manufacturing the elastomer). For future work, a more robust image processor should be used to identify and quantify other materials that may be present on the material surface. EDX spectroscopy can also be used to identify and quantify foreign materials on the surface of the elastomers.

9. For future work involving larger aging vessels (with proven hydrogen compatibility), a broader range of pressures and temperatures, and longer aging periods, morphological analysis of elastomer surface before and after aging should be more thorough. It should investigate, identify, and quantify the number, size, and orientation of cavities after aging and how decompression rates affect these properties and material deterioration in general. Furthermore, the material should be probed more to identify blisters, sizes, and orientations.

9. References

Abdalla, A. M., Hossain, S., Nisfindy, O. B., Azad, A. T., Dawood, M., & Azad, A. K. 2018. "Hydrogen Production, Storage, Transportation and Key Challenges with Applications: A Review". *Energy Conversion and Management*.

<https://doi.org/10.1016/j.enconman.2018.03.088>

Aftab, A., Hassanpouryouzband, A., Xie, Q., Machuca, L. L., & Sarmadivaleh, M. 2022. "Toward A Fundamental Understanding of Geological Hydrogen Storage". *Industrial & Engineering Chemistry Research*, 61(9), 3233-3253.

<https://doi.org/10.1021/acs.iecr.1c04380>

Agrawal, R., Singh, N. R., Ribeiro, F. H., & Delgass, W. N. 2007. "Sustainable Fuel for The Transportation Sector". *Proceedings of the National Academy of Sciences*, 104(12), 4828-4833.

<https://doi.org/10.1073/pnas.0609921104>

Ahmadpour, S. 2022. "Hydrogen Co-Storage with CO₂ in Depleted Gas Reservoirs: Challenges and Opportunities".

<https://hdl.handle.net/11250/3059610>

Ahmed, S., & Salehi, S. 2021. "Failure Mechanisms of the Wellbore Mechanical Barrier Systems: Implications for Well Integrity". *Journal of Energy Resources Technology*, 143(7).

<https://doi.org/10.1115/1.4050694>

Ahmed, S., Patel, H., & Salehi, S. 2020. "Numerical Modeling and Experimental Study Of Elastomer Seal Assembly In Downhole Wellbore Equipment: Effect Of Material And Chemical Swelling". *Polymer Testing*, 89, 106608.

<https://doi.org/10.1016/j.polymertesting.2020.106608>

Ahmed, S., Patel, H., Salehi, S., Ahmed, R., & Teodoriu, C. 2021. "Performance Evaluation of Liner Dual Barrier System In CO₂-Rich Geothermal Wells". *Geothermics*, 95, 102121.

<https://doi.org/10.1016/j.geothermics.2021.102121>

Ahmed, S., Salehi, S., Ezeakacha, C., & Teodoriu, C. 2019. "Experimental Investigation of Elastomers In Downhole Seal Elements: Implications For Safety". *Polymer Testing*, 76, 350-364.

<https://doi.org/10.1016/j.polymertesting.2019.03.041>

Ajanovic, A., Sayer, M., & Haas, R. 2022. "The Economics and The Environmental Benignity of Different Colors Of Hydrogen". *International Journal of Hydrogen Energy*, 47(57), 24136-24154.

<https://doi.org/10.1016/j.ijhydene.2022.02.094>

Akhlaghi, S., Gedde, U. W., Hedenqvist, M. S., Braña, M. T. C., & Bellander, M. 2015. "Deterioration Of Automotive Rubbers in Liquid Biofuels: A Review". *Renewable and Sustainable Energy Reviews*, 43, 1238-1248.

<https://doi.org/10.1016/j.rser.2014.11.096>

Akhtar, M., Qamar, S. Z., & Pervez, T. 2012. "Swelling Elastomer Applications In Oil And Gas Industry". *J. Trends Dev. Mach. Assoc. Technol*, 16(1), 71-74.

Akiba, M. A., & Hashim, A. S. 1997. "Vulcanization And Crosslinking in Elastomers". *Progress In Polymer Science*, 22(3), 475-521.

[https://doi.org/10.1016/S0079-6700\(96\)00015-9](https://doi.org/10.1016/S0079-6700(96)00015-9)

Alarifi, I. M. 2021. "Synthetic Engineering Materials and Nanotechnology".

Alcock, J. L., Shirvill, L. C., & Cracknell, R. F. 2001. "Compilation Of Existing Safety Data On Hydrogen And Comparative Fuels". Deliverable Report, EIHP2, May.

Aldy, J. E. 2012. "A Preliminary Review of The American Recovery and Reinvestment Act's Clean Energy Package". Resources For the Future Discussion Paper.

<https://dx.doi.org/10.2139/ssrn.1986948>

Aldy, J. E., Kotchen, M. J., & Leiserowitz, A. A. 2012. "Willingness To Pay and Political Support for A US National Clean Energy Standard". *Nature Climate Change*, 2(8), 596-599.

Al-Hallaj, S., & Kiszynski, K. 2011. "Hybrid hydrogen systems: Stationary and Transportation Applications". Springer Science & Business Media.

All Consulting LLC. 2016. "Underground Hydrogen Storage in the United States". Prepared for StatesFirst-An Initiative of the IOGCC & GWPC.

Altfeld, K., & Pinchbeck, D. 2013. "Admissible Hydrogen Concentrations in Natural Gas Systems". *Gas Energy*, 2103(03), 1-2.

Ameduri, B., Boutevin, B., & Kostov, G. 2001. "Fluoroelastomers: Synthesis, Properties And Applications". *Progress in Polymer Science*, 26(1), 105-187.

[https://doi.org/10.1016/S0079-6700\(00\)00044-7](https://doi.org/10.1016/S0079-6700(00)00044-7)

Amid, A., Mignard, D., & Wilkinson, M. 2016. "Seasonal Storage of Hydrogen In A Depleted Natural Gas Reservoir". *International Journal of Hydrogen Energy*, 41(12), 5549-5558.

<https://doi.org/10.1016/j.ijhydene.2016.02.036>

Amigáň, P., Greksak, M., Kozánková, J., Buzek, F., Onderka, V., & Wolf, I. 1990. "Methanogenic Bacteria as a Key Factor Involved in Changes Of Town Gas Stored In an Underground Reservoir". *FEMS Microbiology Ecology*, 6(3), 221-224.

<https://doi.org/10.1111/j.1574-6968.1990.tb03944.x>

Amsden, B. G. 2008. "Biodegradable Elastomers in Drug Delivery. Expert Opinion on Drug Delivery", 5(2), 175-187.

<https://doi.org/10.1517/17425247.5.2.175>

Ansaloni, L., Alcock, B., & Peters, T. A. 2020. "Effects Of CO₂ On Polymeric Materials In The CO₂ Transport Chain: A Review". *International Journal of Greenhouse Gas Control*, 94, 102930.

<https://doi.org/10.1016/j.ijggc.2019.102930>

Aprem, A. S., Joseph, K., & Thomas, S. 2005. "Recent Developments in Crosslinking Of Elastomers. Rubber Chemistry and Technology". 78(3), 458-488.

<https://doi.org/10.5254/1.3547892>

Asif, M., & Muneer, T. 2007. "Energy Supply, Its Demand and Security Issues For Developed And Emerging Economies. Renewable And Sustainable Energy Reviews" 11(7), 1388-1413.

<https://doi.org/10.1016/j.rser.2005.12.004>

ASTM Committee. 2001. ASTM D575-91 Standard Test Methods for Rubber Properties in Compression. American Society for Testing and Materials. (ASTM International: West Conshohocken).

ASTM, D. 2015. ASTM D-2240.

Azzuni, A., & Breyer, C. 2018. "Energy Security and Energy Storage Technologies". *Energy Procedia*, 155, 237-258.

<https://doi.org/10.1016/j.egypro.2018.11.053>

Bai, M., Song, K., Sun, Y., He, M., Li, Y., & Sun, J. 2014. "An Overview of Hydrogen Underground Storage Technology and Prospects In China". *Journal Of Petroleum Science and Engineering*, 124, 132-136.

<https://doi.org/10.1016/j.petrol.2014.09.037>

- Baaser, H., Ziegler, C., & KG, F. F. 2006. Simulation von Setz-und Relaxationsvorgängen von Elastomer-bauteilen mit Hilfe des mehrachsigen formulierten Freudenberg-Alterungsmodells. In Proceedings of the 7th Kautschuk-Herbst-Kolloquium (Hanover, 08.–11.11. 2006). Deutsches Institut für Kautschuktechnologie, Hanover (pp. 393-406).
- Balasoorya, W., Schritteser, B., Pinter, G., & Schwarz, T. 2018. “Induced Material Degradation of Elastomers In Harsh Environments”. *Polymer Testing*, 69, 107-115.
<https://doi.org/10.1016/j.polymertesting.2018.05.016>
- Ball, M., & Weeda, M. 2015. “The Hydrogen Economy–Vision or Reality?”. *International Journal of Hydrogen Energy*, 40(25), 7903-7919.
<https://doi.org/10.1016/j.ijhydene.2015.04.032>
- Balopi, B., Moyo, M., & Gorimbo, J. 2022. “Autothermal Reforming Of Bio-Ethanol: A Short Review Of Strategies Used To Synthesize Coke-Resistant Nickel-Based Catalysts”. *Catalysis Letters*, 1-13.
<https://doi.org/10.1007/s10562-021-03892-2>
- Barrufet, M. A., Bacquet, A., & Falcone, G. 2010. “Analysis Of the Storage Capacity For CO2 Sequestration Of a Depleted Gas Condensate Reservoir And a Saline Aquifer”. *Journal of Canadian Petroleum Technology*, 49(08), 23-31.
<https://doi.org/10.2118/139771-PA>
- Bhattacharya, A. B., Chatterjee, T., & Naskar, K. 2020. “Automotive Applications Of Thermoplastic Vulcanizates”. *Journal of Applied Polymer Science*, 137(27), 49181.
<https://doi.org/10.1002/app.49181>
- Bhattacharya, S., Sharma, D. K., Saurabh, S., De, S., Sain, A., Nandi, A., & Chowdhury, A. 2013. “Plasticization Of Poly (Vinylpyrrolidone) Thin Films Under Ambient Humidity: Insight From Single-Molecule Tracer Diffusion Dynamics”. *The Journal of Physical Chemistry B*, 117(25), 7771-7782.
<https://doi.org/10.1021/jp401704e>
- Bhowmick, A. K., & Mangaraj, D. 2018. “Vulcanization And Curing Techniques. In Rubber Products Manufacturing Technology”.
- Birol, F. 2019. “The Future of Hydrogen: Seizing Today’s Opportunities. IEA Report Prepared For The G-20”.

Blanco, H., & Faaij, A. 2018. “A Review at The Role Of Storage In Energy Systems With A Focus On Power To Gas And Long-Term Storage”. *Renewable And Sustainable Energy Reviews*, 81, 1049-1086.

<https://doi.org/10.1016/j.rser.2017.07.062>

Blizzard, W. A. 1989. “Metallic Sealing Technology in Downhole Completion Equipment”. In *Offshore Technology Conference*. 1-4 May. 1989.

<https://doi.org/10.4043/6087-MS>

Blow, S. 1998. *Handbook of Rubber Technology*.

Bo, Z., Zeng, L., Chen, Y., & Xie, Q. 2021. “Geochemical Reactions-Induced Hydrogen Loss During Underground Hydrogen Storage in Sandstone Reservoirs”. *International Journal of Hydrogen Energy*, 46(38), 19998-20009.

<https://doi.org/10.1016/j.ijhydene.2021.03.116>

Boersheim, E. C., Reitenbach, V., Albrecht, D., Pudlo, D., & Ganzer, L. 2019. “Experimental Investigation of Integrity Issues of UGS Containing Hydrogen”. In *SPE EUROPEC featured at 81st EAGE Conference and Exhibition*. 3-6 June 2019.

<https://doi.org/10.2118/195555-MS>

Bonart, R. 1979. Thermoplastic elastomers. *Polymer*, 20(11), 1389-1403.

[https://doi.org/10.1016/0032-3861\(79\)90280-5](https://doi.org/10.1016/0032-3861(79)90280-5)

Boopathy, R., & Daniels, L. 1991. “Effect Of pH On Anaerobic Mild Steel Corrosion by Methanogenic Bacteria”. *Applied And Environmental Microbiology*, 57(7), 2104-2108.

<https://doi.org/10.1128/aem.57.7.2104-2108.1991>

Bos, A., Pünt, I. G. M., Wessling, M., & Strathmann, H. 1999. “CO₂-Induced Plasticization Phenomena in Glassy Polymers”. *Journal of Membrane Science*, 155(1), 67-78.

[https://doi.org/10.1016/S0376-7388\(98\)00299-3](https://doi.org/10.1016/S0376-7388(98)00299-3)

Bosma, M., Ravi, K., Driel, W. V., & Schreppers, G. J. 1999. “Design Approach to Sealant Selection for The Life Of The Well”. In *SPE Annual Technical Conference and Exhibition*. 3-6 October 1999.

<https://doi.org/10.2118/56536-MS>

Bossel, U., Eliasson, B., & Taylor, G. 2004. “The Future of The Hydrogen Economy: Bright or Bleak?” *Journal of KONES*, 11(1-2), 87-111.

<https://www.infona.pl/resource/bwmeta1.element.baztech-article-BUJ6-0023-0128>

Breysse, D. 2010. "Deterioration Processes in Reinforced Concrete: An Overview. Non-Destructive Evaluation Of Reinforced Concrete Structures".

<https://doi.org/10.1533/9781845699536.1.28>

Briscoe, B. J., & Liatsis, D. 1992. "Internal Crack Symmetry Phenomena During Gas-Induced Rupture Of Elastomers". *Rubber Chemistry and Technology*, 65(2), 350-373.

<https://doi.org/10.5254/1.3538617>

Briscoe, B. J., Savvas, T., & Kelly, C. T. 1994. "Explosive Decompression Failure of Rubbers: A Review of The Origins of Pneumatic Stress Induced Rupture In Elastomers". *Rubber Chemistry and Technology*, 67(3), 384-416.

<https://doi.org/10.5254/1.3538683>

Brisse, A., Schefold, J., & Zahid, M. 2008. "High Temperature Water Electrolysis in Solid Oxide Cells". *International Journal of Hydrogen Energy*, 33(20), 5375-5382.

<https://doi.org/10.1016/j.ijhydene.2008.07.120>

Brun, K., & Kurz, R. (Eds.). 2018. "Compression Machinery for Oil and Gas". Gulf Professional Publishing.

Bülbül, Ş., Yaşar, M., & Akçakale, N. 2014. "Effect of Changing of Filling Materials In NR-SBR Type Elastomer Based Rubber Materials on Mechanical Properties".

<https://doi.org/10.7317/pk.2014.38.5.664>

Bünger, U., Michalski, J., Crotogino, F., & Kruck, O. 2016. "Large-Scale Underground Storage of Hydrogen for The Grid Integration of Renewable Energy and Other Applications". In *Compendium Of Hydrogen Energy* (pp. 133-163). Woodhead Publishing.

<https://doi.org/10.1016/B978-1-78242-364-5.00007-5>

Caglayan, D. G., Weber, N., Heinrichs, H. U., Linßen, J., Robinius, M., Kukla, P. A., & Stolten, D. 2020. "Technical Potential of Salt Caverns for Hydrogen Storage in Europe. *International Journal of Hydrogen Energy*", 45(11), 6793-6805.

<https://doi.org/10.1016/j.ijhydene.2019.12.161>

Campion, R. P., Thomson, B., & Harris, J. A. 2005. "Elastomers for Fluid Containment In Offshore Oil And Gas Production": Guidelines And Review. HSE Books.

Cashdollar, K. L., Zlochower, I. A., Green, G. M., Thomas, R. A., & Hertzberg, M. 2000. "Flammability of Methane, Propane, And Hydrogen Gases". *Journal Of Loss Prevention In The Process Industries*, 13(3-5), 327-340.

[https://doi.org/10.1016/S0950-4230\(99\)00037-6](https://doi.org/10.1016/S0950-4230(99)00037-6)

Chai, A. B., Andriyana, A., Verron, E., Johan, M. R., & Haseeb, A. S. M. A. 2011. "Development of A Compression Test Device for Investigating Interaction Between Diffusion Of Biodiesel And Large Deformation In Rubber". *Polymer Testing*, 30(8), 867-875.

<https://doi.org/10.1016/j.polymertesting.2011.08.009>

Chalk, S., & Inouye, L. 2004. "The President's US Hydrogen Initiative". In *The Hydrogen Energy Transition*. Academic Press.

<https://doi.org/10.1016/B978-012656881-3/50009-5>

Chao, Y., Huang, C. T., Lee, H. M., & Chang, M. B. 2008. "Hydrogen Production Via Partial Oxidation of Methane with Plasma-Assisted Catalysis". *International Journal of Hydrogen Energy*, 33(2), 664-671.

<https://doi.org/10.1016/j.ijhydene.2007.09.024>

Chen, H., Zheng, M., Sun, H., & Jia, Q. 2007. "Characterization And Properties of Sepiolite/Polyurethane Nanocomposites". *Materials Science and Engineering: A*, 445, 725-730.

<https://doi.org/10.1016/j.msea.2006.10.008>

Chen, X., Zonoz, R. H., Salem, H. A., & Lim, H. K. 2019. "Extrusion Resistance and High-Pressure Sealing Performance of Hydrogenated Nitrile-Butadiene Rubber (HNBR)". *Polymer Testing*, 76, 499-504.

<https://doi.org/10.1016/j.polymertesting.2019.04.008>

Chen, X., Zonoz, R., & Salem, H. A. 2021. "The Challenge of Elastomer Seals for Blowout Preventer BOP and Wellhead/Christmas Trees under High Temperature". In *Offshore Technology Conference*. 6-19 August 2021.

<https://doi.org/10.4043/30945-MS>

Chi, J., & Yu, H. 2018. "Water Electrolysis Based on Renewable Energy for Hydrogen Production". *Chinese Journal of Catalysis*.

[https://doi.org/10.1016/S1872-2067\(17\)62949-8](https://doi.org/10.1016/S1872-2067(17)62949-8)

Chou, C. H., & World Health Organization. 2003. "Hydrogen Sulfide: Human Health Aspects". World Health Organization.

Christensen, R. 2012. Theory Of Viscoelasticity: An Introduction. Elsevier.

Chugh, S., Posina, V. A., Sonkar, K., Srivatsava, U., Sharma, A., & Acharya, G. K. 2016. “Modeling & Simulation Study to Assess the Effect of CO₂ On Performance And Emissions Characteristics Of 18% HCNG Blend On A Light Duty SI Engine”. International Journal of Hydrogen Energy, 41(14), 6155-6161.

<https://doi.org/10.1016/j.ijhydene.2015.09.138>

Clarkin, J. 2003. “Hydrogen: Opportunities and Challenges. In AIAA International Air and Space Symposium and Exposition: The Next 100 Years” (p. 2881).

<https://doi.org/10.2514/6.2003-2881>

Colvin, H. 2004. General-Purpose Elastomers. In Rubber Compounding.

<https://doi.org/10.1201/9781420030464>

Cong, C. B., Cui, C. C., Meng, X. Y., Lu, S. J., & Zhou, Q. 2013. “Degradation of Hydrogenated Nitrile-Butadiene Rubber in Aqueous Solutions of H₂S or HCl. Chemical Research in Chinese Universities, 29, 806-810.

Coran, A. Y. 1995. Vulcanization: Conventional and Dynamic. Rubber Chemistry and Technology, 68(3), 351-375.

<https://doi.org/10.5254/1.3538748>

Cord-Ruwisch, R., Seitz, H. J., & Conrad, R. 1988. “The Capacity of Hydrogenotrophic Anaerobic Bacteria to Compete For Traces Of Hydrogen Depends On The Redox Potential Of The Terminal Electron Acceptor”. Archives of Microbiology, 149, 350-357.

<https://doi.org/10.1007/BF00411655>

Cormos, C. C. 2011. “Hydrogen Production from Fossil Fuels with Carbon Capture And Storage Based On Chemical Looping Systems”. International Journal of Hydrogen Energy.

<https://doi.org/10.1016/j.ijhydene.2011.01.170>

Cornelio, C., Spagnuolo, E., Di Toro, G., Nielsen, S., & Violay, M. 2019. “Mechanical Behaviour of Fluid-Lubricated Faults”. Nature communications, 10(1), 1274.

<https://doi.org/10.1038/s41467-019-09293-9>

Cornot-Gandolphe, S. 2018. Underground Gas Storage in The World–2017 Status. Cedigaz Insights, 31, 1-17.

Correas, L., & Simón, M. J. 2013. HyUnder Project.

Crabtree, G. W., & Dresselhaus, M. S. 2008. “The Hydrogen Fuel Alternative”. MRS Bulletin, 33(4), 421-428.

<https://doi.org/10.1557/mrs2008.84>

Crabtree, G. W., Dresselhaus, M. S., & Buchanan, M. V. 2004. “The Hydrogen Economy”. Physics today, 57(12), 39-44.

<https://doi.org/10.1063/1.1878333>

Crotogino, F., & Huebner, S. 2008. “Energy Storage in Salt Caverns: Developments and Concrete Projects for Adiabatic Compressed Air And For Hydrogen Storage”. In KBB Underground Technologies GMBh, Hannover, Germany. SMRI Spring Technical Meeting, Porto, Portugal (pp. 28-29).

Crotogino, F., Donadei, S., Bünger, U., & Landinger, H. 2010. “Large-Scale Hydrogen Underground Storage for Securing Future Energy Supplies”. In 18th World hydrogen energy conference (Vol. 78, pp. 37-45).

Crotogino, Fritz. 2022. “Large-Scale Hydrogen Storage”. In Storing energy: Elsevier (pp. 613-632).

Csavina, J., Field, J., Félix, O., Corral-Avitia, A. Y., Sáez, A. E., & Betterton, E. A. 2014. “Effect Of Wind Speed and Relative Humidity on Atmospheric Dust Concentrations In Semi-Arid Climates”. Science Of the Total Environment, 487, 82-90.

<https://doi.org/10.1016/j.scitotenv.2014.03.138>

Das, L. M. 2016. “Hydrogen-Fueled Internal Combustion Engines”. In Compendium of hydrogen energy (pp. 177-217). Woodhead Publishing.

<https://doi.org/10.1016/B978-1-78242-363-8.00007-4>

Datta, R. N. 2002. Rubber curing systems (Vol. 12). iSmithers Rapra Publishing.

Datta, S. 2004. Special-Purpose Elastomers. In Rubber Compounding (pp. 114-141). CRC Press.

<https://doi.org/10.1201/9781420030464>

Dautriat, J., Gland, N., Guelard, J., Dimanov, A., & Raphanel, J. L. 2009. “Axial And Radial Permeability Evolutions of Compressed Sandstones: End Effects And Shear-Band Induced Permeability Anisotropy”. Pure and Applied Geophysics, 166, 1037-1061.

<https://doi.org/10.1007/s00024-009-0495-0>

Davey, M. E., Gevertz, D., Wood, W. A., Clark, J. B., & Jenneman, G. E. 1998. "Microbial Selective Plugging Of Sandstone Through Stimulation Of Indigenous Bacteria In A Hypersaline Oil Reservoir". *Geomicrobiology Journal*, 15(4), 335-352.

<https://doi.org/10.1080/01490459809378087>

Dawood, F., Anda, M., & Shafiullah, G. M. 2020. "Hydrogen Production For Energy: An Overview." *International Journal of Hydrogen Energy*, 45(7), 3847-3869.

<https://doi.org/10.1016/j.ijhydene.2019.12.059>

de Sena Costa, B. L., de Oliveira Freitas, J. C., Santos, P. H. S., da Silva Araújo, R. G., dos Santos Oliveira, J. F., & de Araújo Melo, D. M. 2018. "Study Of Carbonation in A Class G Portland Cement Matrix At Supercritical And Saturated Environments". *Construction and Building Materials*, 180, 308-319.

<https://doi.org/10.1016/j.conbuildmat.2018.05.287>

Deepalekshmi, P., Visakh, P. M., Mathew, A. P., Chandra, A. K., & Thomas, S. 2013. "Advances In Elastomers: Their Blends and Interpenetrating Networks-State of Art, New Challenges and Opportunities". *Advances In Elastomers I: Blends and Interpenetrating Networks*, 1-9.

https://doi.org/10.1007/978-3-642-20925-3_1

Denecour, R. L., & Gent, A. N. 1968. Bubble Formation in Vulcanized Rubbers. *Journal of Polymer Science Part A-2: Polymer Physics*, 6(11), 1853-1861.

<https://doi.org/10.1002/pol.1968.160061103>

Deng, J., Ma, F., Li, S., He, Y., Wang, M., Jiang, L., & Zhao, S. 2011. "Experimental Study On Combustion And Emission Characteristics Of A Hydrogen-Enriched Compressed Natural Gas Engine Under Idling Condition". *International Journal of Hydrogen Energy*, 36(20), 13150-13157.

<https://doi.org/10.1016/j.ijhydene.2011.07.036>

Deutch, J., Moniz, E., Ansolabehere, S., Driscoll, M., Gray, P., Holdren, J., ... & Todreas, N. 2003. "The future of nuclear power". an MIT Interdisciplinary Study, <http://web.mit.edu/nuclearpower>.

Deveci, M. 2018. "Site Selection for Hydrogen Underground Storage Using Interval Type-2 Hesitant Fuzzy Sets". *International Journal of Hydrogen Energy*, 43(19), 9353-9368.

<https://doi.org/10.1016/j.ijhydene.2018.03.127>

Di Lullo, G., Oni, A. O., & Kumar, A. 2021. “Blending Blue Hydrogen with Natural Gas for Direct Consumption: Examining the Effect of Hydrogen Concentration On Transportation And Well-To-Combustion Greenhouse Gas Emissions”. *International Journal of Hydrogen Energy*, 46(36), 19202-19216.

<https://doi.org/10.1016/j.ijhydene.2021.03.062>

Dincer, I. 2012. “Green Methods for Hydrogen Production. *International Journal Of Hydrogen Energy*”, 37(2), 1954-1971.

<https://doi.org/10.1016/j.ijhydene.2011.03.173>

Dluzneski, P. R. 2001. “Peroxide Vulcanization of Elastomers”. *Rubber chemistry and technology*, 74(3), 451-492.

<https://doi.org/10.5254/1.3547647>

Donadei, S., Zander-Schiebenhöfer, D., Horvath, P. L., Zapf, D., Staudtmeister, K., Rokahr, R. B., ... & von Goerne, G. 2015. “Project InSpEE-Rock Mechanical Design for CAES and H₂ Storage Caverns & Evaluation of Storage Capacity in NW-Germany”. In *The Third Sustainable Earth Sciences Conference and Exhibition (Vol. 2015, No. 1, pp. 1-5)*. EAGE Publications BV.

<https://doi.org/10.3997/2214-4609.201414255>

Doornhof, D., Kristiansen, T. G., Nagel, N. B., Pattillo, P. D., & Sayers, C. 2006. “Compaction And Subsidence”. *Oilfield Review*, 18(3), 50-68.

Dopffel, N., Jansen, S., & Gerritse, J. 2021. “Microbial Side Effects of Underground Hydrogen Storage—Knowledge Gaps, Risks and Opportunities For Successful Implementation”. *International Journal Of Hydrogen Energy*, 46(12), 8594-8606.

<https://doi.org/10.1016/j.ijhydene.2020.12.058>

Drobny, J. G. 2014. *Handbook of thermoplastic elastomers*. Elsevier.

Drolet, B., & Gretz, J. 2002. “The Euro-Quebec Hydro-Hydrogen Pilot Project: The Beginning Of The Industrialisation Of Hydrogen Part 2: The View From North America”.

Duffy, J., & Wilson, G. J. 1993. “Synthesis Of Butyl Rubber by Cationic Polymerization. *Ullman’s Encyclopedia of Industrial Chemistry*”. 5th Edn. Elsevier, Amsterdam.

Dusseault, M. B., Jackson, R. E., & Macdonald, D. 2014. “Towards A Road Map for Mitigating The Rates And Occurrences Of Long-Term Wellbore Leakage”. Waterloo, ON, Canada: University of Waterloo.

Dwivedi, S. K., & Vishwakarma, M. 2018. “Hydrogen Embrittlement In Different Materials: A Review”. *International Journal Of Hydrogen Energy*, 43(46), 21603-21616.

<https://doi.org/10.1016/j.ijhydene.2018.09.201>

Ebigbo, A., Golfier, F., & Quintard, M. 2013. “A Coupled, Pore-Scale Model for Methanogenic Microbial Activity in Underground Hydrogen Storage”. *Advances In Water Resources*, 61, 74-85.

<https://doi.org/10.1016/j.advwatres.2013.09.004>

Ebrahimiyehta, A. 2017. “Characterization Of Geochemical Interactions and Migration of Hydrogen in Sandstone Sedimentary Formations: Application To Geological Storage (Doctoral Dissertation, Université d'Orléans)”.

Eddaoui, N., Panfilov, M., Ganzer, L., & Hagemann, B. 2021. “Impact Of Pore Clogging by Bacteria on Underground Hydrogen Storage”. *Transport in Porous Media*, 139, 89-108.

<https://doi.org/10.1007/s11242-021-01647-6>

Edmond, K. S. 2003. *Elastomer Explosive Decompression Modelling* (Doctoral dissertation, Cranfield University).

<https://ethos.bl.uk/OrderDetails.do?uin=uk.bl.ethos.486100>

Edwards, P. P., Kuznetsov, V. L., & David, W. I. 2007. “Hydrogen energy. *Philosophical Transactions of The Royal Society A: Mathematical, Physical And Engineering Sciences*”.

<https://doi.org/10.1098/rsta.2006.1965>

Edyvean, R. G. J., Benson, J., Thomas, C. J., Beech, I. B., & Videla, H. A. 1997. “Biological Influences on Hydrogen Effects In Steel In Seawater”. In *Corrosion97*. OnePetro.

Ehlig-Economides, C., & Hatzignatiou, D. G. 2021. “Blue Hydrogen Economy-A New Look at an Old Idea”. In *SPE Annual Technical Conference and Exhibition*. OnePetro.

<https://doi.org/10.2118/206282-MS>

EIA, U. 2022. *Annual energy outlook 2022*. Washington: US Energy Information Administration.

El-Emam, R. S., Ozcan, H., & Zamfirescu, C. 2020. “Updates On Promising Thermochemical Cycles for Clean Hydrogen Production Using Nuclear Energy”. *Journal of Cleaner Production*, 262, 121424.

<https://doi.org/10.1016/j.jclepro.2020.121424>

Elhard, J. D., Duguid, A., & Heinrichs, M. 2017. *Research on Safety Technology Verification for Materials and Pressure High Temperature (HPHT) Continental Shelf (OCS), High Corrosions in*

the US Outer Material Evaluation. Technical Assessment Program Report (TAP 767AA) Prepared for Bureau of Safety and Environmental Enforcement.

<https://www.bsee.gov/research-record/tap-767-safety-technology-verification-materials-and-corrosions-us-ocs-hpht-material> . Date Accessed: 28 August 2022.

Elias, H. G. 2003. “An introduction to plastics”. John Wiley & Sons.

Elias, H. G. 1997. “An Introduction to Polymer Science”.

El-Shafie, M., Kambara, S., & Hayakawa, Y. 2019. “Hydrogen Production Technologies Overview”.

Embury, P. 2004. “High-Pressure Gas Testing of Elastomer Seals and A Practical Approach to Designing For Explosive Decompression Service”. Sealing technology, 2004(6), 6-11.

[https://doi.org/10.1016/S1350-4789\(04\)00231-4](https://doi.org/10.1016/S1350-4789(04)00231-4)

ENTSOG, E. 2019. “2050 Roadmap for Gas Grids”.

Ertekin, A., & Sridhar, N. 2009. “Performance Of Elastomeric Materials in Gasoline-Ethanol Blends-A Review”. CORROSION 2009.

Evans, D. J. 2009. “A Review of Underground Fuel Storage Events and Putting Risk Into Perspective With Other Areas Of The Energy Supply Chain”. Geological Society, London, Special Publications, 313(1), 173-216.

<https://doi.org/10.1144/SP313.12>

Evans, D. J. 2007. “An Appraisal of Underground Gas Storage Technologies and Incidents, For the Development of Risk Assessment Methodology”. Volume 1, Text. Volume 2, Figures and Tables.

Evans, D. J. 2007. “An Appraisal of Underground Gas Storage Technologies and Incidents, For the Development of Risk Assessment Methodology”. Volume 1, Text. Volume 2, Figures and Tables.

<http://hdl.handle.net/1721.1/106782>

Fan, L., Tu, Z., & Chan, S. H. 2021. “Recent Development of Hydrogen and Fuel Cell Technologies: A Review”. Energy Reports, 7, 8421-8446.

<https://doi.org/10.1016/j.egy.2021.08.003>

Fancy, M. A., Joseph, R., & Varghese, S. 2013. “Elastomer Processing. Advances In Elastomers I: Blends and Interpenetrating Networks”.

Farhana, K., Kadirgama, K., Mahamude, A. S. F., & Mica, M. T. 2022. “Energy Consumption, Environmental Impact, And Implementation of Renewable Energy Resources in Global Textile Industries: An Overview Towards Circularity And Sustainability”. *Materials Circular Economy*, 4(1), 15.

<https://doi.org/10.1007/s42824-022-00059-1>

Federal Energy Regulatory Commission. 2004. “Current State of And Issues Concerning Underground Natural Gas Storage”. Energy, Washington DC Retrieved from www.ferc.gov/eventcalendar/files/20041020081349-final-gsreport.pdf.

Feyzullahoğlu, E. 2015. “Abrasive Wear, Thermal and Viscoelastic Behaviors Of Rubber Seal Materials Used In Different Working Conditions”. *Proceedings of the Institution of Mechanical Engineers, Part J: Journal of Engineering Tribology*, 229(1), 64-73.

<https://doi.org/10.1177/1350650114541750>

Fincke, J. R., Anderson, R. P., Hyde, T. A., & Detering, B. A. 2002. “Plasma Pyrolysis of Methane To Hydrogen And Carbon Black”. *Industrial & Engineering Chemistry Research*”.

<https://doi.org/10.1021/ie010722e>

Flesch, S., Pudlo, D., Albrecht, D., Jacob, A., & Enzmann, F. 2018. “Hydrogen Underground Storage—Petrographic and Petrophysical Variations in Reservoir Sandstones From Laboratory Experiments Under Simulated Reservoir Conditions”. *International Journal of Hydrogen Energy*.

<https://doi.org/10.1016/j.ijhydene.2018.09.112>

Folga, S., Portante, E., Shamsuddin, S., Tompkins, A., Talaber, L., McLamore, M., . & Levin, T. 2016. “US natural gas storage risk-based ranking methodology and results” (No. ANL-16/19). Argonne National Lab.(ANL), Argonne, IL (United States).

<https://doi.org/10.2172/1337151>

Freifeld, B. M., Oldenburg, C. M., Jordan, P., Pan, L., Perfect, S., Morris, J., & Rose, K. 2016. “Well Integrity for Natural Gas Storage in Depleted Reservoirs and Aquifers” (No. LBNL-1006165). Lawrence Berkeley National Lab. (LBNL), Berkeley, CA (United States).

<https://doi.org/10.2172/1338936>

Freund, H. J., & Messmer, R. P. 1986. “On The Bonding and Reactivity Of CO₂ On Metal Surfaces”. *Surface science*, 172(1), 1-30.

[https://doi.org/10.1016/0039-6028\(86\)90580-7](https://doi.org/10.1016/0039-6028(86)90580-7)

Freyer, R., & Huse, A. 2002. "Swelling Packer for Zonal Isolation In Open Hole Screen Completions". In European Petroleum Conference. OnePetro. 29 October 2002. SPE-78312-MS <https://doi.org/10.2118/78312-MS>

Fries, H., & Pandit, R. R. 1982. "Mastication Of Rubber". Rubber Chemistry and Technology, 55(2), 309-327. <https://doi.org/10.5254/1.3535880>

Fujiwara, H., Ono, H., & Nishimura, S. 2015. "Degradation Behavior Of Acrylonitrile Butadiene Rubber After Cyclic High-Pressure Hydrogen Exposure". International Journal of Hydrogen Energy, 40(4), 2025-2034. <https://doi.org/10.1016/j.ijhydene.2014.11.106>

Gabrielli, P., Poluzzi, A., Kramer, G. J., Spiers, C., Mazzotti, M., & Gazzani, M. 2020. "Seasonal Energy Storage for Zero-Emissions Multi-Energy Systems Via Underground Hydrogen Storage". Renewable and Sustainable Energy Reviews, 121, 109629.

Gaines, L. G. 2023. "Historical And Current Usage of Per-And Polyfluoroalkyl Substances (PFAS)": A Literature Review. American Journal of Industrial Medicine, 66(5), 353-378. <https://doi.org/10.1016/j.rser.2019.109629>

Galan, I., Glasser, F. P., Baza, D., & Andrade, C. 2015. "Assessment of The Protective Effect of Carbonation On Portlandite Crystals". Cement and Concrete Research, 74, 68-77. <https://doi.org/10.1016/j.cemconres.2015.04.001>

Gallandat, N., Romanowicz, K., & Züttel, A. 2017. "An Analytical Model for The Electrolyser Performance Derived From Materials Parameters". Journal of Power and Energy Engineering, 5(10), 34-49. [10.4236/jpee.2017.510003](https://doi.org/10.4236/jpee.2017.510003)

Gangloff, R. P., & Somerday, B. P. (Eds.). 2012. "Gaseous Hydrogen Embrittlement Of Materials In Energy Technologies: The Problem, Its Characterisation And Effects On Particular Alloy Classes".

Garbis, P., Kern, C., & Jess, A. 2019. "Kinetics And Reactor Design Aspects Of Selective Methanation Of CO Over A Ru/γ-Al₂O₃ Catalyst In CO₂/H₂ Rich Gases". Energies, 12(3), 469. <https://doi.org/10.3390/en12030469>

Gardiner, J. 2014. "Fluoropolymers: Origin, Production, And Industrial and Commercial Applications". Australian Journal of Chemistry, 68(1), 13-22.

<https://doi.org/10.1071/CH14165>

Gardner, D. 2009. "Hydrogen production from renewables. Renewable Energy Focus".9(7), 34-37.

[https://doi.org/10.1016/S1755-0084\(09\)70036-5](https://doi.org/10.1016/S1755-0084(09)70036-5)

Garfield, G., & Mackenzie, G. 2007. "Zonal Isolation Applications Utilizing New Metal-To-Metal Sealing Technology Demonstrates Potential for Offshore and Deepwater Environments". In Offshore Mediterranean Conference and Exhibition. OnePetro.

[https://doi.org/10.1016/S1755-0084\(09\)70036-5](https://doi.org/10.1016/S1755-0084(09)70036-5)

Gasda, S. E., Bachu, S., & Celia, M. A. 2004. "Spatial Characterization of The Location Of Potentially Leaky Wells Penetrating A Deep Saline Aquifer In A Mature Sedimentary Basin". Environmental geology, 46, 707-720.

Gaucher, C., Sial, A. N., Halverson, G. P., & Frimmel, H. E. (Eds.). 2009. "Neoproterozoic-Cambrian Tectonics, Global Change and Evolution: A Focus On Southwestern Gondwana". Elsevier.

Gent, A. N. 1990. "Cavitation In Rubber: A Cautionary Tale. Rubber Chemistry and Technology", 63(3), 49-53.

<https://doi.org/10.5254/1.3538266>

Gent, A. N., & Tompkins, D. A. 1969. "Surface Energy Effects For Small Holes Or Particles In Elastomers". Journal of Polymer Science Part A-2: Polymer Physics, 7(9), 1483-1487.

<https://doi.org/10.1002/pol.1969.160070904>

George, J., Varughese, K. T., & Thomas, S. 2000. "Dynamically Vulcanized Thermoplastic Elastomer Blends Of Polyethylene And Nitrile Rubber". Polymer, 41(4), 1507-1517.

[https://doi.org/10.1016/s0032-3861\(99\)00302-x](https://doi.org/10.1016/s0032-3861(99)00302-x)

Ghasemi, R. 2011. "Hydrogen-Assisted Stress Corrosion Cracking of High Strength Steel".

Gholami, R., Raza, A., & Iglauer, S. 2021. "Leakage Risk Assessment of A CO₂ Storage Site: A Review". Earth-Science Reviews, 223, 103849.

<https://doi.org/10.1016/j.earscirev.2021.103849>

Ginic-Markovic, M., Choudhury, N. R., Dimopoulos, M., Williams, D. R., & Matisons, J. 1998. "Characterization Of Elastomer Compounds by Thermal Analysis". *Thermochimica Acta*, 316(1), 87-95.

[https://doi.org/10.1016/s0040-6031\(98\)00290-1](https://doi.org/10.1016/s0040-6031(98)00290-1)

Gniese, C., Bombach, P., Rakoczy, J., Hoth, N., Schlömann, M., Richnow, H. H., & Krüger, M. 2014. "Relevance Of Deep-Subsurface Microbiology for Underground Gas Storage And Geothermal Energy Production". *Geobiotechnology II: Energy Resources, Subsurface Technologies, Organic Pollutants and Mining Legal Principles*, 95-121.

Götz, M., Lefebvre, J., Mörs, F., Koch, A. M., Graf, F., Bajohr, S., ... & Kolb, T. 2016. "Renewable Power-To-Gas: A Technological and Economic Review". *Renewable Energy*, 85, 1371-1390.

<https://doi.org/10.1016/j.renene.2015.07.066>

Gradisher, L., Dutcher, B., & Fan, M. 2015. "Catalytic Hydrogen Production from Fossil Fuels Via The Water Gas Shift Reaction". *Applied Energy*, 139, 335-349.

<https://doi.org/10.1016/j.apenergy.2014.10.080>

Gronowski, A. A. 2003. "Synthesis Of Butyl Rubber In Hexane Using A Mixture Of Et₂AlCl And EtAlCl₂ In The Initiating System". *Journal Of Applied Polymer Science*, 87(14), 2360-2364.

<https://doi.org/10.1002/app.11924>

Guiltinan, E. J., Cardenas, M. B., Bennett, P. C., Zhang, T., & Espinoza, D. N. 2017. "The Effect of Organic Matter And Thermal Maturity On The Wettability Of Supercritical CO₂ On Organic Shales". *International Journal of Greenhouse Gas Control*.

Standard, A. S. T. M. 2010. "Standard Test Method for Rubber Property-Durometer Hardness".

<https://doi.org/10.1016/j.ijggc.2017.08.006>

Harwood, H. J. (1983). Ethylene-propylene-diene monomer (EPDM) and fluorocarbon (FKM) elastomers in the geothermal environment. *Journal of testing and evaluation*, 11(4), 289-298.

Hardy, C. 2003. "The Hydrogen Economy for A Sustainable Future And The Potential Contribution Of Nuclear Power".

Haronabadi, L., Dashti, A., & Najipour, M. 2018. "Investigation of the Effect of Thermal Aging On Rapid Gas Decompression (RGD) Resistance Of Nitrile Rubber". *Polymer Testing*, 67, 37-45.

<https://doi.org/10.1016/j.polymertesting.2018.02.014>

Hashemi, L., Glerum, W., Farajzadeh, R., & Hajibeygi, H. 2021. “Contact Angle Measurement For Hydrogen/Brine/Sandstone System Using Captive-Bubble Method Relevant For Underground Hydrogen Storage”. *Advances In Water Resources*, 154, 103964.

<https://doi.org/10.1016/j.advwatres.2021.103964>

Hassanpouryouzband, A., Joonaki, E., Edlmann, K., & Haszeldine, R. S. 2021. “Offshore Geological Storage Of Hydrogen: Is This Our Best Option To Achieve Net-Zero?”. *ACS Energy Letters*, 6(6), 2181-2186.

<https://doi.org/10.1021/acsenergylett.1c00845>

Heideman, G., Datta, R. N., Noordermeer, J. W., & Van Baarle, B. 2004. “Activators In Accelerated Sulfur Vulcanization. *Rubber Chemistry and Technology*”.

<https://doi.org/10.5254/1.3547834>

Heinemann, N., Alcalde, J., Miocic, J. M., Hangx, S. J., Kallmeyer, J., Ostertag-Henning, C., ... & Rudloff, A. 2021. “Enabling Large-Scale Hydrogen Storage In Porous Media–The Scientific Challenges”. *Energy & Environmental Science*, 14(2), 853-864.

Heinemann, N., Booth, M. G., Haszeldine, R. S., Wilkinson, M., Scafidi, J., & Edlmann, K. 2018. “Hydrogen Storage in Porous Geological Formations–Onshore Play Opportunities In The Midland Valley (Scotland, Uk)”. *International Journal of Hydrogen Energy*, 43(45), 20861-20874.

<https://doi.org/10.1016/j.ijhydene.2018.09.149>

Heller, M., Legare, J., Wang, S., & Fukuhara, S. 1999. “Thermal Stability and Sealing Performance Of Perfluoroelastomer Seals As A Function Of Crosslinking Chemistry”. *Journal of Vacuum Science & Technology A: Vacuum, Surfaces, And Films*, 17(4), 2119-2124.

<https://doi.org/10.1116/1.581736>

Hematpur, H., Abdollahi, R., Rostami, S., Haghighi, M., & Blunt, M. J. 2023. “Review of Underground Hydrogen Storage: Concepts and Challenges”. *Advances In Geo-Energy Research*, 7(2), 111-131.

<https://doi.org/10.46690/ager.2023.02.05>

Hemme, C., & Van Berk, W. 2018. “Hydrogeochemical Modeling to Identify Potential Risks Of Underground Hydrogen Storage In Depleted Gas Fields”. *Applied Sciences*, 8(11), 2282.

<https://doi.org/10.3390/app8112282>

Henkel, S., Pudlo, D., Werner, L., Enzmann, F., Reitenbach, V., Albrecht, D., . & Gaupp, R. 2014. "Mineral Reactions in The Geological Underground Induced by H₂ And CO₂ Injections". Energy Procedia, 63, 8026-8035.

<https://doi.org/10.1016/j.egypro.2014.11.839>

Hermesmann, M., & Müller, T. E. 2022. "Green, Turquoise, Blue, Or Grey? Environmentally Friendly Hydrogen Production in Transforming Energy Systems". Progress In Energy and Combustion Science, 90, 100996.

<https://doi.org/10.1016/j.pecs.2022.100996>

Higman, C., Van Der Burgt, M., Higman, C., & Vanderburgt, M. 2008. "The Thermodynamics Of Gasification. Gasification". Amsterdam, Boston: Gulf Professional Pub./Elsevier Science, 11-31.

<http://dx.doi.org/10.1016/b978-0-7506-8528-3.00002-x>

Hilado, C. J. 1998. "Flammability Handbook for Plastics". Crc Press.

Hill, David M.. "4. Degradation Of Elastomers". Latex Dipping: Science and Technology, Berlin, Boston: De Gruyter, 2019, Pp. 73-78.

<https://doi.org/10.1515/9783110638097-004>

Hirata, Y., Kondo, H., & Ozawa, Y. 2014. "Natural Rubber (Nr) For the Tyre Industry". In Chemistry, Manufacture and Applications of Natural Rubber (Pp. 325-352). Woodhead Publishing.

<https://doi.org/10.1533/9780857096913.2.325>

Holden, G., Bishop, E. T., & Legge, N. R. 1969. "Thermoplastic Elastomers". In Journal of Polymer Science Part C: Polymer Symposia (Vol. 26, No. 1, Pp. 37-57). New York: Wiley Subscription Services, Inc., A Wiley Company.

<https://doi.org/10.1002/polc.5070260104>

Holladay, J. D., Hu, J., King, D. L., & Wang, Y. 2009. "An Overview of Hydrogen Production Technologies". Catalysis Today, 139(4), 244-260.

<https://doi.org/10.1016/j.cattod.2008.08.039>

Hosseini, S. E., & Wahid, M. A. 2016. "Hydrogen Production from Renewable and Sustainable Energy Resources: Promising Green Energy Carrier For Clean Development". Renewable And Sustainable Energy Reviews, 57, 850-866.

<https://doi.org/10.1016/j.rser.2015.12.112>

Howarth, R. W., & Jacobson, M. Z. 2021. “How Green Is Blue Hydrogen?”. *Energy Science & Engineering*, 9(10), 1676-1687.

<https://doi.org/10.1002/ese3.956>

Huang, Y. 2014. “Drivers Of Rising Global Energy Demand: The Importance of Spatial Lag And Error Dependence”. *Energy*, 76, 254-263.

<https://doi.org/10.1016/j.energy.2014.07.093>

Council, H. 2017. “Hydrogen Scaling Up: A Sustainable Pathway for The Global Energy Transition”.

Ibarra, L., & Alzoriz, M. 2007. “Ionic Elastomers Based on Carboxylated Nitrile Rubber and Magnesium Oxide”. *Journal Of Applied Polymer Science*, 103(3), 1894-1899.

Iglauer, S., Ali, M., & Keshavarz, A. 2021. “Hydrogen Wettability of Sandstone Reservoirs: Implications for Hydrogen Geo-Storage”. *Geophysical Research Letters*, 48(3), E2020gl090814.

<https://doi.org/10.1029/2020gl090814>

Imato, K., Kanehara, T., Nojima, S., Ohishi, T., Higaki, Y., Takahara, A., & Otsuka, H. 2016. “Repeatable Mechanochemical Activation of Dynamic Covalent Bonds in Thermoplastic Elastomers”. *Chemical Communications*, 52(69), 10482-10485.

Iordache, I., Schitea, D., Gheorghe, A. V., & Iordache, M. 2014. “Hydrogen Underground Storage In Romania, Potential Directions Of Development, Stakeholders And General Aspects”. *International Journal Of Hydrogen Energy*, 39(21), 11071-11081.

<https://doi.org/10.1016/j.ijhydene.2014.05.067>

Iqbal, K., Saxena, A., Pande, P., Tiwari, A., Joshi, N. C., Varma, A., & Mishra, A. 2022. “Microalgae-Bacterial Granular Consortium: Striding Towards Sustainable Production Of Biohydrogen Coupled With Wastewater Treatment”. *Bioresource Technology*, 127203.

<https://doi.org/10.1016/j.biortech.2022.127203>

Bianco, E., & Blanco, H. 2020. “Green Hydrogen: A Guide to Policy Making”.

Iso, N. 2017. “Petroleum And Natural Gas Industries-Well Integrity-Part 1: Life Cycle Governance”.

Jaravel, J., Castagnet, S., Grandidier, J. C., & Benoît, G. 2011. “On Key Parameters Influencing Cavitation Damage Upon Fast Decompression In A Hydrogen Saturated Elastomer”. *Polymer Testing*, 30(8), 811-818.

<https://doi.org/10.1016/j.polymertesting.2011.08.003>

Jaunich, M., Von Der Ehe, K., Wolff, D., Völzke, H., & Stark, W. 2011. “Understanding Low Temperature Properties Of Elastomer Seals”. *Packaging, Transport, Storage & Security Of Radioactive Material*, 22(2), 83-88.

<https://doi.org/10.1179/1746510911y.0000000004>

Jayasekara, D. W., Ranjith, P. G., Wanniarachchi, W. A. M., & Rathnaweera, T. D. 2020. “Understanding The Chemico-Mineralogical Changes of Caprock Sealing In Deep Saline CO₂ Sequestration Environments: A Review Study”. *The Journal of Supercritical Fluids*, 161, 104819.

<https://doi.org/10.1016/j.supflu.2020.104819>

Jiang, Y., Li, W. J., Xu, P., Tang, S. K., & Xu, L. H. 2006. “Study On Diversity of Actinomycetes Under Salt and Alkaline Environments”. *Wei Sheng Wu Xue Bao= Acta Microbiologica Sinica*, 46(2), 191-195.

Jin, H. H., Hong, C. K., Cho, D. L., & Kaang, S. Y. 2008. “Effects Of Temperature on Hardness Of Rubber Materials With Different Curing System”. *Elastomers And Composites*, 43(4), 213-220.

John, V., & John, V. 1992. “Elastomers”. *Introduction To Engineering Materials*, 270-275.

Johnson, P. R. 1976. “Polychloroprene Rubber”. *Rubber Chemistry and Technology*, 49(3), 650-702.

<https://doi.org/10.5254/1.3534978>

Jurkowska, B., Olkhov, Y. A., & Jurkowski, B. 1998. “Thermomechanical Study Of Butyl Rubber Mastication During Compounding”. *Journal Of Applied Polymer Science*, 68(13), 2159-2167.

[https://doi.org/10.1002/\(sici\)1097-4628](https://doi.org/10.1002/(sici)1097-4628)

Kakooei, S., Ismail, M. C., & Ariwahjoedi, B. 2012. “Mechanisms Of Microbiologically Influenced Corrosion: A Review”. *World Appl. Sci. J*, 17(4), 524.

Kalamaras, C. M., & Efstathiou, A. M. 2013. “Hydrogen Production Technologies: Current State And Future Developments”. In *Conference Papers in Science*. Hindawi.

<http://dx.doi.org/10.1155/2013/690627>

Kalfayan, S. H., Silver, R. H., Mazzeo, A. A., & Lui, S. T. 1972. “Long Term Aging Of Elastomers: Chemorheology Of Viton B Fluorocarbon Elastomer”.

Kampman, N., Busch, A., Bertier, P., Snippe, J., Hangx, S., Pipich, V., ... & Bickle, M. J. 2016. “Observational Evidence Confirms Modelling of The Long-Term Integrity Of CO₂-Reservoir Caprocks”. *Nature Communications*, 7(1), 12268.

<https://doi.org/10.1038/ncomms12268>

Kanaani, M., Sedaee, B., & Asadian-Pakfar, M. 2022. “Role Of Cushion Gas on Underground Hydrogen Storage In Depleted Oil Reservoirs”. *Journal Of Energy Storage*, 45, 103783.

<https://doi.org/10.1016/j.est.2021.103783>

Karakilcik, H., & Karakilcik, M. 2020. “Underground Large-Scale Hydrogen Storage. Accelerating The Transition to A 100% Renewable Energy Era”.

Karpeles, R., & Grossi, A. V. 2000. “EPDM Rubber Technology”. In *Handbook of Elastomers* (Pp. 863-894). Crc Press.

Katz, D. L., & Tek, M. R. 1981. “Overview On Underground Storage of Natural Gas. *Journal Of Petroleum Technology*”. 33(06), 943-951.

<https://doi.org/10.2118/9390-pa>

Kennedy, G., Lawless, A., Shaikh, K., & Alabi, T. 2005. “The Use Of Swell Packers As A Replacement And Alternative To Cementing”. In *SPE Annual Technical Conference And Exhibition*. 9-12 October 2005.

<https://doi.org/10.2118/95713-ms>

Kim, Y. S., & Kim, J. G. 2017. “Electroplating Of Reduced-Graphene Oxide on Austenitic Stainless Steel to Prevent Hydrogen Embrittlement”. *International Journal of Hydrogen Energy*, 42(44), 27428-27437.

<https://doi.org/10.1016/j.ijhydene.2017.09.033>

King, G. E., & King, D. E. 2013. “Environmental Risk Arising from Well-Construction Failure—Differences Between Barrier and Well Failure, And Estimates Of Failure Frequency Across Common Well Types, Locations, And Well Age”. *SPE Production & Operations*, 28(04), 323-344.

<https://doi.org/10.2118/166142-pa>

Kiran, R., Teodoriu, C., Dadmohammadi, Y., Nygaard, R., Wood, D., Mokhtari, M., & Salehi, S. 2017. "Identification And Evaluation of Well Integrity And Causes Of Failure Of Well Integrity Barriers: A Review". *Journal Of Natural Gas Science and Engineering*, 45, 511-526.

<https://doi.org/10.1016/j.jngse.2017.05.009>

Kleinitz, W., & Boehling, E. 2005. "Underground Gas Storage In Porous Media—Operating Experience With Bacteria On Gas Quality". In 67th Eage Conference & Exhibition (Pp. Cp-1). Eage Publications Bv.

<https://doi.org/10.3997/2214-4609-pdb.1.p252>

Kobos, P. H., Lord, A. S., Borns, D. J., & Klise, G. T. 2011. "A Life Cycle Cost Analysis Framework for Geologic Storage Of Hydrogen": A User's Tool (No. Sand2011-6221). Sandia National Laboratories (SNL), Albuquerque, Nm, And Livermore, Ca (United States).

<https://doi.org/10.2172/1029761>

Kodal, M., & Özkoç, G. 2021. "Lab-Scale Twin-Screw Micro-Compounders As A New Rubber-Mixing Tool: 'A Comparison On EPDM/Carbon Black And EPDM/Silica Composites". *Polymers*, 13(24), 4391.

<https://doi.org/10.3390/polym13244391>

Kohjiya, S. 2015. "Natural Rubber". *Smithers Rapra*.

Kömmling, A., Jaunich, M., & Wolff, D. 2016." Revealing Effects Of Chain Scission During Ageing Of EPDM Rubber Using Relaxation And Recovery Experiment". *Polymer Testing*, 56, 261-268.

<https://doi.org/10.1016/j.polymertesting.2016.10.026>

Kong, M., Feng, S., Xia, Q., Chen, C., Pan, Z., & Gao, Z. 2021. "Investigation Of Mixing Behavior of Hydrogen Blended To Natural Gas In Gas Network". *Sustainability*, 13(8), 4255.

<https://doi.org/10.3390/su13084255>

Kubena, E., Ross, K. C., Pugh, T., & Huycke, J. 1991. "Performance Characteristics Of Drilling Equipment Elastomers Evaluated In Various Drilling Fluids". In SPE/IADC Drilling Conference, Amsterdam Netherlands, 11-14 March, 1991. SPE-21960-MS.

<https://doi.org/10.2118/21960-ms>

Von Wolzogen Kühr, C. A. H., & Van Der Vlugt, L. S. 1964. "Graphitization Of Cast Iron As An Electrochemical Process In Anaerobic Soils". *Army Biological Labs Frederick Md*.

Kulkarni, S. S., Choi, K. S., Kuang, W., Menon, N., Mills, B., Souلامي, A., & Simmons, K. 2021. "Damage Evolution In Polymer Due To Exposure To High-Pressure Hydrogen Gas". *International Journal Of Hydrogen Energy*, 46(36), 19001-19022.

<https://doi.org/10.1016/j.ijhydene.2021.03.035>

Kwatia, G. O. 2018. "Studying "Fitness for Service" Of The Sealing Assemblies And Cement System".

<https://hdl.handle.net/11244/299822>

Labus, K., & Tarkowski, R. 2022. "Modeling Hydrogen–Rock–Brine Interactions for The Jurassic Reservoir and Cap Rocks From Polish Lowlands". *International Journal of Hydrogen Energy*, 47(20), 10947-10962.

<https://doi.org/10.1016/j.ijhydene.2022.01.134>

Lachat, V. 2008. "Understanding Oil Resistance of Nitrile Rubber: Cn Group Interactions at Interfaces". The University of Akron.

Lancaster, J. K. 1969. "Abrasive Wear Of Polymers". *Wear*, 14(4), 223-239.

[https://doi.org/10.1016/0043-1648\(69\)90047-7](https://doi.org/10.1016/0043-1648(69)90047-7)

Lankof, L., & Tarkowski, R. 2020. "Assessment Of the Potential for Underground Hydrogen Storage In Bedded Salt Formation". *International Journal of Hydrogen Energy*, 45(38), 19479-19492.

<https://doi.org/10.1016/j.ijhydene.2020.05.024>

Lanz, A., Heffel, J., & Messer, C. 2001. "Hydrogen Fuel Cell Engines and Related Technologies (No. Fta-Ca-26-7022-01.1). United States. Department Of Transportation". Federal Transit Administration.

Le Saout, G., Lécolier, E., Rivereau, A., & Zanni, H. 2006. "Chemical Structure of Cement Aged At Normal And Elevated Temperatures And Pressures: Part I. Class G Oilwell Cement". *Cement And Concrete Research*, 36(1), 71-78.

<https://doi.org/10.1016/j.cemconres.2004.09.018>

Lee, D. S., Lewis, P. M., Cape, J. N., Leith, I. D., & Espenhahn, S. E. 2003. "The Effects of Ozone On Materials—Experimental Evaluation Of The Susceptibility Of Polymeric Materials To Ozone". In *The Effects of Air Pollution On The Built Environment* (Pp. 267-287).

Lee, T. C. P., & Morrell, S. H. 1973. "Network Changes in Nitrile Rubber At Elevated Temperatures". *Rubber Chemistry and Technology*, 46(2), 483-503.

<https://doi.org/10.5254/1.3542918>

Leicher, J., Schaffert, J., Cigarida, H., Tali, E., Burmeister, F., Giese, A., ... & Schweitzer, J. 2022. "The Impact Of Hydrogen Admixture Into Natural Gas On Residential And Commercial Gas Appliances". *Energies*, 15(3), 777.

<https://doi.org/10.3390/en15030777>

Leighty, W. C. 2008, January. "Running The World on Renewables: Hydrogen Transmission Pipelines with Firming Geologic Storage". In *ASME Power Conference* (Vol. 48329, Pp. 601-613).

<https://doi.org/10.1115/power2008-60031>

Lemieux, A., Sharp, K., & Shkarupin, A. 2019. "Preliminary Assessment of Underground Hydrogen Storage Sites in Ontario, Canada". *International Journal of Hydrogen Energy*, 44(29), 15193-15204.

<https://doi.org/10.1016/j.ijhydene.2019.04.113>

Leung, S. N. 2018. "Thermally Conductive Polymer Composites and Nanocomposites: Processing-Structure-Property Relationships". *Composites Part B: Engineering*, 150, 78-92.

<https://doi.org/10.1016/j.compositesb.2018.05.056>

Lewandowska-Śmierchalska, J., Tarkowski, R., & Uliasz-Misiak, B. 2018. "Screening And Ranking Framework for Underground Hydrogen Storage Site Selection In Poland". *International Journal Of Hydrogen Energy*, 43(9), 4401-4414.

<https://doi.org/10.1016/j.ijhydene.2018.01.089>

Li, C. E., Kuan, B., Lee, W. J., Burke, N., & Patel, J. 2018. "The Non-Catalytic Partial Oxidation of Methane In A Flow Tube Reactor Using Indirect Induction Heating—An Experimental And Kinetic Modelling Study". *Chemical Engineering Science*, 187, 189-199.

<https://doi.org/10.1016/j.ces.2018.04.070>

Lin, S., Harada, M., Suzuki, Y., & Hatano, H. 2002. "Hydrogen Production from Coal By Separating Carbon Dioxide During Gasification". *Fuel*, 81(16), 2079-2085.

[https://doi.org/10.1016/s0016-2361\(02\)00187-4](https://doi.org/10.1016/s0016-2361(02)00187-4)

Lion, A., & Jöhrlitz, M. 2012. "On The Representation Of Chemical Ageing Of Rubber In Continuum Mechanics". *International Journal of Solids and Structures*, 49(10), 1227-1240.

<https://doi.org/10.1016/j.ijsolstr.2012.01.014>

Liu, J., Wang, S., Javadpour, F., Feng, Q., & Cha, L. 2022. “Hydrogen Diffusion in Clay Slit: Implications for The Geological Storage”. *Energy & Fuels*, 36(14), 7651-7660.

<https://doi.org/10.1021/acs.energyfuels.2c01189>

Liu, W., Zhang, Z., Chen, J., Jiang, D., Wu, F., Fan, J., & Li, Y. 2020. “Feasibility Evaluation Of Large-Scale Underground Hydrogen Storage In Bedded Salt Rocks Of China: A Case Study In Jiangsu Province”. *Energy*, 198, 117348.

<https://doi.org/10.1016/j.energy.2020.117348>

Loadman, M. J. R. 1985. “The Glass Transition Temperature of Natural Rubber”. *Journal Of Thermal Analysis and Calorimetry*, 30(4), 929-941.

<https://doi.org/10.1007/bf01913321>

Lodewijks, G. 2011. “The Next Generation Low Loss Conveyor Belts”. *Bulk Solids Handling*, 32(1), 52-56.

Logothetis, A. L. 1989. “Chemistry Of Fluorocarbon Elastomers”. *Progress In Polymer Science*, 14(2), 251-296.

[https://doi.org/10.1016/0079-6700\(89\)90003-8](https://doi.org/10.1016/0079-6700(89)90003-8)

Lord, A. S., Kobos, P. H., & Borns, D. J. 2014. “Geologic Storage of Hydrogen: Scaling Up To Meet City Transportation Demands”. *International Journal of Hydrogen Energy*, 39(28), 15570-15582.

<https://doi.org/10.1016/j.ijhydene.2014.07.121>

Lorge, O., Briscoe, B. J., & Dang, P. 1999. “Gas Induced Damage in Poly (Vinylidene Fluoride) Exposed To Decompression”. *Polymer*, 40(11), 2981-2991.

[https://doi.org/10.1016/s0032-3861\(98\)00527-8](https://doi.org/10.1016/s0032-3861(98)00527-8)

Lu, Z., Zhang, X., Tian, D., Li, H., & Lu, C. 2012. “Mechanochemical Preparation of Devulcanized Ground Flouroelastomers for The Enhancement of The Thermal Stability of Nitrile–Butadiene Rubber Vulcanizates”. *Journal Of Applied Polymer Science*, 126(4), 1351-1358.

<https://doi.org/10.1002/app.36638>

Lago, W. S. R., Aymes-Chodur, C., Ahoussou, A. P., & Yagoubi, N. 2017. Physico-chemical ageing of ethylene–norbornene copolymers: a review. *Journal of Materials Science*, 52, 6879-6904.

Mahajan, D., Tan, K., Venkatesh, T., Kileti, P., & Clayton, C. R. 2022. “Hydrogen Blending in Gas Pipeline Networks—A Review”. *Energies*, 15(10), 3582.

<https://doi.org/10.3390/en15103582>

Fazal, M. 2019. “In-Situ Investigation of Cavity Nucleation and Growth In Hydrogen-Exposed EPDM During Decompression” (Doctoral Dissertation, Isae-Ensm Ecole Nationale Supérieure De Mécanique Et D'aérotechnique-Poitiers).

Mao, Y., Talamini, B., & Anand, L. 2017. “Rupture Of Polymers by Chain Scission”. *Extreme Mechanics Letters*, 13, 17-24.

<https://doi.org/10.1016/j.eml.2017.01.003>

Mark, J. E. 2017. “Thermoset Elastomers”. In *Applied Plastics Engineering Handbook* (Pp. 109-125). William Andrew Publishing.

<https://doi.org/10.1016/b978-0-323-39040-8.00006-7>

Mark, J. E., Erman, B., & Roland, M. (Eds.). 2013. “The Science and Technology of Rubber”. Academic Press.

Melaina, M. W., Antonia, O., & Penev, M. 2013. “Blending Hydrogen into Natural Gas Pipeline Networks: A Review of Key Issues”.

Melnichuk, M., Thiébaud, F., & Perreux, D. 2020. “Non-Dimensional Assessments to Estimate Decompression Failure in Polymers for Hydrogen Systems”. *International Journal of Hydrogen Energy*, 45(11), 6738-6744.

<https://doi.org/10.1016/j.ijhydene.2019.12.107>

Menon, N. C., Kruizenga, A. M., Alvine, K. J., San Marchi, C., Nissen, A., & Brooks, K. 2016, July. “Behaviour Of Polymers in High Pressure Environments As Applicable To The Hydrogen Infrastructure. In *Pressure Vessels and Piping Conference* (Vol. 50435, P. V06bt06a037)”. American Society Of Mechanical Engineers.

<https://doi.org/10.1115/pvp2016-63713>

Michalski, J., Bünger, U., Crotogino, F., Donadei, S., Schneider, G. S., Pregger, T., ... & Heide, D. 2017. “Hydrogen Generation by Electrolysis and Storage In Salt Caverns: Potentials, Economics And Systems Aspects With Regard To The German Energy Transition”. *International Journal Of Hydrogen Energy*, 42(19), 13427-13443.

<https://doi.org/10.1016/j.ijhydene.2017.02.102>

Midilli, A., Kucuk, H., Topal, M. E., Akbulut, U., & Dincer, I. 2021. “A Comprehensive Review on Hydrogen Production from Coal Gasification: Challenges And Opportunities”. *International Journal Of Hydrogen Energy*, 46(50), 25385-25412.

<https://doi.org/10.1016/j.ijhydene.2021.05.088>

Midilli, A., Dincer, I., & Ay, M. 2006. “Green Energy Strategies for Sustainable Development”. *Energy Policy*, 34(18), 3623-3633.

<https://doi.org/10.1016/j.enpol.2005.08.003>

Miroslav Penchev, Taehoon Lim, Michael Todd, Oren Lever, Ernest Lever, Suveen Mathaudhu, Alfredo Martinez-Morales, And Arun S.K. Raju*. 2022. Hydrogen Blending Impacts Study Final Report. Agreement Number: 19ns1662.

Mishra, V. 2021, April. “Effect Of Carbon Black and Graphene on The Performance Of EPDM Rubber Composites: A Short Review”. In *Iop Conference Series: Materials Science and Engineering* (Vol. 1116, No. 1, P. 012004). Iop Publishing.

Mitra, S., Ghanbari-Siahkali, A., Kingshott, P., Almdal, K., Rehmeier, H. K., & Christensen, A. G. 2004. “Chemical degradation of fluoroelastomer in an alkaline environment. *Polymer Degradation and Stability*”. 83(2), 195-206.

[https://doi.org/10.1016/S0141-3910\(03\)00235-0](https://doi.org/10.1016/S0141-3910(03)00235-0)

Mitsugi, C., Harumi, A., & Kenzo, F. 1998. “We-Net: Japanese Hydrogen Program”. *International Journal Of Hydrogen Energy*, 23(3), 159-165.

[https://doi.org/10.1016/s0360-3199\(97\)00042-6](https://doi.org/10.1016/s0360-3199(97)00042-6)

Miyazaki, B. 2009. “Well Integrity: An Overlooked Source of Risk and Liability For Underground Natural Gas Storage”. *Lessons Learned from Incidents in The USA*. Geological Society, London, Special Publications, 313(1), 163-172.

<https://doi.org/10.1144/sp313.11>

Mody, R., Gerrard, D., & Goodson, J. 2013. “Elastomers In the Oil Field”. *Rubber Chemistry and Technology*, 86(3), 449-469.

<https://doi.org/10.5254/rct.13.86999>

Mohamed, A. O., & Al-Zuraigi, A. 2013. “Liner Hangers Technology Advancement and Challenges”. In *SPE Middle East Oil and Gas Show and Conference*. 10 March 2013. SPE-164367-MS

<https://doi.org/10.2118/164367-ms>

Moore, M. J., Campo, D. B., Hockaday, J., & Ring, L. 2002, May. "Expandable Liner Hangers: Case Histories". In Offshore Technology Conference.

<https://doi.org/10.4043/14313-ms>

Morgan, T. 2006. "The Hydrogen Economy: A Non-Technical Review".

Mori, K., Tsurumaru, H., & Harayama, S. 2010. "Iron Corrosion Activity of Anaerobic Hydrogen-Consuming Microorganisms Isolated from Oil Facilities". *Journal Of Bioscience and Bioengineering*, 110(4), 426-430.

<https://doi.org/10.1016/j.jbiosc.2010.04.012>

Morton, M. 1987. "Rubber Technology, Van Nostrand Reinhold Company Co. Molly Millars Lane, Wokingham, UK".

Muhammed, N. S., Haq, M. B., Al Shehri, D. A., Al-Ahmed, A., Rahman, M. M., Zaman, E., & Iglauer, S. 2023. "Hydrogen Storage in Depleted Gas Reservoirs: A Comprehensive Review". *Fuel*, 337, 127032.

<https://doi.org/10.1016/j.fuel.2022.127032>

Naskar, K. 2007. "Thermoplastic Elastomers Based on Pp/EPDM Blends By Dynamic Vulcanization". *Rubber Chemistry and Technology*, 80(3), 504-519.

<https://doi.org/10.5254/1.3548176>

Nehrir, M. H., & Wang, C. 2009. "Modeling And Control of Fuel Cells: Distributed Generation Applications (Vol. 41)". John Wiley & Sons.

Nieuwenhuizen, P. J. 2001. "Zinc Accelerator Complexes.: Versatile Homogeneous Catalysts In Sulfur Vulcanization". *Applied Catalysis A: General*, 207(1-2), 55-68.

[https://doi.org/10.1016/s0926-860x\(00\)00613-x](https://doi.org/10.1016/s0926-860x(00)00613-x)

Nishimura, S. 2013. "Fracture Behavior of Ethylene Propylene Rubber For Hydrogen Gas Sealing Under High-Pressure Hydrogen". *Nippon Gomu Kyokaishi*, 86(12), 360-366.

Niyogi, U. K. 2007. "Natural And Synthetic Rubber".

Nohilé, C., Dolez, P. I., & Vu-Khanh, T. 2008. "Parameters Controlling the Swelling of Butyl Rubber By Solvents". *Journal Of Applied Polymer Science*, 110(6), 3926-3933.

<https://doi.org/10.1002/app.29004>

Noor, M. M., Wandel, A. P., & Yusaf, T. 2013. "Design And Development of Mild Combustion Burner". *Journal Of Mechanical Engineering and Sciences*, 5, 662-676.
<https://doi.org/10.15282/jmes.5.2013.13.0064>

NORSOK, D. 2013. "Well Integrity in Drilling and Well Operations". NORSOK Standard D-010 Rev, 4.

NORSOK, D. 1998. 001. NORSOK Standard, Drilling Facilities, D-001, Rev, 2.

Nortey, N. O. 1999. "Enhanced Mixing in The Intermeshing Batch Mixer". *Rubber World*, 219(6).

Noussan, M., Raimondi, P. P., Scita, R., & Hafner, M. 2020. "The Role Of Green And Blue Hydrogen In The Energy Transition—A Technological And Geopolitical Perspective". *Sustainability*, 13(1), 298.
<https://doi.org/10.3390/su13010298>

Obergassel, W., Arens, C., Hermwille, L., Kreibich, N., Mersmann, F., Ott, H. E., & Wang-Helmreich, H. 2015. "Phoenix From the Ashes: An Analysis Of The Paris Agreement To The United Nations Framework Convention On Climate Change; Part 1".

O'hara, S. 2009. "The Importance of The United States Staying the Course While Implementing Environmental Policy in Accordance With The American Recovery And Reinvestment Act Of 2009". *U. Balt. J. Envntl. L.*, 17, 85.

Ohi, J. 2005. "Hydrogen Energy Cycle: An Overview". *Journal Of Materials Research*, 20(12), 3180-3187.
<https://doi.org/10.1557/jmr.2005.0408>

Ohm, R. F. 1990. "The Vanderbilt Rubber Handbook, Rt Vanderbilt Company. Inc. Ed. Norwalk".

Omosebi, O., Maheshwari, H., Ahmed, R., Shah, S., Osisanya, S., Hassani, S., ... & Simon, D. 2016. "Degradation Of Well Cement in HPHT Acidic Environment: Effects Of CO₂ Concentration And Pressure". *Cement And Concrete Composites*, 74, 54-70.
<https://doi.org/10.1016/j.cemconcomp.2016.09.006>

Ono, H., Nait-Ali, A., Kane Diallo, O., Benoit, G., & Castagnet, S. 2018. "Influence Of Pressure Cycling On Damage Evolution In An Unfilled EPDM Exposed To High-Pressure Hydrogen". *International Journal Of Fracture*, 210, 137-152.

Ostermeier, R. M. 1995. “Deepwater Gulf of Mexico Turbidites—Compaction Effects on Porosity And Permeability”. SPE Formation Evaluation, 10(02), 79-85. 01 June 1995. SPE-26468-PA
<https://doi.org/10.2118/26468-pa>

Ozturk, M., & Dincer, I. 2021. “A Comprehensive Review on Power-To-Gas with Hydrogen Options for Cleaner Applications”. International Journal of Hydrogen Energy, 46(62), 31511-31522.
<https://doi.org/10.1016/j.ijhydene.2021.07.066>

Panfilov, M., Gravier, G., & Fillacier, S. 2006, September. “Underground Storage of H₂ And H₂-CO₂-CH₄ Mixtures”. In ECMOR X-10th European Conference on The Mathematics of Oil Recovery (Pp. Cp-23). Eage Publications Bv.
<https://doi.org/10.3997/2214-4609.201402474>

Panić, I., Cuculić, A., & Ćelić, J. 2022. “Color-Coded Hydrogen: Production and Storage In Maritime Sector”. Journal Of Marine Science and Engineering, 10(12), 1995.
<https://doi.org/10.3390/jmse10121995>

Patel, H., Salehi, S., Ahmed, R., & Teodoriu, C. 2019. “Review Of Elastomer Seal Assemblies in Oil & Gas Wells: Performance Evaluation, Failure Mechanisms, And Gaps In Industry Standards”. Journal Of Petroleum Science and Engineering, 179, 1046-1062.
<https://doi.org/10.1016/j.petrol.2019.05.019>

Patil, A. O., & Coolbaugh, T. S. 2005. “Elastomers: A Literature Review with Emphasis On Oil Resistance”. Rubber Chemistry and Technology, 78(3), 516-535.
<https://doi.org/10.5254/1.3547894>

Pellegrini, M., Guzzini, A., & Sacconi, C. 2020. “A Preliminary Assessment of the Potential of Low Percentage Green Hydrogen Blending in The Italian Natural Gas Network”. Energies, 13(21), 5570.
<https://doi.org/10.3390/en13215570>

Peng, T., Wan, J., Liu, W., Li, J., Xia, Y., Yuan, G., ... & Liu, H. 2023. “Choice Of Hydrogen Energy Storage in Salt Caverns and Horizontal Cavern Construction Technology”. Journal Of Energy Storage, 60, 106489.
<https://doi.org/10.1016/j.est.2022.106489>

Peters, E. N. 2002. “Plastics: Thermoplastics, Thermosets, And Elastomers” (Pp. 335-355). Wiley-Interscience, New York.

Pichler, M. 2019, April. "Underground Sun Storage Results And Outlook. In Eage/Dgmk Joint Workshop on Underground Storage Of Hydrogen" (Vol. 2019, No. 1, Pp. 1-4). Eage Publications Bv.

Plaat, H. 2009. "Underground Gas Storage: Why And How". Geological Society, London, Special Publications, 313(1), 25-37.

<https://doi.org/10.3997/2214-4609.201900257>

Policy, U. 2011. "Clean Energy Standards: State And Federal Policy Options And Implications".

Ponnamma, D., Jose Chirayil, C., Sadasivuni, K. K., Somasekharan, L., Yaragalla, S., Abraham, J., & Thomas, S. 2013. "Special Purpose Elastomers: Synthesis, Structure-Property Relationship, Compounding, Processing and Applications". *Advances In Elastomers I: Blends and Interpenetrating Networks*, 47-82.

Princi, E. 2019. "Rubber: Science and Technology". Walter De Gruyter Gmbh & Co Kg.

Pudlo, D., And S. Henkel. 2016. "H2STORE And HyINTEGER—Studies on The Effect Of Hydrogen Storage In (Pore) Underground Gas Reservoirs—An Overview." In *Proceedings Of The 3rd Hips-Net Workshop, Brussels, Belgium, June, Pp. 23-24.*

<https://doi.org/10.1115/1.4052626>

Pudlo, D., Ganzer, L., Henkel, S., Kühn, M., Liebscher, A., De Lucia, M., ... & Gaupp, R. 2013. *The H2store Project: Hydrogen Underground Storage—A Feasible Way in Storing Electrical Power In Geological Media? In Clean Energy Systems in The Subsurface: Production, Storage and Conversion: Proceedings Of The 3rd Sino-German Conference "Underground Storage Of CO2 And Energy", Goslar, Germany, 21-23 May 2013 (Pp. 395-412). Springer Berlin Heidelberg.*

Raad, S. M. J., Leonenko, Y., & Hassanzadeh, H. 2022. "Hydrogen Storage In Saline Aquifers: Opportunities And Challenges". *Renewable And Sustainable Energy Reviews*, 168, 112846.

<https://doi.org/10.1016/j.rser.2022.112846>

Rabenstein, G., & Hacker, V. 2008. "Hydrogen For Fuel Cells from Ethanol By Steam-Reforming, Partial-Oxidation And Combined Auto-Thermal Reforming: A Thermodynamic Analysis". *Journal Of Power Sources*, 185(2), 1293-1304.

<https://doi.org/10.1016/j.jpowsour.2008.08.010>

Rajesh Babu, R., Shibulal, G. S., Chandra, A. K., & Naskar, K. 2013. "Compounding And Vulcanization". *Advances In Elastomers I: Blends and Interpenetrating Networks*, 83-135.

Rashid, M. D., Al Mesfer, M. K., Naseem, H., & Danish, M. 2015. "Hydrogen Production By Water Electrolysis: A Review Of Alkaline Water Electrolysis, Pem Water Electrolysis And High Temperature Water Electrolysis". *International Journal of Engineering and Advanced Technology*.

Raza, A., Gholami, R., Rezaee, R., Rasouli, V., Bhatti, A. A., & Bing, C. H. 2018. "Suitability Of Depleted Gas Reservoirs for Geological CO₂ Storage: A Simulation Study". *Greenhouse Gases: Science And Technology*, 8(5), 876-897.

<https://doi.org/10.1002/ghg.1802>

Reitenbach, V., Ganzer, L., Albrecht, D., & Hagemann, B. 2015. "Influence Of Added Hydrogen on Underground Gas Storage: A Review Of Key Issues". *Environmental Earth Sciences*, 73, 6927-6937.

Revie, R. W. 2008. "Corrosion And Corrosion Control: An Introduction to Corrosion Science And Engineering". John Wiley & Sons.

Rezaee, R., Saeedi, A., Iglauer, S., & Evans, B. 2017. "Shale Alteration After Exposure to Supercritical Co₂". *International Journal of Greenhouse Gas Control*, 62, 91-99.

<https://doi.org/10.1016/j.ijggc.2017.04.004>

Richter B., And Blobner U 2017. "Expert Knowledge Failure Analysis of Elastomer Components-Chemical Degradation and Swelling Destruction Of Network Structure By Contact Medium".

Rigas, F., & Amyotte, P. 2013. Myths And Facts About Hydrogen Hazards. In 13th International Symposium on Loss Prevention And Safety Promotion In The Process Industries, Florence, Italy (May 12-15, 2013).

Rinnbauer, M. 2007. "Technical Elastomers, The Basis of High-Tech Sealing and Vibration Control Technology Solutions". Sv Corporate Media Gmbh: Munich, Germany.

Rivard, E., Trudeau, M., & Zaghbi, K. 2019. "Hydrogen Storage for Mobility: A Review". *Materials*, 12(12), 1973.

<https://doi.org/10.3390/ma12121973>

Rudolph, T. 2019, April. "Underground Hydrogen Storage–Current Developments and Opportunities". In Eage/Dgmk Joint Workshop on Underground Storage Of Hydrogen (Vol. 2019, No. 1, Pp. 1-2). Eage Publications Bv.

<https://doi.org/10.3997/2214-4609.201900256>

Rueda, F., Marquez, A., Otegui, J. L., & Frontini, P. M. 2016. "Buckling Collapse of HDPE Liners: Experimental Set-Up And Fem Simulations". *Thin-Walled Structures*, 109, 103-112.

<https://doi.org/10.1016/j.tws.2016.09.011>

Ruscic, B. 2015. "Active Thermochemical Tables: Sequential Bond Dissociation Enthalpies of Methane, Ethane, And Methanol And The Related Thermochemistry". *The Journal of Physical Chemistry A*, 119(28), 7810-7837.

<https://doi.org/10.1021/acs.jpca.5b01346>

Sáinz-García, A., Abarca, E., Rubí, V., & Grandía, F. 2017. "Assessment Of Feasible Strategies for Seasonal Underground Hydrogen Storage In A Saline Aquifer". *International Journal Of Hydrogen Energy*, 42(26), 16657-16666.

<https://doi.org/10.1016/j.ijhydene.2017.05.076>

Saleesung, T., Reichert, D., Saalwächter, K., & Sirisinha, C. 2015. "Correlation Of Crosslink Densities Using Solid State NMR And Conventional Techniques In Peroxide-Crosslinked EPDM Rubber". *Polymer*, 56, 309-317.

<https://doi.org/10.1016/j.polymer.2014.10.057>

Salehi, S., Ezeakacha, C. P., Kwatia, G., Ahmed, R., & Teodoriu, C. 2019. "Performance Verification of Elastomer Materials in Corrosive Gas and Liquid Conditions". *Polymer Testing*, 75, 48-63.

<https://doi.org/10.1016/j.polymertesting.2019.01.015>

Schrittesser, B., Pinter, G., Schwarz, T., Kadar, Z., & Nagy, T. 2016. "Rapid Gas Decompression Performance of Elastomers—A Study Of Influencing Testing Parameters". *Procedia Structural Integrity*, 2, 1746-1754.

<https://doi.org/10.1016/j.prostr.2016.06.220>

Schultz, R. A., & Evans, D. J. 2020. "Occurrence Frequencies and Uncertainties for US Underground Natural Gas Storage Facilities By State". *Journal Of Natural Gas Science and Engineering*, 84, 103630.

<https://doi.org/10.1016/j.jngse.2020.103630>

Schweitzer, P. A. 2000. "Mechanical And Corrosion-Resistant Properties Of Plastics And Elastomers".

Scott, K. 2019. "Introduction To Electrolysis, Electrolyzers and Hydrogen Production".

<https://doi.org/10.1039/9781788016049-00001>

Sercombe, J., Vidal, R., Gallé, C., & Adenot, F. 2007. “Experimental Study of Gas Diffusion In Cement Paste”. *Cement And Concrete Research*, 37(4), 579-588.

<https://doi.org/10.1016/j.cemconres.2006.12.003>

Hosseini, S. E. 2022. “Hydrogen Has Found Its Way to Become The Fuel Of The Future”. *Future Energy*, 1(3), 11-12.

<https://orcid.org/0000-0002-0907-9427>

Shafiee, M., Elusakin, T., & Enjema, E. 2020. “Subsea Blowout Preventer (BOP): Design, Reliability, Testing, Deployment, And Operation and Maintenance Challenges”. *Journal Of Loss Prevention In The Process Industries*, 66, 104170.

<https://doi.org/10.1016/j.jlp.2020.104170>

Shakiba, M., & Najmeddine, A. 2021. “Physics-Based Constitutive Equation for Thermo-Chemical Aging In Elastomers Based On Crosslink Density Evolution”. *Arxiv Preprint Arxiv:2104.09001*.

<https://doi.org/10.48550/arxiv.2104.09001>

Shamoon, A., Haleem, A., Bahl, S., Javaid, M., Garg, S. B., Sharma, R. C., & Garg, J. 2022. “Environmental Impact of Energy Production and Extraction Of Materials-A Review”. *Materials Today: Proceedings*.

<https://doi.org/10.1016/j.matpr.2022.03.159>

Shanks, R. A., & Kong, I. 2013. “General Purpose Elastomers: Structure, Chemistry, Physics And Performance”. *Advances In Elastomers I: Blends and Interpenetrating Networks*, 11-45.

Sharma, S., & Ghoshal, S. K. 2015. “Hydrogen The Future Transportation Fuel: From Production To Applications”. *Renewable And Sustainable Energy Reviews*, 43, 1151-1158.

<https://doi.org/10.1016/j.rser.2014.11.093>

Shaw, J. A., Jones, A. S., & Wineman, A. S. 2005. Chemorheological Response of Elastomers at Elevated Temperatures: Experiments and Simulations. *Journal of the Mechanics and Physics of Solids*, 53(12), 2758-2793.

<https://doi.org/10.1016/j.jmps.2005.07.004>

Shen, J., Wen, S., Du, Y., Li, N., Zhang, L., Yang, Y., & Liu, L. 2013. “The Network and Properties Of The NR/SBR Vulcanizate Modified By Electron Beam Irradiation”. *Radiation Physics And Chemistry*, 92, 99-104.

<https://doi.org/10.1016/j.radphyschem.2013.07.022>

Shen, M. X., Dong, F., Zhang, Z. X., Meng, X. K., & Peng, X. D. 2016. "Effect of Abrasive Size on Friction and Wear Characteristics Of Nitrile Butadiene Rubber (Nbr) In Two-Body Abrasion". *Tribology International*, 103, 1-11.

<https://doi.org/10.1016/j.triboint.2016.06.025>

Sherif, S. A., Barbir, F., & Veziroglu, T. N. 2003. "Principles Of Hydrogen Energy Production, Storage And Utilization".

<http://nopr.niscpr.res.in/handle/123456789/17577>

Shi, Z., Jessen, K., & Tsotsis, T. T. 2020. "Impacts Of The Subsurface Storage of Natural Gas And Hydrogen Mixtures". *International Journal Of Hydrogen Energy*, 45(15), 8757-8773.

<https://doi.org/10.1016/j.ijhydene.2020.01.044>

Siddique, S., Kwoffie, L., Addae-Afoakwa, K., Yates, K., & Njuguna, J. 2017, May. "Oil Based Drilling Fluid Waste: An Overview On Environmentally Persistent Pollutants". In *IOP Conference Series: Materials Science And Engineering* (Vol. 195, No. 1, P. 012008). IOP Publishing.

Doi 10.1088/1757-899x/195/1/012008

Simmons, K. L., Kuang, W., Burton, S. D., Arey, B. W., Shin, Y., Menon, N. C., & Smith, D. B. 2021. "H-Mat Hydrogen Compatibility Of Polymers And Elastomers". *International Journal Of Hydrogen Energy*, 46(23), 12300-12310.

<https://doi.org/10.1016/j.ijhydene.2020.06.218>

Simpson, R. B. (Ed.). 2002. "Rubber Basics". Ismithers Rapra Publishing.

Singh, A. P., Pal, A., & Agarwal, A. K. 2016. "Comparative Particulate Characteristics Of Hydrogen, CNG, HCNG, Gasoline And Diesel Fueled Engines". *Fuel*, 185, 491-499.

<https://doi.org/10.1016/j.fuel.2016.08.018>

Singh, V. K. 2010. "Geological Storage: Underground Gas Storage".

Sinigaglia, T., Lewiski, F., Martins, M. E. S., & Siluk, J. C. M. 2017. "Production, Storage, Fuel Stations of Hydrogen And Its Utilization In Automotive Applications-A Review". *International Journal of Hydrogen Energy*, 42(39), 24597-24611.

<https://doi.org/10.1016/j.ijhydene.2017.08.063>

Skogdalen, J. E., Utne, I. B., & Vinnem, J. E. 2011. "Developing Safety Indicators For Preventing Offshore Oil And Gas Deepwater Drilling Blowouts". *Safety Science*, 49(8-9), 1187-1199.

<https://doi.org/10.1016/j.ssci.2011.03.012>

Slikkerveer, P. J., Van Dongen, M. H. A., & Touwslager, F. J. 1999. "Erosion of Elastomeric Protective Coatings". *Wear*, 236(1-2), 189-198.

[https://doi.org/10.1016/s0043-1648\(99\)00268-9](https://doi.org/10.1016/s0043-1648(99)00268-9)

Smart, B. E. 1983. "The Chemistry of Functional Groups, Supplement D; Patai, S., Rappoport, Z., Eds".

Speer, M. 2006. "Introduction To Wellhead Systems". *Petroleum Engineering Handbook*, 2, 344-369.

Spiegelhalder, B., & Preussmann, R. 1983. "Occupational Nitrosamine Exposure". 1. Rubber And Tyre Industry. *Carcinogenesis*, 4(9), 1147-1152.

<https://doi.org/10.1093/carcin/4.9.1147>

Stahl, W. M. 2006. "Choosing The Right Elastomer for the Right Application". *World Pumps*, 2006(481), 30-33.

[https://doi.org/10.1016/s0262-1762\(06\)71110-5](https://doi.org/10.1016/s0262-1762(06)71110-5)

Stella, G., & Cheremisinoff, N. P. 1989. "Designing EPDM for Production Efficiency". *Polymer-Plastics Technology And Engineering*, 28(2), 185-199.

<https://doi.org/10.1080/03602558908048593>

Anil, K. B., & Howard, L. S. 2001. "Handbook Of Elastomers".

Stevenson, A., & Morgan, G. 1995. "Fracture Of Elastomers by Gas Decompression". *Rubber Chemistry And Technology*, 68(2), 197-211.

<https://doi.org/10.5254/1.3538735>

Stiegel, G. J., & Ramezan, M. 2006. "Hydrogen From Coal Gasification: An Economical Pathway To A Sustainable Energy Future". *International Journal of Coal Geology*, 65(3-4), 173-190.

<https://doi.org/10.1016/j.coal.2005.05.002>

Stolten, D., & Emonts, B. (Eds.). 2016. *Hydrogen Science and Engineering*, 2 Volume Set: Materials, Processes, Systems, And Technology (Vol. 1). John Wiley & Sons.

Strazisar, B., Kutchko, B., & Huerta, N. 2009. "Chemical Reactions of Wellbore Cement Under CO₂ Storage Conditions: Effects Of Cement Additives". *Energy Procedia*, 1(1), 3603-3607.

<https://doi.org/10.1016/j.egypro.2009.02.155>

Subramaniam, A. 1987. "Natural Rubber". *Rubber Technology*, 179-208.

Sweet, G. C. 1980. "Special Purpose Elastomers". *Developments In Rubber Technology*, 1, 86.

Szummer, A., Jezierska, E., & Lublińska, K. 1999. "Hydrogen Surface Effects in Ferritic Stainless Steels". *Journal Of Alloys and Compounds*, 293, 356-360.

[https://doi.org/10.1016/s0925-8388\(99\)00401-6](https://doi.org/10.1016/s0925-8388(99)00401-6)

Tabibzadeh, M., Stavros, S., Ashtekar, M. S., & Meshkati, N. 2017. "A Systematic Framework For Root-Cause Analysis of the Aliso Canyon Gas Leak Using The Accimap Methodology: Implication For Underground Gas Storage Facilities". *Journal Of Sustainable Energy Engineering*, 5(3), 212-242.

<https://doi.org/10.7569/jsee.2017.629515>

Tan, J., Chao, Y. J., Van Zee, J. W., & Lee, W. K. 2007. "Degradation of Elastomeric Gasket Materials In Pem Fuel Cells". *Materials Science and Engineering: A*, 445, 669-675.

<https://doi.org/10.1016/j.msea.2006.09.098>

Tarkowski, R. 2019. "Underground Hydrogen Storage: Characteristics and Prospects". *Renewable And Sustainable Energy Reviews*, 105, 86-94.

<https://doi.org/10.1016/j.rser.2019.01.051>

Tarkowski, R., & Czapowski, G. 2018. "Salt Domes in Poland–Potential Sites for Hydrogen Storage In Caverns". *International Journal Of Hydrogen Energy*, 43(46), 21414-21427.

<https://doi.org/10.1016/j.ijhydene.2018.09.212>

Temin, S. C. 1990. "Pressure-Sensitive Adhesives for Tapes and Labels". *Handbook Of Adhesives*, 641-663.

Tetteh, D. A., & Salehi, S. 2023. "The Blue Hydrogen Economy: A Promising Option For The Near-To-Mid-Term Energy Transition". *Journal Of Energy Resources Technology*, 145(4), 042701.

<https://doi.org/10.1115/1.4055205>

Thaysen, E. M., McMahon, S., Strobel, G. J., Butler, I. B., Ngwenya, B. T., Heinemann, N., ... & Edlmann, K. 2021. "Estimating Microbial Growth And Hydrogen Consumption In Hydrogen Storage In Porous Media". *Renewable And Sustainable Energy Reviews*, 151, 111481.

<https://doi.org/10.1016/j.rser.2021.111481>

The Engineering Toolbox, Air-Diffusion Coefficients Of Gases In Excess Air, Accessed: 01/24/2023. https://www.engineeringtoolbox.com/air-diffusion-coefficient-gas-mixture-temperature-d_2010.html.

Date Accessed: 11/24/2022

Thiyagarajan, S. R., Emadi, H., Hussain, A., Patange, P., & Watson, M. 2022. "A Comprehensive Review of The Mechanisms and Efficiency of Underground Hydrogen Storage". *Journal of Energy Storage*, 51, 104490.

<https://doi.org/10.1016/j.est.2022.104490>

Tokita, N., & White, J. L. 1966. "Milling Behavior of Gum Elastomers: Experiment and Theory". *Journal of Applied Polymer Science*, 10(7), 1011-1026.

<https://doi.org/10.1002/app.1966.070100705>

Twum, E. B., Mccord, E. F., Fox, P. A., Lyons, D. F., & Rinaldi, P. L. 2013. "Characterization of Backbone Structures in Poly (Vinylidene Fluoride-Co-Hexafluoropropylene) Copolymers By Multidimensional ¹⁹F NMR Spectroscopy". *Macromolecules*, 46(12), 4892-4908.

Ursua, A., Gandia, L. M., & Sanchis, P. 2011. "Hydrogen Production from Water Electrolysis: Current Status and Future Trends". *Proceedings Of The IEEE*, 100(2), 410-426.

V Bevervoorde-Meilof, E. E. 1998. "Improving Mechanical Properties Of EPDM Rubber By Mixed Vulcanisation".

Deepalekshmi, P., Visakh, P. M., Mathew, A. P., Chandra, A. K., & Thomas, S. 2013. "Advances In Elastomers: Their Blends and Interpenetrating Networks-State Of Art, New Challenges And Opportunities". *Advances In Elastomers I: Blends and Interpenetrating Networks*, 1-9.

Vohra, A., Filiatrault, H. L., Amyotte, S. D., Carmichael, R. S., Suhan, N. D., Siegers, C., ... & Carmichael, T. B. 2016. "Reinventing Butyl Rubber for Stretchable Electronics". *Advanced Functional Materials*, 26(29), 5222-5229.

<https://doi.org/10.1002/adfm.201601283>

Wan, Q., Masters, R. C., Lidzey, D., Abrams, K. J., Dapor, M., Plenderleith, R. A., ... & Rodenburg, C. 2016. "Angle Selective Backscattered Electron Contrast in The Low-Voltage Scanning Electron Microscope: Simulation and Experiment For Polymers". *Ultramicroscopy*, 171, 126-138.

<https://doi.org/10.1016/j.ultramic.2016.09.006>

Wang, L., Yu, C., Zhang, Y., Luo, L., & Zhang, G. 2018. "An Analysis of The Characteristics of Road Traffic Injuries and A Prediction of Fatalities in China from 1996 to 2015". *Traffic Injury Prevention*, 19(7), 749-754.

<https://doi.org/10.1080/15389588.2018.1487061>

Wang, Y., Liu, H., Li, P., & Wang, L. 2022. "The Effect Of Cross-Linking Type On EPDM Elastomer Dynamics And Mechanical Properties: A Molecular Dynamics Simulation Study". *Polymers*, 14(7), 1308.

<https://doi.org/10.3390/polym14071308>

Warmuzinski, K. 2008. "Harnessing Methane Emissions From Coal Mining". *Process Safety And Environmental Protection*, 86(5), 315-320.

<https://doi.org/10.1016/j.psep.2008.04.003>

Warren, J. K., & Warren, J. K. 2016. "Solution Mining and Salt Cavern Usage". *Evaporites: A Geological Compendium*, 1303-1374.

Watfa, M. 1991. "Downhole Casing Corrosion Monitoring and Interpretation Techniques to Evaluate Corrosion In Multiple Casing Strings". *SPE Production Engineering*, 6(03), 283-290. 10 March 2013. SPE-164367-MS

<https://doi.org/10.2118/17931-pa>

Wentinck, H. M., & Busch, A. 2017. "Modelling Of CO₂ Diffusion and Related Poro-Elastic Effects In A Smectite-Rich Cap Rock Above A Reservoir Used For CO₂ Storage". *Geological Society, London, Special Publications*, 454(1), 155-173.

<https://doi.org/10.1144/sp454.4>

Windslow, R. J., & Busfield, J. J. C. 2019. "Viscoelastic Modeling Of Extrusion Damage In Elastomer Seals". *Soft Materials*, 17(3), 228-240.

<https://doi.org/10.1080/1539445x.2019.1575238>

Woo, C. S., & Park, H. S. 2011. "Useful Lifetime Prediction of Rubber Component". *Engineering Failure Analysis*, 18(7), 1645-1651.

<https://doi.org/10.1016/j.engfailanal.2011.01.003>

Wood, L. A. 1957. "The Elasticity of Rubber". *Journal Of the Washington Academy of Sciences*, 47(9), 281-299.

<https://www.jstor.org/stable/24533824>

Wuebbles, D. J., & Jain, A. K. 2001. “Concerns About Climate Change And The Role Of Fossil Fuel Use”. *Fuel Processing Technology*, 71(1-3), 99-119.

[https://doi.org/10.1016/s0378-3820\(01\)00139-4](https://doi.org/10.1016/s0378-3820(01)00139-4)

Xiao, G., Zhimin, D., Ping, G., Yuhong, D., Yu, F., & Tao, L. 2006. “Design and Demonstration of Creating Underground Gas Storage In A Fractured Oil Depleted Carbonate Reservoir”. In *SPE Russian Oil And Gas Technical Conference And Exhibition*. OnePetro. 03 October 2006. SPE-102397-MS

<https://doi.org/10.2118/102397-ms>

Xu, L., Wang, Y., Shah, S. A. A., Zameer, H., Solangi, Y. A., Walasai, G. D., & Siyal, Z. A. 2019. “Economic Viability And Environmental Efficiency Analysis Of Hydrogen Production Processes For The Decarbonization Of Energy Systems”. *Processes*, 7(8), 494.

<https://doi.org/10.3390/pr7080494>

Xu, R., Li, R., Ma, J., He, D., & Jiang, P. 2017. “Effect Of Mineral Dissolution/Precipitation And Co₂ Exsolution on CO₂ Transport In Geological Carbon Storage”. *Accounts Of Chemical Research*, 50(9), 2056-2066.

<https://doi.org/10.1021/acs.accounts.6b00651>

Yamabe, J., & Nishimura, S. 2009. “Influence Of Fillers On Hydrogen Penetration Properties And Blister Fracture of Rubber Composites for O-Ring Exposed to High-Pressure Hydrogen Gas”. *International Journal Of Hydrogen Energy*, 34(4), 1977-1989.

<https://doi.org/10.1016/j.ijhydene.2008.11.105>

Yamabe, J., Nakao, M., Fujiwara, H., & Nishimura, S. 2008. “Influence Of Fillers On Hydrogen Penetration Properties And Blister Fracture Of Epdm Composites Exposed to 10 MPa Hydrogen Gas”. *Nihon Kikai Gakkai Ronbunshu, A Hen/Transactions Of The Japan Society Of Mechanical Engineers, Part A*, 74(743), 971-981.

<https://doi.org/10.1299/kikaia.74.971>

Yekta, A. E., Manceau, J. C., Gaboreau, S., Pichavant, M., & Audigane, P. 2018. “Determination of Hydrogen–Water Relative Permeability and Capillary Pressure In Sandstone: Application to Underground Hydrogen Injection In Sedimentary Formations”. *Transport In Porous Media*, 122(2), 333-356.

<https://doi.org/10.1007/s11242-018-1004-7>

Yu, L., Zhu, Q., Song, S., Mcelhenny, B., Wang, D., Wu, C., ... & Ren, Z. 2019. “Non-Noble Metal-Nitride Based Electrocatalysts For High-Performance Alkaline Seawater Electrolysis”. *Nature Communications*, 10(1), 5106.

<https://doi.org/10.1038/s41467-019-13092-7>

Yue, X. Y. 2005. “Research Development of Thermoplastic Elastomers”. *Special Purpose Rubber Products*, 26, 51.

Zaghoudi, M., Kömmling, A., Jaunich, M., & Wolff, D. 2019. “Scission, Cross-Linking, And Physical Relaxation During Thermal Degradation Of Elastomers”. *Polymers*, 11(8), 1280.

<https://doi.org/10.3390/polym11081280>

Zamehrian, M., & Sedaee, B. 2022. “Underground Hydrogen Storage In A Naturally Fractured Gas Reservoir: The Role of Fracture”. *International Journal Of Hydrogen Energy*, 47(93), 39606-39618.

<https://doi.org/10.1016/j.ijhydene.2022.09.116>

Zeng, L., Sarmadivaleh, M., Saeedi, A., Al-Yaseri, A., Dowling, C., Buick, G., & Xie, Q. 2022. “Thermodynamic Modelling on Wellbore Cement Integrity During Underground Hydrogen Storage In Depleted Gas Reservoirs”. In *SPE Asia Pacific Oil & Gas Conference And Exhibition*. OnePetro. 14 October 2022. SPE-210639-MS

<https://doi.org/10.2118/210639-ms>

Zeng, L., Sarmadivaleh, M., Saeedi, A., Chen, Y., Zhong, Z., & Xie, Q. 2022. “Storage Integrity During Underground Hydrogen Storage In Depleted Gas Reservoirs”.

<https://doi.org/10.31223/x54647>

Zhang, B., Zhang, S. X., Yao, R., Wu, Y. H., & Qiu, J. S. 2021. “Progress And Prospects Of Hydrogen Production: Opportunities And Challenges”. *Journal Of Electronic Science And Technology*, 19(2), 100080.

<https://doi.org/10.1016/j.jnlest.2021.100080>

Zheng, J., Wang, C. G., Zhou, H., Ye, E., Xu, J., Li, Z., & Loh, X. J. 2021. “Current Research Trends And Perspectives On Solid-State Nanomaterials In Hydrogen Storage”. *Research*, 2021.

<https://doi.org/10.34133/2021/3750689>

Zhong, A., Fan, Z., Purohit, A., & Jutu Mothilal, B. P. 2022, April. “Optimizations of Downhole Sealing Devices and Their Validations”. In *Offshore Technology Conference*. OnePetro.

<https://doi.org/10.4043/31830-ms>

Zoulias, E., Varkaraki, E., Lymberopoulos, N., Christodoulou, C. N., & Karagiorgis, G. N. 2004. “A Review on Water Electrolysis”. *Tcjst*, 4(2), 41-71.

10. Appendix

Equations for Statistical T and F Tests

F- TEST

(1)

$H_0: \sigma_1^2 = \sigma_2^2$ (Null Hypothesis)

$H_1: \sigma_1^2 \neq \sigma_2^2$ (Null Hypothesis)

$\sigma_1^2 =$ Population variance for sampled number of cavities before exposure

$\sigma_2^2 =$ Population variance for sampled number of cavities after exposure

Test Statistic

$$F_o = s_1^2 / s_2^2$$

$s_1 =$ Standard deviation of sampled data before gaseous exposure

$s_2 =$ Standard deviation of sampled data after gaseous exposure

T-Test

(2)

$H_0: \mu_1 \geq \mu_2$ (null hypothesis)

$H_1: \mu_1 < \mu_2$ (alternate hypothesis)

$\mu_1 =$ Population mean number of cavities for sampled data before exposure

$\mu_2 =$ population mean number of cavities for sampled data after exposure

Test Statistic (For Unknown and unequal variance)

$$t_o = \frac{(\gamma_1 - \gamma_2) - (\mu_1 - \mu_2)}{\sqrt{\frac{s_1^2}{n_1} + \frac{s_2^2}{n_2}}}$$

$\gamma_1 =$ Sample mean number of cavities for sampled data before exposure

$\gamma_2 =$ Sample mean number of cavities for sampled data after exposure

$n_1 =$ Sample size for population 1

$n_2 =$ Sample size for population 2

Test Statistic (For Unknown and Equal variance)

$$t_o = \frac{(\gamma_1 - \gamma_2) - (\mu_1 - \mu_2)}{\sqrt{\frac{(n_1 - 1)s_1^2 + (n_2 - 1)s_2^2}{n_1 + n_2 - 2}} \times \sqrt{\frac{1}{n_1} + \frac{1}{n_2}}}$$